

https://dspace.org/

A study of methods to improve the performance of drag bits used to cut hard rock

Hood, Michael

2015-08-06
http://hdl.handle.net/10539/18193

Downloaded from a DSpace repository. https://dspace.org/

A STUDY OF METHODS TO IMPROVE THE PERFORMANCE OF DRAG BITS USED TO CUT HARD ROCK.

Michael Hood

A Thesis Submitted to the Faculty of Engineering
University of t Witwatersrand, Johannesburg
for the Degree of Doctor of Philosophy.

Johannesburg 1977

SUMMARY

The motivation for undertaking this study of drag bits for use in hard rock applications was provided by ongoing field trials of rockcutting machines at gold mines of the Witwatersrand system. Investigations were carried out to determine the mode of failure of bits used at these trial sites and laboratory experiments were conducted to identify the weak aspects of the bit design. It was established that a major cause of failure of the bits in service underground was thermal deterioration of the tungsten carbide bit inserts and of the bit braze joint. A further series of tests was then carried out, both in the laboratory and underground, with modified bits in an attempt to improve the bit strength.

In addition, a suite of experiments was conducted with the aim of improving the rate of cutting by reducing the mean force acting on the bit during the cutting operation. Three different methods were evaluated as a means of achieving this objective, these being, reducing the area of the bit wearflat in contact with the rock, impacting the bit during the cutting operation, and directing a high pressure water jet immediately ahead of the bit during the cutting stroke. Each of these methods did result in decreases in at least one component of the bit force, but the technique that was selected as presenting the most promising direction for further investigation was the use of water jets.

Laboratory experiments showed that when coherent water jets at fifty megapascals pressure were directed towards the corners of the

bit inserts, approximately two millimetres ahead of the leading face of the bit, significant reductions of the forces acting on the bit were achieved. The bit cutting force was reduced by a factor of about two and the bit penetrating force by a factor of about three. The bit penetrating force was found to be consistently sensitive to changes both in the pressure of the water jets and in the point of impingement of the jets relative to the bit. On the other hand, the reduction in the bit cutting force was for the most part unaltered despite changes in these parameters, except when the jets were directed ten millimetres or more ahead of the leading face of the bit.

In order to investigate the influence on the rock breaking process of high pressure water jets directed ahead of a drag bit, initial experiments were carried out to establish the mechanism by which the bit cut the rock when water jets were not used. It was shown that in hard rock a drag bit broke the rock in a fashion similar to that of a flat indentor. A theoretical analysis was employed and the stresses in the rock adjacent to an indentor, together with stress trajectories, were calculated.

A series of indentation tests demonstrated that cracks were initiated along lines of calculated maximum principal stress. It was shown that when high pressure water jets were directed ahead of the bit the indentation force required to form a rock chip was reduced by a factor of approximately two. It was inferred from these experiments that water was injected into cracks which were formed in the rock by the bit. The pressure of the water then caused the crack to propagate and form a rock chip.

The discovery that high pressure water jets can reduce significantly the forces acting on a drag bit cutting in hard rock may lead to a more widespread use of this cheap efficient tool in hard rock applications. In addition, it is possible that water jets could be used to assist other methods of rockbreaking, for example disc cutters on various types of boring machines.

CONTENTS

	Page No
CHAPTER 1	
1. INTRODUCTION	1
1.1 General	1
1.2 Geological background of the Witwatersrand gold deposits	1
1.3 Motivation for selective mining	2
1.4 Choice of a selective mining system	4
1.4.1 Rockbreaking considerations	4
1.4.2 Rockcutting system	5
1.5 Development of rockcutting machines	6
1.6 Pilot production trials of mining by rockcutting	7
CHAPTER 2	
2. PREVIOUS WORK WITH DRAG BITS	10
2.1 Evans model	11
2.2 Drag bits used to cut in strong rocks	12
2.2.1 Studies conducted by the Chamber of Mines	14
2.2.2 Investigations with blunt bits	16
2.3 The development of bits for the pilot production trials	19
CHAPTER 3	
3. IDENTIFICATION OF PROBLEMS ASSOCIATED WITH THE BITS	24
3.1 The strength of the bit	24
3.2 Thermal deterioration of the bits	27

Page No.

3.2.1 The tungsten carbide 27

3.2.2 The bit braze joint 29

CHAPTER 4

4. TEST EQUIPMENT 31

4.1 Test frame 31

4.1.1 Comparison of the properties of norite and quartzite 31

4.1.2 Load cells 32

4.2 Instrumentation of test rig 33

4.2.1 Calibration of test rig instrumentation 37

4.3 Rockcutting machine and hydraulic power packs 39

4.3.1 Power packs used for high pressure water jets 40

CHAPTER 5

5. EXPERIMENTAL METHODS AND PROCEDURES 41

5.1 Laboratory experiments using the test rig 41

5.2 Experiments conducted underground 42

5.2.1 Bit failure 43

CHAPTER 6

6. EXPERIMENTAL PROGRAMME 45

6.1 Investigations into the heat generated during the cutting operation 46

6.1.1 Temperature measurements 46

6.1.2 Computer study 48

Page No.

6.2 Experiments designed to increase the strength of the bit 50

6.2.1 Tungsten carbide grade 51

6.2.2 Braze joint 51

6.2.3 Bit geometry 59

6.3 Experiments to reduce the mean bit force 63

6.3.1 Bits with a narrow wearflat 63

6.3.2 Vibration of the bit 65

6.3.3 Pre-weakening the rock 67

6.3.4 Directing a 'flat-fan' water jets towards the bit 71

6.4 The use of 'coherent' water jets to assist the cutting operation 72

6.4.1 Effect of water jet pressure 74

6.4.2 Effect of direction of the water jets relative to the corners of the tungsten carbide inserts 76

6.4.3 Point of impingement of the jets 80

6.5 Testing water jets at the underground site 82

CHAPTER 7

7. INVESTIGATION OF THE MECHANISM OF FAILURE OF HARD ROCK, USING DRAG BITS ASSISTED BY WATER JETS 86

7.1 The mechanism of fracture of strong rock using a drag bit with no water jets 86

7.2 Indentation tests - using a drag bit to indent a rock surface 89

Page No.

7.2.1 Rock chips formed by an indentation force applied normal to the rock surface 90

7.2.2 Indentation tests with a shear force superimposed between the bit and the rock 92

7.3 The propagation of fracture in rock caused by a bit indenting the rock surface with the force applied normal to the surface 96

7.4 Calculation of the stress distribution in the rock adjacent to the bit 99

7.4.1 Calculation of stress contours 102

7.4.2 Regions of excess stress 108

7.4.3 Stress trajectories 108

7.5 Experiments to study the effect of high pressure water jets on the rock breaking process 110

7.5.1 Examination of hypothesis 110

7.5.2 Indentation tests using high pressure water jets 112

7.6 A model to explain how high pressure water jets affect the cutting operation 115

CHAPTER 8

8. SUMMARY OF CONCLUSIONS 118

APPENDICES 122

ACKNOWLEDGEMENTS 130

REFERENCES 131

LIST OF FIGURES

Figure 1. Specific energy of rockbreaking as a function of mineral particle size for processes of excavation, (after Cook and Joughin, 1970).

Figure 2. Diagramatic representation of a rockcutting machine.

Figure 3. Diagramatic representation of a wedge shaped drag bit.

Figure 4. Sketch showing a wedge pressed into a brittle material, (after Evans, 1962).

Figure 5 a) Original design of rockcutting bit.
b) Modified design of rockcutting bit.

Figure 6. A blunt rotary drilling drag bit (after Fairhurst and Lacabanne, 1957).

Figure 7. The components of force acting on a drag bit.

Figure 8. Diagram illustrating method of rock fracture using a blunt drag bit to cut hard rock, (after Kiemann, 1974).

Figure 9. Detachable rockcutter bit, 23 mm thick, in use at the start of the pilot production trials of mining by rock-cutting.

Figure 10. Schematic diagram illustrating cracks in the rock surrounding a deep-level stope.

Figure 11. Plan view of a section of the Doornfontein rockcutter stope illustrating the extent of the fractured condition of the rock.

Figure 12. Magnified section of a tungsten carbide bit insert, showing plastic deformation of the insert ahead of the leading face.

Figure 13. Thermal deterioration-producing wear of tungsten carbide bit insert.

Figure 14. Rockcutter bit, showing method of breaking open to examine the braze joint.

Figure 15. Oxidation of front braze face.

Figure 16. Oxidation of rear braze face.

Figure 17. Diagram of test frame. Plan view illustrating the rockcutting machine set up to cut against the norite block.

Figure 18. Rockcutting machine in test frame, side view.

Figure 19. Indentation strength of quartzite as a function of the quartz content of the rock specimen.

Figure 20. Strain gauge instrumented load cell billet.

Figure 21. Section through a test frame load cell.

Figure 22. Mounting of load cell billets relative to the block of rock.

Figure 23. Instrumentation connection diagrams.

Figure 24. Extract from chart recording.

Figure 25. Pulley-driven potentiometer for velocity transducer.

Figure 26. Rockcutting machine.

Figure 27. Hydraulic power pack to drive the rockcutting machine.

Figure 28. Power pack used for high pressure water jets.

Figure 29. Categories of bit failure.

Figure 30. Diagram illustrating the position of thermocouples mounted in the bit.

Figure 31. Temperatures measured at the bit braze joint during the cutting operation plotted against depth of cut.

Figure 32. Extract from chart recordings illustrating temperature measurements, and reduced amplitudes of force components with water cooling.

Figure 33. Initial parameters used for computer calculation of bit temperatures.

Figure 34. Temperatures calculated in the tungsten carbide bit insert after twelve seconds, with 5 kW applied to the bit wearflat.

Figure 35. Hardness and transverse rupture strength of cemented tungsten carbide as a function of the particle grain size and the cobalt content.

Figure 36. Detachable rockcutter bit, 35 mm thick.

Figure 37. Mean peak cutting force plotted against depth of cut for 35 mm thick bits and 23 mm thick bits.

Figure 38. Mean bit cutting force plotted against depth of cut for 35 mm thick bits and 23 mm thick bits.

Figure 39. Mean peak bit penetrating force plotted against depth of cut for 35 mm thick bits and 23 mm thick bits.

Figure 40. Mean bit penetrating force plotted against depth of cut for 35 mm thick bits and 23 mm thick bits.

Figure 41. Detachable, 35 mm rockcutter bit with a 2 mm wearflat width.

Figure 42. Mean peak bit cutting force using a standard wearflat and a narrow wearflat bit.

Figure 43. Mean bit cutting force using a standard wearflat and a narrow wearflat bit.

Figure 44. Mean peak bit penetrating force using a standard wearflat and a narrow wearflat bit.

Figure 45. Mean bit penetrating force using a standard wearflat and a narrow wearflat bit.

Figure 46. Extract from chart recording using a stiff hydraulic drive to the rockcutting machine.

Figure 47. Extract from chart recording using a compliant hydraulic drive to the rockcutting machine.

Figure 48. Mean peak bit cutting force plotted against depth of cut, comparing a stiff hydraulic drive to the machine with a compliant hydraulic drive.

Figure 49. Mean bit cutting force plotted against depth of cut, comparing a stiff hydraulic drive to the machine with a compliant hydraulic drive.

Figure 50. Mean peak bit penetrating force plotted against depth of cut, comparing a stiff hydraulic drive to the machine with a compliant hydraulic drive.

Figure 51. Mean bit penetrating force plotted against depth of cut, comparing a stiff hydraulic drive to the machine with a compliant hydraulic drive.

Figure 52. Igniting jet channeling torch.

Figure 53. Weakening the rock using a jet channeling torch.

Figure 54. Nozzle for flat-fan water jet.

Figure 55. Position of the nozzle relative to the drag bit.

Figure 56. Mean peak bit cutting plotted against depth of cut, with a 'flat-fan' water jet and with no water jets.

Figure 57. Mean bit cutting force plotted against depth of cut, with a 'flat-fan' water jet and with no water jets.

Figure 58. Mean peak bit penetrating force plotted against depth of cut, with a 'flat-fan' water jet and with no water jets.

Figure 59. Mean bit penetrating force plotted against depth of cut, with a 'flat-fan' water jet and with no water jets.

Figure 60. Nozzle used for 'coherent' water jets.

Figure 61. Method of mounting nozzles in the blade. White markers have been inserted into the nozzles to indicate the position of the jets relative to the bit.

Figure 62. Diagram illustrating the different positions of the water jets relative to the bit.

Figure 63. Mean peak bit cutting force plotted against depth of cut illustrating the reduction of the force required to cut the rock with 50 MPa water jets directed ahead of the bit.

Figure 64. Mean bit cutting force plotted against depth of cut illustrating the reduction of the force required to cut the rock with 50 MPa water jets directed ahead of the bit.

Figure 65. Mean peak bit penetrating force plotted against depth of cut illustrating the reduction of the force required to cut the rock with 50 MPa water jets directed ahead of the bit.

Figure 66. Mean bit penetrating force plotted against depth of cut illustrating the reduction of the force required to cut the rock with 50 MPa water jets directed ahead of the bit.

Figure 67. Mean peak bit cutting force plotted against depth of cut, illustrating the reduction of the force required to cut the rock with 10 MPa water jets directed ahead of the bit.

Figure 68. Mean bit cutting force plotted against depth of cut, illustrating the reduction of the force required to cut the rock with 10 MPa water jets directed ahead of the bit.

Figure 69. Mean peak bit penetrating force plotted against depth of cut, illustrating the reduction of the force required to cut the rock with 10 MPa water jets directed ahead of the bit.

Figure 70. Mean bit penetrating force plotted against depth of cut, illustrating the reduction of the force required to cut the rock with 10 MPa water jets directed ahead of the bit.

Figure 71. Mean peak bit cutting force plotted against depth of cut with 10 MPa water jets directed adjacent to the corners of the tungsten carbide bit inserts.

Figure 72. Mean bit cutting force plotted against depth of cut with 10 MPa water jets directed adjacent to the corners of the tungsten carbide bit inserts.

Figure 73. Mean peak bit penetrating force plotted against depth of cut with 10 MPa water jets directed adjacent to the corners of the tungsten carbide bit inserts.

Figure 74. Mean bit penetrating force plotted against depth of cut with 10 MPa water jets directed adjacent to the corners of the tungsten carbide bit inserts.

Figure 75. Photograph showing damage to a tungsten carbide bit insert when a water jet was not directed towards the insert during the cutting operation.

Figure 76. Photograph showing wear of steel bit body when a water jet was not used.

Figure 77. Diagram illustrating the influence of water jets on the side force acting on the bit.

Figure 78. Mean peak bit cutting force plotted against depth of cut, with water jets directed 10 mm ahead of the bit.

Figure 79. Mean bit cutting force plotted against depth of cut, with water jets directed 10 mm ahead of the bit.

Figure 80. Mean peak bit penetrating force plotted against depth of cut, with water jets directed 10 mm ahead of the bit.

Figure 81. Mean bit penetrating force plotted against depth of cut, with water jets directed 10 mm ahead of the bit.

Figure 82. Mean peak bit cutting force plotted against depth of cut, comparing force measurements using two water jets directed towards the bit corners with a single jet directed along the centre of the leading face of the bit.

Figure 83. Mean bit cutting force plotted against depth of cut, comparing force measurements using two water jets directed towards the bit cotners with a single jet directed along the centre of the leading face of the bit.

Figure 84. Mean peak bit penetrating force plotted against depth of cut, comparing force measurements using two water jets directed towards the bit corners with a single jet directed along the centre of the leading face of the bit.

Figure 85. Mean bit penetrating force plotted against depth of cut, comparing force measurements using two water jets directed towards the bit corners with a single jet directed along the centre of the leading face of the bit.

Figure 86. High-speed camera.

Figure 87. Diagramatic representation of discontinuous chip formation during the cutting process.

Figure 88. Stiff compression testing machine.

Figure 89. Method of mounting the bit and the rock in the testing machine for indentation experiments.

Figure 90. Diagram illustrating formation of a rock chip during indentation tests.

Figure 91. Indentation force required to form a rock chip in norite, plotted against penetration of the bit.

Figure 92. Indentation force required to form a rock chip in quartzite, plotted against penetration of the bit.

Figure 93. Indentation force required to form a rock chip behind the bit, plotted against bit penetration.

Figure 94. Geometric similarity between rock chips formed during the cutting operation and those formed during indentation tests.

Figure 95. Method by which a shear force was applied to the rock during indentation tests.

Figure 96. Section through rock specimen, illustrating the position of a rock chip relative to the bit.

Figure 97. Diagram illustrating cracks which developed as a result of the limited size of the specimen.

Figure 98. Indentation load plotted against bit penetration for the first norite specimen.

Figure 99. Indentation load plotted against bit penetration for the second norite specimen.

Figure 100. Indentation load plotted against bit penetration for the first quartzite specimen.

Figure 101. Indentation load plotted against bit penetration for the second quartzite specimen.

Figure 102. Photo-micrograph of a section through the first norite specimen.

Figure 103. Photo-micrograph of a section through the second norite specimen.

Figure 104. Photo-micrograph of a section through the first quartzite specimen.

Figure 105. Photo-micrograph of a section through the second quartzite specimen.

Figure 106. Mohr envelope plotted for norite rock specimens.

Figure 107. Diagram illustrating the criterion used to determine the state of stress at points in the rock underneath an indentor.

Figure 108. Evidence of rock fracture parallel to the direction of the maximum principal stress, illustrated by slabbing on the sidewalls of a tunnel.

Figure 109. Nomenclature for calculations of the stress induced in an elastic body when a punch is applied to the surface of the body.

Figure 110. Stress contours σ_{xx} when a normal pressure 1 050 MPa is applied to the surface of the body.

Figure 111. Stress contours σ_{yy} when a normal pressure 1 050 MPa is applied to the surface of the body.

Figure 112. Stress contours τ_{xy} when a normal pressure 1 050 MPa is applied to the surface of the body.

Figure 113. Stress contours σ_1 (maximum principal stress) when a normal pressure 1 050 MPa is applied to the surface of the body.

Figure 114. Stress contours σ_3 (minimum principal stress) when a normal pressure 1 050 MPa is applied to the surface of the body.

Figure 115. Stress contours τ_{max} (maximum shear stress) when a normal pressure 1 050 MPa is applied to the surface of the body.

Figure 116. Stress contours σ_{xx} when both a normal pressure 1 050 MPa and a shear pressure 700 MPa are applied to the surface of the body.

Figure 117. Stress contours σ_{yy} when both a normal pressure 1 050 MPa and a shear pressure 700 MPa are applied to the surface of the body.

Figure 118. Stress contours τ_{xy} when both a normal pressure 1 050 and a shear pressure 700 MPa are applied to the surface of the body.

Figure 119. Stress contours σ_1 when both a normal pressure 1 050 MPa and a shear pressure 700 MPa are applied to the surface of the body.

Figure 120. Stress contours σ_1 when both a normal pressure 1 050 and a shear pressure 700 MPa are applied to the surface of the body.

Figure 121. Stress contours τ_{max} when both a normal pressure 1 050 MPa and a shear pressure 700 MPa are applied to the surface of the body.

Figure 122. Stress contours σ_1 when both a normal pressure 760 MPa and a shear pressure 700 MPa are applied to the surface of the body.

Figure 123. Stress contours τ_{max} when both a normal pressure 760 MPa and a shear pressure 700 MPa are applied to the surface of the body.

Figure 124. Stress contours σ_1 when a normal pressure 2 000 MPa is applied to the surface of the body.

Figure 125. Stress contours τ_{max} when a normal pressure 2 000 MPa is applied to the surface of the body.

Figure 126. Stress contours σ_1 when both a normal pressure 1 430 MPa and a shear pressure 240 MPa are applied to the surface of the body.

Figure 127. Stress contours τ_{max} when both a normal pressure 1 430 MPa and a shear pressure 240 MPa are applied to the surface of the body.

Figure 128. Zone of excess stress when both a normal pressure 1 050 MPa and a shear pressure 700 MPa are applied to the surface of the body.

Figure 129. Zone of excess stress when both a normal pressure 760 MPa and a shear pressure 700 MPa are applied to the surface of the body.

Figure 130. Zone of excess stress when a normal pressure 2 000 MPa is applied to the surface of the body.

Figure 131. Zone of excess stress when both a normal pressure 1 430 MPa and a shear pressure 240 MPa are applied to the surface of the body.

Figure 132. Stress trajectories when a normal pressure only is applied to the surface of the body.

Figure 133. Stress trajectories when both a normal pressure and a shear pressure are applied to the surface of the body.

Figure 134. Press used for indentation tests with high pressure water jets.

Figure 135. Drag bits with nozzles for high pressure water jets built in to the steel bit body.

Figure 136. Method of mounting bit and rock specimen in the press prior to conducting indentation tests assisted by water jets.

Figure 1.1 (a) Instrumentation of the test frame used for experiments cutting rock.

Figure 1.1 (b) Block diagram of instrumentation.

Figure 1.2 Pre-amplifier and bridge supply for test frame instrumentation.

Figure 1.3 Peak-level detector circuit diagram.

Figure 1.4 Low-pass filter diagram.

Figure 1.5 Differentiator circuit diagram.

Figure 2.1 Calibration of 300 kN hydraulic jack.

Figure 2.2 Calibration of test frame load cells in the direction of cutting.

Figure 2.3 Calibration of test frame load cells normal to the cutting direction.

Figure 2.4 Calibration of test frame load cells orthogonal to the cutting and normal directions.

Figure 2.5 Thermocouple calibrations.

Figure 4.1 (a) Program used for stress contour plots.

Figure 4.1 (b) Program used for stress contour plots.

Figure 4.2 An example of the computer plot of stress contours.

Figure 4.3 Computer program used for calculation of zones of excess stress.

CHAPTER I

1. INTRODUCTION

1.1 General

The Chamber of Mines Mining Technology Laboratory is engaged in a number of projects aimed at mechanising stoping operations on the gold mines of the Witwatersrand. The project which has received the most attention is "rockcutting", using drag bits to cut a slot in close proximity to the gold reef. Pilot production trials to assess the mining potential of a number of rockcutting machines operating in the underground environment on a long term basis, were commenced in 1973.

The study described in this thesis, which was started at the beginning of 1974, was undertaken to improve the performance of drag bits used for cutting hard rock.

1.2 Geological Background of the Witwatersrand gold deposits

The Witwatersrand gold deposits and its associated host rocks belong to the Witwatersrand System, (Stokes 1961). This System consists of a succession of arenaceous and argillaceous rocks deposited in a sedimentary basin with a periphery measuring some 800 kilometres, (Borchers 1961). The dominant rock-types of the Witwatersrand System are alternations of shales, quartzites, grits and conglomerates. The gold deposits are found at some of these conglomerate horizons and are known as "reefs". The thickness of the gold reefs varies from a few metres down to a few millimetres and much of the ore currently being mined is from narrow reefs,

typically of the order of a few centimetres thick.

Some of reefs outcrop, and this led to the original discovery of the conglomerate gold deposits in Johannesburg. These shallow deposits, however, are largely worked out and the majority of the gold mined today is from reefs which sub-outcrop at depth. With the exception of the Evander Goldfield where mining takes place at relatively shallow levels, the average depth of the workings on many of the mines is approximately 2 000 metres. Western Deep Levels, the deepest mine in the world, is currently mining at 3 500 metres below surface.

The quartzites and conglomerates in these deposits are strong, highly abrasive rocks and typically the uniaxial compressive strength varies between 150 MPa and 300 MPa while the quartz content falls in the range from 30 per cent up to 98 per cent. The rocks in the deposit are layered, being separated by planes of weakness which run approximately parallel to the plane of the reef and are known as parting planes. Weak shales, varying in thickness from a few millimetres to a few centimetres, are found often along these parting planes.

1.3 Motivation for selective mining

Current mining practice in the South African gold mines is extraction of the reef from underground stopes using the drill and blast technique. A minimum working height of approximately one metre is necessary in the stopes and thus, with blasting, massive dilution of the ore by country rock occurs in the narrow reefs, which account for at least 50 per cent of the known reserves

(Jager 1976).

A study was conducted by Cook et al (1969) to investigate potential improvements in the mining operations on deep-level South African gold mines which would enhance the profitability of these mines. A hypothetical gold mine of the Witwatersrand System was considered and improvements were based on possible developments in mining technology. Marginal improvements in the rate of financial return on investment were computed when realistic reductions in the time or capital expenditure required to reach full production were estimated. Also, possible reductions in the working costs or improvements in labour productivity indicated only small financial gains. In contrast, a marked increase in the rate of return was demonstrated for the case whereby the tonnage trammed from the stope was halved. A further substantial improvement of the financial return was calculated for the situation where the tramming width was reduced by a factor of two and to compensate, so that the volume of rock milled was not decreased, the rate of mining was doubled.

One proposal for halving the tramming width for increased profitability of the gold mines, was to develop a [illegible] cutting the rock, as opposed to blasting, to enable manual separation of reef from the waste rock. In such a system the reef would be trammed from the stope and the country rock packed into a stone wall behind the working face as roof support.

In addition to the calculated economic advantages of selective mining, it was claimed that a number of technological benefits would be realised. The most important of these would be derived from the

packing of the waste area. This would improve the strata control by reducing the effective stoping width and therefore, the amount of gravitational energy released per unit area mined would be proportionally reduced. This parameter has been shown by Joughin (1966), and other workers to be of great importance in minimising rockbursts. Stonewall packing also would reduce the heat pick-up and consequently the ventilation requirements, since by waste filling of the worked out regions the exposed surface area, from which heat could be radiated, would be decreased substantially. In addition all of the ventilation air would be channelled through the working places, which would also reduce the volume of air required.

The results of this report (Cook et al, 1969), prompted the Chamber of Mines to investigate in detail the feasibility of developing a selective mining system by employing a method of cutting the rock.

1.4 Choice of a selective mining system

1.4.1 Rockbreaking considerations

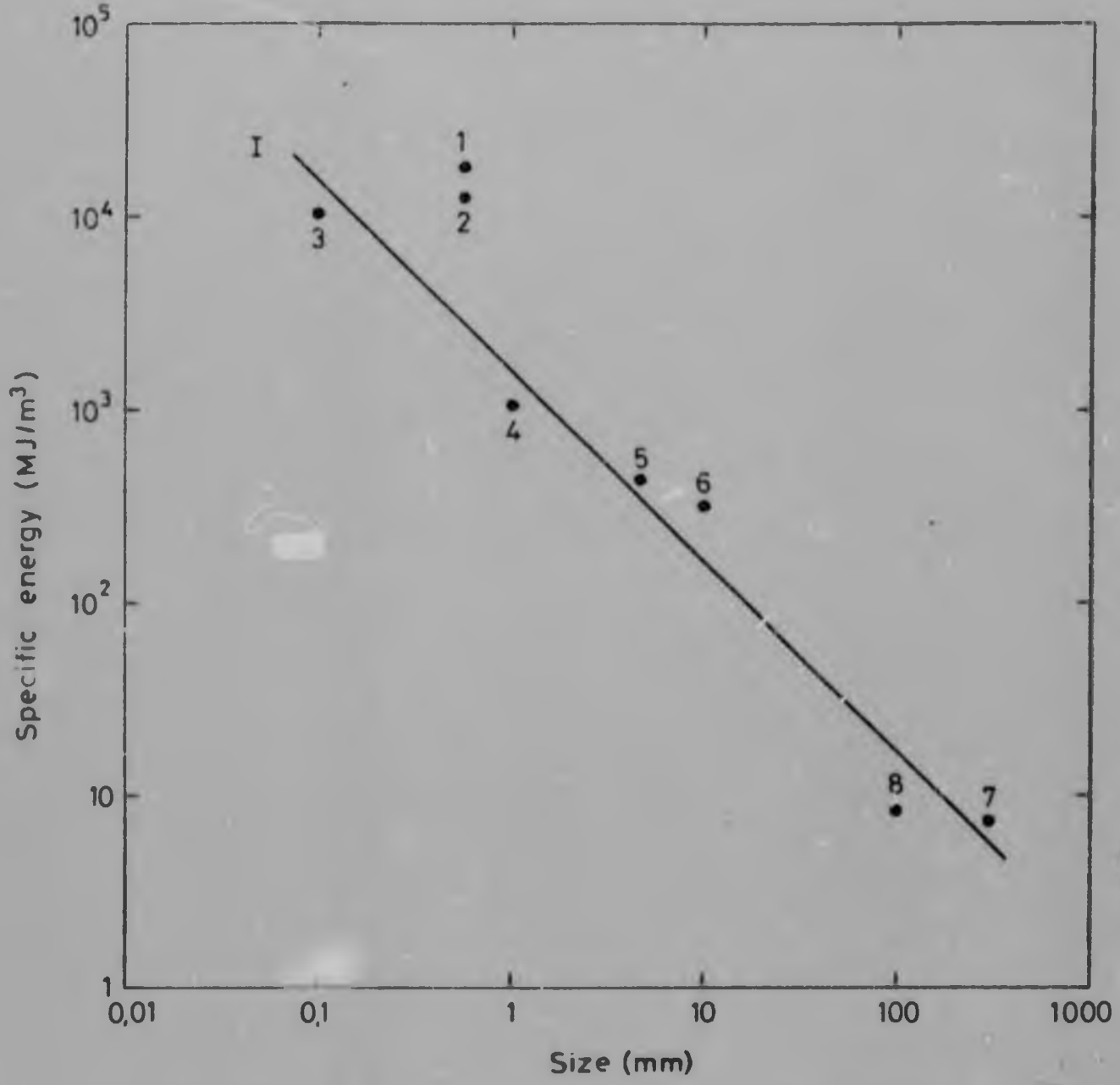
In order to enable a method of cutting rock to be chosen, a measure of the effectiveness of the available rockbreaking techniques is required. One method of measuring the efficiency of a rockbreaking process is to consider the energy required to break a unit volume of rock. This is defined as the specific energy. Rittinger (1867), demonstrated that the specific energy required to fracture rock is inversely proportional to the size of the rock particles produced. The results of a study by Cook and Joughin (1970), where different primary rockbreaking techniques in rocks of

similar uniaxial compressive strength were compared with the size of particles produced, is illustrated in Figure 1. A section of the conclusions contained in this study noted that the relative efficiency of the breakage methods, measured in terms of the specific energy, is fairly constant. Thus in order to minimise the total energy requirement, the only effective method is to minimise production of small rock fragments.

In another report (Cook et al, 1968), it was argued that from considerations of specific energy, a mechanical method of rock excavation would offer the most immediate prospect for success in the search for a selective mining method. The authors conducted laboratory experiments to assess the cuttability of Witwatersrand quartzite. A strain-gauge instrumented tungsten carbide tipped drag bit was used to cut slots in quartzite blocks and force measurements were made during the cutting operation. These tests showed that tungsten carbide drag bits could cut this strong, abrasive rock at a rate which, when converted for the mining situation, would give an acceptable rate of mining. The wear of the bits was found not to be prohibitive, but it was recognised that the design of any machine that would use this type of bit underground, should make allowance for the bits to be changed easily.

1.4.2 Rockcutting system

Following these laboratory tests (Cook et al, 1968), a mining system was proposed where drag bits would be used to cut two slots in the stope face, one immediately above and the other below the reef. The machine then would be moved to an adjoining panel and



1. Jet piercing
2. Erosion drilling
3. Diamond cutting
4. Percussive drilling
5. Drag-bit cutting
6. Roller bit boring
7. Impact-driven wedge
8. Explosives

(after Cook and Joughin, 1970.)

FIGURE 1. Specific energy of rockbreaking as a function of mineral particle size for processes of excavation.

other workers would break out the rock between the two slots and remove it from the stope. The waste rock then could be removed and packed in convenient size blocks in the worked out area. It was proposed to u[illegible]pact-driven wedges to assist with these operations to remove the ro[illegible] from the stope face. The rock-slotting operation was termed rockcutt[illegible]g and the rock removal using impact-drive wedges was termed secondary breaking.

1.5 Development of rockcutting mach[illegible]es

A prototype rockcutting machine designed to work in underground stopes was manufactured. The cutting action of this prototype, illustrated in Figure 2, used a drag bit mounted on a toolblade which in turn was attached to a slide, or saddle, by a feedscrew. The bit was traversed through the rock by activating a hydraulic ram which moved the saddle along the fixed guide. The bit was advanced into the rock by turning the feedscrew. The anchors at each end of the machine were hydraulic jacks which were extended to support the hangingwall and footwall (roof and floor) of the stope. A detailed account of the concepts and principles involved in the design and operation of this prototype rockcutting machine, much of which applies to the modern machines, is found in the paper by Hojem et al,(1971).

Operation of this prototype rockcutter demonstrated that the basic mining concept of cutting slots in close proximity to the reef and breaking the rock from the face into the slot using drills and wedges was feasible. To assist with the development of machines which would operate efficiently and reliably in the hostile deep-level mining environment, the Chamber of Mines entered into develop-

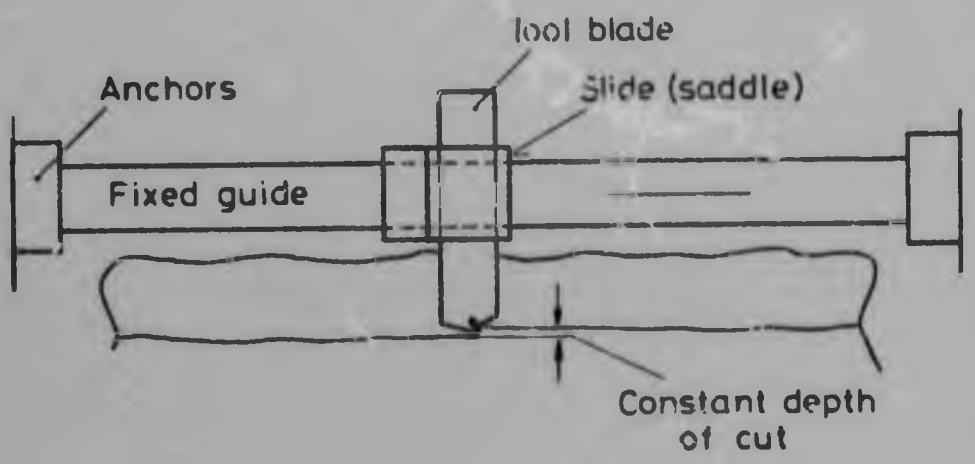


FIGURE 2 : Diagramatic representation of a rockcutting machine.

ment contracts with three manufacturers and a series of prototype rockcutters was produced. This programme continued for two years with ancilliary equipment such as hydraulic power packs, a plug-in electrical system, conveyors and secondary rockbreakers being developed in parallel with the rockcutting machines. By the end of 1972 a total of about 10 000 centares had been mined by rockcutting machines at various underground test sites, (Joughin, 1976).

1.6 Pilot production trials of mining by rockcutting

The successful results achieved by the prototype rockcutting machines during underground tests, encouraged the Chamber of Mines during 1973 to initiate two separate trials at Doornfontein and Stilfontein Gold Mines, using two series of rockcutting machines built to two standard designs. The main objective of these trials was to establish whether the stope tramming width could be halved consistently over a long period of time, using a mining system based on rockcutting machines and by packing the waste rock in the worked out area. If this objective was achieved, the cost effectiveness of the rockcutting system was to be assessed.

Major differences in the depth of operation and geological conditions existed between the two rockcutting sites. The Doornfontein trial site was at a depth of approximately 2,4 kilometres and the face length was about 250 metres. The rate of energy release in the stope, which affects the extent of fracturing of the rock at the working face, varied from 10 MJ/centare to 35 MJ/centare . The rock above the reef was a very hard, glassy quartzite and that below it was a slightly argillaceous quartzite of medium hardness.

At Stilfontein the trial site was at a depth of 1,5 kilometres, the face length was 200 metres and the average rate of energy release in the stope was 5,6 MJ/centare. Above the reef the rock was a soft argillaceous quartzite, while the rock below the reef was a slightly argillaceous quartzite. An important part of the experiment was to assess how these different geological and rock stress conditions affected the rockcutting operations.

A review of the progress of the pilot production trials with rockcutting machines after approximately one year of operation, demonstrated that the eighteen machines at the two trial sites had succeeded in halving the stope tramming width, (Joughin, 1974). Detailed analysis of the stoping costs revealed that the rockcutting costs were only slightly higher than stoping costs with conventional mining. Since stoping costs represent only between a quarter and a third of the total working costs on most gold mines (Joughin, 1974), a small increase is not significant when compared to the substantial improvement of the financial return which is realised by a mining system with the stope tramming width halved, (Section 1.3).

Because of the depth at which these trials were conducted, the stress on the stope face generally exceeded the compressive strength of the rock and therefore the rock on the face was fractured. It was found during these trials that because the rock was in this fractured condition, the reef was readily removed from the face when only one slot was cut in close proximity to the reef. Consequently the mining operation was carried out cutting one slot only.

Both the extent of fracturing of the rock and the strength of the rock were found to be important parameters which influenced the rate of cutting and rate of wear of the bits.

Following this review of progress in mid-1974 the trial site at Stilfontein Gold Mine was closed. For this reason, the tests conducted underground during the research programme described in this thesis were all carried out at Doornfontein Gold Mine.

CHAPTER II

2. PREVIOUS WORK WITH DRAG BITS

Drag bits are widely used in weak to medium strength rock-cutting applications; for example, virtually all coal getting machines and many coal roadheading machines use a form of drag bit as a cutting tool. The mechanics of penetration of drag bits into the weak and medium strength strata has been the subject of extensive studies. Laboratory and field experiments which defined basic principles for the efficient cutting of coal have been outlined by Evans (1962), Pomeroy (1968), and Pomeroy and Brown (1968), amongst other workers. Experiments using drag bits for cutting other relatively low strength rocks have been conducted by Roxborough (1973), Roxborough and Rispin (1973), and Hewitt (1975). Two of the most important theories of the mechanism of rock fracture caused by drag bits were proposed by Evans (1962), for brittle materials and by Potts and Shuttleworth (1958), for elastic-plastic materials. This latter theory was a development of the Ernst - Merchant theory of metal cutting (1945). Both of these theories assume that a bit with a wedge shape is used to penetrate the material.

The conventional design of drag bit which is used to cut in the weaker rock types is wedge shaped, (Figure 3). These bits are provided with a clearance angle underneath the bit to minimise the area of contact between the tool and the rock. The usual design of bit is with a zero or a positive rake angle, that is, the bit included angle plus the bit clearance angle is equal to or less than ninety degrees (Figure 3), (Roxborough, 1973).

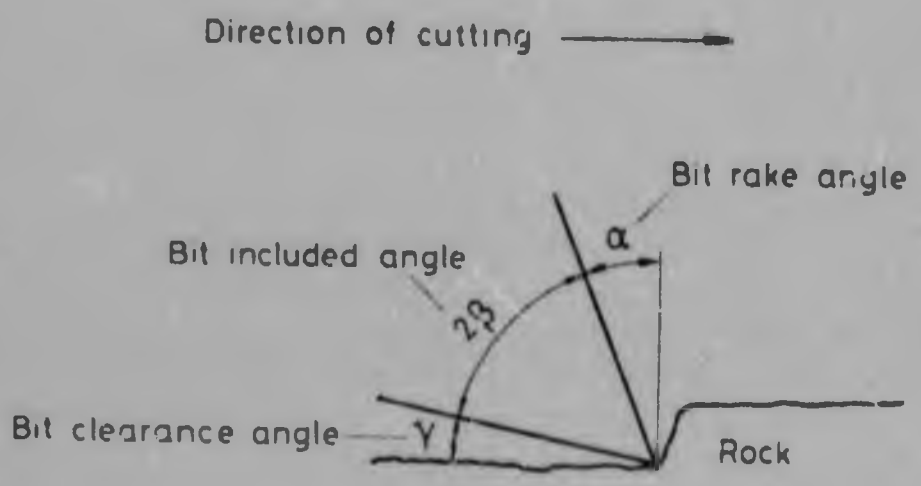


FIGURE 3 : Diagramatic representation of a wedge shaped drag bit.

2.1 Evans model

Witwatersrand quartzite behaves as an elastic-brittle material (Wagner and Schümann, 1971), therefore it is instructive to examine the fracture theory proposed by Evans, (1962). This author considered a sharp wedge with an included angle 2θ which was pressed into a brittle material with an applied force P. The wedge was applied close to a right-angled corner in the material and it was assumed that failure of the material occurred due to a tensile crack which developed along a line c - d, (Figure 4). Thus, a diagram of the forces acting in this model show that :

(i) A reaction force R^1 is applied to the material by the wedge, normal to the face of the wedge.

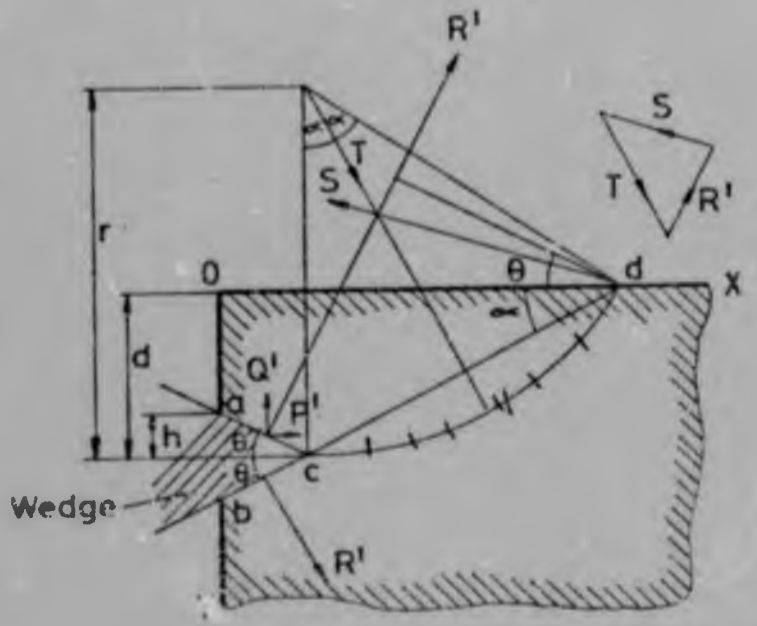
(ii) A resultant of the tensile forces that acted perpendicular to c - d. This was termed T.

(iii) A third force is required to maintain limiting equilibrium in the material. It was shown by experiment that the chip that formed tended to rotate about point d. Thus a force S was assumed, acting through the point d, (Figure 4).

Two further assumptions were made in the development of the simplified theory :

(a) That there was zero friction between the wedge and the brittle material.

(b) That the depth of penetration by the wedge into the material was negligible when compared with the depth of cut d. Thus $h \ll d$.



(after Evans, 1962.)

FIGURE 4 : Sketch showing a wedge pressed into a brittle material, (after Evans, 1962).

Then by taking moments about point d and using a minimum work hypothesis, Evans derived the equation

$$P = \frac{2\,td\sin\theta}{1-\sin\theta}$$

where t is the tensile strength of the material.
The variation of P with friction was calculated by assuming an angle of friction ϕ between the wedge and the brittle material, then

$$P = \frac{2\,td\sin(\theta+\phi)}{1-\sin(\theta+\phi)}$$

Evans, (1962) conducted experiments cutting in two different types of coal, and the forces that were measured correlated well with this theory.

2.2 Drag bits used to cut in strong rocks

When the uniaxial compressive strength of rock exceeds 100 MPa the rock may be defined as strong. Because of high rates of wear and breakage, drag bits have found little application in situations where it is required to cut strong rock. Consequently the majority of strong rock machining is carried out using some form of roller cutter, these generally have a lower instantaneous cutting rate than drag bits and the unit cost of this type of cutter is much higher. However, they do achieve an acceptable life, in terms of the amount of rock cut before the cutter is discarded. One of the few applications in current practice where drag bits are used to cut strong rocks is in rotary drilling applications.

A review of the fracture mechanisms resulting from the various methods of drilling, including rotary drilling, was presented by

Maurer, (1966).

In this review it was stated that different authors had found that the factors which affected the forces acting on the bit during the cutting operation were :

(i) Depth of cut (defined as the advance per stroke of the bit).

(ii) Bit rake angle.

(iii) Extent of bluntness of the bit.

(iv) Type of rock.

A 'full-face' tunnelling machine and a small machine 'a mini full-facer', manufactured by a Swedish company, employs drag bits mounted on rotary heads which machine the rock using an under-cutting principle, (Parendsen, 1970). Little detailed information relating to bits had been published by this company for reasons of commercial competition. These Swedish machines, together with the rockcutting machines produced by manufacturers in collaboration with the Chamber of Mines, are the only examples of equipment which have been built in order to cut strong rocks with drag bits and have been subjected to extensive field trials.

Thus, throughout the world, little work has been carried out in this field, and where studies have been made, generally these have been sponsored by commercial organisations and the results have not been published.

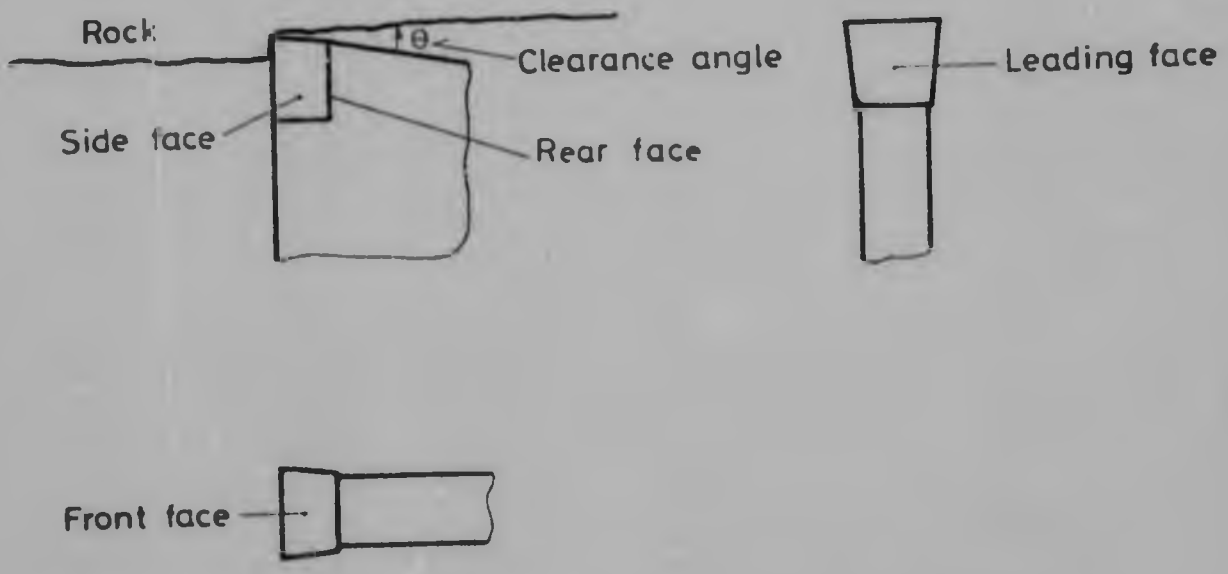
2.2.1 Studies conducted by the Chamber of Mines

The basic parameters affecting drag bits which are used to cut in strong rock, have been studied by previous research workers at the Chamber of Mines. Much of this work has remained unpublished. The early experiments, using tungsten carbide tipped tools to cut in quartzite, demonstrated that the wear of the tungsten carbide was related to a critical cutting speed. The rate of wear of the bits was found to be almost independent of the cutting speed below this critical value, but at greater speeds the bit wear increased suddenly, (Cook et al, 1968). It was deduced that drag bits could only be used to cut strong, siliceous rock at relatively low cutting speeds.

The original design of bits used for the early experimental programme with rockcutting machines is illustrated in Figure 5a, (Hojem et al, 1971). The tungsten carbide insert with zero rake angle was brazed into a notch in the steel bit body. Clearance angles were provided in the insert on the front and side faces of the insert. The early experiments carried out at the Chamber of Mines showed that when cutting strong abrasive quartzites a high rate of wear of the tungsten carbide inserts was experienced. Thus, after only a few traverses of the rock by the bit, the front face of the tool had worn to form a flat and the tool effectively was blunt. It was recognised that the bits would have to operate in a blunt condition and the bit design was modified so that the clearance angle behind the face of the bit became zero. The area of this front face of the bit that was in contact with the rock was termed the bit wearflat, (Figure 5b).

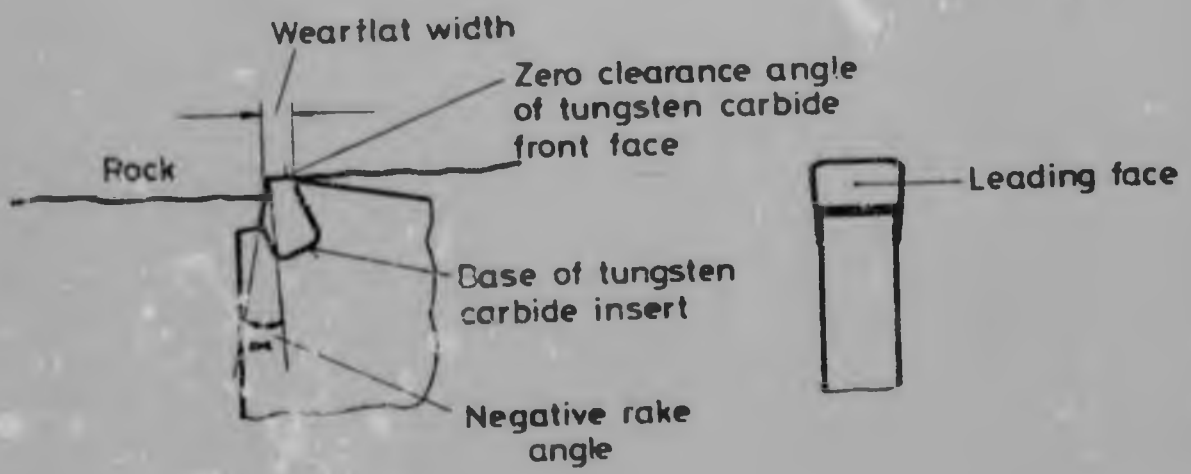
These experiments showed also, that the tungsten carbide bit inserts cracked along the rear face of the inserts, (Figure 5a). These cracks were attributed to the high penetrating force generated during the cutting operation which induced tensile stresses in the tungsten carbide insert since the leading face of the insert was not supported. Another major cause of failure of these bits was at the braze joint, where the tungsten carbide broke away completely from the steel bit body. This type of failure occurred either during the return stroke, when the tungsten carbide fouled the rock which put the braze in tension, or when excessive sideloads were applied to the insert causing the braze joint to shear.

Additional experiments showed that tungsten carbide bit inserts had a tendency to flake pieces from the leading face of the bit when a positive rake angle or a zero rake angle was employed. In order to overcome these various weaknesses, the bit was redesigned, (Figure 5b). The tungsten carbide insert was angled to resist the resultant force on the bit through the base of the insert. A negative rake angle was adopted to increase the strength of the leading face of tungsten carbide. The front of the insert was buttressed by the steel bit holder in order to reduce tensile stresses along the rear face of the tungsten carbide. In addition this increased the braze area which enhanced the strength of the braze joint. The typical modes of bit failure that had been experienced with the original design of bit were successfully eliminated by these modifications. Therefore in order for drag bits to work successfully in strong rocks, three main conclusions were drawn, these were :



Original design of rockcutting bit

(a)



Modified design of rockcutting bit

(b)

FIGURE 5. a) Original design of rockcutting bit.
b) Modified design of rockcutting bit.

(i) The bits must operate at relatively low cutting speeds.

(ii) Because of the high loads imposed on the bits, a negative rake angle is necessary to give sufficient strength.

(iii) As a result of high rates of wear of the tungsten carbide inserts, the bits must be able to cut when no clearance angle is provided on the front face of the bit.

2.2.2. Investigations with blunt bits

Previous experimentation concerned with drag bit cutting or rotary drilling conducted by other workers, has concentrated largely on the mechanism of rock breakage assuming that sharp bits are used to cut the rock. In order to reflect more closely the performance of actual bits in the mining situation, Fairhurst and Lacabanne (1957), made a study of a blunt, rotary drilling drag bit, (Figure 6). In this work the authors propose that the forces acting on the bit are :

Thrust force = $p.a$

Torque force = (Cutting forces) + $\mu.p.a$

where 'a' is the area of the bit wearflat

'p' is the contact pressure underneath the bit and

'μ' is the coefficient of friction between the bit and the rock.

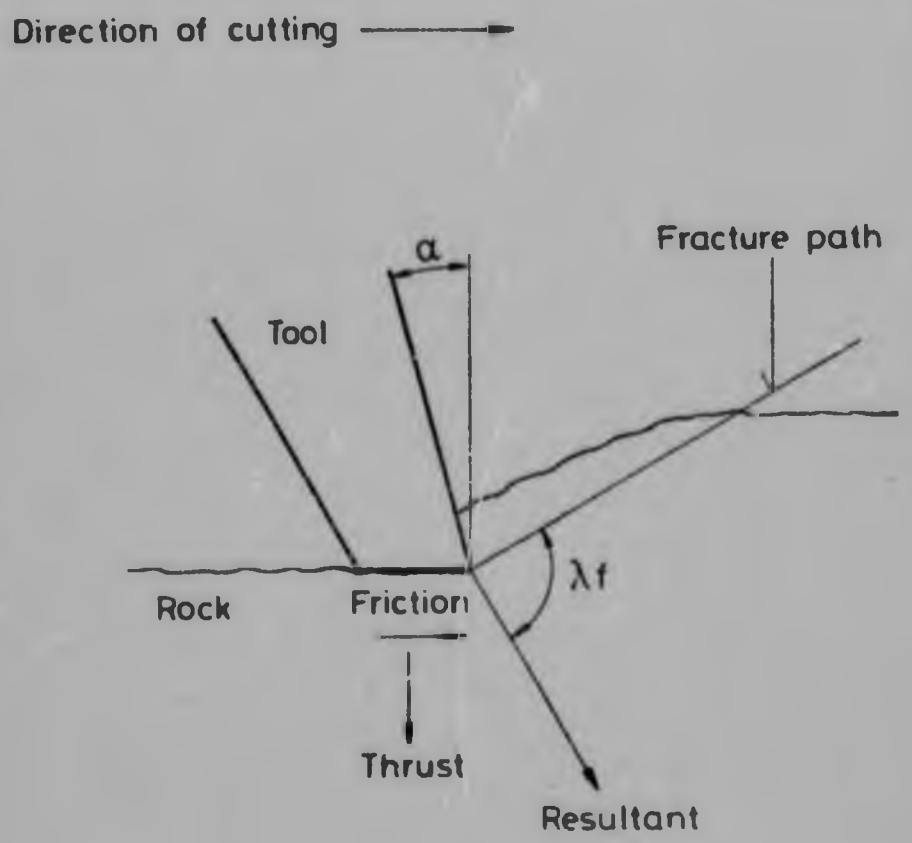


FIGURE 6 : A blunt rotary drilling drag bit (after Fairhurst and Lacabanne, 1957).

In addition it was proposed that the thrust is directly proportional to the contact area and the torque remains only partly affected. It was suggested by these authors that the angle of the resultant force applied to the bit during the cutting operation was affected by the bit rake angle. They postulated that fracture occurs at some constant angle with the resultant force, (Figure 6). Thus a change of the bit rake angle would alter the angle of the resultant force. This in turn would cause the length of the fracture path to vary (Figure 6), and affect the forces to cause the rock to fracture.

Using a modification of his original theory (Evans 1962), Evans derived equations to calculate the cutting force required to cut coal with blunt wedges, (Evans, 1965). No explaration of the high normal forces that were measured during experiments cutting coal with blunt wedges was given in this paper.

The parameters relating to the geometry of the bits which affect the forces acting on blunt bits when cutting in strong rocks, were defined by Riemann (1974). A number of different rock types were used by this author during the course of his investigations, but most of the experimental work was carried out using blocks of Witwatersrand quartzite and norite. The uniaxial compressive strength of these two rock types is similar, but whereas the former is highly abrasive, the latter has a very low quartz content and consequently has low abrasive qualities, (Section 4.1.1).

Riemann (1974) conducted experiments where he resolved the resultant force acting on the bit during the cutting operation into two components, a force in the direction of cutting, called the bit

cutting force, and the force normal to this direction, called the bit penetrating force, (Figure 7). The results obtained by Riemann showed that values of the bit penetrating force were significantly higher than those of the bit cutting force. This result was directly the opposite of measurements taken when cutting in weaker rock types using wedge shaped bits, where the bit cutting force was greater than the normal or penetrating force. (Evans, 1965). When using a nineteen millimetres thick tungsten carbide tipped tool to make a cut six millimetres deep in strong quartzite, Riemann (1974), found that typical mean values of these forces were :

penetrating force	130 kN and
cutting force	80 kN.

The results from Riemann's experiments showed that :-

(i) A large increase in the thickness of the bits required a relatively small increase in the applied bit force. This result contradicts the findings of Fairhurst and Lacabanne (1957), and indicates that the fracture mechanism when cutting in strong rocks such as Witwatersrand quartzites, may be substantially different to the mechanism when cutting in weaker rock types.

(ii) The width of the bit wearflat, (Figure 5b), was shown to affect significantly the forces acting on the bit.

(iii) The bit rake angle was varied within a wide range, from plus twenty degrees to minus twenty degrees, and changes of this parameter were found not to affect the bit forces.

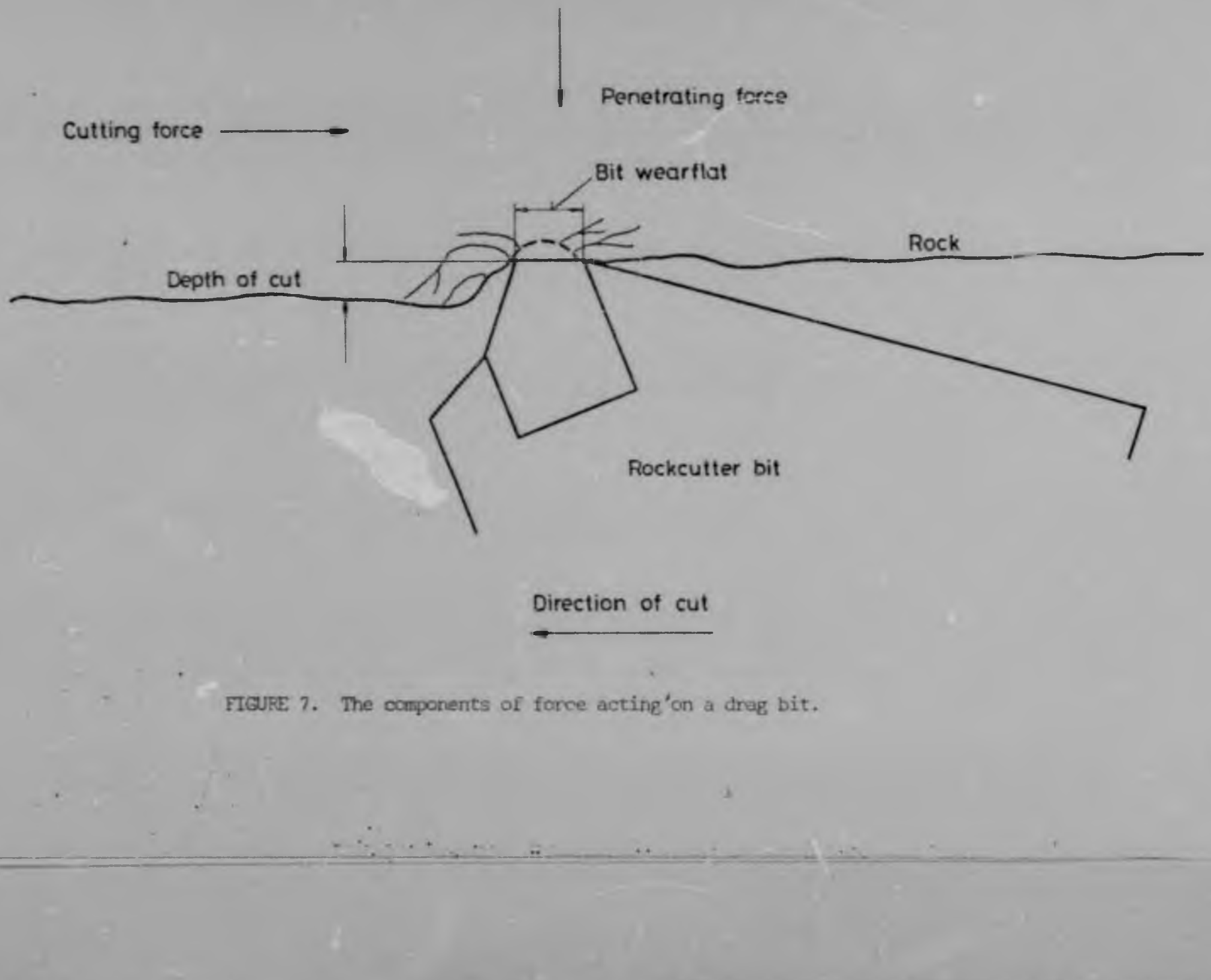


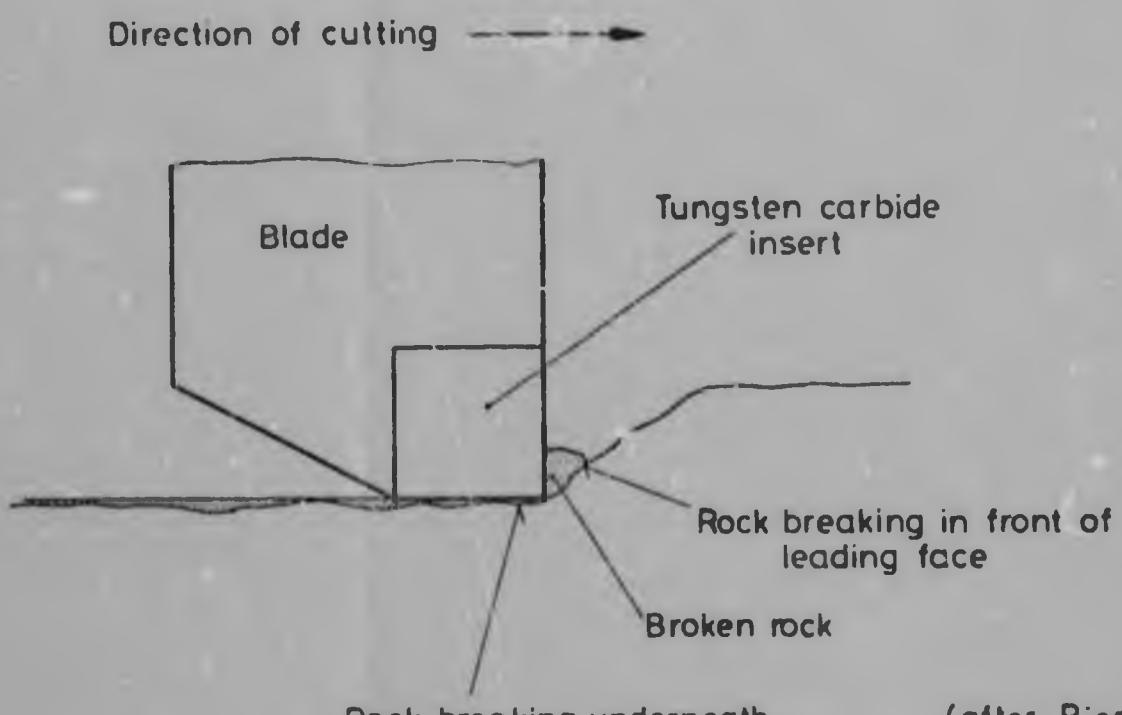
FIGURE 7. The components of force acting on a drag bit.

This finding is in marked contrast to experiments that have been conducted cutting in coal and other weak rock types (Whittaker, 1967) (Evans, 1962) (Evans, 1965), where the bit rake angle has been shown to be one of the most important parameters which influence the design of bits.

Riemann concluded that the fracture mechanism which had been suggested by Evans (1962) and other workers for cutting weak rocks with drag bits did not apply for strong rock situations. He proposed that in the strong rock types, fracture was initiated underneath the bit wearflat and that cracks formed in this region caused the rock to spall ahead of the leading face of the bit. Therefore, it was suggested that the reason the bit angle was found not to influence the bit forces during the cutting operation was because the leading face of the bit usually was not in contact with the rock, (Figure 8).

2.3 The development of bits for the pilot production trials

In order to be economically viable in the mining situation, research workers at the Chamber of Mines calculated that the area of the slot cut by each bit would need to average three centares, (square metres). Therefore, during the period when prototype machines were being developed (Section 1.5), an experimental programme was carried out by these workers to develop the bits in order to achieve this required bit life. Details of these experiments were not published, but the reasons for undertaking certain tests, the test programme and a summary of the results are described in this Section.



E 8. Diagram illustrating method of rock fracture using a blunt drag bit to cut hard rock.

A number of different materials which could be used as the cutting element were assessed. Diamond was rejected on ground of cost; it was estimated that the cost of bits which utilised diamonds as the cutting element would exceed the cost of bits that used cemented tungsten carbide by approximately two orders of magnitude. Ceramics were considered too brittle for use in rock cutting situations. Titanium carbide, which is a surface coating applied to tungsten carbide and which has shown advantages in metal cutting applications, is not used for cutting rock as this causes the surface layer of the tool to be eroded rapidly. Therefore,cemented tungsten carbide was selected as the only practical material to use for the cutting element and experiments were directed towards finding the grade of tungsten carbide which would give optimum performance in terms of low rates of wear and low incidence of brittle fracture. A large number of different grades of tungsten carbide were investigated systematically at various underground test sites. The results of these tests showed that a tungsten carbide grade normally used for percussive drilling with approximately 9 per cent cobalt gave the best overall performance. Cobalt acts as the matrix for the tungsten carbide grains. When the cobalt fraction was reduced below 9 per cent, brittle fracture of the tungsten carbide was found to take place; when the fraction was increased above 9 per cent, plastic deformation of this cutting element occurred.

Fixing the tungsten carbide element to a holder by mechanical means was considered impractical in the mining environment and since brazing of tungsten carbide to steel holders is common practice for rock drill bits, attention was paid to the choice of a strong braze metal. The most frequent cause of premature removal of the

bits from service during this test programme was because of failure of the bit braze joint. Therefore considerable attention was paid to this problem and a large number of different braze metals were tested. The thickness of the braze joint was examined also, to optimise the strength of this joint. These experiments were carried out systematically at underground test sites using a large number of bits for each different parameter that was being investigated. From the many different types of braze metals that were tested, the most successful was a compound material consisting of a silver solder braze with copper layers. This had a relatively low melting temperature, about 680 degrees Celsius, and a fairly thick braze joint, about 0,5 millimetres.

It was considered necessary for the steel bit body to have the following properties :

(i) High strength in the vicinity of the tungsten carbide cutting element. Riemann's experiments (1974), (Section 2.2.2), had shown that high forces were applied to this element during the cutting operation and adequate steel strength was required in this region adjacent to the tungsten carbide to prevent the steel from exceeding its yield point and deforming plastically.

(ii) Resistance to impact loading. Riemann (1974), showed that the mechanism of rock breakage caused the bit to travel through the rock with a 'slip-stick' motion. This could induce impulsive forces at the bit and it was necessary for the steel bit body to withstand these forces.

A grade of steel that satisfied these requirements was En 30 B. This is an air-hardening steel with high-harderability due to its molybdenum content, and therefore, provided the bit was heated to above the temperature required to form martensite, it would be hardened locally around the tungsten carbide cutting element during the brazing operation. Also, En 30 B is an alloy steel with a high nickle content, about 4,25 per cent, and this gives it good 'toughness' characteristics. A further property of this grade of steel is that little distortion takes place during the heat treatment process because one of the alloying elements, silicon, reduces the expansion during the phase from austenite to martensite (Rollason, 1968). This low distortion would minimise the stress that may be applied to the tungsten carbide during the brazing operation. For these reasons En 30 B is widely used by different manufacturers for applications where it is required to braze a tungsten carbide cutting element to a steel bit body. Consequently no experiments were conducted with other types of steel for the cutting bits.

Therefore, the design of bit development for the start of the pilot production trials, employed a tungsten carbide insert twenty three millimetres thick, with a wearflat width of six millimetres when the bit was new. The insert, with a twenty degrees negative rake angle, was brazed into the bit body so that the resultant force vector was normal to the base of the insert, (Figure 5b). A silver-solder braze metal was used and the thickness of the braze joint was 0,5 millimetres. The steel bit body was machined with a "V" cross-section which mated with a 'socket' machined in the blade, (Figure 9). The bit was fitted into this 'blade pocket' and was

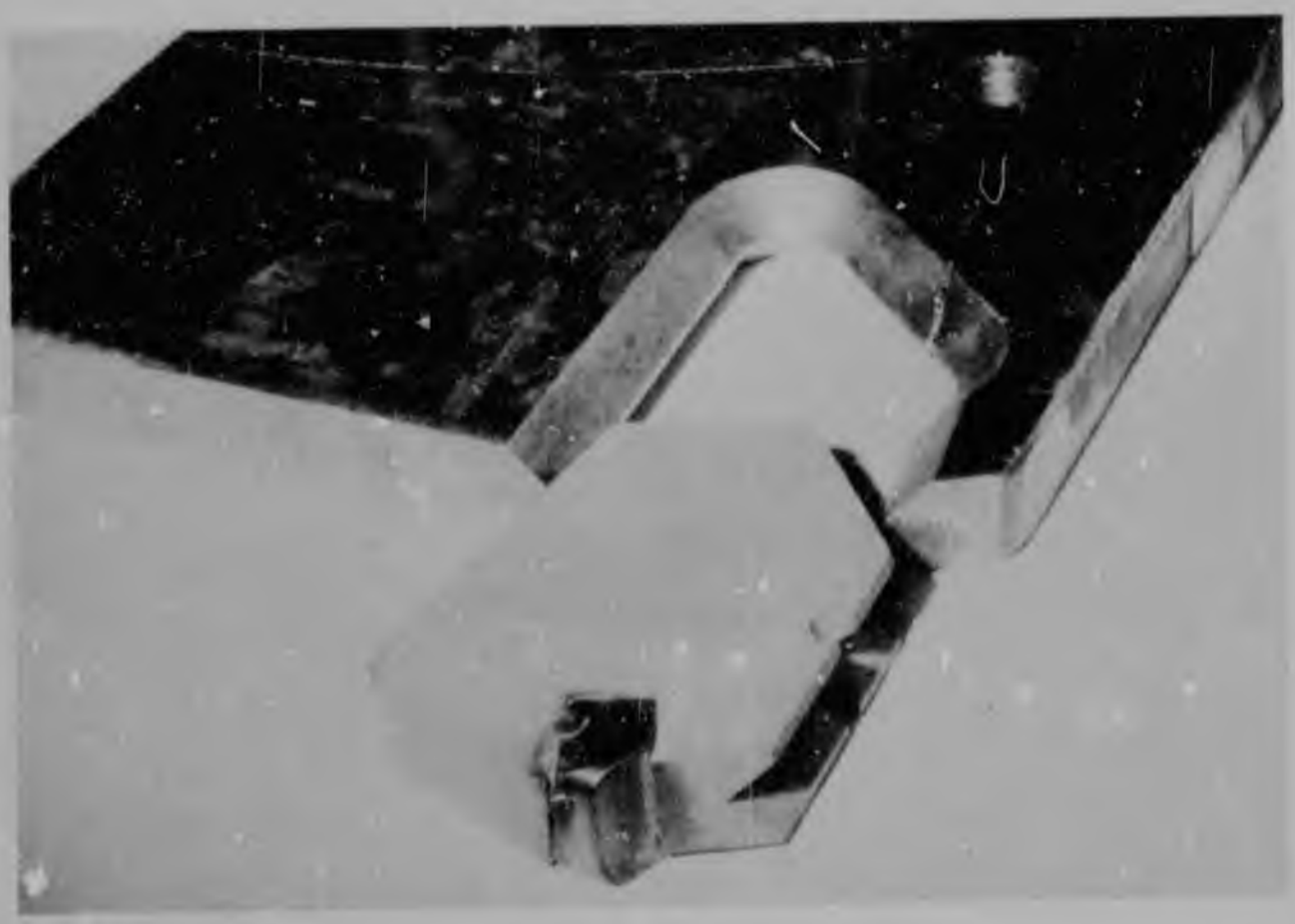


FIGURE 9. Detachable rockcutter bit, 23 mm thick, in use at the start of the pilot production trials of mining by rockcutting.

retained by a pin. The required average bit life of three centares was achieved using these bits.

CHAPTER 3

3. IDENTIFICATION OF PROBLEMS ASSOCIATED WITH THE BITS

The work described in this thesis was commenced at the beginning of 1974 and, after reviewing the previous studies relevant to this subject, (Chapter 2), the author set out to identify the problems relating to the use of bits for the underground trials. Details of these problems are discussed in this Chapter.

3.1 The strength of the bits

A study of the different parameters affecting the cutting operation at the Doornfontein trial site revealed that the effectiveness of the rock breaking process was influenced markedly by the extent of fracturing of the rock on the stope face and by the strength of the rock. The nature and extent of rock failure in a stope, is a subject currently being studied by research workers at the Chamber of Mines, Mining Technology Laboratory. These investigations have shown that cracks develop in the rock ahead of the stope face, parallel to the face, (Figure 10). The cracks have been observed a considerable distance, up to 10 metres, ahead of the face, (van Proctor, 1977).

The extent of fracturing on the stope face at the Doornfontein trial site has been classified by van Proctor (1977) into four different categories :

(a) 'Well fractured' - where the maximum distance between fractures is less than 20 cm and more than 70 per cent

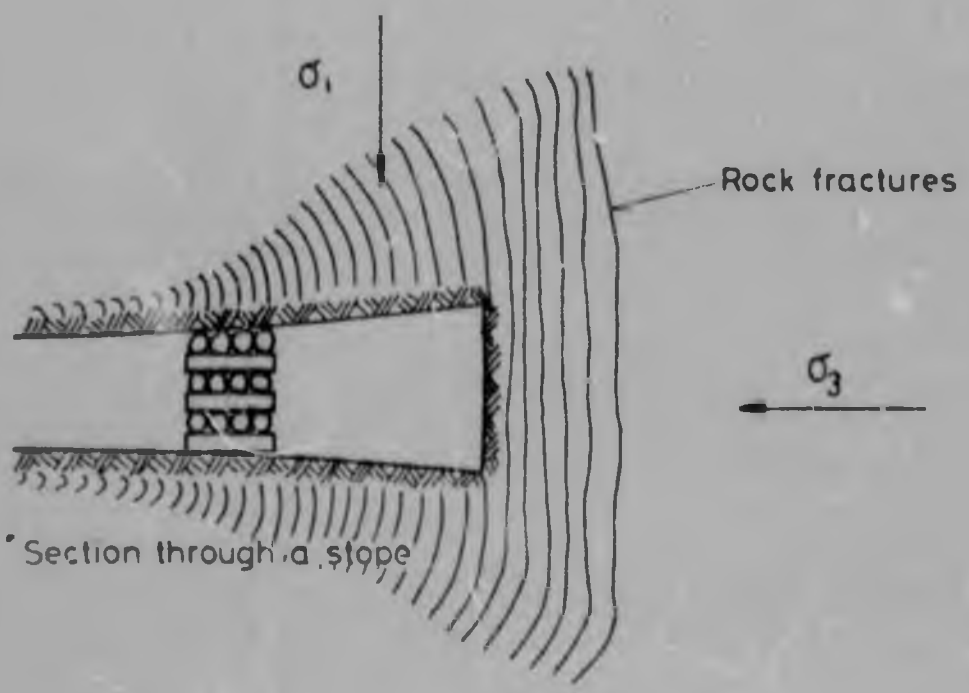


FIGURE 10. Schematic diagram illustrating cracks in the rock surrounding a deep-level stope.

of fractures are separated by a distance of less than 10cm.

(b) 'Fractured' - where the maximum distance between fractures was 30 cm.

(c) 'Slightly fractured' - with a maximum distance of 50 cm between fractures.

(d) 'Solid' - indicates that no fractures were observed for at least 1 m ahead of the face.

Using these definitions, observations made of the condition of the rock above the reef at the Doornfontein site over a four month period showed that approximately half of the face was classified as either 'well fractured' or 'fractured'. About 10 per cent of the face was classified as 'solid' and therefore the remainder was 'slightly fractured'. It has been found also that the fractured condition of the rock on the stope face changes continuously as the face is advanced, (Figure 11).

When these observations were related to the ability of the bits to cut the rock it was shown that when the machine moved from a 'well fractured' region of the face to a 'solid' region, then the maximum depth of cut, which was defined as the advance per stroke of the bit, was reduced by four or five times for a given machine force. In addition, the life of the bits, in terms of the area of the slot cut before the bit was discarded, was reduced by an order of magnitude in these unfractured rock conditions.

A further factor which was made analysis of the performance of the bits difficult, was the variation in the strength of the rock above and below the reef, (Section 1.5). This was found to

DOORNFONTEIN ROCKCUTTER STOPE

Scale: 0 10 metres



Figure legend:

——— Solid rock

-·-·- Slightly fractured

------ Fractured

——— Well fractured

Blank spaces - Observation not made

FIGURE 11 : Plan view of a section of the Doornfontein rockcutter stope illustrating the extent of the fractured condition of the rock.

influence markedly the life of the bits and the rate of cutting. A serious problem caused by this variation of the strength of the rock on the face, was the deflection of the rockcutter blade during the cutting operation. The weaker rock below the reef often used to break up and fall away from beneath the slot that was being machined. This left the bit unsupported on one side of the slot and severe sideloads were imposed on the tungsten carbide bit insert. In this situation a shear force was applied to the bit braze joint. Also, the strength of the 19 mm thick blades was insufficient to resist these sideloads and the blades frequently were deflected past the yield point of the steel.

Because of the limitation of the strength of the bits, the rock-cutting machines at the Doornfontein site generally were positioned to cut in the weaker rock below the reef, (Section 1.6). Work studies carried out at this site indicated that if the system was changed and the slot was cut above the reef, this would reduce the secondary rockbreaking operations and a substantial improvement in the labour productivity in the stope would be achieved. This provided further incentive to improve the strength of the bits.

A major problem which became apparent during the trials with rockcutting machines was that the rate of mining was some 40 per cent below the projected target value. Work studies showed that a reorganisation of the system, to make the machine cutting time a greater proportion of the operation cycle time, would give a limited improvement in the rate of mining. It was shown that a marked increase in the mining rate would be achieved only by increasing the instantaneous rate of cutting. It was recognised that this was

a fundamental problem since previous experiments (Cook et al., 1968), (Section 2.2), had demonstrated that the rate of bit wear became intolerable above a critical cutting speed. Also, examination of the bits that were returned from the pilot production trials revealed that the majority of bits were discarded from service due to failure of either the tungsten carbide bit insert or of the bit braze joint, (Section 6.2). This indicated that the bits were working close to the limits of these materials and therefore increasing the force applied to the bit in order to increase the maximum depth of cut was not considered justified. Consequently techniques were sought to reduce the mean bit force during the cutting operation and thereby to increase the depth of cut for a given available machine force.

3.2 Thermal deterioration of the bit

A study was conducted to investigate the most important factors which caused failure of the bits during the cutting operation at the underground trial sites. The results of this work indicated that thermal deterioration of both the tungsten carbide bit insert and the bit braze joint were major causes of bit failure.

3.2.1 The tungsten carbide

Bits that were returned to the laboratory after service in the machines underground, commonly showed plastic deformation of the tungsten carbide bit insert. This is illustrated in a magnified section in Figure 12. This Figure shows that the tungsten carbide was deformed ahead of the insert adjacent to the bit wearflat. A brittle material such as cemented tungsten carbide can be deformed

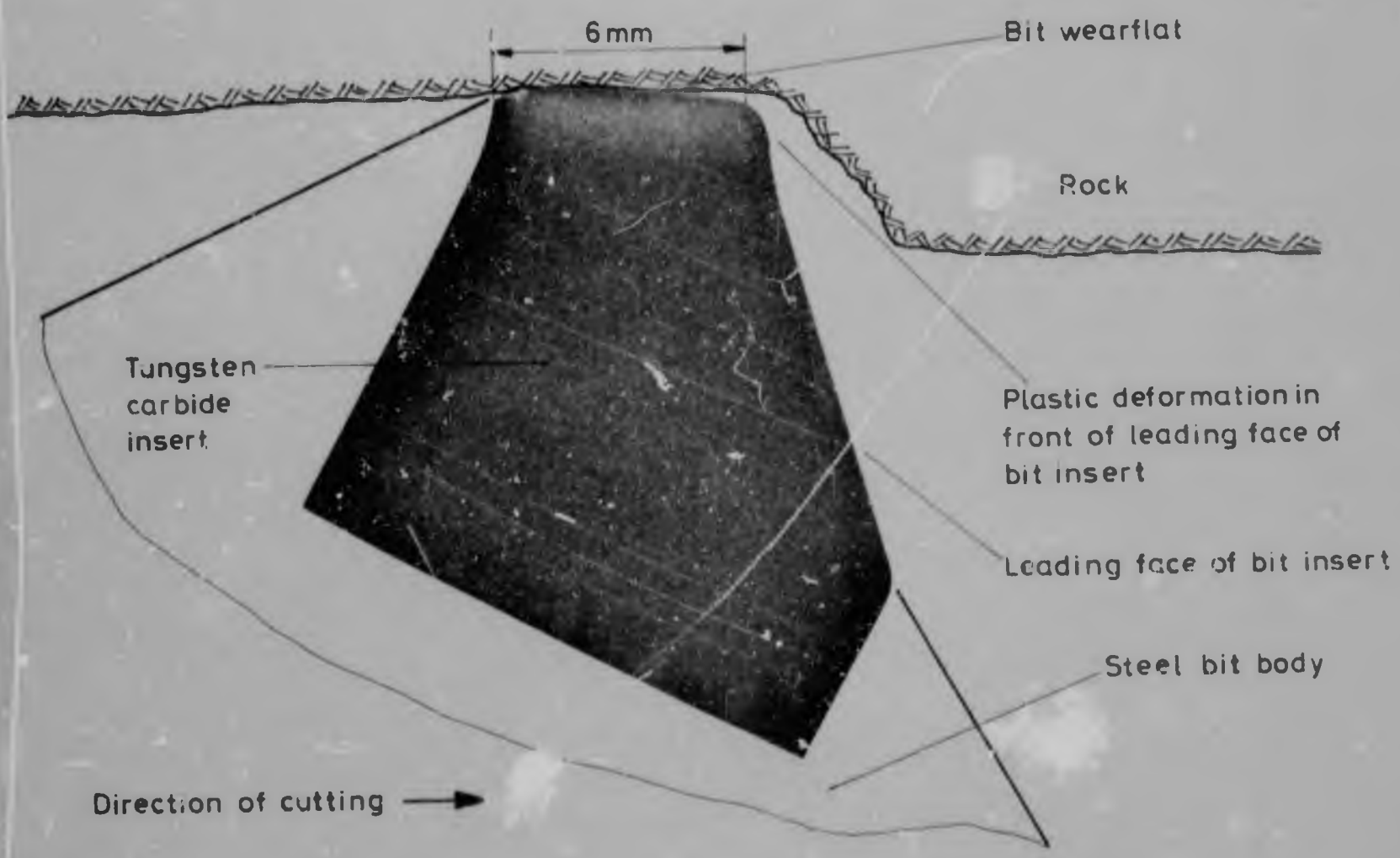


FIGURE 12 : Magnified section of a tungsten carbide bit insert, showing plastic deformation of the insert ahead of the leading face.

plastically only by the application of heat. Therefore it was concluded that the heat generated in the vicinity of the wearflat during the cutting operation, together with the applied forces, caused this damage to the bit cutting element.

The forward direction of flow of the tungsten carbide provides evidence to support the contention by Riemann (1974), that, when cutting in strong rock, the leading face of the bit generally is not in contact with the rock. If this was not true, and the theories which have been developed for cutting in weak rock by Evans (1962) and by Fairhurst and Lacabanne (1957), applied in these strong rock situation, then the load exerted by the rock on the leading face of the bit would prevent plastic deformation from taking place ahead of this face.

In addition, when cutting in relatively unfractured rock underground, it was observed occasionally that black streaks were left on the rock surface in the bottom of the slot behind the bit. These streaks were studied in the laboratory, using an energy dispersive X-ray analyser, and a significant amount of tungsten, a mineral normally not found in the quartzite, was detected within the samples. This implied that the tungsten carbide insert had melted at the interface between the bit and the rock. In this situation the bit insert was found to wear rapidly, reducing the bit life significantly. An example of one of these bits, compared with a new bit, is given in Figure 13.



FIGURE 13. Thermal deterioration producing wear of tungsten carbide bit insert.

3.2.2 The bit braze joint

Measurements were made in order to investigate whether the strength of the bit braze joint was affected by the heat applied to the bit during the cutting process. The bit, supported by a clamp holding the steel bit body, was mounted in a press and a side force was applied to the tungsten carbide bit insert, The force required to fracture the braze joint between the insert and the steel body with a number of unused bits, was compared with the force necessary to cause this failure with bits which had been used in the laboratory to cut only a small volume of rock. This test showed that a force between 100 kN and 150 kN caused the braze joint to fail with new, unused bits. This force was reduced to between 60 kN and 95 kN for bits which had been used to cut only a little rock.

A study of the damage to the bit braze joint as a result of the cutting process was made using a number of bits from this same laboratory test series. The bits were sectioned by sawing through the steel bit body and then breaking the tungsten carbide from the steel along the braze joint, (Figures 14, 15 and 16). The braze joint of all the bits which had been used to cut in the block of rock showed signs of serious damage, indicated by oxidation of the braze metal which caused a black discolouration. By comparison, the braze joints of bits which had not been used for cutting, were found to have a uniform copper colour with no blackened areas. The extent of these oxidized areas of the braze joint was less marked along the front brazed face of the insert, (Figure 15), than along the rear face of the insert (Figure 16). This was attributed to the heat being generated at the area of contact between the bit and the rock,



FIGURE 14. Rockcutter bit, showing method of breaking open to examine the braze joint.



FIGURE 15. Oxidation of front braze face.



FIGURE 16. Oxidation of rear braze face.

that is, the bit wearflat. Since the rear face of the tungsten carbide insert is adjacent to the bit wearflat with this design of bit, whereas the front face of the insert is several millimetres away from the wearflat, the more severe damage would be expected at the braze joint along the rear of the insert.

CHAPTER 4

4. TEST EQUIPMENT

4.1 Test frame

Laboratory experiments with a full-scale rockcutting machine were carried out in a test frame. This equipment consisted of a strong steel framework in the shape of a rectangular hollow box, 6 m long and 3 m wide with a working height inside a box of approximately 1 m, (Figure 17). A block of rock 3 m long with a cross-section of 0,75 m square was mounted on load cells within this box frame. The rock was cemented into a steel tray and was then bolted with tiebars against a backing plate. The backing plate was suspended by spigots from four load cells, which were designed to measure the force applied to the rock by the bit during the cutting operation and to resolve this force into three orthogonal directions, (Section 4.1.2). A rigid connection between the rock and the load cells was ensured by filling the space between the steel tray and the backing plate with epoxy resin prior to finally tensioning the tiebars. The rockcutting machine was set up square against the rock and anchored against the roof and the floor of the box by hydraulic staking jacks,(Figure 18).

4.1.1 Comparison of the properties of norite and quartzite

The rock used for experiments carried out using this test apparatus was norite; this is a strong basic rock that is quarried in the Rustenburg, Transvaal area. Norite was used for these tests,

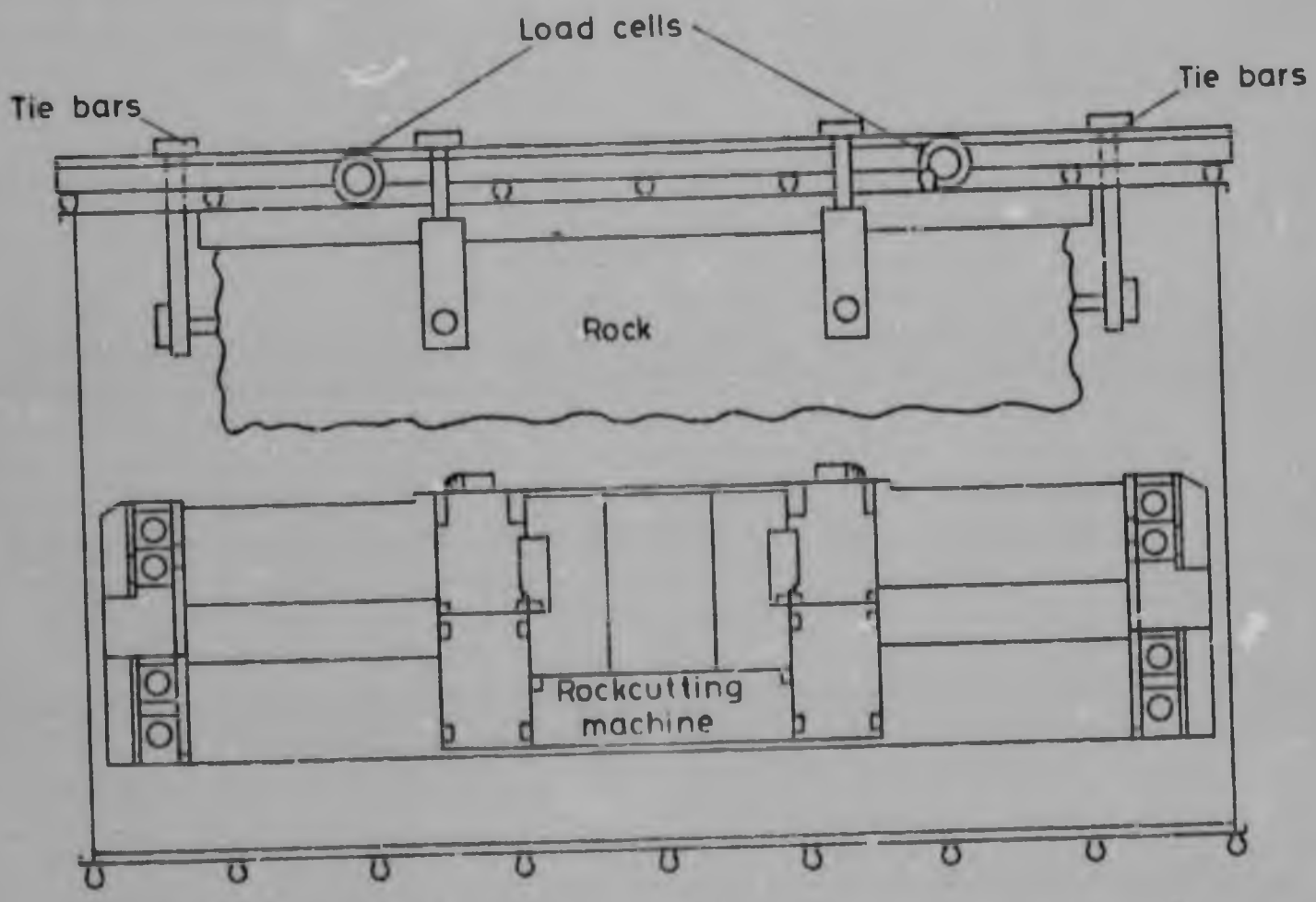


FIGURE 17 : Diagram of test frame. Plan view illustrating the rockcutting machine set up to cut against the norite block.

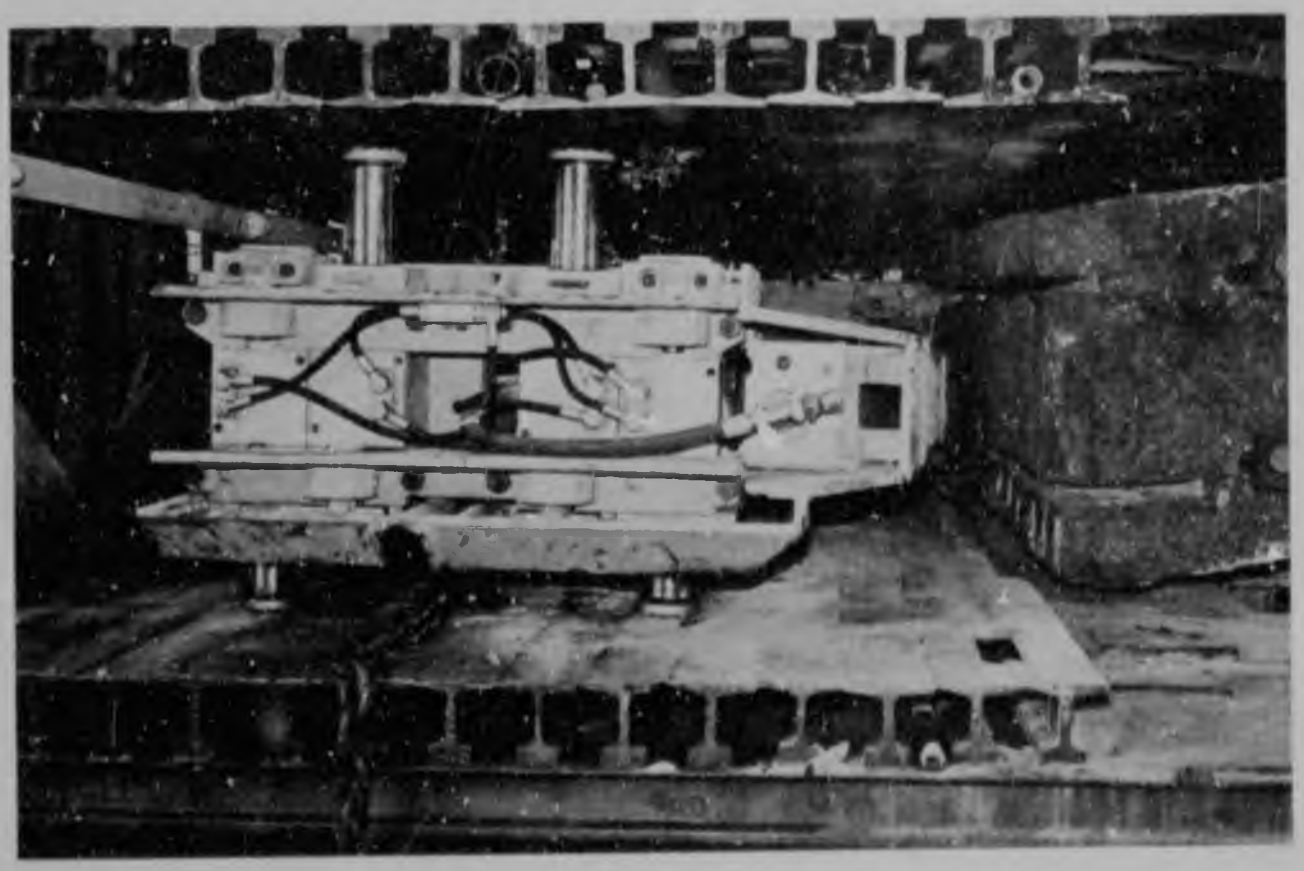


FIGURE 18. Rockcutting machine in test frame, side view.

as quartzite, the country rock adjacent to the gold reefs, was fractured as a result of stresses induced by mining (Section 3.1), and therefore was unobtainable in the large size of blocks required. Quartzite, sampled from gold mining stopes, has uniaxial compressive strength values ranging from 150 MPa to 300 MPa; 250 MPa is a representative mean value. The uniaxial compressive strength of norite is approximately 300 MPa. The indentation strength of quartzite, using a 10 mm diameter ball to indent the rock specimen, is found to be related to the quartz content of the rock, (Joughin 1976). A relatively constant strength value of about 20 kN is measured when the rock has a quartz content below 75 per cent, above this the indentation strength rises steeply to over 100 kN at 95 per cent quartz content, (Figure 19). An average value for the indentation strength of norite, which has less than 2 per cent quartz, is 26 kN. Therefore, the major difference between the two rock types is that, although they are rocks of essentially similar strengths, quartzite is far more abrasive, which is important from the viewpoint of bit wear. These figures provide justification for relating laboratory results involving bit force measurements in norite to the bit forces required to cut unstressed quartzite in the underground mining situation, but they indicate also that tests relating to wear of the bits could not be carried out in the laboratory.

4.1.2 Load cells

Five cylindrical strain gauge instrumented steel billets (Figure 20), were mounted inside each of the four load cells. Four strain gauges connected in series were attached to each billet. The

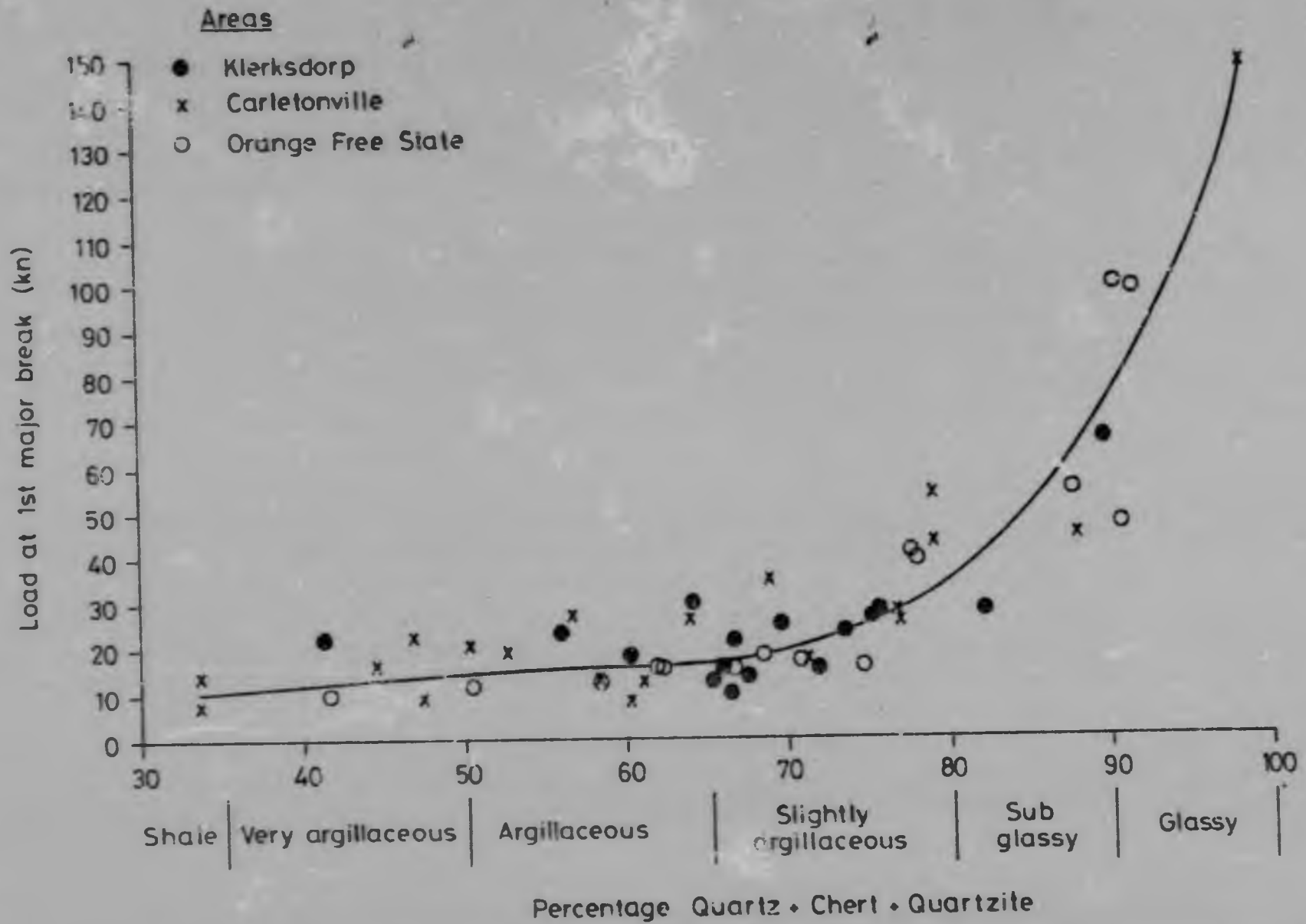


FIGURE 19 : Indentation strength of quartzite as a function of the quartz content of the rock specimen.



FIGURE 20. Strain gauge instrumented load cell billet.

billets were retained rigidly against the spigot of the test rig backing plate inside each load cell by pre-tensioned bolts, (Figure 21). The position of the instrumented billets inside the load cells relative to the rock is shown in Figure 22. Four of the billets from each load cell were mounted in the horizontal plane. Two of these billets had the main axes of the cylinders aligned parallel to the cutting direction. The two remaining billets in the horizontal plane were mounted at right angles to these, that is, with their cylinder axes normal to the cutting direction. The fifth billet from each load cell was mounted in the vertical plane, perpendicular to the horizontal billets.

The force acting on the bit during the cutting operation was resolved therefore into three orthogonal components by the load cell billets. Figure 7 shows the component of bit force in the direction of cutting, the bit cutting force, and the force normal to this direction, the bit penetrating force. The third force component, the bit side force, was orthogonal to these two.

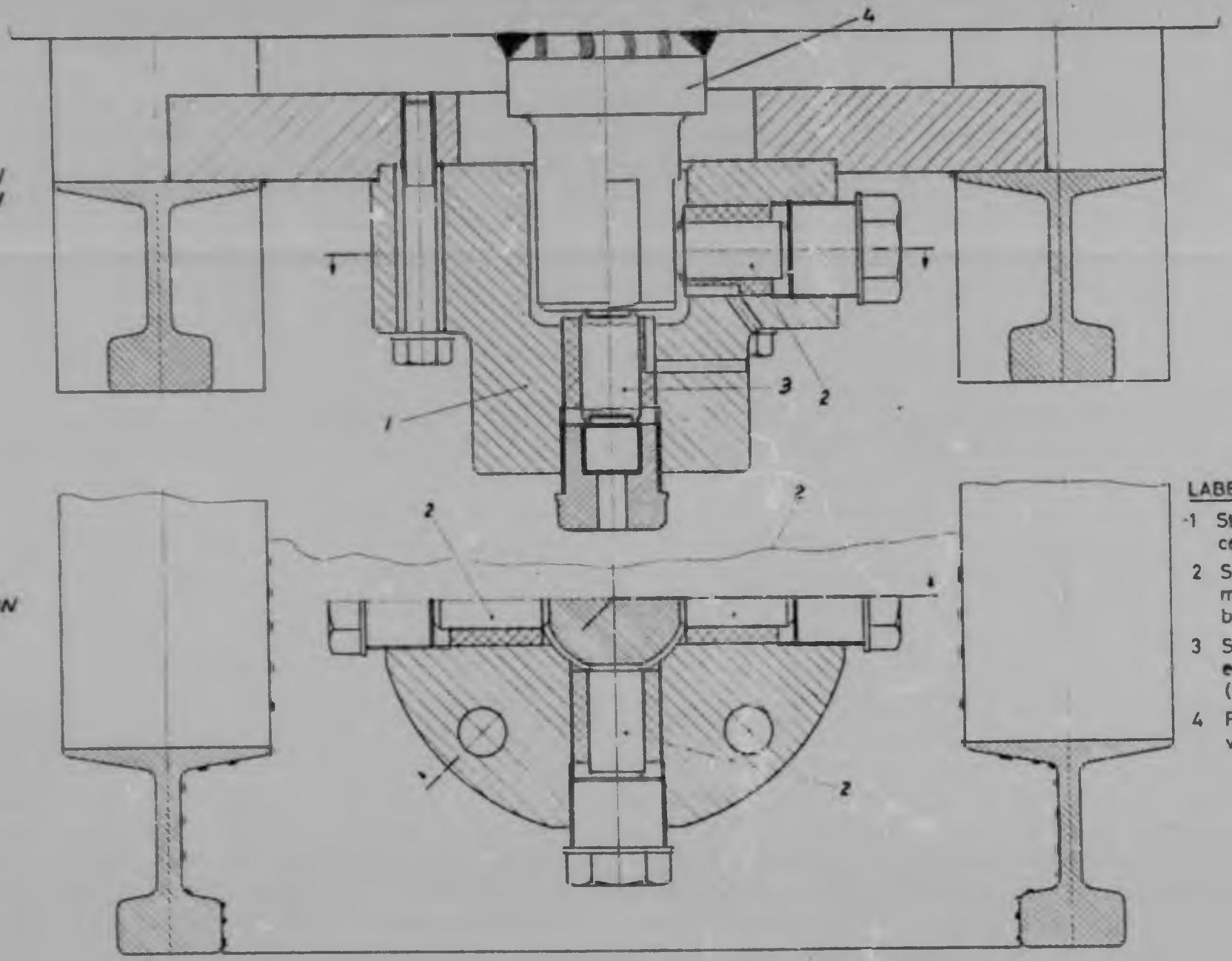
The four load cells were positioned along the length of the backing plate towards the ends of the block of rock, two at the top and two underneath the rock, (Figure 22). The circuit diagram showing the method of connecting the strain gauges from individual billets into bridge configurations given in Appendix (i).

4.2 Instrumentation of test rig

Signals from the load cell strain gauges were amplified and displayed on a twelve channel oscillograph. A differential input amplifier was used and facility was incorporated within the amplifier

SIDE ELEVATION
CROSS-SECTION

PLAN
CROSS-SECTION



LABELS.

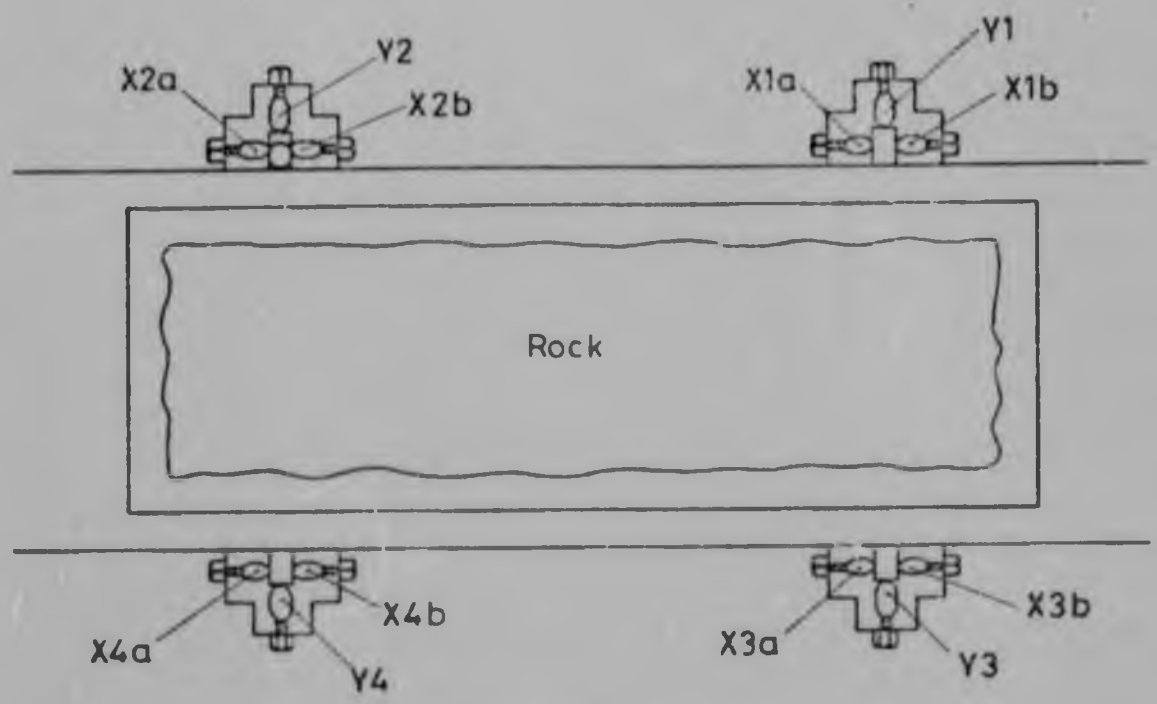
1 Steel casing of load cell.

2 Strain-gauge instrumented horizontal billet (4 of per cell).

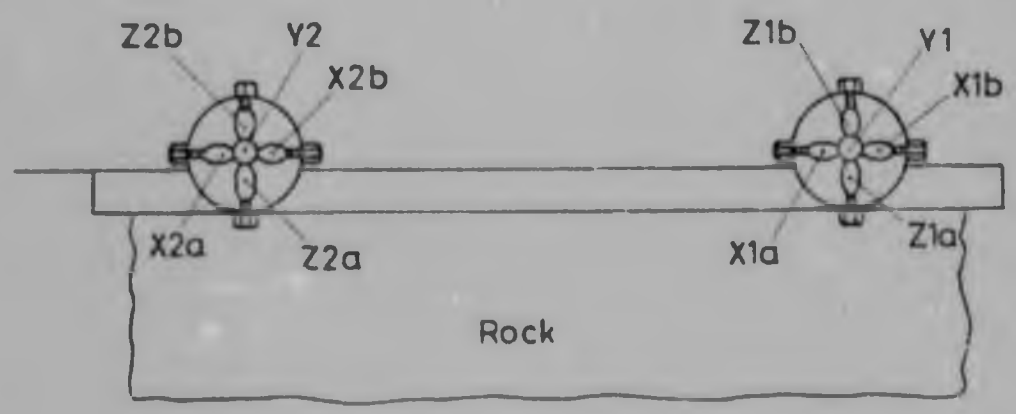
3 Strain gauge instrumented vertical billet (1 of per cell).

4 Pin joining load cell with rock tray.

FIGURE 21. Section through a test frame load cell.



Front view



Plan view

FIGURE 22 : Mounting of load cell billets relative to the block of rock.

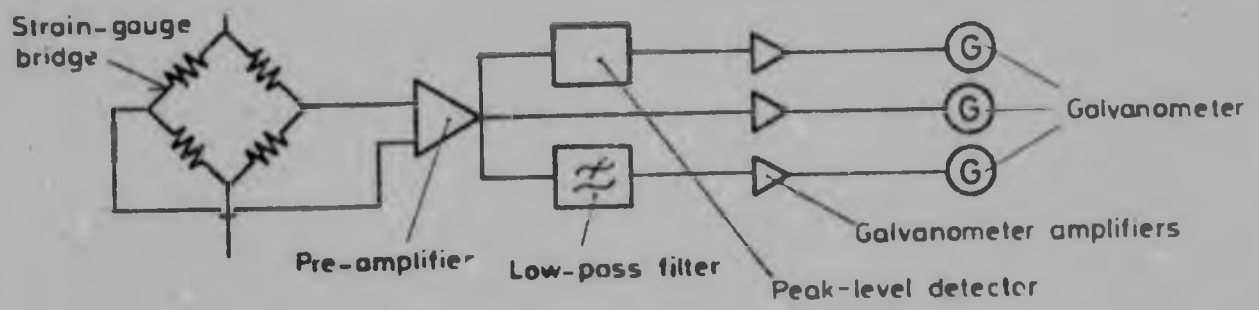
for balancing the three bridges of the orthogonal force components at zero load. The amplifier frequency response was from zero to 20 kHz, the input impedence was 10 000 ohms and the peak output voltage swing was 27 volts. A gain of 425 times was applied to the signals from the load cell strain gauges which measured the bit cutting force and the bit penetrating force. The amplifier gain was doubled to 850 times when recording the bit side force signal, since the number of strain gauge instrumented billets that were used to measure this force component was only half of those used for the other two force components, (Section 4.1.1). The circuit diagram of this amplifier is given in Appendix (i).

In order to assist with the interpretation of data from the fluctuating traces which represented the bit cutting force and the bit penetrating force on the chart recordings, two electronic devices were constructed. One of these was a low-pass filter from which the 'mean force' values were determined. This filter consisted of a second-order Chebyshev filter with a 25 Hz cut-off frequency in series with a passive twin-T, 45 Hz notch filter. The notch filter was included in order to eliminate the normal frequency of oscillation of the force traces which was about 45 Hz. The output from the notch filter was buffered by an amplifier of variable gain, arranged such that the overall D.C. gain of the filter and amplifier system was unity. The second electronic device was a half-wave rectifier with a storage capacitor and an output buffer amplifier; this was used as a 'peak-level detector' to determine the mean of the peak force values. The negative feedback potentiometer on the output buffer amplifier of this 'peak-level detector' was adjusted during the calibration procedure to

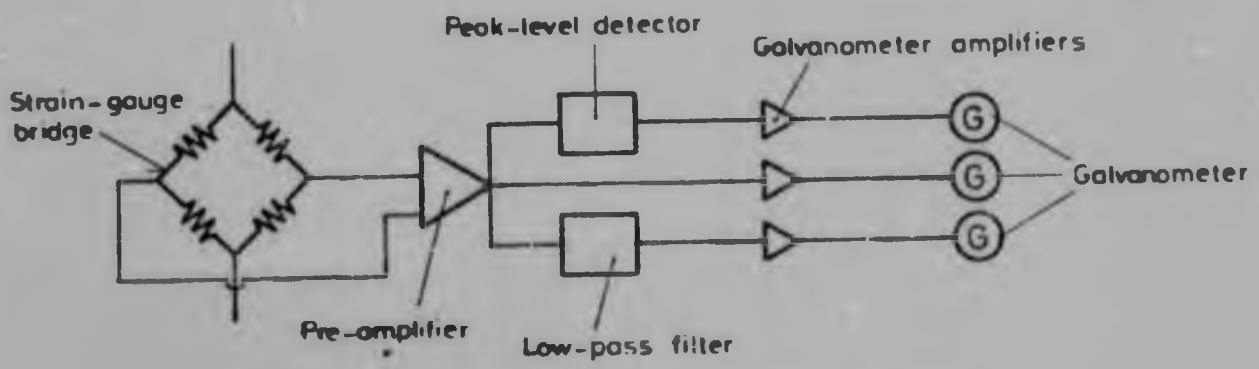
give the same gain as the unprocessed signal, and the 'decay' potentiometer was adjusted to cause the output waveform to follow accurately the input voltage peaks. The circuit diagrams of both this device and the low-pass filter are given in Appendix (i).

Therefore the bit cutting force and bit penetrating force signals, were displayed on the oscillograph using three connections from each of the two output terminals of the amplifier channels which corresponded to these two forces. One of these three signals from each amplifier channel was connected directly through the galvanometer amplifier to the oscillograph (Figure 23), this was termed the unprocessed signal. The second signal was connected through the low-pass filter and from there to the galvanometer amplifier and oscillograph. The third signal was connected through the 'peak-level detector' and the galvanometer amplifier to the oscillograph, (Figure 23). The three oscillograph galvanometers corresponding to either the bit cutting force or the bit penetrating force, were brought to a common zero prior to starting the tests. The amplifier gain of the signal to each galvanometer was adjusted as a part of the calibration procedure, (Section 4.2.1), so that the galvanometer deflections from the low-pass filter and the 'peak-level detector' were the same as the galvanometers deflection connected directly through the amplifiers to the strain gauges.

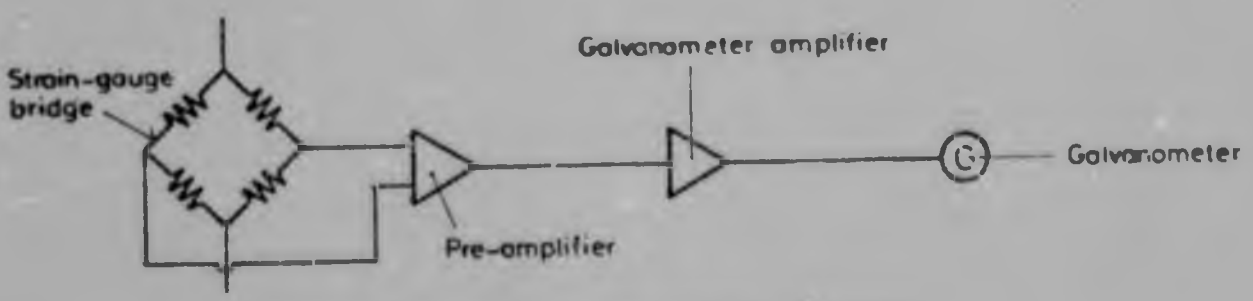
A typical extract from a chart recording using this equipment is given in Figure 24. The mean peak values and the mean values of both the bit cutting force and the bit penetrating force are shown in this Figure superimposed on the unprocessed signal. The bit



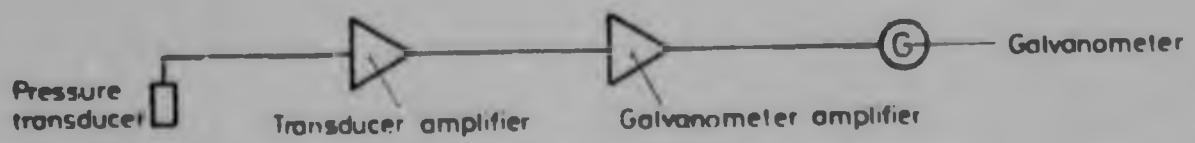
Cutting force instrumentation diagram.



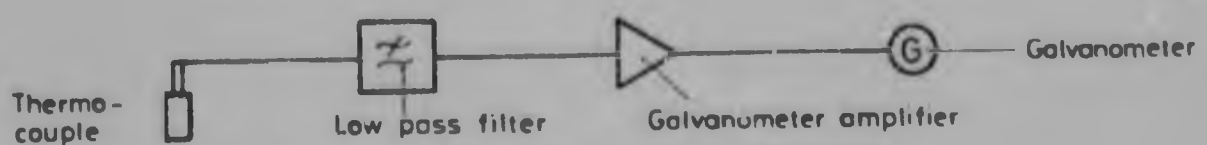
Penetration force instrumentation diagram.



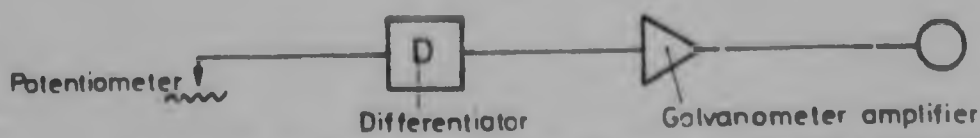
Vertical force instrumentation diagram.



Pressure transducer instrumentation diagram.



Thermocouple instrumentation diagram.



Velocity transducer instrumentation diagram.

FIGURE 23 : Instrumentation connection diagrams.

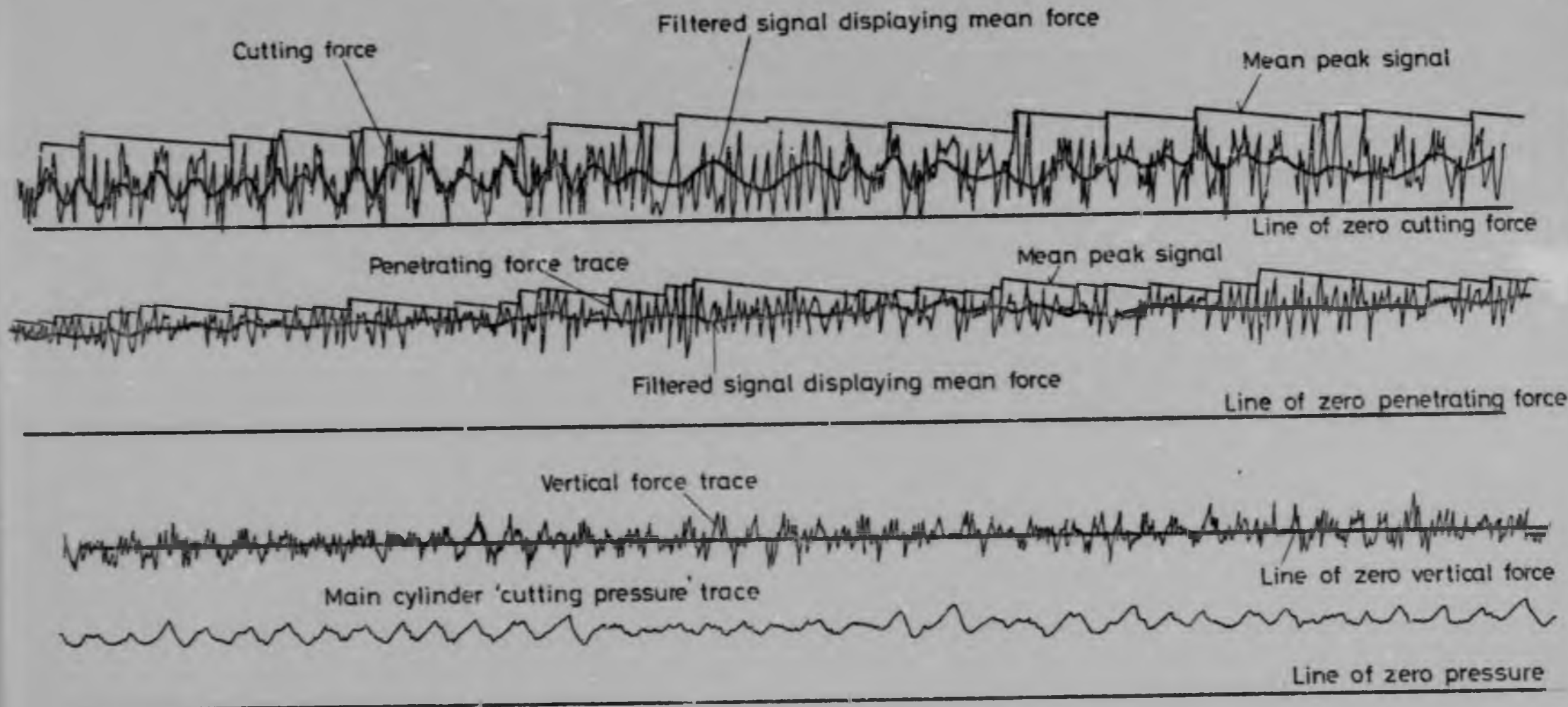


FIGURE 24. Extract from chart recording.

side force, unprocessed, is also shown.

Piezzoresistive pressure transducers were used for measuring hydraulic pressure on both sides of the piston in the main cylinder of the rockcutting machine, (Section 4.3). Commercially available pressure transducers and transducer amplifiers were employed. The manufacturers specifications of this pressure measuring equipment showed a frequency response of 10 kHz and an accuracy of better than 0,5 per cent; these figures were better than the measuring accuracy of the oscillograph, which had galvanometers with a frequency of 5 kHz, and the degree of resolution which was possible from the chart recordings.

Chromel-alumel thermocouples were used for the experiment to measure temperatures at the bit braze joint during the cutting operation, (Section 6.1.1). The thermocouples were sheathed and ungrounded with a 1,6 millimetres outside diameter. It was found necessary to conduct signals from the thermocouples through an active low-pass filter with an attenuation of 70 db at 50 Hz prior to display on the oscillograph, to remove oscillatory interference induced in the relatively long transducer leads by the close promimity of machine tools. This was aggravated by electrical impedance matching problems.

An instrument to measure the instantaneous velocity of the bit was constructed, in order to observe and quantify the vibration of the bit during the cutting operation. The velocity readings were obtained by measuring the displacement of the blade and then differentiating this signal electronically using a simple

differentiating circuit, (Appendix i).

A rotary potentiometer was used to measure the blade displacement. The drive spindle of the potentiometer was mounted on a pulley at one end of the test frame. A high yield strength wire, connected to the blade, was wound over this pulley and over one similar at the other end of the test frame. Thus a movement of the blade caused the pulleys to rotate and this provided the drive for the potentiometer, (Figure 25).

The oscillograph and the galvanometer amplifier used for this instrumentation were commercially available units. These galvanometers have a frequency range from zero to 5 kHz with an updamped natural frequency of 8 kHz. The overall system voltage sensitivity was 2,08 v/cm, to an accuracy of plus or minus 5 per cent.

4.2.1 Calibration of test rig instrumentation

The load cells which were used to measure the bit forces during the cutting operation were calibrated by applying a series of known static loads to the rock in the three orthogonal directions which corresponded to the components of the resultant bit force. Deflections of the oscillograph galvanometers were measured with known loads applied separately to the mid-points on three orthogonal faces of the block of rock using a pre-calibrated 300 kN hydraulic jack. Calibration curves of applied load plotted against oscillograph galvanometer deflection are given in Appendix (ii). The jack was precalibrated by conducting a compression test using an accurate strain-gauge instrumented load cell in series with the jack



FIGURE 25. Pulley-driven potentiometer for velocity transducer.

to obtain force values for given jack hydraulic pressures, (Appendix ii).

The pressure transducers were calibrated using a Budenberg dead-weight pressure tester and measuring deflections of the oscillograph galvanometers at known pressures. Calibration of the thermocouples was achieved by heating each of these transducers separately to known temperatures in a furnace and recording the deflections that were produced on the oscillograph galvanometers. The measured calibration points for these transducers were found to conform to the manufacturers specifications. These were, accuracies better than 0,5 per cent for the pressure transducers, and better than 3 per cent for the thermocouples.

The velocity transducer was calibrated using a stopwatch to time the movement of the machine saddle over a known distance. From this test, a calculated value of blade velocity was obtained and this was related to the displacement of the oscillograph galvanometer. A linear relationship between blade velocity and galvanometer displacement was assumed. Accurate readings of velocity were not required for the experiment; the main purpose of this transducer was to show the extra vibration that was superimposed on the blade when the compliance of the rockcutter hydraulic drive was increased, (Section 6.3.3).

Calibration curves of these transducers are given in Appendix (ii).

4.3 Rockcutting machine and hydraulic power packs

A double acting linear rockcutting machine, (Figure 26) was used for laboratory experiments. The principle of operation of the machine was similar to that of the prototype described in Section 1.5, with a cutting bit fixed to a tool blade mounted on the machine saddle. The double acting machine had been designed to cut two slots one above the gold reef and one below it although this facility was not used during the underground trials, (Section 1.6). The non-productive return stroke of the saddle was eliminated by using two bits to cut one slot, the one bit cutting in one direction of saddle travel and the other bit cutting in the opposite direction. This rockcutting machine therefore was equipped with four blades, two for each slot, (Figure 26). A screw mechanism was employed to feed the blade and bit towards the rock face.

This rockcutting machine was designed to work within a stoping width of about one metre. The height of the machine with the staking jacks fully retracted was 0,55 m. The overall length of the machine, which included the staking jacks at both ends, was approximately 5 m. The length of the fixed guide on which the saddle moved, and therefore the lengths of the cut made by the machine, was 4 m. The width of the rockcutting machine was about 1,4m.

The machine main ram and the staking jacks were powered hydraulically from an external power pack, (Figure 27), using flexible hydraulic hoses to connect the power pack to the machine. A fixed delivery, axial piston pump operating at 14 MPa pressure with a flow rate of 2,1 ℓ/sec, connected to a 30 kW electric motor,



FIGURE 26. Rockcutting machine.

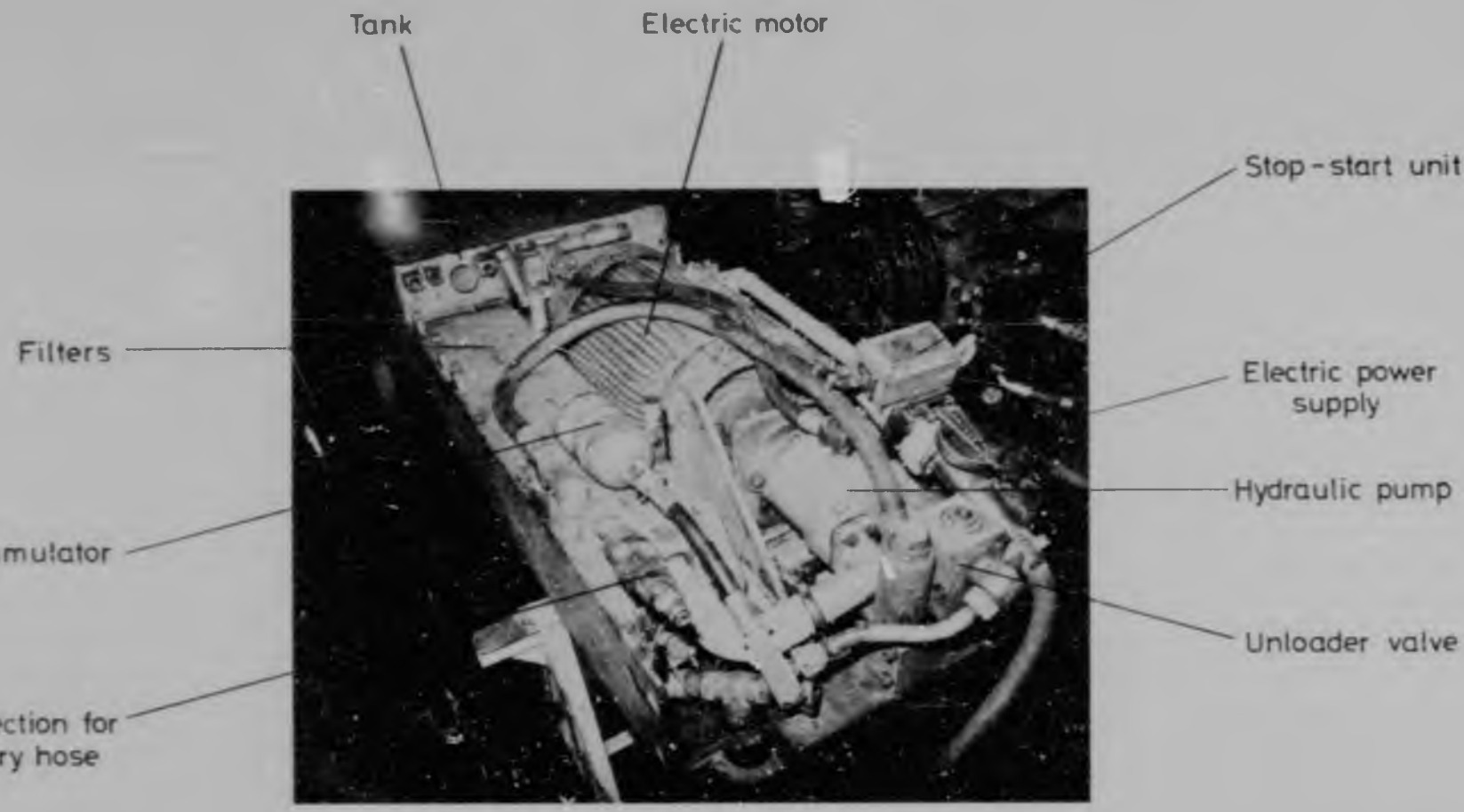


FIGURE 27. Hydraulic power pack to drive the rockcutting machine.

was used as the driving unit of the power pack. In addition this unit was equipped with a 300 ℓ tank for the hydraulic fluid, a 15μm filter to remove extraneous particles from the fluid and a heat exchanger which used a continuous flow of water to cool the hydraulic fluid. An emulsion, 95 per cent water with 5 per cent soluble oil was used as the hydraulic fluid for this system.

The machines that were operated using these power packs had a theoretical maximum cutting force of 169 kN. In practice this was reduced by friction losses along the slide to about 150 kN. The cutting speed of the saddle was fixed at 150 mm/sec.

4.3.1 Power packs used for high-pressure water jets

The experiments which were carried out using a 'flat-fan' water jet directed towards the drag bit (Section 6.3.4), employed a fixed delivery, three-throw, in-line piston pump driven by a 7,5 kW electric motor. The experiments which were conducted using coherent water jets (Section 5.4), used a larger version of the same design of pump. A 30 kW electric motor was used to drive this larger pump, and these, together with a bank of 15 μm filters, were assembled into a low profile unit (Figure 28), to enable it to be used in narrow gold mining stopes.

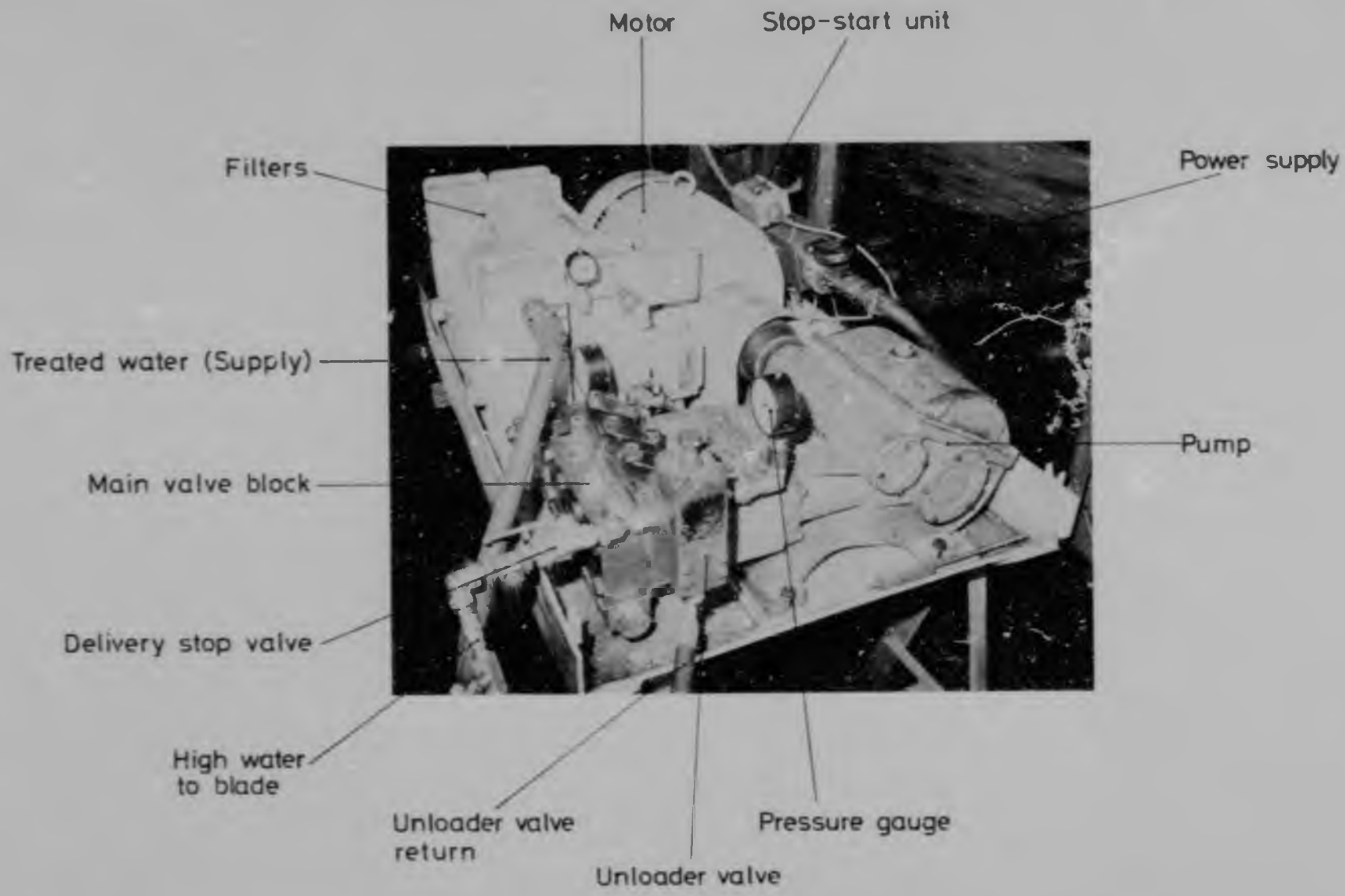


FIGURE 28 : Power pack used for high pressure water jets.

CHAPTER 5

5. EXPERIMENTAL METHODS AND PROCEDURES

5.1 Laboratory experiments using the test rig

A factor which affected the control of experiments carried out using the test apparatus was the lateral stiffness of the rockcutting machine during the cutting operation. The machine frame was anchored at both ends of the staking jacks (Section 4.3), and lateral deflection of the machine was caused by the bit penetrating force. This deflection of the machine could be calculated by considering the machine frame as a beam, rigidly supported at both ends, with a moving concentrated load applied to the beam. Calculations and tests showed that this compliance of the machine caused the depth of cut to change continuously over the length of the slot by up to 2 mm. It was shown by experiment that this machine deflection was constant after about four cuts. Therefore throughout the test programme using this apparatus, these preliminary cuts were taken in order to establish an even depth of cut along the length of the slot, prior to recording measurements of the parameters that were being investigated.

Each parameter was tested individually during the experimental programme and ten cuts were made at each depth of cut where measurements were recorded. This enabled representative mean values of the measurements to be tabled. The parameters of interest for a particular test were recorded at a given depth of cut which was then increased incrementally up to a value where the bit cutting force

approached the maximum available force of the machine. The majority of the experiments were conducted in this fashion and the results were plotted with the depth of cut measurements along the abscissa of the graphs.

5.2 Experiments conducted underground

Control of the rockcutting bits which were tested at the Doornfontein trial site was exercised by using a comprehensive system of numbering for each individual bit and blade. The machines that used the bits were numbered also and detailed records of which bits were used in the various machines were kept by a clerk who worked in an underground store. In addition, the number of benches, or slots, cut by the machine was recorded. Every month the amount of rock cut by each machine was measured by surveyors, in terms of advance of stope face multiplied by the length of the panel where the machine was stationed. Therefore, this measurement was given in terms of an area, and a nominal one metre stoping width was assumed. This area cut per month was related back to individual bits by dividing the area cut on a machine panel by the total number of benches cut on that panel during the month. This figure was then multiplied by the number of benches cut by a particular bit, to give the area cut in terms of square metres, or centares, per bit.

The bits that were used underground were removed from the machines either because of :

(i) excessive wear of the tungsten carbide insert

(ii) fracture of this insert

(iii) failure of the bit braze joint

(iv) failure of the steel bit body.

5.2.1 Bit failure

The most common types of failure and wear suffered by the bits during tests underground were classified by the author into the following categories. These are illustrated in Figure 29.

The 'insert' failure classification defines a group of bits which were discarded because the tungsten carbide insert fractured during the cutting operation. The 'braze' failure category refers to bits where the strength of the bit braze joint had been exceeded, possibly due to thermal deterioration of this joint (Section 3.2.2), and the insert had been removed completely from the steel bit body. The 'insert and braze' failure classification applies to bits where parts of the broken tungsten insert remained, together with evidence of a braze joint failure. The category 'unknown' represents bits where all traces of the original tungsten carbide insert and braze joint were destroyed leaving only the worn steel bit body. With these bits the machine operator had not recognised the failure and continued to use the bit, thereby destroying all evidence as to the original cause of failure. The term 'no failure' implies that the reason for discarding the bit was excessive wear of the tungsten carbide insert which caused the area of the bit wearflat to be increased. Laboratory experiments conducted by both Riemann (1974) and by the author (Section 6.3.2), showed that the force required to cut the rock was increased as the area of the bit wearflat was increased. Therefore as the wear of this insert progressed during the cutting operation, the maximum



Insert failure



Braze failure



Insert and Braze failure



Unknown failure



No failure

FIGURE 29 : Categories of bit failure.

depth of cut, which was limited by the maximum available machine force, was reduced to the point where the bit no longer was effective as a cutting tool.

The bits were returned to the laboratory, after service in the rockcutting machines underground, for examination and to enable the bit failure classification records to be completed. A computer program was developed by the Chamber of Mines, Mining Operation Laboratory in consultation with the author, in order to process the above data and to assist in assessing the merits of different types of bits.

CHAPTER 6

6. EXPERIMENTAL PROGRAMME

The objectives of the research project described in this thesis were twofold. Firstly to improve the life of the drag bits used in the field trials and secondly to investigate the possibilities of increasing the rate of cutting by decreasing the forces acting on the bit during the machine cutting stroke.

A programme was undertaken to improve the strength of the bits and thereby to increase the bit life. Previous studies had shown that thermal damage to the tungsten carbide inserts and to the bit braze joint was a major cause of failure of the bits underground, (Section 3.2). Consequently investigations were conducted to establish the temperatures generated in the bits during the cutting operation and to determine methods of controlling these temperatures. In addition, systematic tests with an alternative grade of tungsten carbide, different braze metals, and with bits of a modified geometry were carried out.

The investigation to reduce the forces acting on the bit was pursued by conducting four series of experiments. The first of these involved changing the geometry of the tungsten carbide cutting element by decreasing the area of the bit wearflat. Thus the stress required to cause the rock to fail was induced with lower forces applied to the rock by the bit. The second series of tests was conducted with the bit subjected to vibration during the cutting operation. In addition experiments were carried out to determine

the extent of damage caused to the rock by heat using a jet channelling torch. Finally experiments were conducted in which the rock was cut with drag bits assisted by high pressure water jets.

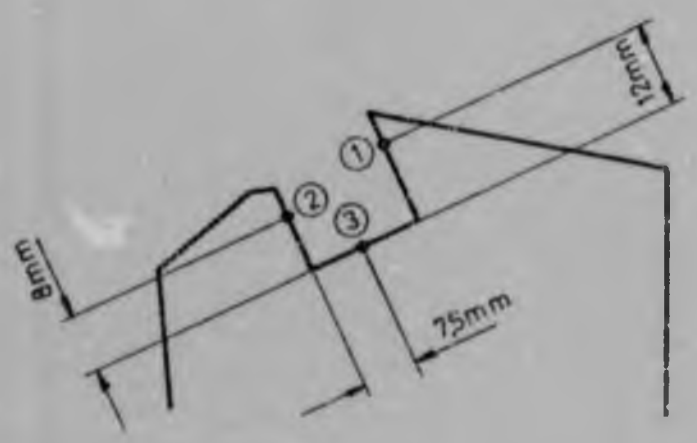
6.1 Investigations into the heat generated during the cutting operation

6.1.1 Temperature measurements

The objectives of this experiment were to determine temperatures generated at the bit braze joint during the cutting operation when no water cooling was used, and to investigate whether these temperatures could be reduced appreciably when the bit was flooded with water.

These experiments were carried out using the test rig apparatus; the temperatures were measured using thermocouples that were inserted into the braze joint at the positions marked in Figure 30. Three bits were instrumented with thermocouples but unfortunately the thermocouples which were inserted at position 1 in Figure 30 were damaged during the brazing process in all three bits. Therefore no temperature readings were made along this face of the braze joint. It was anticipated that this area of the braze would have yielded higher temperature values than the other two braze faces since this was the position closest to the area of heat generation, the bit wearflat.

Five traverses of the rock were made at a given depth of cut prior to recording measurements of temperature or bit forces. This procedure was followed not only to establish an even depth of cut along the length of the slot (Section 5.1), but also to ensure that steady conditions prevailed and that the temperatures measured were



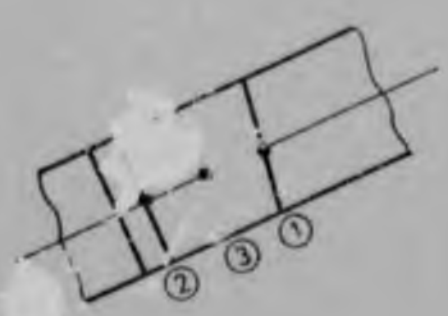


FIGURE 30 : Diagram illustrating the position of thermocouples mounted in the bit.

repeated consistently on successive cuts.

The results of this experiment are illustrated in Figure 31. This shows that when water was not used to cool the bit, temperatures were measured which approached 400 degrees Celsius at position 3 in Figure 30 and which were in excess of 300 degrees Celsius at position 2 in Figure 30. When the bit was flooded with a large volume of water, (2 litres/second); the temperatures were at all times less than 100 degrees Celsius and 50 degrees Celsius at positions 3 and 2 in Figure 30, respectively.

Extracts from two chart recordings which were both made at a depth of cut of 2,8 mm are given in Figure 32. One of these recordings represents a cut where no water cooling was used and the other where the water was applied to the bit during the cutting operation. With no water cooling the temperature increased in a relatively linear fashion over the complete length of the cut. When water was directed towards the bit the temperature increased linearly during the first half of the cut, equivalent to a distance of about 1 m. The temperature then reached a maximum value and maintained this value for the remainder of the cut. These observations were consistent at both depths of cut and at both positions of the braze joint where measurements were made.

It was observed during these tests that the amplitudes of the oscillations of the bit cutting force and the bit penetrating force were reduced when water cooling was applied to the bit during the cutting operation, (Figure 32). Thus it was anticipated that two benefits would be derived by applying a continuous water jet to the

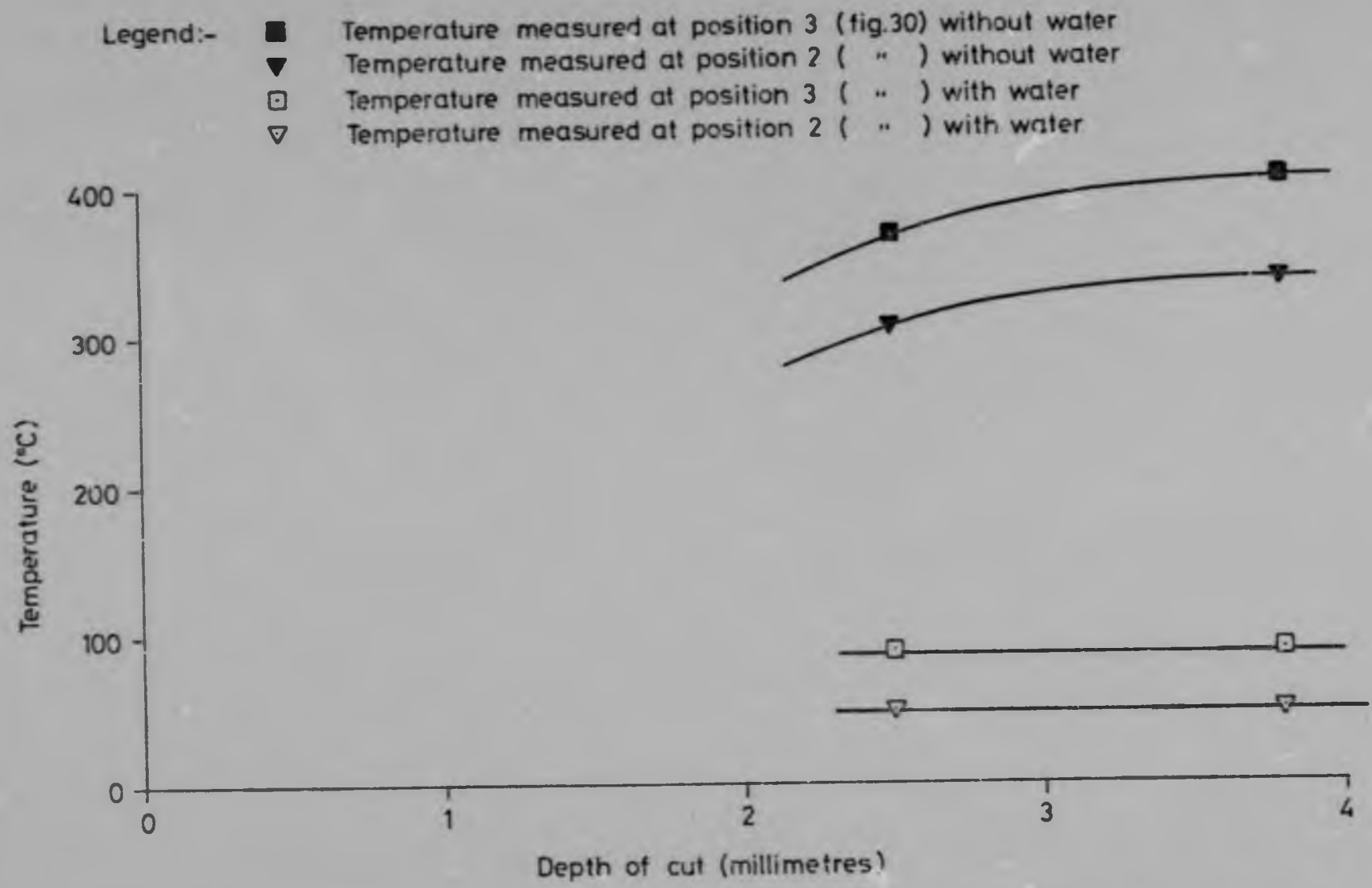


FIGURE 31 : Temperatures measured at the bit braze joint during the cutting operation plotted against depth of cut.

38mm cut - no water cooling



High amplitude cutting force

-Temperature

High amplitude penetrating force

38mm cut - powerful water cooling



Low amplitude cutting force

-Temperature

Low amplitude penetrating force

Figure 37 : Extract from chart recordings illustrating temperature measurements and reduced amplitudes of force components with water cooling.

to the bit while cutting rock. The first and most significant advantages was that adequate cooling was expected to reduce the thermal damage to the bits. A second advantage was that a reduction of the mean of the peak forces for a given depth of cut should decrease the mechanical load on the bit and thereby enhance the bit life.

6.1.2 Computer study

A computer calculation, using conventional non-steady-state heat transfer theory to predict temperatures at given points within the tungsten carbide insert and steel bit body, was carried out by Whillier (1974), in discussion with the author.

This study enabled temperatures to be estimated at regions in the bit where thermocouples would be susceptible to damage and therefore where direct measurements were not feasible. The calculations were made using the two dimensional theory and a computer was used to solve the standard finite difference approximation to the non-steady-state heat conduction equation. The properties of the braze metal were not considered in this analysis and estimates of the temperatures at the braze joint were made from the calculated temperatures at the interface between the tungsten carbide and the steel. A simplified bit geometry was assumed, similar to that illustrated in Figure 8.

The initial parameters used for this calculation are given in Figure 33. This shows that a heat flux of 5 kW was assumed to pass into the tungsten carbide at the bit wearflat. The actual power

HEAT FLOW INTO CUTTING TOOL

REDUCTION OF TUNGSTEN TOOL BODY BEING MELTED		= 0.250
TOTAL HEAT FLUX RATE INTO TOOL	(W)	= 9000.
CONDUCTIVITY OF TUNGSTEN CARBIDE	(W/MC)	= 163.00
CONDUCTIVITY OF STEEL	(W/MC)	= 43.00
TIME INCREMENT	(S)	= 0.100
DIFFUSIVITY OF TUNGSTEN CARBIDE	(M**2/S)	= .00006230
DIFFUSIVITY OF STEEL	(M**2/S)	= .00001170
TUNGSTEN CARBIDE BLOCK SIZE	(M)	= 0.04000
THICKNESS OF CUTTING TOOL	(M)	= 0.02000
GRID SPACING	(M)	= 0.00500

TEMPERATURE AFTER 1.00 SECONDS

Carbide-steel interface

Tungsten carbide insert

Carbide steel interface

Steel bit body

1727.	1697.	1537.	823.	255.	64.	34.	9.	3.	0.	0.	0.	0.	0.	0.	0.	0.	0.	0.
960.	-20.	790.	423.	142.	79.	24.	8.	2.	0.	0.	0.	0.	0.	0.	0.	0.	0.	0.
475.	448.	367.	222.	113.	45.	17.	4.	1.	0.	0.	0.	0.	0.	0.	0.	0.	0.	0.
209.	194.	159.	101.	60.	23.	7.	2.	0.	0.	0.	0.	0.	0.	0.	0.	0.	0.	0.
77.	71.	59.	38.	2	8.	1.	1.	0.	0.	0.	0.	0.	0.	0.	0.	0.	0.	0.
24.	23.	17.	12.		3.	1.	0.	0.	0.	0.	0.	0.	0.	0.	0.	0.	0.	0.
6.	6.	5.	3.	1	0.	0.	0.	0.	0.	0.	0.	0.	0.	0.	0.	0.	0.	0.
1.	1.	1.	1.		0.	0.	0.	0.	0.	0.	0.	0.	0.	0.	0.	0.	0.	0.
0.	0.	0.	0.		0.	0.	0.	0.	0.	0.	0.	0.	0.	0.	0.	0.	0.	0.
0.	0.	0.	0.	0.	0.	0.	0.	0.	0.	0.	0.	0.	0.	0.	0.	0.	0.	0.
0.	0.	0.	0.	0.	0.	0.	0.	0.	0.	0.	0.	0.	0.	0.	0.	0.	0.	0.
0.	0.	0.	0.	0.	0.	0.	0.	0.	0.	0.	0.	0.	0.	0.	0.	0.	0.	0.
0.	0.	0.	0.	0.	0.	0.	0.	0.	0.	0.	0.	0.	0.	0.	0.	0.	0.	0.
0.	0.	0.	0.	0.	0.	0.	0.	0.	0.	0.	0.	0.	0.	0.	0.	0.	0.	0.
0.	0.	0.	0.	0.	0.	0.	0.	0.	0.	0.	0.	0.	0.	0.	0.	0.	0.	0.
0.	0.	0.	0.	0.	0.	0.	0.	0.	0.	0.	0.	0.	0.	0.	0.	0.	0.	0.
0.	0.	0.	0.	0.	0.	0.	0.	0.	0.	0.	0.	0.	0.	0.	0.	0.	0.	0.
0.	0.	0.	0.	0.	0.	0.	0.	0.	0.	0.	0.	0.	0.	0.	0.	0.	0.	0.

TEMPERATURE AFTER 2.00 SECONDS

2113.	2056.	1864.	903.	464.	236.	118.	57.	32.	9.	1.	0.	0.	0.	0.	0.	0.	0.	0.
1146.	1203.	1297.	883.	992.	211.	106.	53.	29.	4.	0.	0.	0.	0.	0.	0.	0.	0.	0.
611.	771.	450.	692.	270.	196.	93.	41.	23.	3.	0.	0.	0.	0.	0.	0.	0.	0.	0.
681.	649.	573.	272.	179.	104.	49.	29.	15.	2.	0.	0.	0.	0.	0.	0.	0.	0.	0.
264.	234.	203.	145.	101.	60.	33.	17.	9.	1.	0.	0.	0.	0.	0.	0.	0.	0.	0.
123.	118.	100.	77.	52.	32.	17.	9.	4.	0.	0.	0.	0.	0.	0.	0.	0.	0.	0.
59.	54.	47.	34.	25.	16.	9.	4.	2.	0.	0.	0.	0.	0.	0.	0.	0.	0.	0.
25.	24.	21.	15.	11.	7.	4.	2.	1.	0.	0.	0.	0.	0.	0.	0.	0.	0.	0.
12.	12.	10.	7.	5.	3.	2.	1.	0.	0.	0.	0.	0.	0.	0.	0.	0.	0.	0.
5.	5.	4.	3.	2.	1.	1.	0.	0.	0.	0.	0.	0.	0.	0.	0.	0.	0.	0.
2.	2.	2.	1.	1.	0.	0.	0.	0.	0.	0.	0.	0.	0.	0.	0.	0.	0.	0.
1.	1.	1.	1.	0.	0.	0.	0.	0.	0.	0.	0.	0.	0.	0.	0.	0.	0.	0.
0.	0.	0.	0.	0.	0.	0.	0.	0.	0.	0.	0.	0.	0.	0.	0.	0.	0.	0.
0.	0.	0.	0.	0.	0.	0.	0.	0.	0.	0.	0.	0.	0.	0.	0.	0.	0.	0.
0.	0.	0.	0.	0.	0.	0.	0.	0.	0.	0.	0.	0.	0.	0.	0.	0.	0.	0.
0.	0.	0.	0.	0.	0.	0.	0.	0.	0.	0.	0.	0.	0.	0.	0.	0.	0.	0.
0.	0.	0.	0.	0.	0.	0.	0.	0.	0.	0.	0.	0.	0.	0.	0.	0.	0.	0.

Figure 33 : Initial parameters used for computer calculation of bit temperatures.

applied to the bit, calculated from the force applied to the bit multiplied by the cutting speed, shows that between 5 kW and 10 kW was applied during the cutting operation. The lower limit of these two values was chosen for the heat input to the bit since some of the applied energy, probably a small proportion, is used in forming rock chips and the remainder is used to generate heat. Some of this heat will be absorbed by the rock.

The bit temperatures in the vicinity of the tungsten carbide insert after one second and two seconds are given in Figure 33. A representative time for the bit to be in contact with the rock during the cutting stroke of the rockcutting machine, is twelve to thirteen seconds. The temperatures calculated after this period of time are plotted as isotherms in Figure 34. This shows temperatures at the interface between the tungsten carbide insert and the steel of between 400 degrees Celsius and 500 degrees Celsius. These correspond closely with the temperatures measured during the cutting operation (Section 6.1.1), therefore giving credence to temperatures calculated in other regions of the bit.

These temperatures provided cause for concern since other experiments showed that the strength of the silver-solder braze joint is reduced significantly at temperatures in excess of 200 degrees Celsius, (Section 6.2.2). Braze temperatures considerably higher than this, were measured during these cutting experiments at points remote from the area of heat input. Furthermore Roxborough (1973), showed that the hardness of tungsten carbide falls off very rapidly with temperature, far more rapidly than the hardness of quartz, and he claimed that at approximately 400 degrees Celsius the

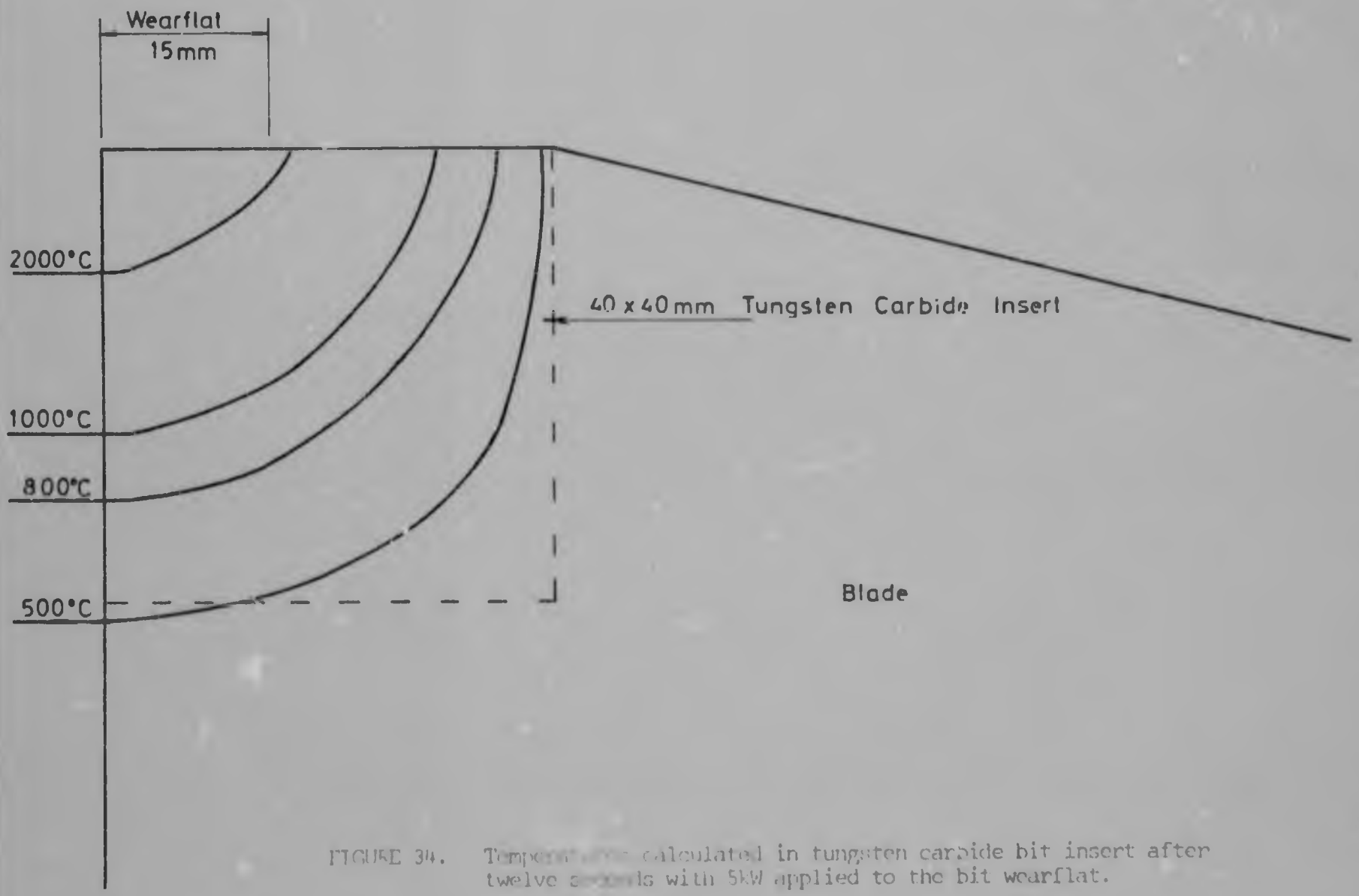


FIGURE 34. Temperatures calculated in tungsten carbide bit insert after twelve seconds with 5kW applied to the bit wearflat.

tungsten carbide becomes softer than quartz. This figure is almost certainly too low since the experiments described in Section 6.1.1 together with the analysis in this Section indicate that the bits in service at the underground trials sites commonly operate at temperatures in excess of this value. Nevertheless experiments where streaks observed on the rock behind the bit were analysed (Section 3.2.1), showed that melting of the tungsten carbide insert did take place on occasions.

Therefore, major problems of thermal deterioration of both the bit braze joint and, to a lesser extent of the tungsten carbide insert, were identified as a result of cutting strong rock with no cooling water. From these results it was considered imperative to reduce these temperatures during the cutting operation in order to prevent severe damage to the tungsten carbide insert.

6.2 Experiments designed to increase the strength of the bit

Considerable effort had been devoted to this topic by other research workers, (Section 2.3). However it was considered that not all of the avenues had been fully explored since new developments in tungsten carbide manufacture had become available recently and because the extent of thermal damage to the bits had not been appreciated previously.

A description is given in this Section, of experiments carried out where large numbers of bits were tested at the Doornfontein field site. These tests were conducted over a long period, up to three years during which time an area of between 10 000 centares and 20 000

centares was mined by rockcutting machines.

The results of the experiments, which define the average life of the bits (expressed in terms of the area cut by each bit before it is discarded), all show very high values of the standard deviation of the mean. This reflects the wide variation in the cutting conditions as a result of the 'fractured' or 'solid' condition of the rock on the stope face, (Section 3.1). The bits used for these tests were distributed randomly to the rockcutting machines along the complete length of the face, and since the experiments took place over a long period of time, it can be assumed that similar proportions of the bits from the various 'test groups' were employed in the different rock conditions.

The 't test' was used in order to test for statistical significance when comparing the mean value for the life of the bits from one group with the mean value from another group. Although the observations were not normally distributed, the samples were sufficiently large for the distribution of their means to approach normality, and consequently the use of the 't test' was justified.

6.2.1 Tungsten carbide grade

In an attempt to reduce the number of bits that were discarded because of fracturing of the tungsten carbide insert, tests were carried out using a grade of tungsten carbide with an increased toughness, measured in terms of greater traverse rupture strength. This strength value is derived from a three-point bending test using oblong specimens of tungsten carbide with a square cross-section.

It is a standard test conducted with tungsten carbide.

The properties of tungsten carbide are affected by two parameters, the particle grain size and the amount of the binder material, cobalt. As the particle grain size is increased and as the percentage of cobalt is increased, the hardness of the tungsten carbide product is reduced and the traverse rupture strength is increased, (Figure 35). The grade of tungsten carbide tests for this experiment was a new development, using a larger grain size than normal for a given cobalt content to contain an increase in the traverse rupture strength.

The results of this experiment, which was carried out underground using a large number of bits, are presented in Tables 1 and 2. The difference in the average bit life between the two groups, from 8,3 centares to 8,9 centares is found to be not significant since :

$$t = \frac{\bar{x}_1 - \bar{x}_2}{\frac{S_1^2}{n_1} \quad \frac{S_2^2}{n_2}}$$

where $\bar{x}$ is the mean of the group

S is the standard deviation of the mean

n is the number of bits in the group

Thus $\bar{x}_1 = 9,3$ $x_2 = 8,9$

$S_1 = 13,4$ $S_2 = 10,9$

$n_1 = 425$ $n_2 = 569$

$\therefore t = 0,5$

and, for a normal distribution a 5 per cent level of significance is realised only when $t > 1,98$.

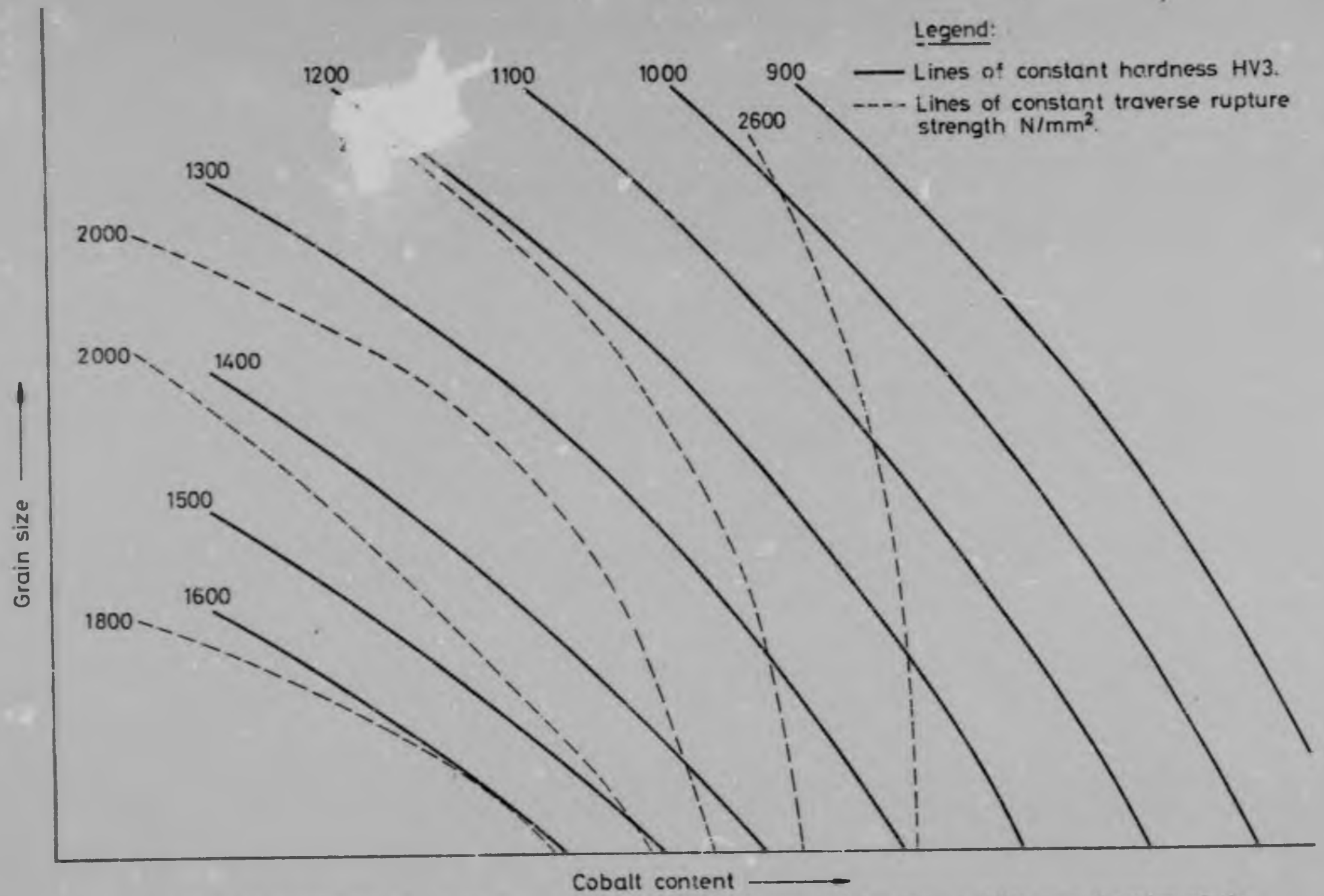


FIGURE 35 : Hardness and transverse rupture strength of cemented tungsten carbide as a function of the particle grain size and the cobalt content.

A study of the detailed breakdown of these results shows that the proportion of bits which were classified as failing in a particular mode was approximately the same for each of the two groups. For example, the bits which were discarded because of fracture of the tungsten carbide inserts accounted for 12,0 per cent of the bits with the original grade of tungsten carbide, and for 12,8 per cent of the bits with the test grade of tungsten carbide. The average life of the bits before they were discarded with failure of the tungsten carbide inserts was 8,9 centares per bit for bits with the original tungsten carbide inserts, compared with 6,0 centares per bits for bits with inserts of the test grade. However, the standard deviation of the mean for the bits with original inserts was 6,5; this was much greater than the standard deviation of 6,2 for the bits with test grade inserts.

The classification 'unknown' accounted for the largest single category of failure for both groups of bits, (Tables 1 and 2). Again the percentage of bits that failed in this category was approximately the same for each group. The average life of the bits before they were discarded with this failure classification was similar also, the bits with the original inserts averaged 11,0 centares per bit and the bits with the test grade inserts averaged 11,8 centares per bit. Thus, when bits were discarded with a failure classification 'unknown' the average life of the bits was generally higher than in other failure categories. Consequently, even if it were practicable, there was little point in directing efforts towards reducing the number of bits in this category. For this reason, although it was not possible to account for the cause of bit failure of a large proportion of the bits, this was not

TABLE 1

ILLUSTRATING BIT LIFE AND MODE OF BIT FAILURE FOR THE SINGLE CARBIDE TWENTY THREE MILLIMETRES THICK BITS WITH ORIGINAL GRADE OF TUNGSTEN CARBIDE

TOTAL NUMBER OF BITS USED = 425

AVERAGE BIT LIFE BEFORE FAILURE = 9,3 CENTARES

STANDARD DEVIATION = 13,4

MODE OF FAILURE	BRAZE	INSERT AND BRAZE	INSERT	UNKNOWN	No FAILURE	OTHERS
NUMBER OF BITS	131	50	51	133	18	42
%AGE OF TOTAL BITS	30,8	11,8	12,0	31,3	4,2	9,9
AVERAGE BIT LIFE (Centares/Bit)	8,7	5,4	8,9	11,0	12,3	9,7
STANDARD DEVIATION	12,6	9,1	16,5	15,3	13,2	8,3

TABLE 7

ILLUSTRATING BIT LIFE AND MODE OF BIT FAILURE FOR THE SINGLE CARBIDE TWENTY THREE MILLIMETRES THICK BITS WITH TEST GRADE OF TUNGSTEN CARBIDE

TOTAL NUMBER OF BITS USED = 569

AVERAGE BIT LIFE BEFORE FAILURE = 8,9 CENTARES

STANDARD DEVIATION = 10,9

MODE OF FAILURE	BROKE	[illegible] BRAZE	[illegible]	[illegible]	No FAILURE	[illegible]
NUMBER OF BITS	129	47	73	195	49	76
%AGE OF TOTAL BITS	22,7	8,3	12,8	34,3	8,6	13,4
AVERAGE BIT LIFE (Centares/Bit)	6,5	4,6	6,0	11,8	9,8	9,8
STANDARD DEVIATION	7,6	7,6	6,2	13,7	11,4	10,4

considered to be a serious problem.

Three main conclusions were drawn from the results of this experiment. Firstly, that the strength of the bit was not improved by substituting tungsten carbide inserts of the test grade for those of the original grade. This result, together with the results from previous experiments (Section 2.3), were taken as demonstrating that the optimum grade of tungsten carbide for use in this application was close to one of these two grades and that probably little further potential existed for improving the life of the bits by conducting additional experiments of this kind.

Secondly, the fact that bits with the test grade tungsten carbide inserts had lower values of the standard deviation of the mean in all of the failure categories (Tables 1 and 2), indicated that the results were more consistent when this grade of tungsten carbide was used. Consequently this grade of tungsten carbide was used when conducting other experiments in order to minimise scatter of the results. Thirdly, the largest number of bits in any single failure category, other than the classification 'unknown', was the 'braze' failure. This was true for both groups of bits and this was taken as an indication that the braze joint was an area of the bit which required further study.

6.2.2. Braze joint

A problem had been identified with heat from the cutting operation generating high temperatures in the bit braze joint which weakened this joint severely, (Section 3.2.2). In order to test the strength of the composite silver-solder braze joint at elevated

temperatures, experiments similar to those described in Section 3.2.2 were conducted, where a press was used to apply a side force to the tungsten carbide bit insert and measurements were made of the force required to fracture the braze joint. When bits at room temperature were tested in this manner, a force of between 100 kN and 150 kN caused the braze joint to fail. However, when the bits were pre-heated in a furnace to about 200 degrees Celsius, the force required to fracture the braze joint was reduced to between 70 kN and 90 kN.

Therefore these tests showed that the strength of the composite silver-solder braze joint dropped rapidly with increasing temperature and, in an attempt to increase the strength of the bit braze joint, the use of alternative braze metals was considered. The criterion used in the selection of other braze materials was that they should have higher melting temperatures than the composite silver-solder braze and that the strength of the braze joint at elevated temperatures should exceed that of the existing braze joint. The Company making the rockcutter bits therefore was requested to manufacture a number of batches of bits, each batch to be brazed with a different braze metal, and then to test the strength of the braze joint of these bits in the manner described above. Following these tests two alternative braze metals were selected as warranting further investigation. These were, a manganese-copper alloy and a copper-zinc brass.

The main differences between these two test braze metals and the composite silver-solder braze metal, were :

(i) The melting-point of the two test metals was about 780 degrees Celsius. This was approximately 100 degrees Celsius higher than the melting-point of the standard braze metal.

(ii) Tests using a press to fracture the bit braze joint showed that, when the bits were pre-heated to 200 degrees Celsius, a force of 90 kN to 105 kN was required to shear the manganese-copper joint, and a force of 110 kN to 130 kN was needed to shear the joint with copper-zinc brass. These figures compare with a force of between 70 kN and 90 kN to fracture the braze joint of bits brazed with the composite silver-solder alloy when tested at the same temperature.

(iii) The braze joint thickness was 0,3mm for bits brazed either with the manganese-copper alloy or with the copper-zinc brass. This compares with a joint thickness of 0,5mm for bits brazed with the composite silver-solder alloy. The maximum thickness of a braze joint is determined by the gap where capilliary flow of the braze metal can take place. A thicker joint was achieved with the composite braze alloy because the copper shim, before it dissolved, encouraged this capilliary flow. Previous experiments (Section 2.3), had demonstrated that a thick braze joint was desirable. Stresses were induced in the tungsten carbide insert when heat was applied to the bit because the coefficient of thermal expansion of steel is about three times that of tungsten carbide. A thick braze joint acted as a cushion, permitting this differential expansion to take place without applying high compressive stresses to the insert.

Initially two batches of bits were manufactured to test these alternative braze metals. The manganese-copper alloy was utilised in one of these batches and the copper-zinc brass was used in the other.

Problems in the use of these braze metals were anticipated because of the difference in the coefficients of thermal expansion between cemented tungsten carbide and steel. It was feared that with the relatively high brazing temperatures combined with the thin braze joint, high compressive stresses might remain in the tungsten carbide insert after the brazing process and this could cause premature failure of the bits when cutting the rock. To overcome these problems a third batch of bits was manufactured using the copper-zinc brass as the braze metal. These bits were 'stress-relieved' after the brazing operation by reheating them to 450 degrees Celsius.

The tungsten carbide grade, described in the previous Section as having a higher transverse rupture strength, was used in the manufacture of these three test batches of bits. The results of the experiment to test the alternative braze metals are given in Tables 3, 4 and 5. Figures from these Tables should be compared with figures given in Table 2 which gives details of the performance and mode of failure of bits, with the same grade of tungsten carbide but with the composite silver-solder braze metal.

No significant difference in the average life of the bits was observed between the bits brazed with the composite silver-solder and the bits, in the non-stress relieved condition, brazed with the copper-zinc brass, (Tables 2 and 3). Furthermore the bits from these two groups failed in similar fashions. In the control group, with the composite braze metal, 22,7 per cent of the bits were discarded because of fracture of the braze joint. The average life of these bits before this failure occurred was 6,5 centares per bit. By comparison, 28,3 per cent of the test group were discarded with this

TABLE 3

ILLUSTRATING BIT LIFE AND MODE OF BIT FAILURE FOR THE SINGLE CARBIDE TWENTY THREE MILLIMETRES THICK BITS BRAZED USING A COPPER-ZINC BRASS

TOTAL NUMBER OF BITS USED = 92

AVERAGE BIT LIFE BEFORE FAILURE = 8,7 CENTARES

STANDARD DEVIATION = 10,2

MODE OF FAILURE	BRAZE	INSERT AND BRAZE	INSERT	UNKNOWN	[illegible] FAILURE	OTHERS
NUMBER OF BITS	26	12	16	33	1	4
%AGE OF TOTAL BITS	28,3	13,0	17,4	35,9	1,1	4,4
AVERAGE BIT LIFE (Centares/Bit)	6,5	2,9	8,0	12,2	36,1	6,4
STANDARD DEVIATION	6,7	2,5	7,0	13,4		3,9

type of failure and the average life of these bits before they were discarded was also 6,5 centares per bit.

In contrast, the average bit life of the second test group of bits which were brazed with the manganese-copper alloy was reduced markedly, (Table 4). Sixty bits were tested and the average bit life was reduced from 8,9 centares per bit with the control group (Table 2), to 5,6 centares per bit (Table 4). The proportion of bits that were discarded because of 'braze' failures was increased from 22,7 per cent in the control group to 33,9 per cent with this test group and the average area cut before the bits were discarded as a result of this type of failure was reduced also, from 6,5 centares per bit (Table 2), to 3,7 centares per bit, (Table 4).

The average life of the bits in the third test group, which were brazed with the copper-zinc brass and then stress relieved, was 11,8 centares per bit, (Table 5). This is higher than the average life of the bits in the control group, at 8,9 centares per bit (Table 2), but calculation of the t statistic gives that t = 1,96, demonstrating that the difference in these mean values is barely significant. The percentage of bits which failed at the braze joint was reduced from 22,7 per cent with the control group to 15,9 per cent with this test group. The average bit life before 'braze' failure of the bits was increased also, from 6,5 centares per bit with the control group to 8,7 centares per bit with the test group. The difference between these two mean values however is not significant and, moreover, the proportion of failures in the 'unknown' category was increased from 34,3 per cent with the control group to 49,3 per cent with this test group, (Table 2 and 3). Thus the

TABLE 4

ILLUSTRATING BIT LIFE AND MODE OF BIT FAILURE FOR THE SINGLE CARBIDE TWENTY THREE MILLIMETRES THICK BITS BRAZED USING A MANGANESE-COPPER ALLOY

TOTAL NUMBER OF BITS USED = 59
AVERAGE BIT LIFE BEFORE FAILURE = 5,6 CENTARES
STANDARD DEVIATION = 6,6

MODE OF FAILURE	BRAZE	[illegible]	[illegible]	UNKNOWN	NO FAILURE	OTHERS
NUMBER OF BITS	20	6	11	18	1	3
%AGE OF TOTAL BITS	33,9	10,2	18,6	30,5	1,7	5,1
AVERAGE BIT LIFE (Centares/Bit)	3,7	2,0	4,4	9,8	6,2	4,5
STANDARD DEVIATION	3,1	2,0	5,2	9,7		3,2

TABLE 5

ILLUSTRATING BIT LIFE AND MODE OF BIT FAILURE FOR THE SINGLE CARBIDE TWENTY THREE MILLIMETRES THICK BITS BRAZED USING A COPPER-ZINC BRASS AND SUBSEQUENTLY STRESS RELIEVED

TOTAL NUMBER OF BITS USED = 69

AVERAGE BIT LIFE BEFORE FAILURE = 11,8 CENTARES

STANDARD DEVIATION = 11,7

MODE OF FAILURE	BRAZE	INSERT AND BRAZE	INSERT	BROKEN	No FAILURE	OTHERS
NUMBER OF BITS	11	6	6	34	6	6
%AGE OF TOTAL BITS	15,9	8,7	8,7	49,3	8,7	8,7
AVERAGE BIT LIFE (Centares/Bit)	8,2	11,5	2,9	14,1	15,6	4,6
STANDARD DEVIATION	6,7	11,6	2,2	13,3	15,7	3,6

percentage of the bits in this test group which failed at the braze joint possibly was similar to that of the control group, but because evidence of this failure had been destroyed, the bits were classified as 'unknown' failures. Nevertheless, this remains an improvement since the average bit life in the 'unknown' category in the standard group was 1[illegible],8 centares per bit and in the test group this was increased to 14,1 centares per bit.

Therefore experiments with different braze metals did not succeed in increasing the life of the bits significantly. It was concluded that all of the braze metals tested were working close to the limit of the materials' strength and therefore that major improvements in the strength of the bits would not be achieved by conducting further experiments. Consequently these tests were discontinued.

6.2.3 Bit geometry

A method to enhance the strength of the bit [illegible] joint, other than changing the braze metal, is to increase the area of contact between the steel bit body and the tungsten carbide bit insert. It was recognised that if the dimensions of the insert were increased in order to strengthen the braze joint then the force required to cut the rock would be increased also. However, Riemann (1974), had shown that the increase in the force applied to the bit was relatively small, for a large increase in the thickness of the bits, (Section 2.2.7). Consequently bits of a modified design, with a larger braze area, were manufactured. Experiments using these bits were conducted initially in the laboratory to measure the increase in the force

necessary to cut the rock, and then subsequently underground to assess any improvements in the life of the bits.

No advantage, other than a larger braze area, was anticipated if the width of the insert was to be increased. However, if the thickness of the insert and the steel bit body was increased, the possibility existed for increasing the thickness of the blades also. This would enhance the lateral stiffness of the blades which would be advantageous in the mining situation, (Section 3.1). Therefore attention was paid to this aspect of the design. It is well known that the strength of a brittle material, such as tungsten carbide, is a maximum when all of the dimensions of the material are approximately the same, thus a sphere or a cube is a strong shape. Hence, the proposal to increase one dimension only of the tungsten carbide insert, the thickness of the insert, would weaken this component of the bit. For this reason two approximately equi-dimensional pieces of tungsten carbide, brazed adjacent to each other, were used in the construction of the modified, thicker bit (Figure 36).

The tungsten carbide bit insert which was 23 mm thick in the original design (Figure 9), was increased to a thickness of 35 mm. The blade thickness was increased from 19 mm to 35 mm. The deflection of a blade with a sideload applied to the bit tip, proportional to the blade thickness to the third power. Thus, for the same blade width, this increase in the blade thickness represents an increase in the blade stiffness in this plane of 2,4 times.



FIGURE 36. Detachable rockcutter bit, 35 mm thick.

The differences between the components of bit cutting force and bit penetrating force which were measured in the laboratory using 23 mm and 35 mm thick bits, are given in Figures 37 to 40. It is evident from these graphs that a substantial increase in bit force was required when the thicker bit was used to cut unfractured rock. However, the force capability of the existing rockcutting machines was such that a reasonable depth of cut could still be maintained using the thicker bit. The potential advantages of a stronger bit, combined with the fact that the majority of the rock in the gold mining stopes is fractured which allowed deeper cuts to be made than was possible in the unfractured norite, resulted in an experiment to test the thicker bits underground.

The bits used for the experiment conducted underground, employed a grade of tungsten carbide for the inserts which were in use at the start of the pilot production trials. These were brazed into the steel bit body using the composite silver-solder braze metal. In order to study the difference in performance between the original 'thin design' and this 'thick design' of bits, the results of this test which are given in Table 6, should be compared with the results presented in Table 1.

One objective of using the 'thick' bits mounted on 'thick' blades was to enable the slot to be cut up against the stope hangingwall, (Section 3.1). This objective was not achieved during these tests. In some instances, in the more highly stressed ground, the machines succeeded in cutting slots in this position up at the top of the stope face, but in general, the high vertical force which was superimposed on the bit (Section 3.1), caused excessive

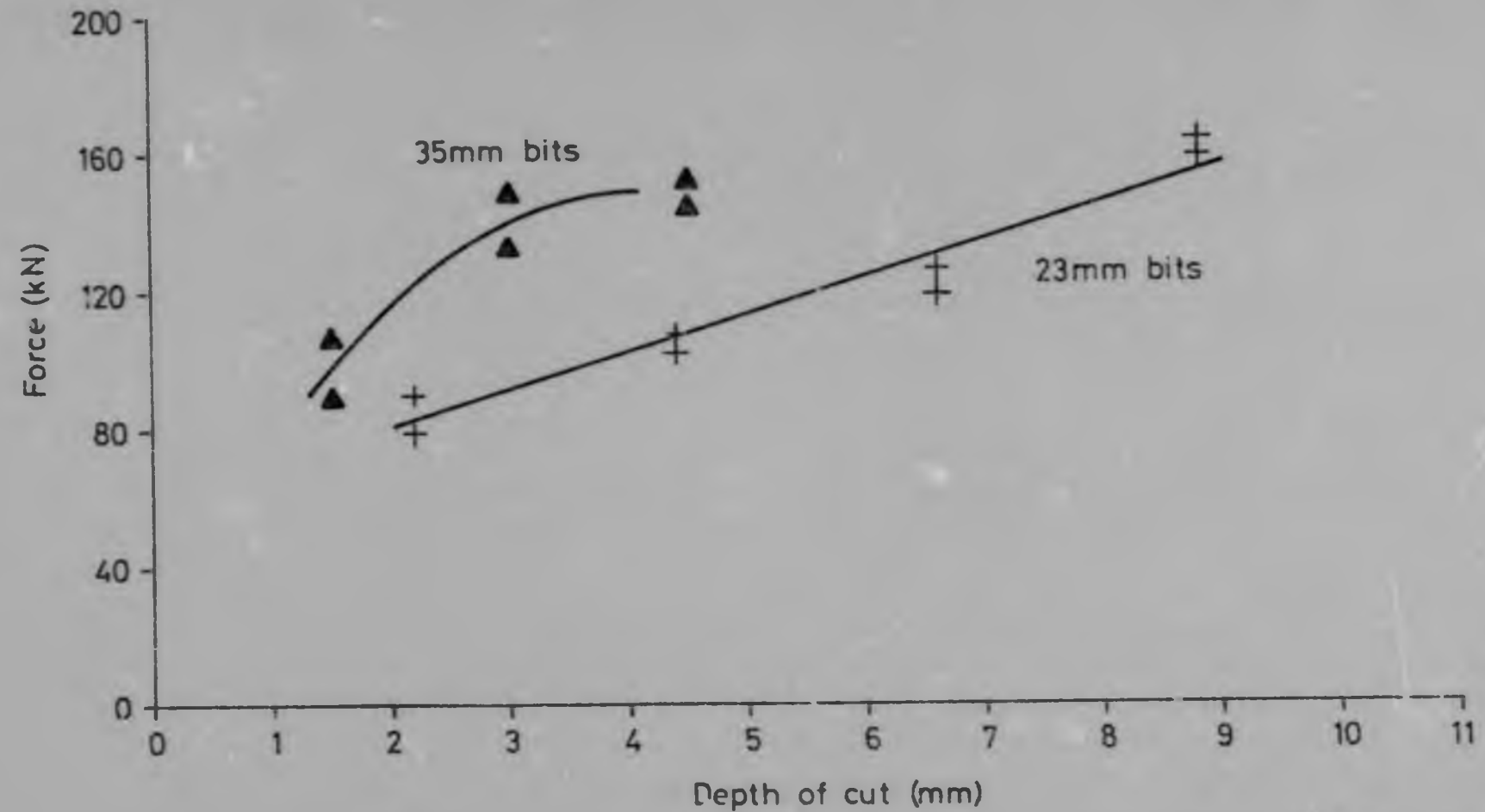


FIGURE 37 : Mean peak bit cutting force plotted against depth of cut for 35 mm thick bits and 23 mm thick bits.

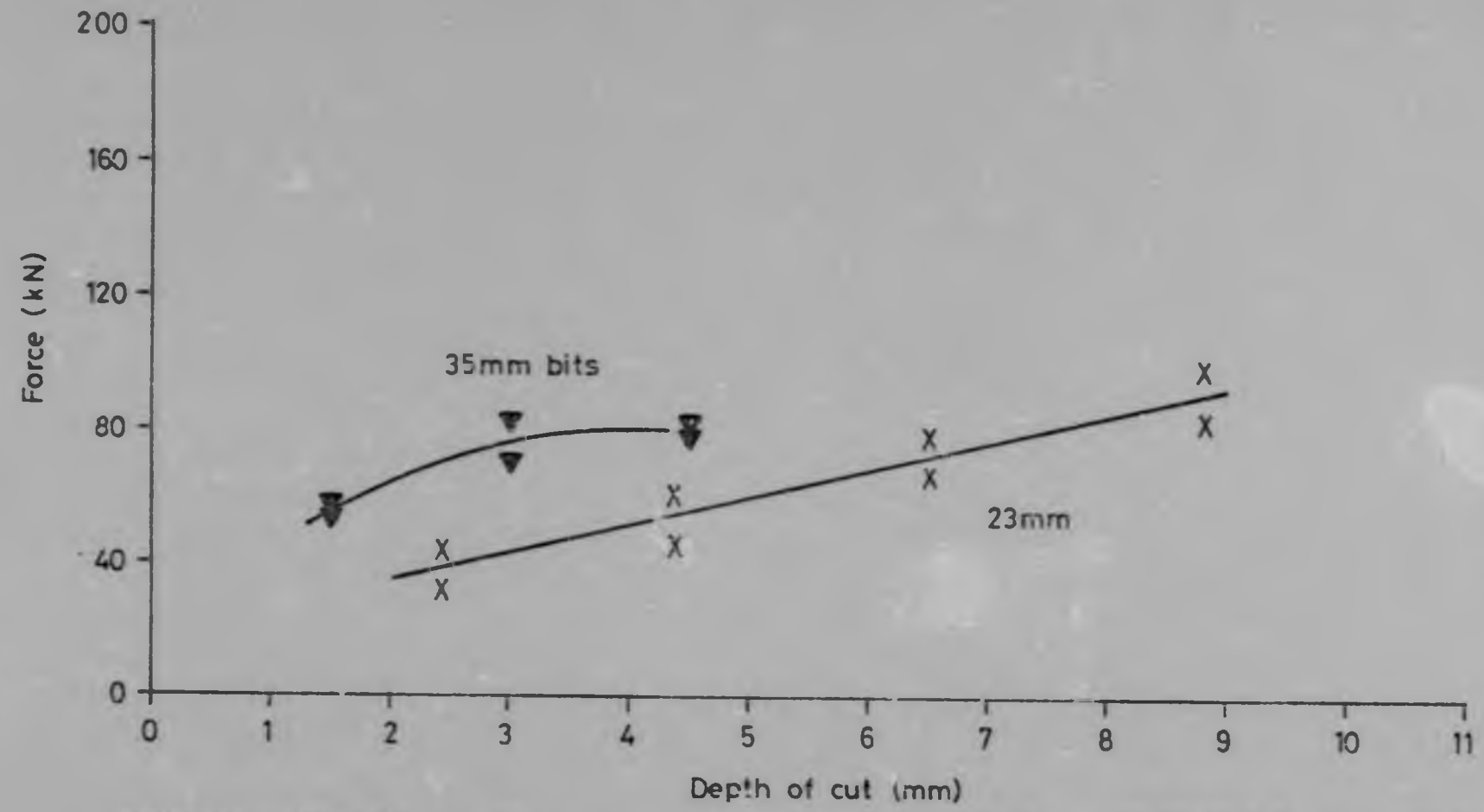


FIGURE 38 : Mean bit cutting force plotted against depth of cut for 35 mm thick bits and 23 mm thick bits.

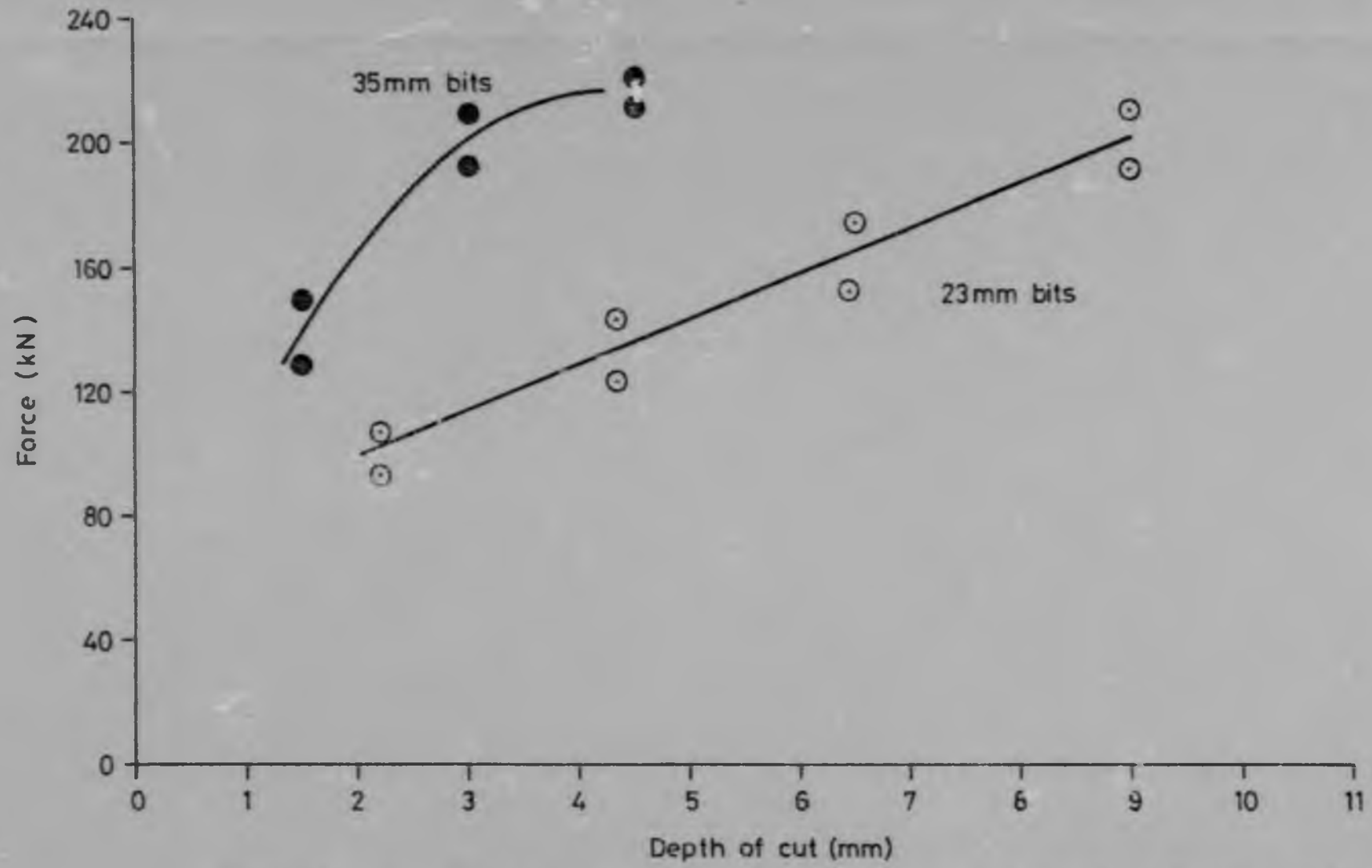


FIGURE 39 : Mean peak bit penetrating force plotted against depth of cut for 35 mm thick bits and 23 mm thick bits.

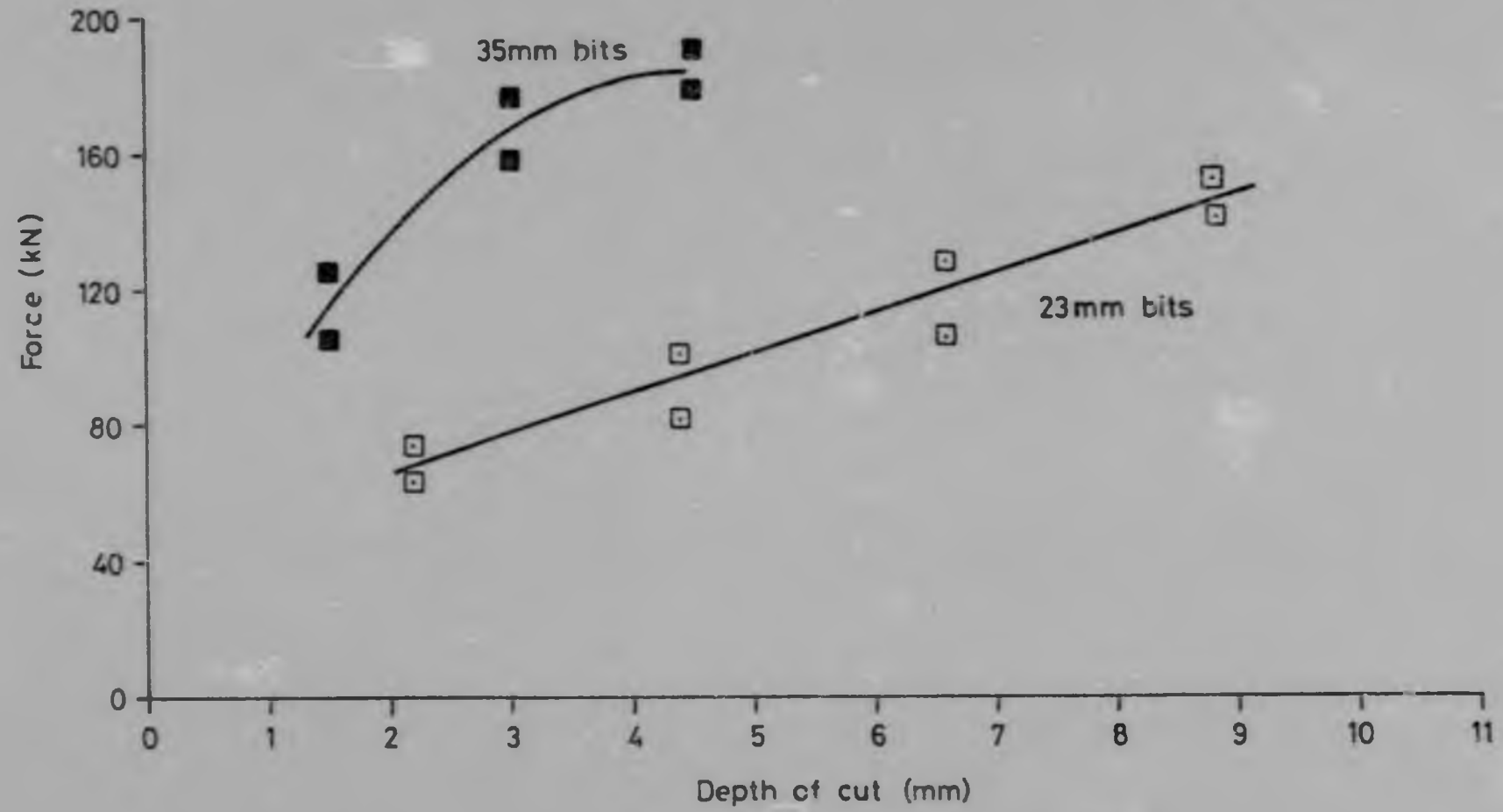


FIGURE 40 : Mean bit penetrating force plotted against depth of cut for 35 mm thick bits and 23 mm thick bits.

deflection of the blade and forced the cutting operation to be carried out in the middle of the face. In addition, the bit life was reduced drastically when cutting in the stronger quartzite above the reef, (Section 3.1). The results presented in Tables 1 and 6 reflect therefore, the difference in performance for two groups of bits of different design but which were used for cutting in similar conditions on a stope face.

The overall average bit life was increased from 9,3 centares per bit to 11,6 centares per bit by the use of the thicker bits, (Tables 1 and 6). Calculation of the t statistic gives that $t = 1,5$ and therefore that this difference is not significant. However a few significant differences did emerge in the mode of failure between the two groups of bits, (Tables 1 and 6). Failure at the braze joint with bits of the 'thick design' occurred after cutting an average of only 4,7 centares. Therefore, although the proportion of bits that were classified as 'braze' failures was reduced from 30,8 per cent with the 'thin' bits to 20,9 per cent with the 'thick' bits, the braze joint remained a weak area of the bit design. An encouraging feature of the breakdown of the failure classification for the 'thick' bits was that the proportion of the bits that were discarded due to excessive wear of the tungsten carbide inserts, as opposed to failure of the bits, was increased to 11,6 per cent from 4,2 per cent.

It was concluded from these tests, which were designed to improve the strength of the bits by experimenting with different grades of tungsten carbide, different braze metals and different bit geometries, that each of these factors was important. From Tables 1

TABLE 6

TABLE ILLUSTRATING BIT LIFE AND MODE OF BIT FAILURE FOR THE THIRTY FIVE MILLIMETRES THICK BITS

TOTAL NUMBER OF BITS USED = 88

AVERAGE BIT LIFE BEFORE FAILURE = 11,6 CENTARES

STANDARD DEVIATION = 13,2

MODE OF FAILURE	UPPER TUNGSTEN CARBIDE INSERT	INSERT	BRAZE	INSERT	UNKNOWN	No FAILURE	STEEL FAILURE	OTHERS	NOT RETURNED FROM MINE
	LOWER TUNGSTEN CARBIDE INSERT	No FAILURE	BRAZE	INSERT	UNKNOWN	No FAILURE			
NUMBER OF BITS	14	19	1	13	10	12	19	1	
%AGE OF TOTAL BITS	16,3	20,9	1,2	12,8	11,6	14,0	22,1	1,2	
AVERAGE BIT LIFE (Centares/Bit)	14,7	4,7	6,1	10,7	17,8	15,9	11,2	7,0	
STANDARD DEVIATION	19,1	4,6		12,8	17,5	11,1	10,8		

and 2 it is evident that the 'insert' failures accounted for only about 12 per cent of the total number of bits used. Thus further experiments with other tungsten carbide grades were not continued. The braze joint was established as a weak region of the bits and experiments designed to strengthen this joint showed that the use of a braze metal with a higher melting temperature gave marginal improvements in the overall bit life. In addition the tests with the 'thick design' of bits demonstrated that increasing the area of the braze joint reduced the percentage of 'braze' failures and helped to increase the overall bit life. However, none of these tests produced a dramatic improvement in the life of the bits. The fundamental problem of excessive heat being generated between the rock and the bit and much of this heat being absorbed by the bit, had not been solved.

6.3 Experiments to reduce the mean bit force

6.3.1 Bits with a narrow wearflat

In an effort to compromise and achieve strong braze joint with a reduced bit force, the bit design was modified again. A number of bits were constructed using two inserts to give an overall bit thickness of 35 mm. The wearflat width of these inserts was reduced from 6 mm, which was the standard with all previous designs of bits, to 2 mm, (Figure 41).

How this design change affected the area of the bit wearflat and the total area of the braze joint is illustrated in Table 7. This shows that the wearflat area was reduced markedly when compared with the bits of the two previous designs. The braze area was increased

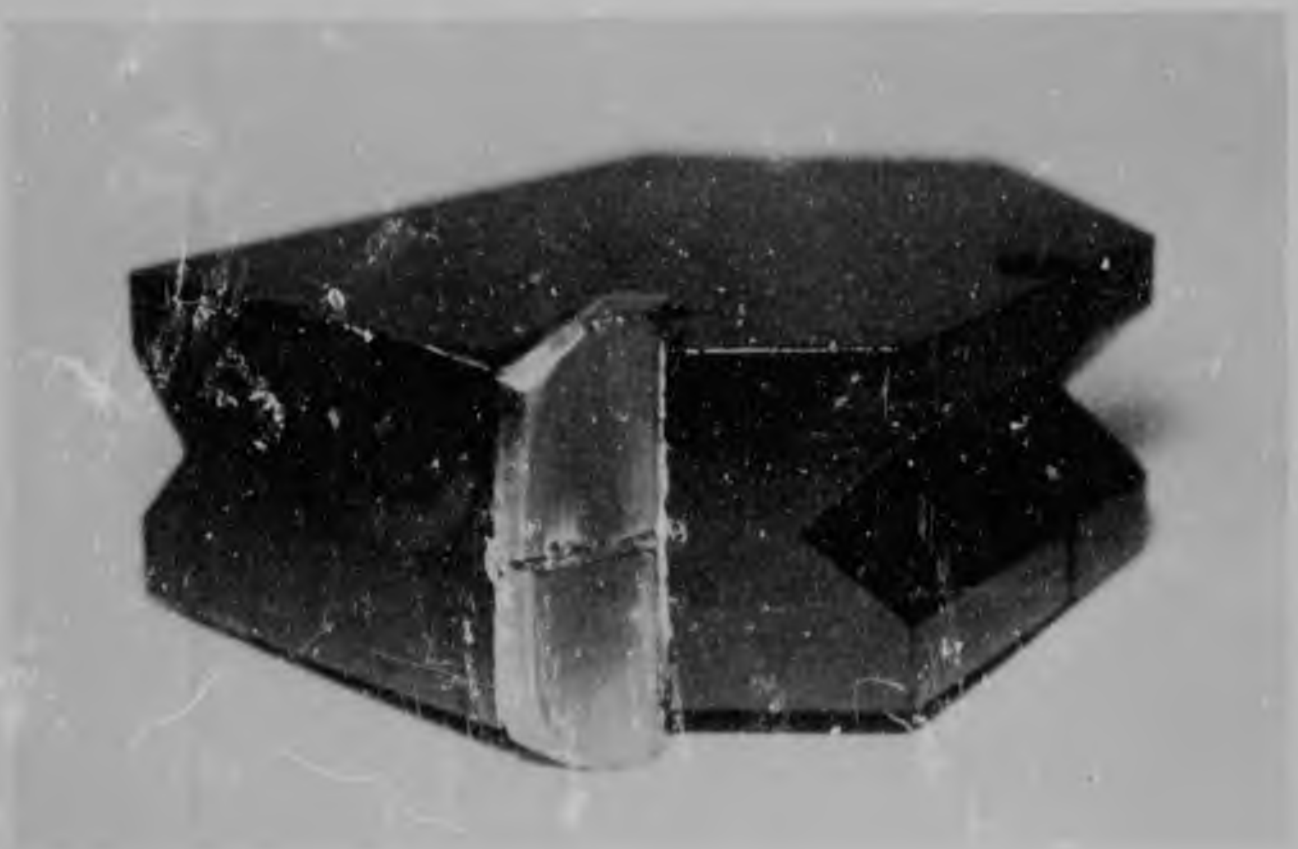


FIGURE 41. Detachable 35 mm rockcutter bit with a 2 mm wearflat width.

TABLE 7 : ILLUSTRATING THE AREAS OF BRAZE JOINTS AND WEARFLATS WITH THE DIFFERENT BIT DESIGNS.

BIT TITLE	THICKNESS OF BITS (mm)	WEAR FLAT AREA (mm^2)	AREA OF BRAZE JOINT (mm^2)
Original Design	23	23 x 6 = 138	798
'Thick Bit' Design	35	35 x 6 = 210	1317
'Narrow Wearflat' Design	35	35 x 2 = 70	1216

substantially compared with the 23 mm thick bits and reduced only slightly compared with the 'thick design' of bits.

Laboratory experiments were conducted to investigate whether an appreciable reduction of the force acting on the bit was achieved using bits with the decreased wearflat area. Subsequently experiments were carried out to test these bits underground.

Force measurements which were recorded during these experiments were plotted against depth of cut (Figures 42 to 45). Reduced mean peak cutting force and the mean cutting force values were measured when the narrow wearflat bits were used. The depth of cut was increased from a maximum of 4,5 mm with the wider wearflat bits to a maximum of 7,0 mm with the narrow wearflat bits. The bit penetrating force, both the peak and the mean force values, was substantially reduced using the narrow wearflat bits, (Figures 44 and 45).

Tests with these narrow wearflat bits were carried out at the Doornfontein trial site to investigate whether the reduced bit force would have a beneficial effect on the cutting operation in the underground situation. Twenty bits of this design were tested; all of these were discarded after each one had been used to cut only a small area, on average less than one centare, of the rock face. The mode of failure of all of these bits was a shattering of the tungsten carbide inserts. The cause of this failure with these bits was attributed to the inability of the narrow tungsten carbide inserts to withstand the bending stresses which were applied by the cutting force component of the bit force. In the laboratory, when cutting an unfractured block of rock the bit penetrating force caused the bit to indent the

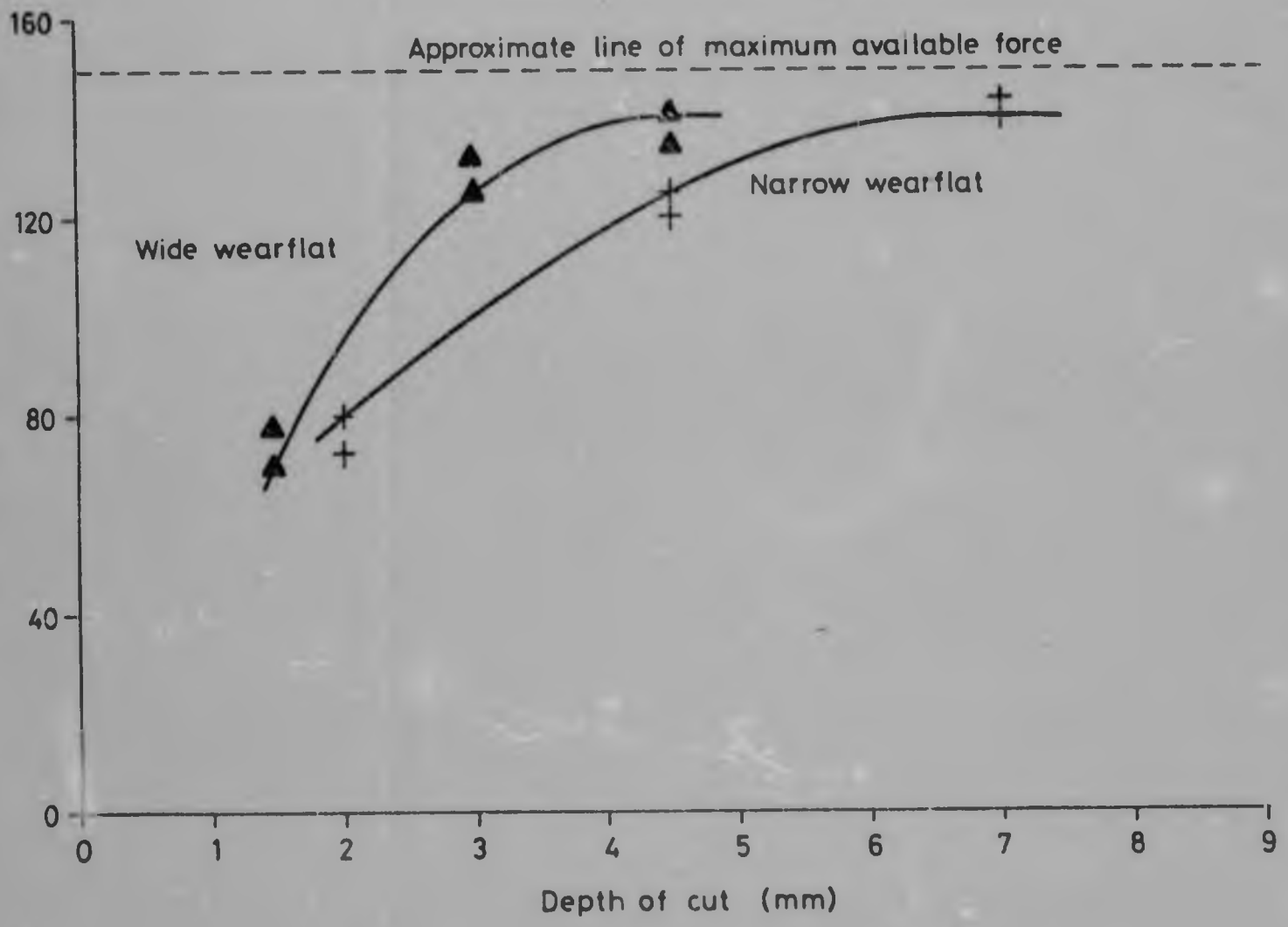


FIGURE 42 : Mean peak bit cutting force using a standard wearflat and a narrow wearflat bit.

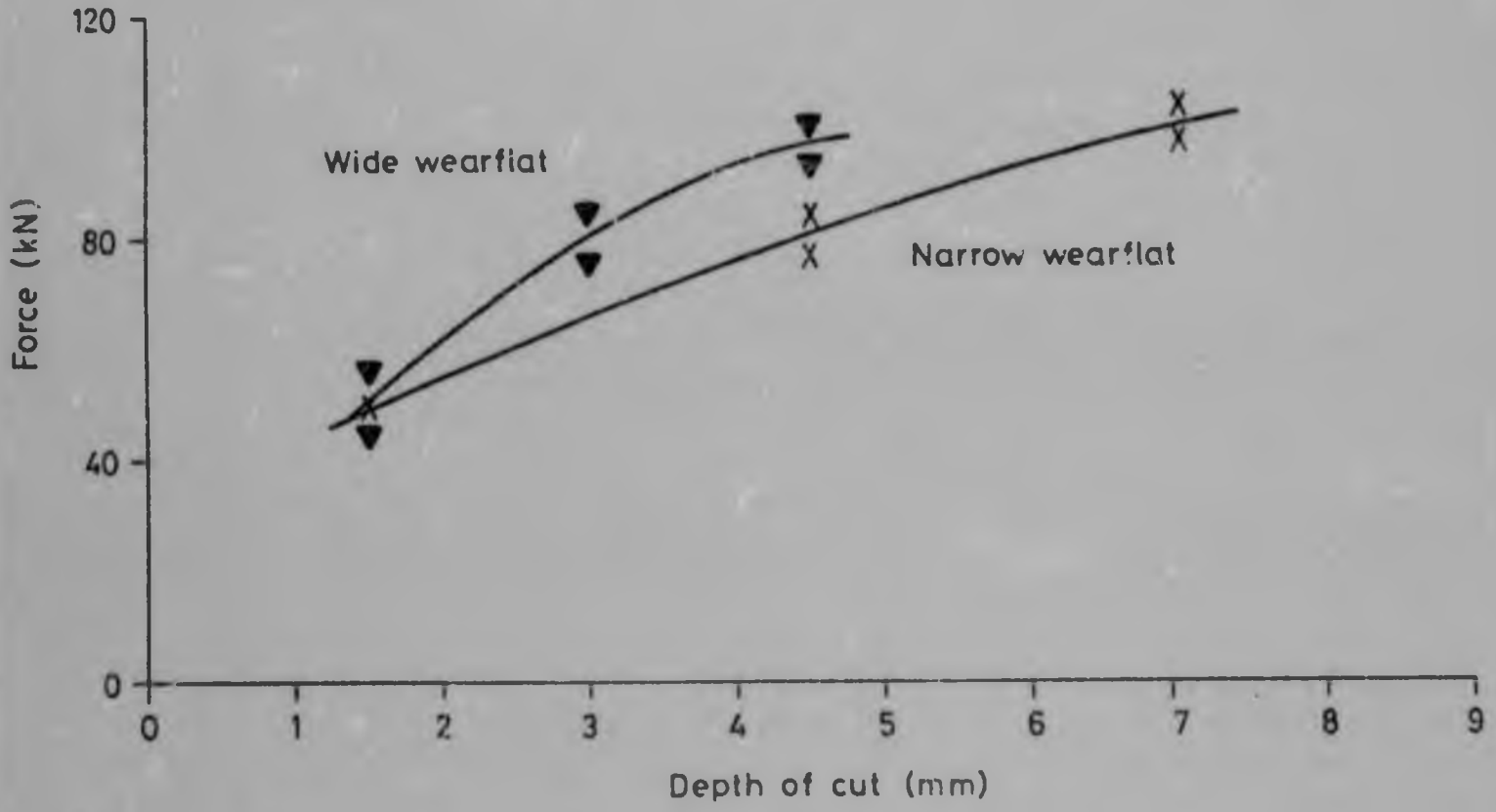


FIGURE 43 : Mean bit cutting force using a standard wearflat and a narrow wearflat bit.

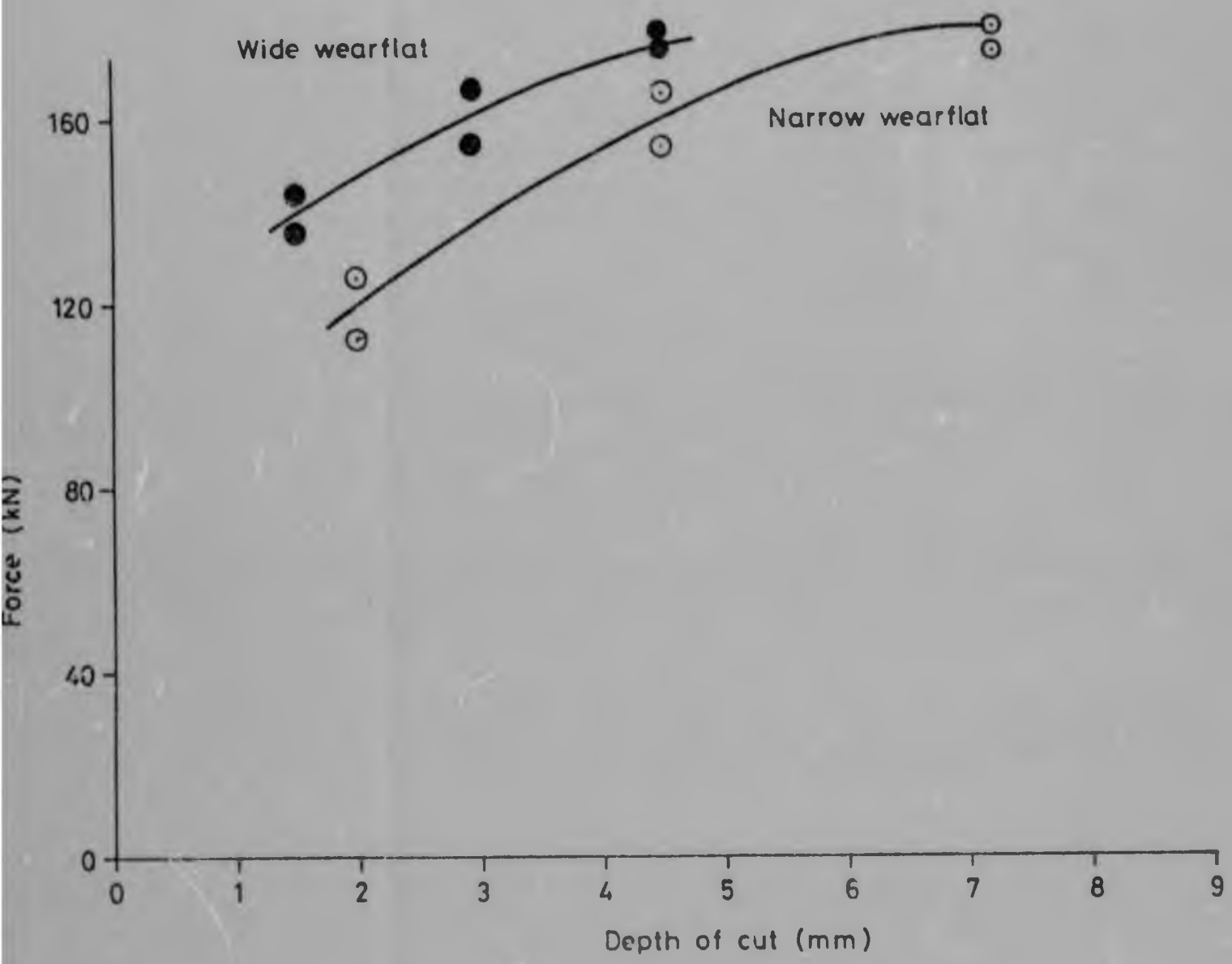


FIGURE 44 : Mean peak bit penetrating force using a standard wearflat and a narrow wearflat bit.

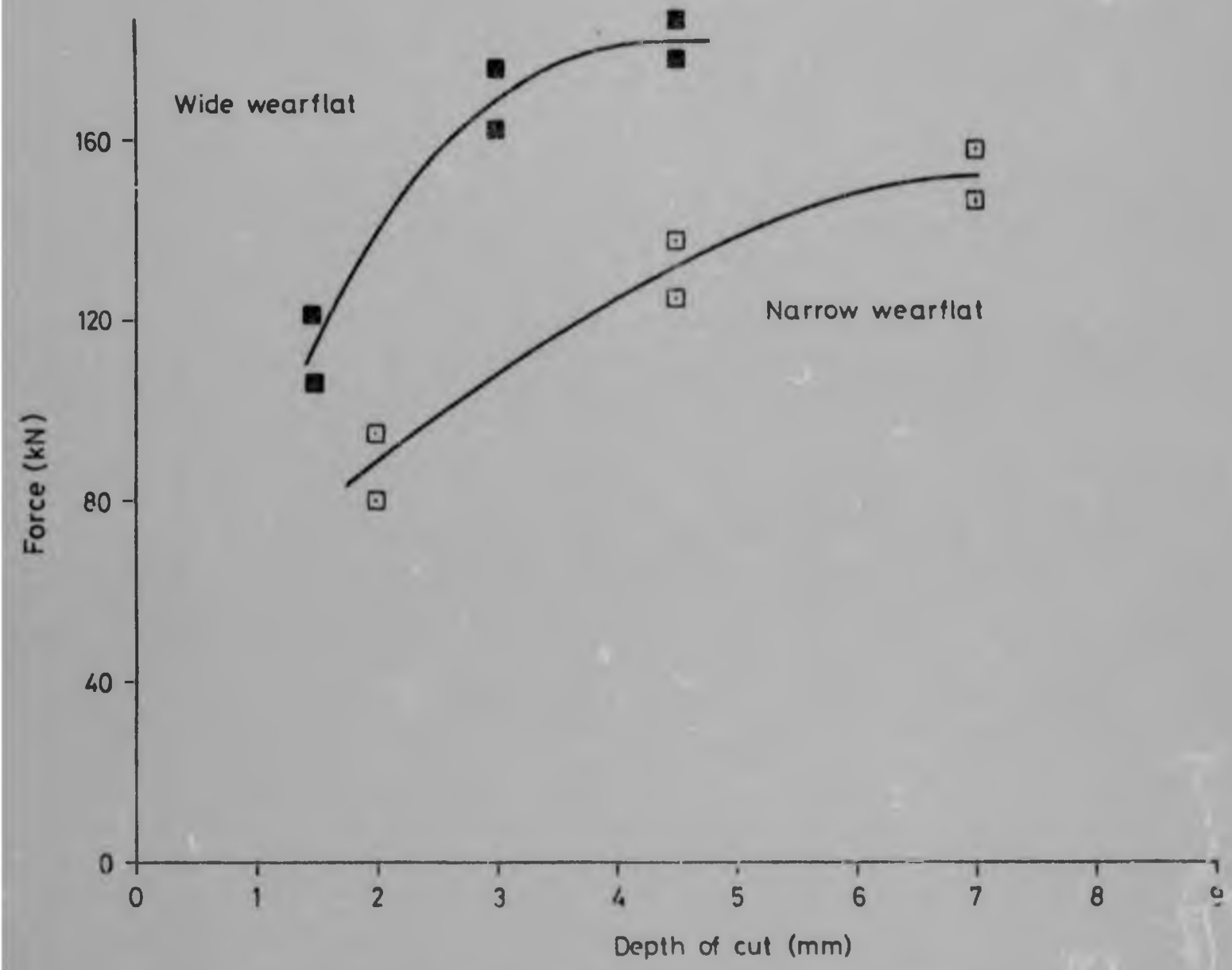


FIGURE 45 : Mean bit penetrating force using a standard wearflat and a narrow wearflat bit.

rock which resulted in the formation of rock chips ahead of the bit. Thus the bit cutting force was always applied together with the bit penetrating force and the bit resultant force was reacted along the base of the tungsten carbide inserts (Figure 5 b). Bit failures caused by fracturing of the tungsten carbide did not occur during the laboratory experiments. Underground, slots were cut in fractured rock which commonly broke away from in front of the bit. In this situation, a load or cutting force was applied to the leading face of the inserts when no penetrating force was applied to the bit. This induced bending stresses into these inserts and caused them to fracture.

Therefore although laboratory tests had demonstrated that the components of the peak and the mean forces were reduced, underground experiments had revealed a fundamental weakness in the design of such bits. Consequently experiments with narrow wearflat bits were not continued.

6.3.2 Vibration of the bit

The principle of operation of a rockcutting machine utilises a ram to move a saddle along a fixed slide, (Figure 2). It was anticipated that the vibration of the saddle during the cutting stroke of the machine would be increased if the compliance of the hydraulic drive to the saddle was increased. Experiments were conducted using a 'stiff' and a 'compliant' machine drive in order to measure any change in the saddle vibration. Attention was paid to the measurement of the force components acting on the bit with these two machine drives, to investigate whether these forces were affected by the saddle vibrations.

Previous investigations had shown that when an impacting action fromanexternal hammer, was superimposed on a drag bit while cutting in strong rock, a marked decrease in the bit force was observed at the start of the groove, (Hood 1973), (Powell 1974). This effect was found to decrease as the groove was deepened, and in deep slots the bit force was found not to be affected significantly by impacting of the bit. The experiments that were conducted for this project, using a compliant machine drive to introduce vibration through the saddle to the bit, were designed to investigate whether the impacting action superimposed on the bit by this vibration was sufficient to affect the forces acting on the bit.

A calculation to show how the stiffness of the hydraulic drive to the rock cutting machine was reduced, by increasing the operating pressure of the system and by reducing the flow rate of the hydraulic fluid, so that the machine was driven at the same speed and with the same effective force, is given in Appendix (iii).

When the compliance of the hydraulic drive to the rockcutting machine was increased a pronounced increase in the vibration of the saddle was observed. This is best illustrated by a study of two extracts from the chart recordings which were made at the same depth of cut with both a stiff hydraulic drive (Figure 46), and a compliant hydraulic drive,(Figure 47). These traces represent measurements of the force components, the hydraulic pressure in the machine main cylinder and the instantaneous velocity of the blade.

From these Figures it is evident that the frequency of the instantaneous blade velocity trace was much higher when the compliant

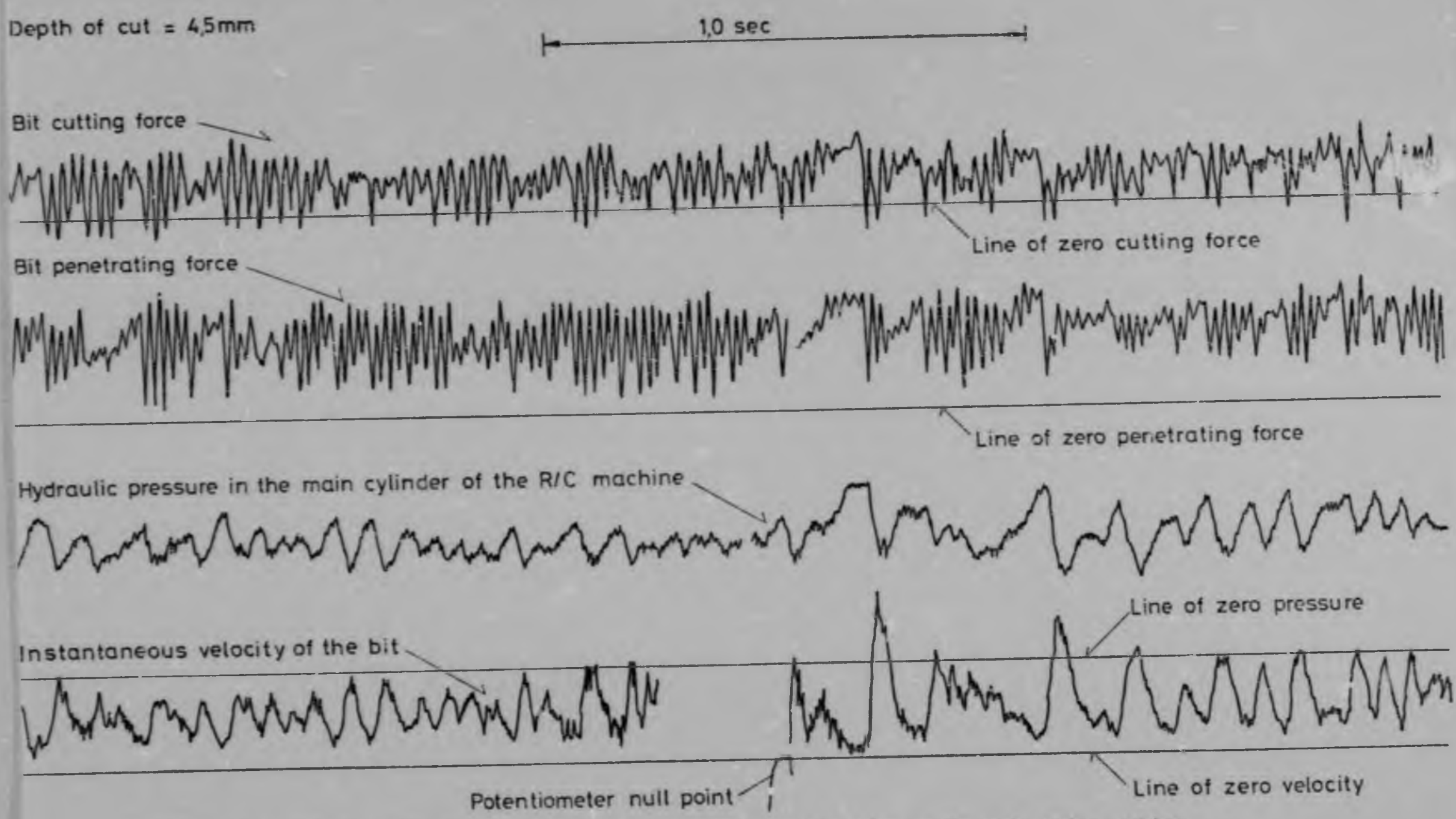


FIGURE 46 : Extract from chart recording using a stiff hydraulic drive to the rockcutting machine.

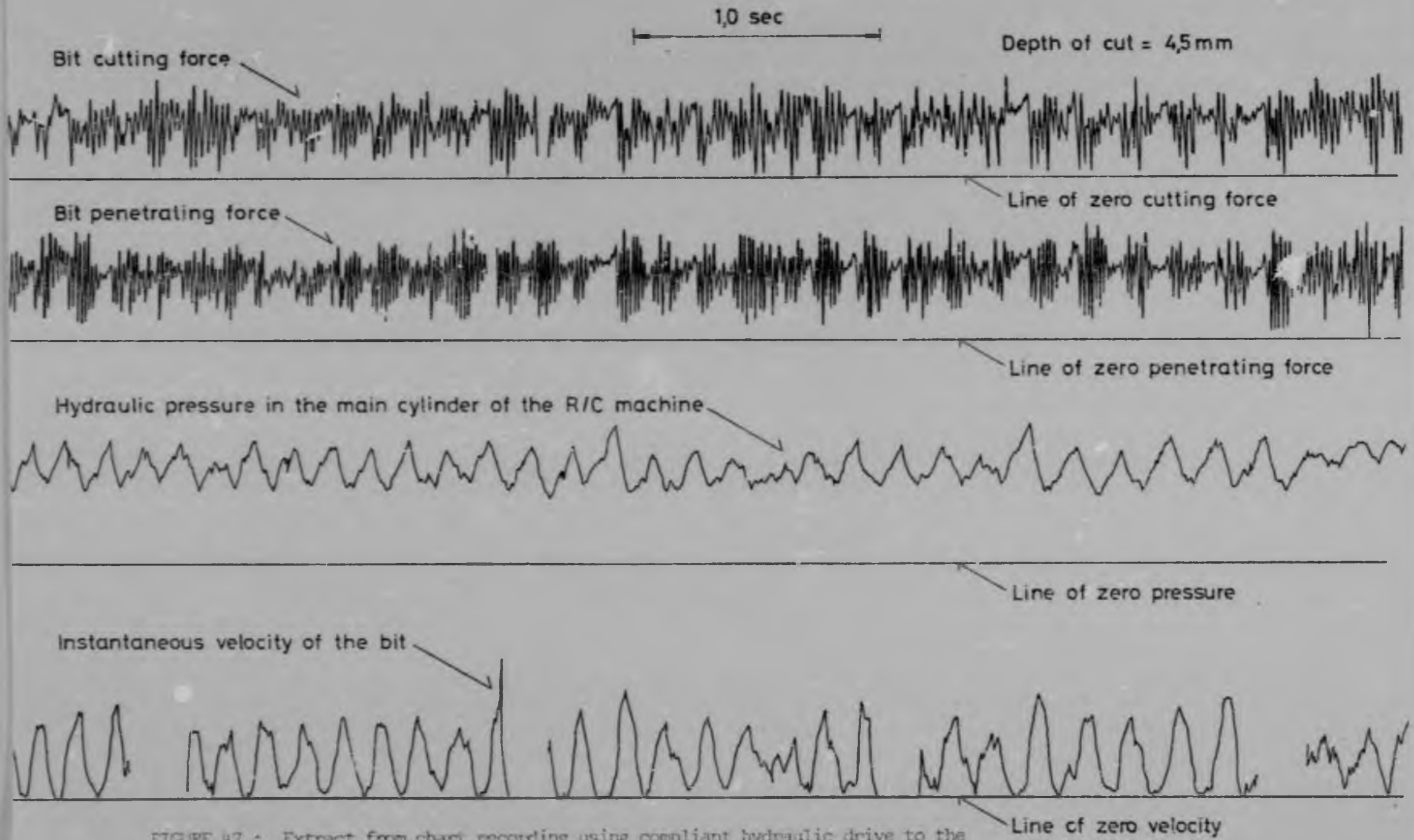


FIGURE 47 : Extract from chart recording using compliant hydraulic drive to the rockcutting machine.

hydraulic drive was used. This drive caused the frequency of the instantaneous velocity trace to be reduced from approximately 10 Hz to about 6 Hz and the oscilliatory component to be increased from about 110 mm/sec to about 170 mm/sec. A change in the mean value of the instantaneous velocity was observed also, the higher mean velocity was recorded when the stiff hydraulic drive was used.

The use of a stiff or a compliant drive to the rockcutting machine was found not to affect the bit cutting force, (Figures 48 and 49). The bit penetrating force was found to be somewhat lower when the compliant drive was used, (Figures 50 and 51). The reduction of this force component was attributed to the higher frequency of vibration of the bit. The amplitude of these vibrations remained constant, therefore the higher frequency caused the velocity of 'impact' of the bit against the rock to be increased.

6.4.3 Pre-weakening the rock

It was considered that the quartzite country rock would be particularly suited to a form of thermal weakening, since quartz has a phase transition from α to β at a relatively low temperature, 573 degrees Celsius. High stresses are induced in the material following change in volume which takes place as a result of this phase transition, (Kanellopoulos and Ball, 1975). In addition it was anticipated that cracks might be induced by the differential thermal expansion and contraction due to temperature gradients within particles of rock.

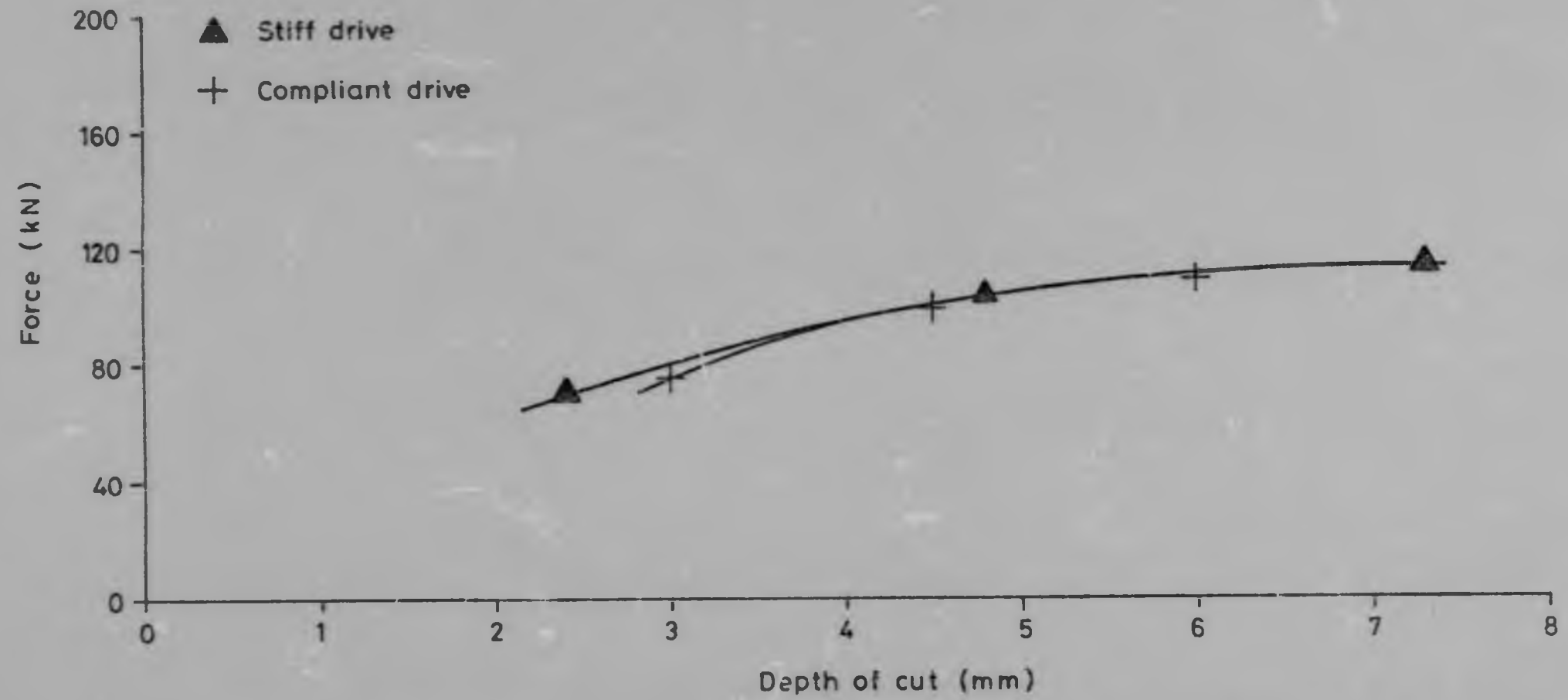


FIGURE 48 : Mean peak bit cutting force plotted against depth of cut, comparing a stiff hydraulic drive to the machine with a compliant hydraulic drive.

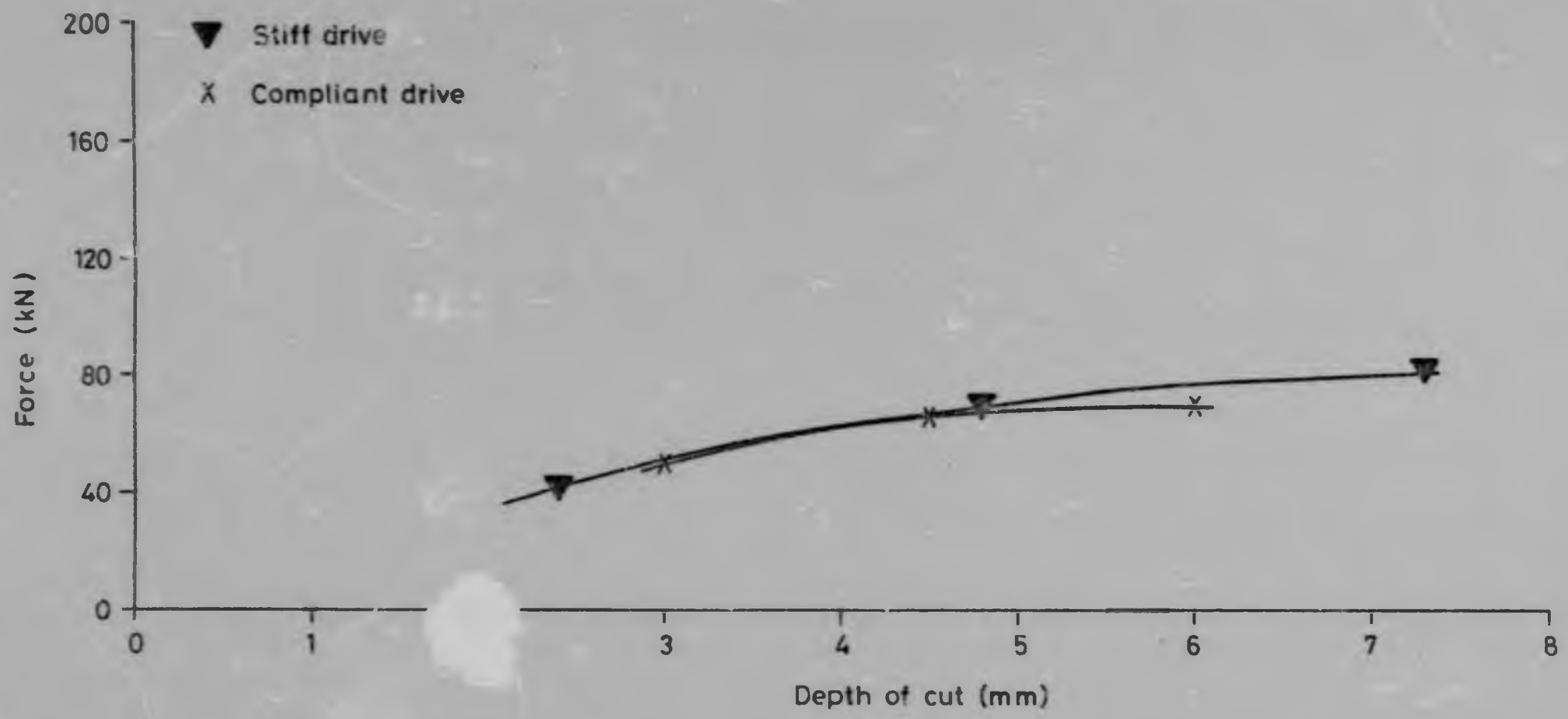


FIGURE 49 : Mean bit cutting force plotted against depth of cut, comparing a stiff hydraulic drive to the machine with a compliant hydraulic drive.

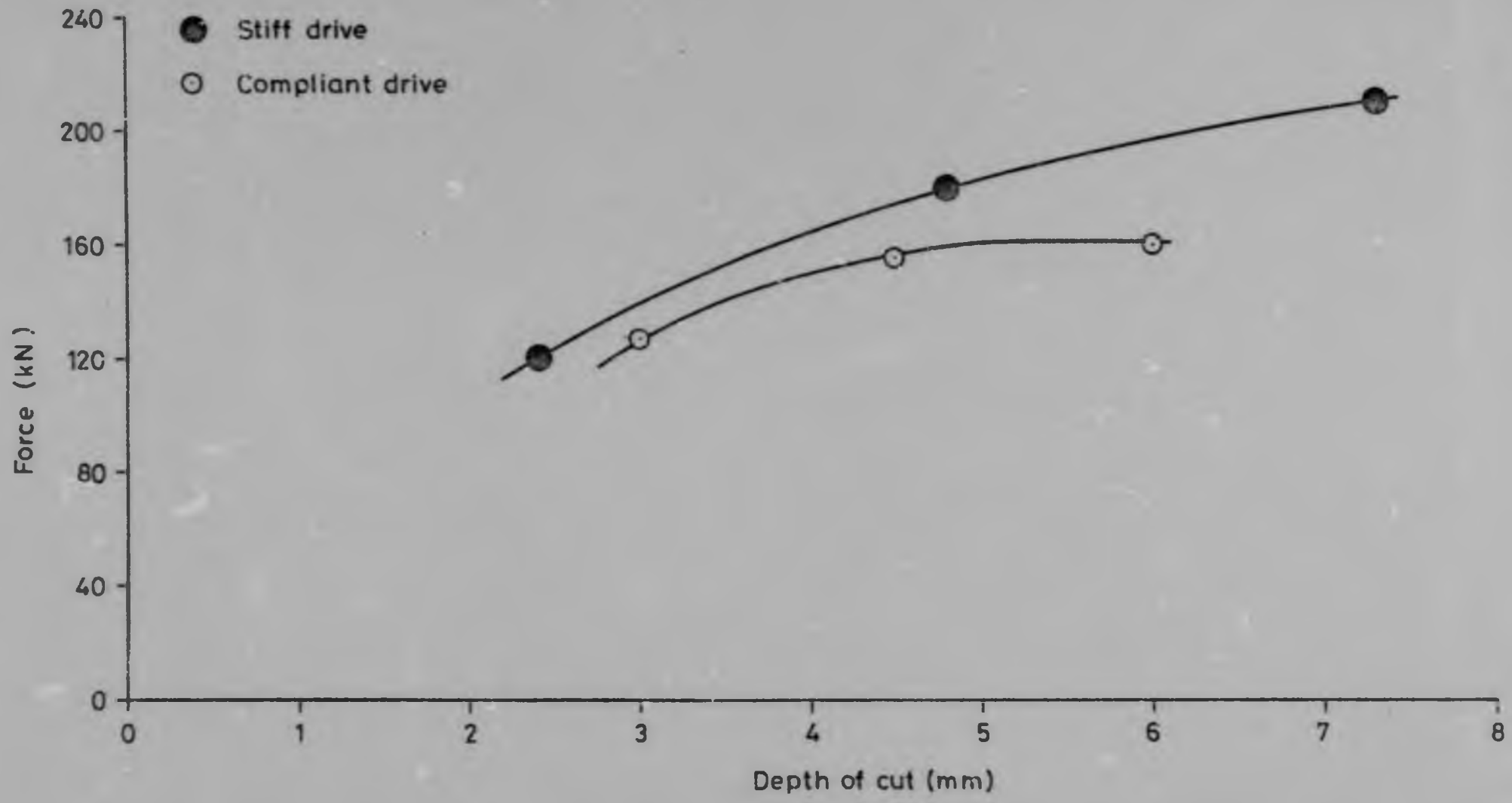


FIGURE 50 : Mean peak bit penetrating force plotted against depth of cut, comparing a stiff hydraulic drive to the machine with a compliant hydraulic drive.

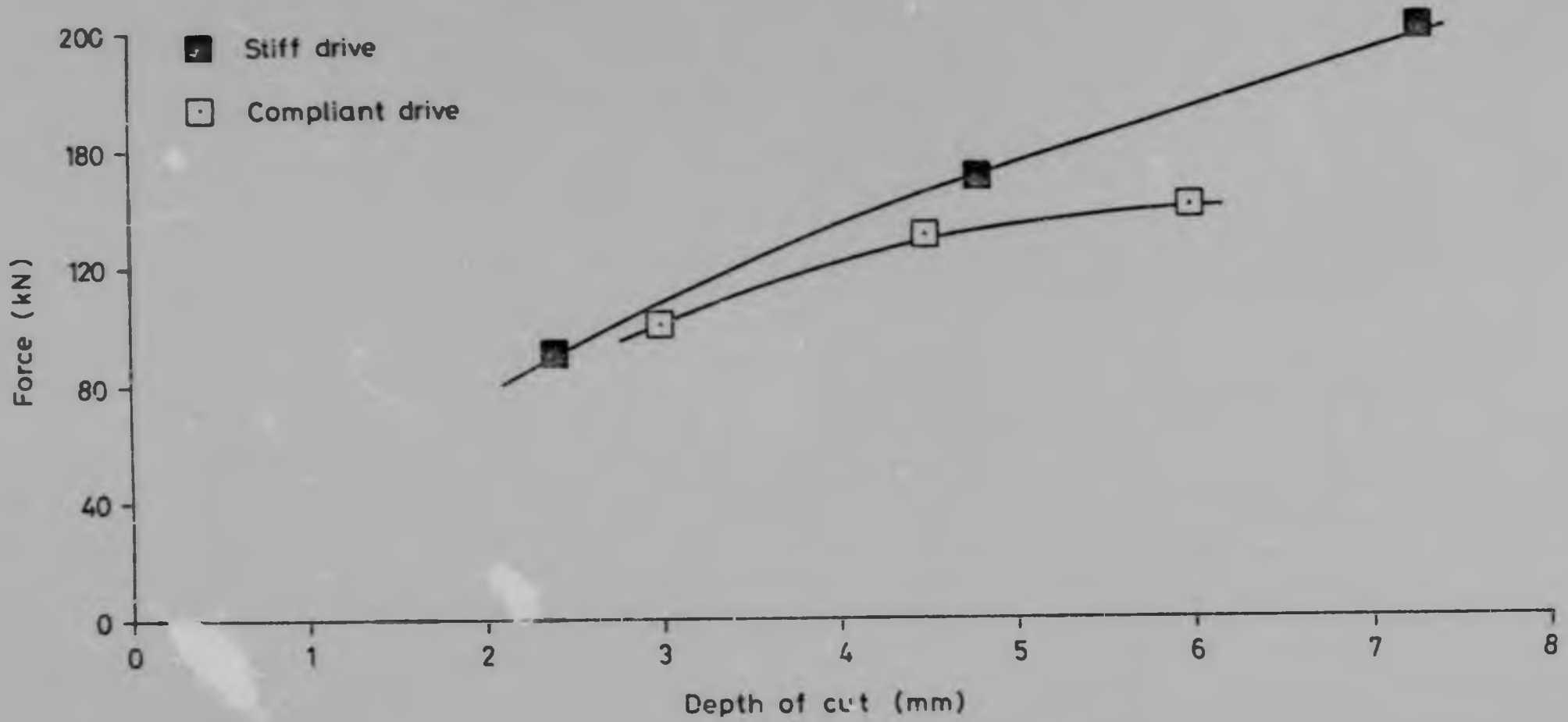


FIGURE 51 : Mean bit penetrating force plotted against depth of cut, comparing a stiff hydraulic drive to the machine with a compliant hydraulic drive.

A review of different techniques available for thermal weakening of rock was published by Lauriello and Fritsch, (1974). These authors examined a wide variety of equipment, including electron beam guns, lasers and flame torches. They concluded that 'the jet torch shows the most promise for heat weakening hard rock in open excavations. Additional cost penalties would be incurred for ventilation in tunnelling applications ...'. The advantages of this method were, the low cost of the equipment and the low cost of the fuel. In addition, the rock breaking process is not one of melting, which is relatively inefficient, instead rock chips are formed using this torch and these are removed from the heated zone by the high flame velocity.

Therefore, this equipment was selected for experiments to investigate the feasibility of pre-weakening the quartzite country rock in the gold mines. Calculations were made prior to conducting these experiments to enable an estimation of the rate at which heat is generated using this equipment. These computations (Appendix iii), showed that the amount of heat required to cause the rock to spall and to cut a slot, using jet channeling equipment without the assistance of a mechanical tool, was unacceptably high for underground applications in deep-level mines. However, it was anticipated that the rock might be weakened using far less heat. Therefore experiments were conducted to investigate the effect of thermal rock weakening using a jet channeling torch, with special attention paid to the heat required to cause damage to the rock.

This experiment was carried out in an unused section of a gold mine. The equipment was operated in a 'travelling way' at about 1 000 m below surface. Tests were conducted to ascertain how effect-

ively the rock on the sides of the raise was weakened by the flame from the jet channeling torch. A petrographic analysis showed that the rock in this raise had a high quartz content, up to 90 per cent. For this reason, because of the volume change associated with the phase transition at a relatively low temperature, this was considered to be a good test site.

A commercially available torch, of the type used commonly in quarrying applications, was used for these tests. The principle of operation of the torch is to ignite a fine spray of the fuel, kerosene, with oxygen in a water cooled combustion chamber. The hot gases pass through a divergent nozzle which increases the gas velocity to about 1 500 m/sec. The temperature of the flame at the nozzle exit is about 2 000 degrees Celsius. The resulting high velocity, high temperature gas stream is directed against the rock, with the torch nozzle some 0,6 m from the rock surface.

The procedure followed was to use a metal bar to remove all of the visibly fractured rock from the face before igniting the torch. The torch was then lit (Figure 52), and directed towards the rock face for a given period of time, (Figure 53). An estimate was made of the amount of rock that spalled from the face when the heat was applied. The metal bar was then employed to remove rock from the face which had been weakened as a result of thermal damage. This technique did not allow accurate calculations of the energy required to remove a given volume of rock, but it did enable an estimate of the heat required to spall the rock and of the heat necessary to cause appreciable damage to the rock.



FIGURE 52. Igniting jet channeling torch.



FIGURE 53. Weakening the rock using a jet channeling torch.

The rate of rock removal, in terms of rock chips spalling from the face during the heating operation, was far lower than had been anticipated in view of the high quartz content of the rock. This was attributed to the rock in the raise being fractured, because of the induced stresses (Section 3.1), and therefore the conduction of heat through the rock was reduced by air gaps in the rock mass. Consequently the use of this torch in this situation was not promising.

However, it was shown that the application of heat to the rock surface did result in a significant weakening of the rock. It was possible using a metal bar, to remove large rock fragments about 300 mm in diameter and 100 mm thick, from the face after a few traverses along the face with the torch. The heat required to cause this type of damage to the rock only needed to be applied intermittantly and it was estimated that when the overall heat applied was about 100 kW the rock could be broken from the face consistently using the metal bar.

It was concluded that this equipment could find an application for weakening the rock ahead of a drag bit, provided that it was used only for short periods of time to minimise the heat input into the stope. However, environmental problems of noise and the formation of gases, as a result of burning sulphides that are present in the rock, motivated the investigation of alternative techniques to reduce the bit forces before proceeding further with thermal rock weakening experiments.

6.3.4 Directing a 'flat-fan' water jet towards the bit

A previous experiment using a high volume, low pressure water jet to cool the bit during the cutting operation, had shown that not only were the temperatures in the bit reduced markedly by the use of the water jet, but the oscillation amplitude of the components of the bit force had been reduced also, (Section 6.1.1). The potential for providing adequate cooling to the bit and reducing the peak force by decreasing the amplitude of the force components, prompted further experiments with a water jet directed towards the bit.

The pressure of the water jet used for these experiments was 8 MPa. The object of using a 'high pressure' jet was an attempt to provide efficient flushing of rock chips from ahead of the bit. Because the higher pressure enabled the jet to be directed more accurately at the interface between the bit and the rock, the water flow rate for these experiments was reduced to 0,67 ℓ/sec per second from 2 ℓ/sec which had been used during the earlier tests, (Section 6.1.1).

The water was directed through a nozzle which consisted of an orifice aimed at a curved plate, (Figure 54). The water therefore struck the plate and formed a 'flat-fan' water jet. The nozzle was mounted on a block which was fitted to the blade, such that the 'fan' water jet covered the full 35 mm thickness of the tungsten carbide bit inserts, (Figure 55). The water jet was directed along the leading face of the inserts to impinge on the rock surface immediately ahead of the bit.



FIGURE 54. Nozzle for flat-fan water jet.

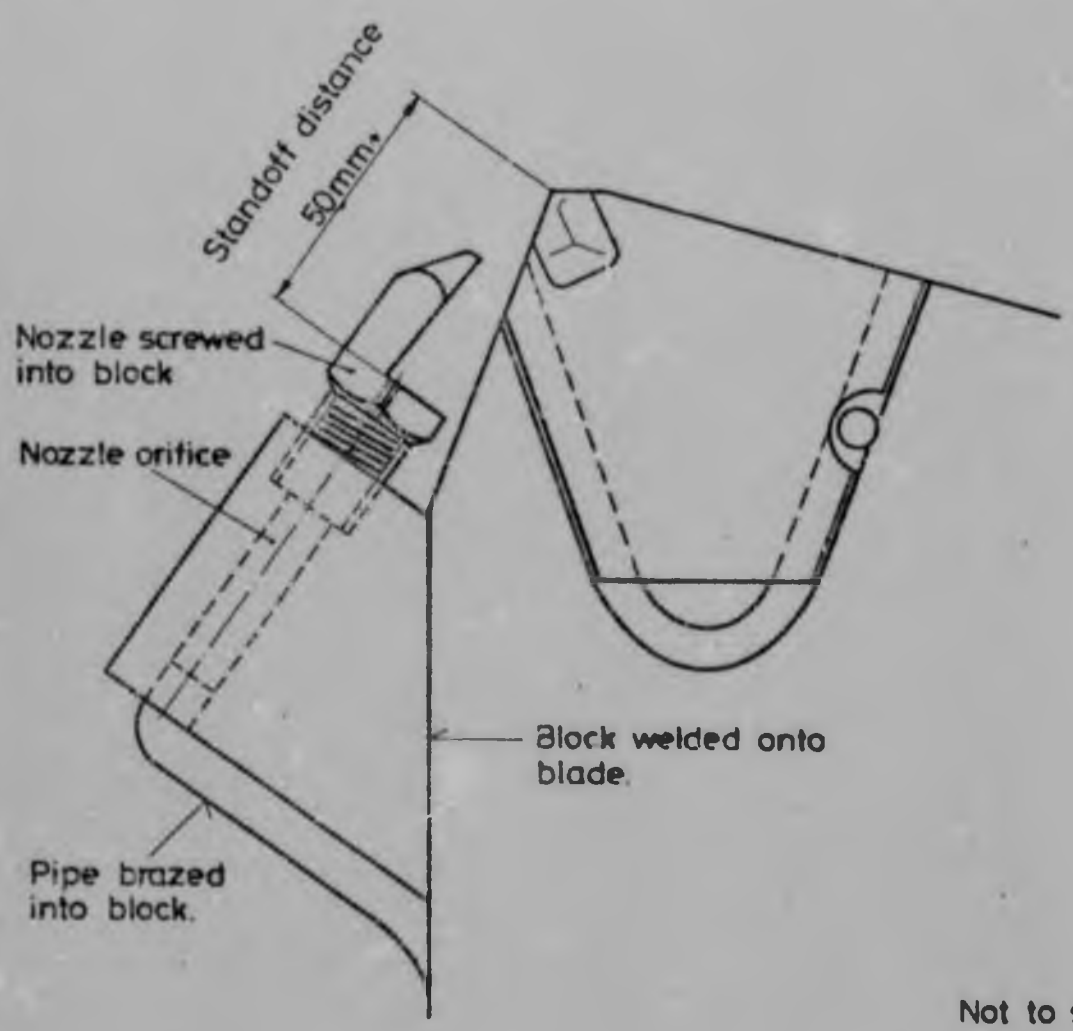


FIGURE 55 : Position of the nozzle relative to the drag bit.

A small reduction of the mean peak bit cutting force (Figure 56), but no appreciable difference in the mean bit cutting force (Figure 57), was measured when the fan jet was directed immediately ahead of the bit. This reduced amplitude in the oscilliatory component of the cutting force trace was similar to that measured using a high volume, low pressure water jet, (Section 6.1.1). The peak and also the mean values of the bit penetrating force showed significant reductions when the water jet was used, (Figures 58 and 59). This result differed from those obtained during the other experiments with a water jet directed towards the bit during the machine cutting stroke (Section 6.1.1), in that throughout this test the mean bit penetrating force was reduced markedly,(Figure 59).

6.4 The use of 'coherent' water jets to assist the cutting operation

The techniques used to reduce the mean values of the bit force, in some cases had shown inherent disadvantages. The field tests using bits with narrow wearflat tungsten carbide inserts had shown that the inserts had a tendency to fracture in the mining situation. The laboratory experiments using a machine with a compliant hydraulic drive had shown that the saddle vibration was increased and lower bit penetrating forces were measured with this system. Nevertheless, the basic problem of thermal deterioration of the bit during the cutting operation was not solved. The results from the experiment using a 'flat-fan' water jet demonstrated that the mean bit forces could be reduced using water jets directed ahead of the bit. In addition, previous experiments had shown that temperatures generated in the bit during the cutting process were reduced considerably with water

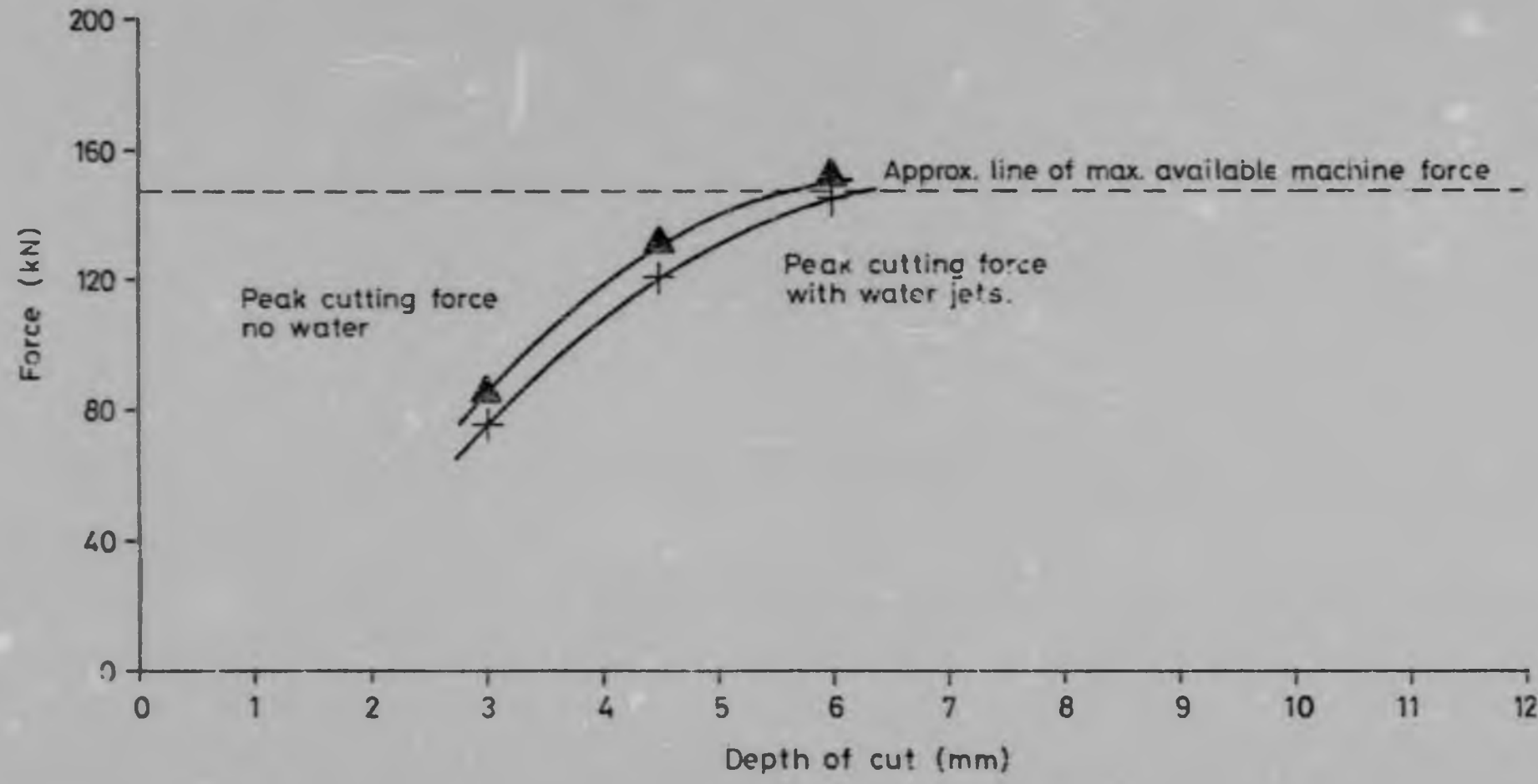


FIGURE 56 : Mean peak bit cutting force plotted against depth of cut, with a 'flat-fan' water jet and with no water jets.

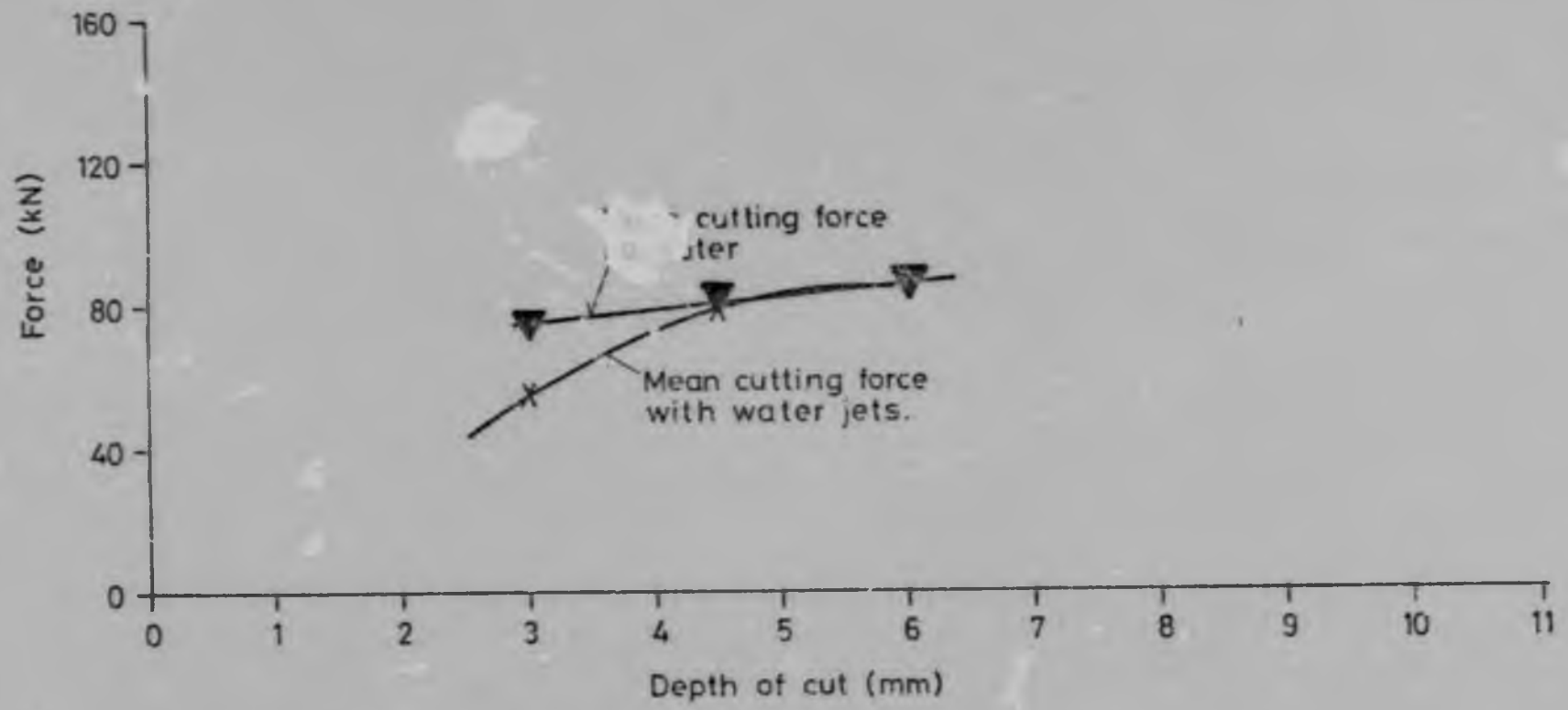


FIGURE 57 : Mean bit cutting force plotted against depth of cut, with a 'Flat-fan' water jet and with no water jets.

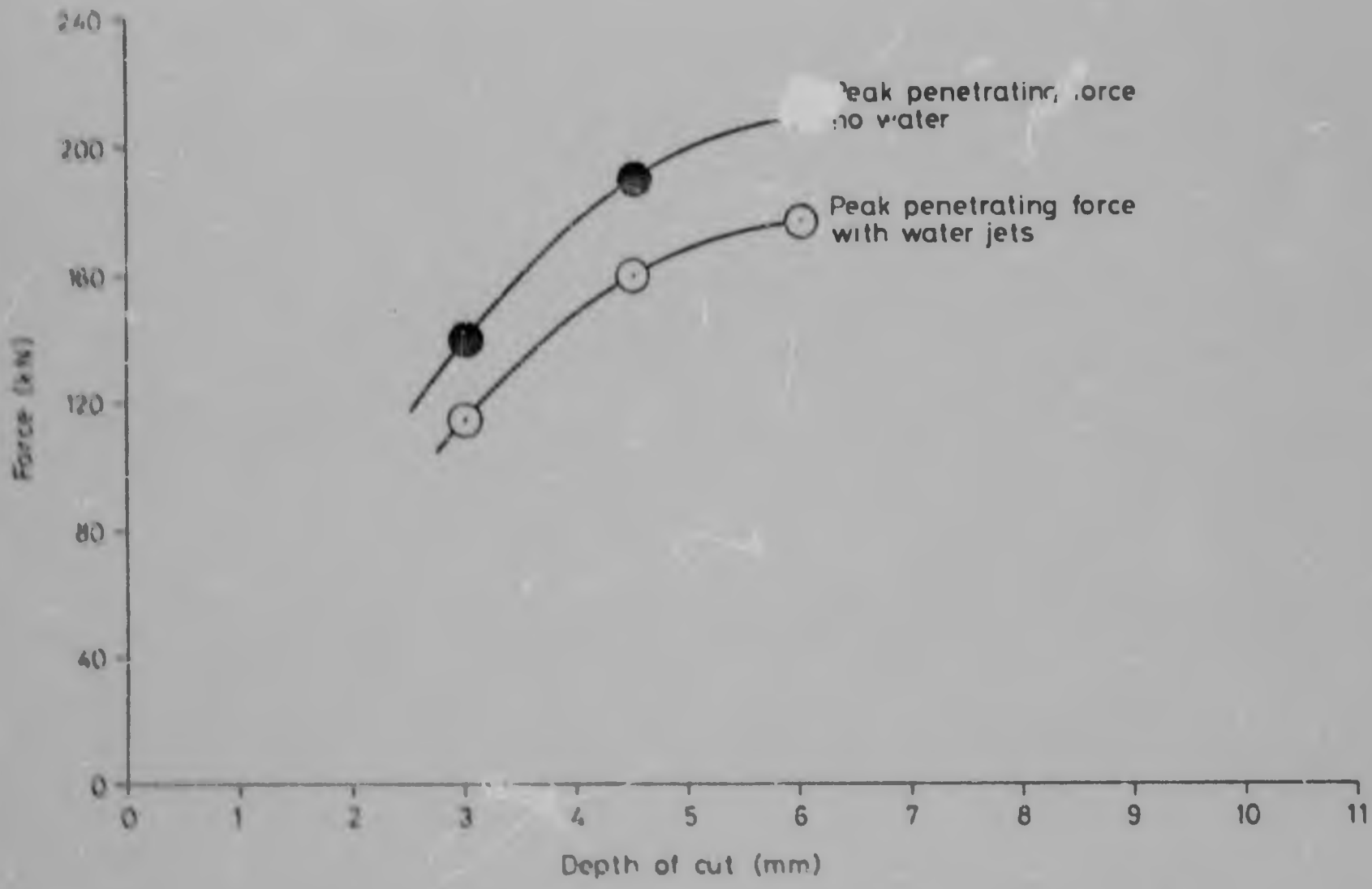


FIGURE 10 : Mean peak bit penetrating force plotted against depth of cut, with a 'flat-fan' water jet and with no water jets.

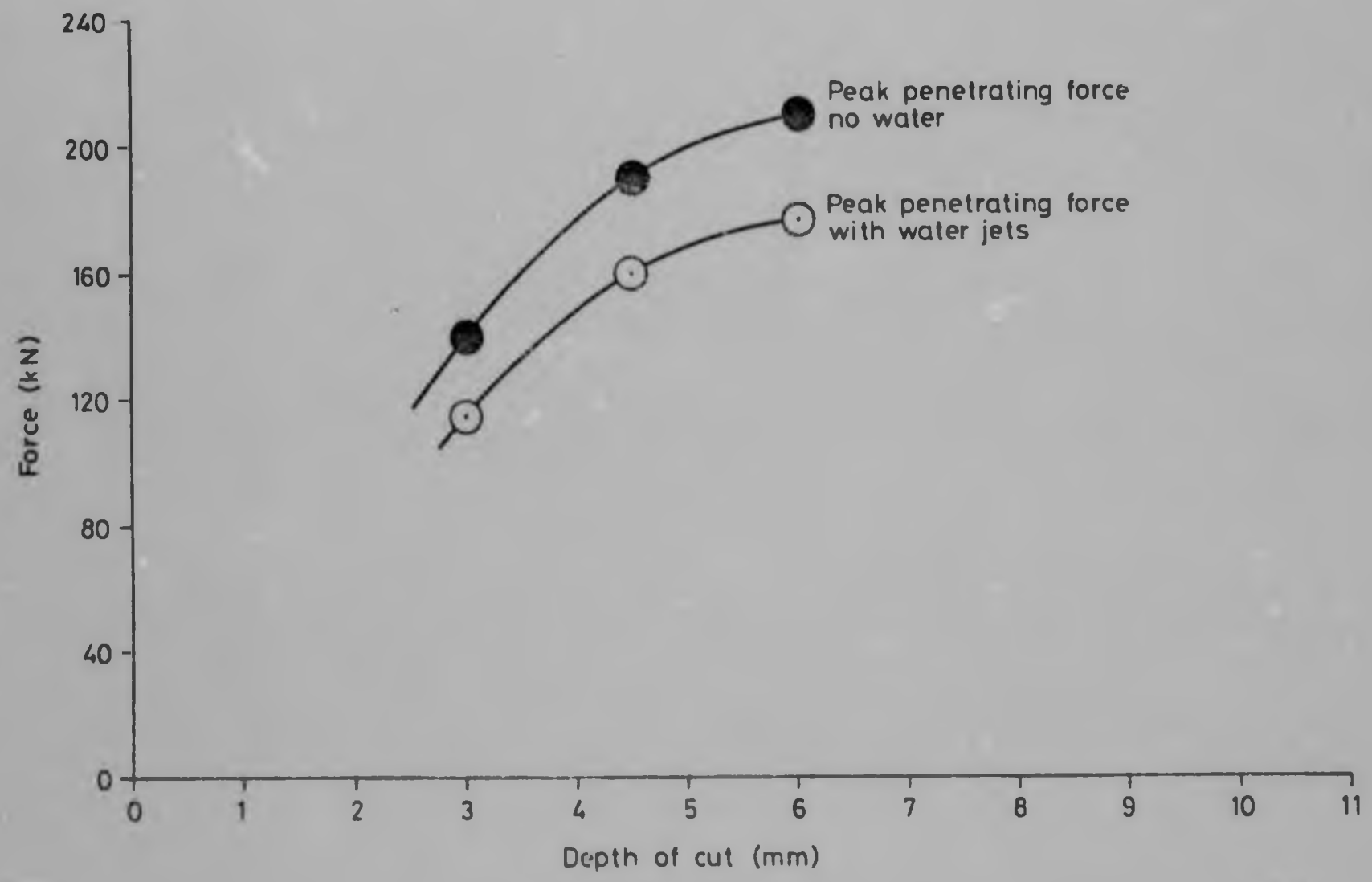


FIGURE 58 : Mean peak bit penetrating force plotted against depth of cut, with a 'flat-fan' water jet and with no water jets.

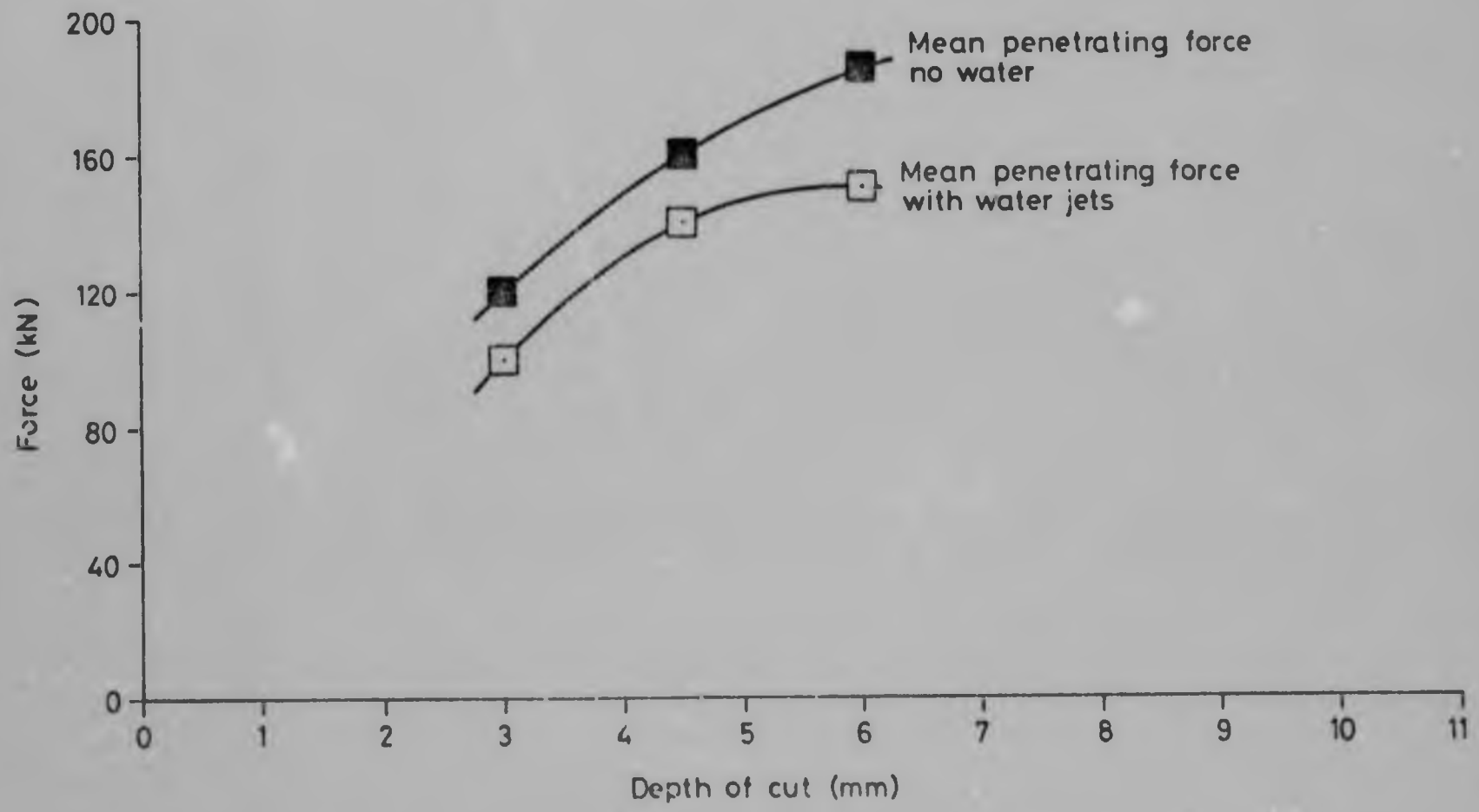


FIGURE 59 : Mean bit penetrating force plotted against depth of cut, with a 'flat-fan' water jet and with no water jets.

jets directed towards the bit, (Section 3.1). Therefore this approach, using high pressure water jets to assist the cutting operation, was considered as holding the most promise for the development of a system to reduce the force acting on the bit and to improve the overall life of the bit. Consequently, further experiments were conducted.

In order to obtain a maximum transfer of energy from the jets to the rock, 'coherent' water jets were employed. Parameters relating to the water jet which were assumed to be relevant to the decrease in the bit force values were : the pressure of the water jets, the point of impingement of the water jets, and the number of jets directed at the interface between the rock and the bit. These parameters were investigated systematically during this experimental investigation.

All of these experiments were carried out using 35 mm thick bits with a wearflat width of 6 mm. The use of thicker, 25 mm blades in conjunction with these bits made it possible to insert a pipe along the length of the blade in order to supply water to the rock ahead of the bit, without weakening the blade severely. A constant water flow rate through the nozzles of 0,67 ℓ/sec was used for these tests. This was not treated as a variable during these experiments since the constraints of the underground mining situation limited the volume of water that it is practicable to supply to a stope. Therefore, the water flow rate was chosen to conform with this requirement.

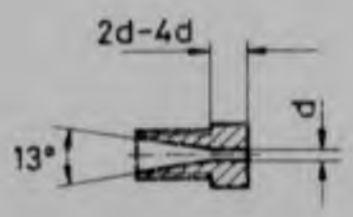
Another parameter which was not investigated during this test series was the distance between the nozzle orifice and the rock.

Previous experiments conducted by Leach and Walker (1966), had shown that the pressure behind a nozzle could be applied to a target one hundred nozzle diameters away without great losses. Consequently the experiments conducted during this test programme, at all times had the nozzles positioned closer than one hundred nozzle diameters from the point of impingement of the jets.

The design of nozzle used to form 'coherent' water jets is illustrated in Figure 60. In cross-section the nozzle had a convergent section with a small included angle, followed by a short parallel orifice section. Previous workers (Nikonov and Shavlovskii 1961), 'Leach and Walker 1966), have shown this to be the optimum nozzle geometry for generating 'coherent' water jets. The nozzles used for these experiments were screwed into a cylindrical chamber which was brazed onto the end of the pipe inserted in the blade, (Figure 61). Therefore, the impingement point of the water jets relative to the bit was controlled by varying the position of the nozzle holes in the cylindrical chamber.

6.4.1 Effect of water jet pressure

Experiments were conducted to investigate the influence of the pressure of the water jets on the bit forces. During these tests the jets were directed past the outside of the corners of the tungsten carbide bit inserts to impinge at the interface between the rock and the bit, (Figure 62a). This point of impingement of the jets relative to the bit was based on the findings by Riemann (1974), relating to the mechanism of fracture of strong rocks using drag bits. Riemann claimed that the leading face of the bit generally was not in contact with the rock during the cutting operation, (Section 2.2.). This implies



d = nozzle diameter

(a) Section through nozzle



Figure 60 : Nozzle used for coherent water jets.

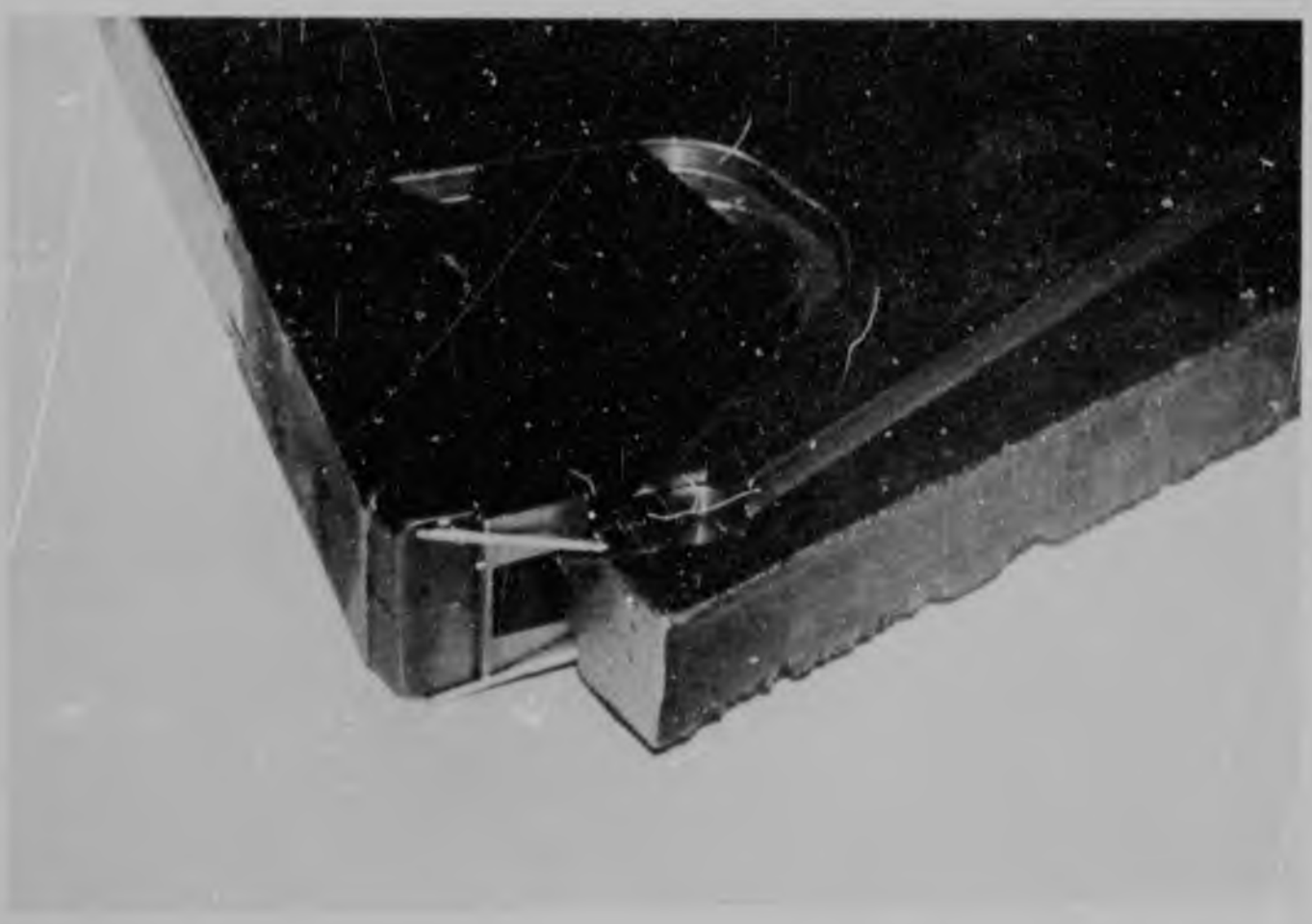
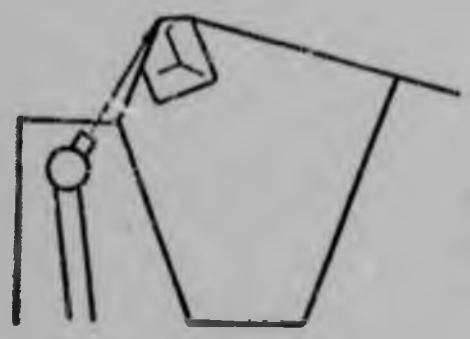
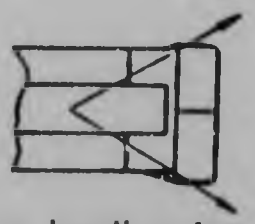


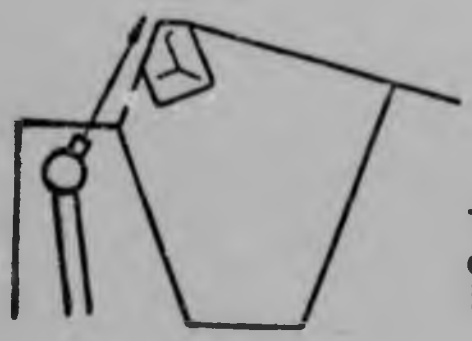
FIGURE 61. Method of mounting nozzles in the blade. White markers have been inserted into the nozzles to indicate the position of the water jets relative to the bit.



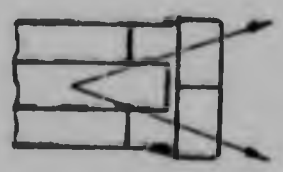
(a)



Two jets directed along leading face of the tungsten carbide inserts, outside the corners of the inserts.



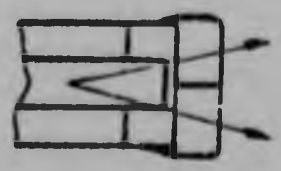
(b)



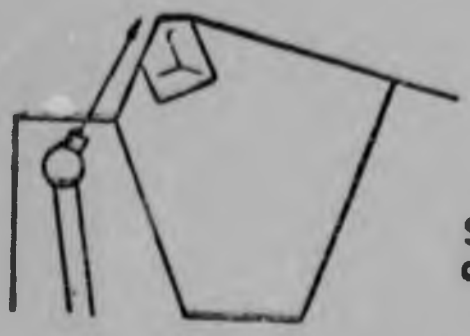
Two jets directed 2mm ahead of the tungsten carbide inserts, inside the corners of the inserts.



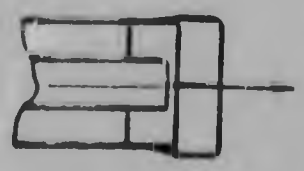
(c)



Two jets directed 10mm ahead of the tungsten carbide inserts, inside the corners of the inserts.



(d)



Single jet directed 2mm ahead of the tungsten carbide inserts, in the centre of the inserts.

FIGURE 62 : Diagram illustrating the different positions of the water jets relative to the bit.

that rock fracture is initiated underneath the bit wearflat which is equivalent to the fracture mechanism employed by a flat-bottomed indentor. It can be shown both mathematically and, by the use of photoelastic techniques, experimentally (Frocht, 1948), that severe stress concentrations are induced in an elastic material underneath the corners of a rigid punch, (Section 7.4). Therefore the water jets were directed towards the corners of the bit to attack the areas of high stress.

Measurements of the bit forces were recorded when water jets, with this nozzle configuration, were directed towards the bit at pressures of both 50 MPa and 10 MPa.

A comparison was made between components of bit cutting forces and bit penetrating forces, both with and without the assistance of 50 MPa water jets, (Figures 63 to 66). Figure 63 shows that the mean peak cutting force at 10,5 mm depth of cut with these jets directed towards the bit, was approximately the same as the mean peak cutting force at 4,5 mm depth of cut when no water jets were used. The values of the mean cutting force were also increased by a similar amount when the water jets were used, (Figure). The bit penetrating force was reduced to a greater extent than the bit cutting force by the use of these water jets. With these jets directed immediately ahead of the bit, values of the bit penetrating force which were measured at 10,5 mm depth of cut, were about the same as those measured at 2 mm depth of cut when no water jets were used. (Figures 65 and 66).

The results of the second series of cuts, which were carried out with the same nozzle configuration but with the pressure reduced to

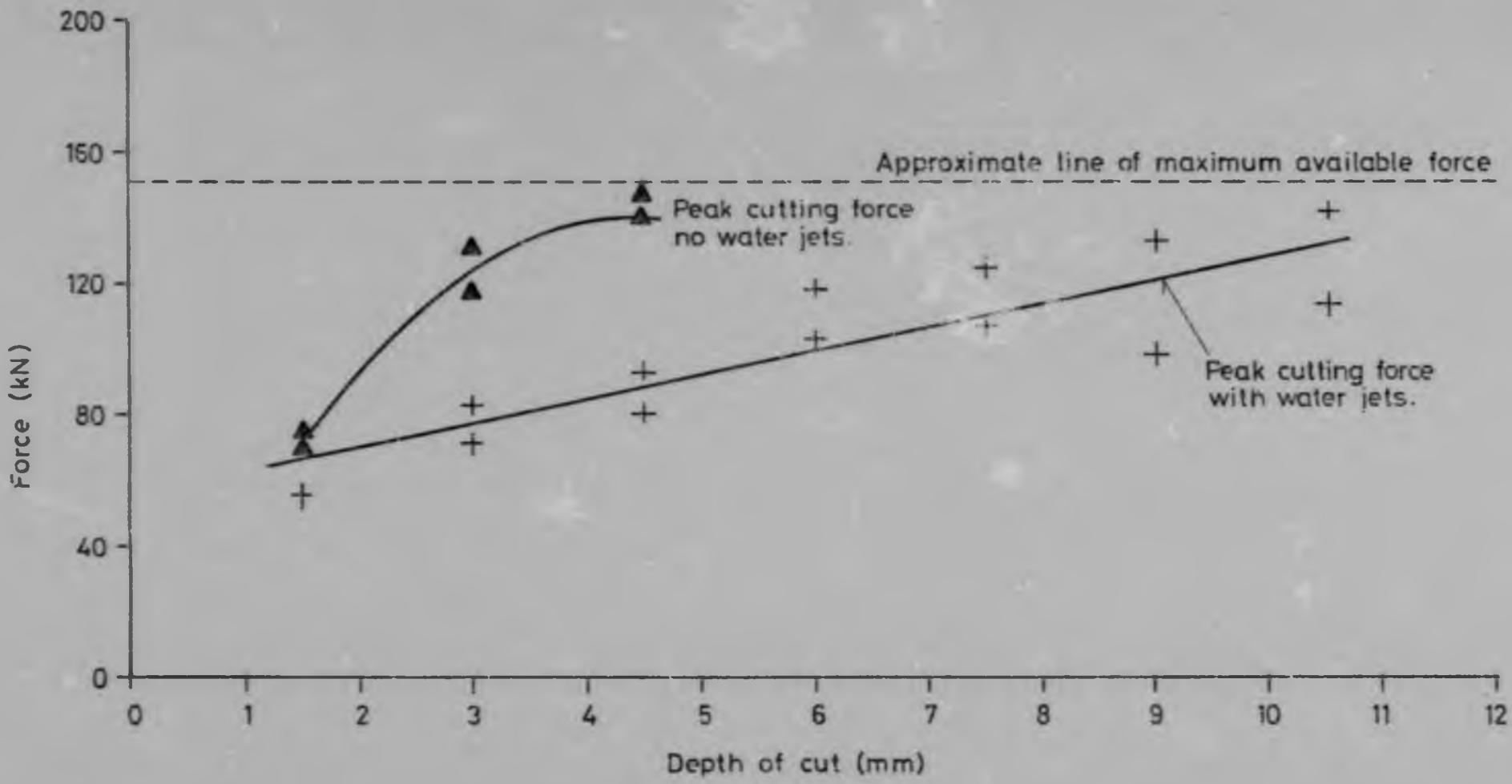


FIGURE 63 : Mean peak bit cutting force plotted against depth of cut illustrating the reduction of the force required to cut the rock with 50 MPa water jets directed ahead of the bit.

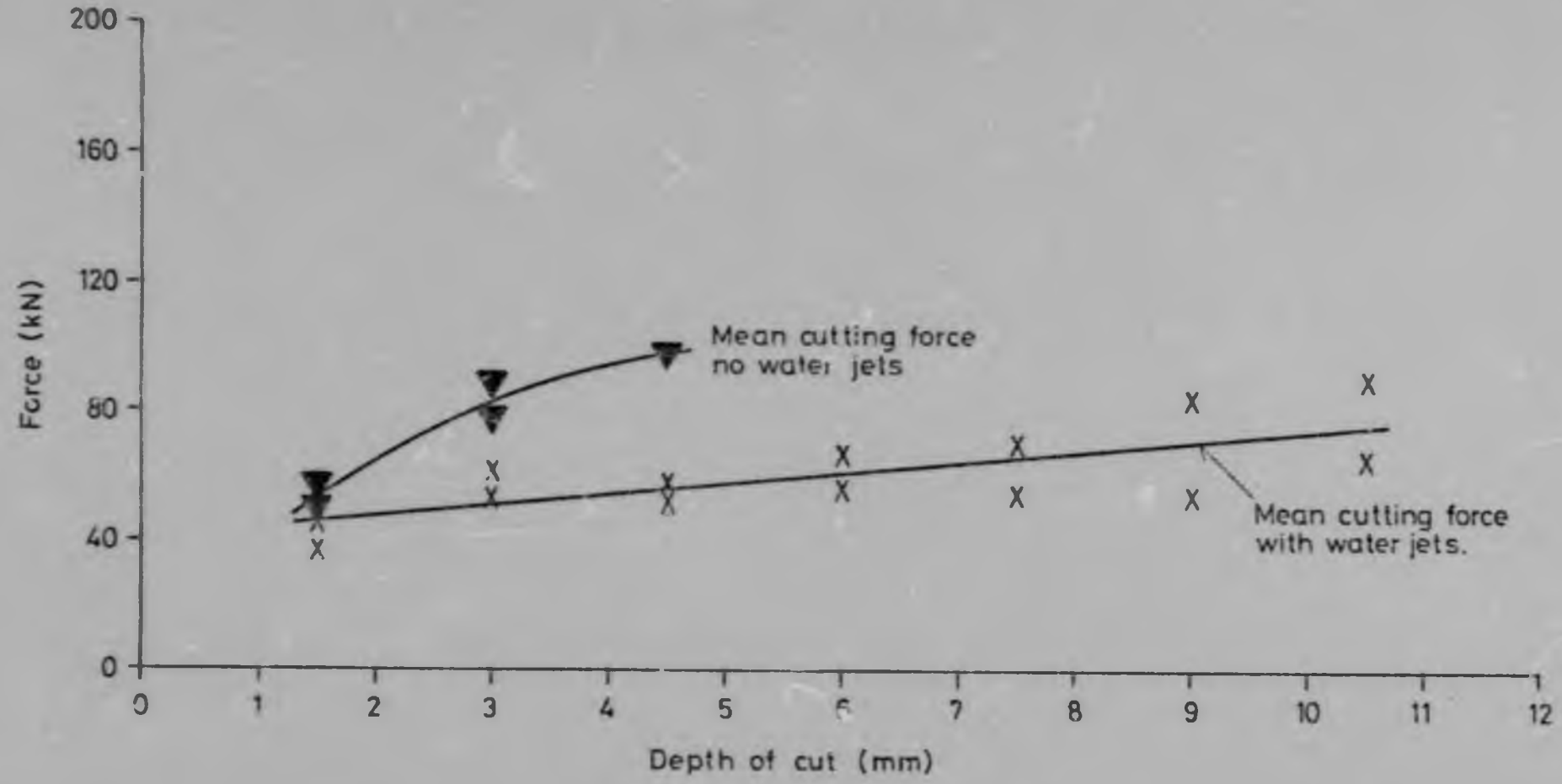


FIGURE 64 : Mean bit cutting force plotted against depth of cut illustrating the reduction of the force required to cut the rock with 50 MPa water jets directed ahead of the bit.

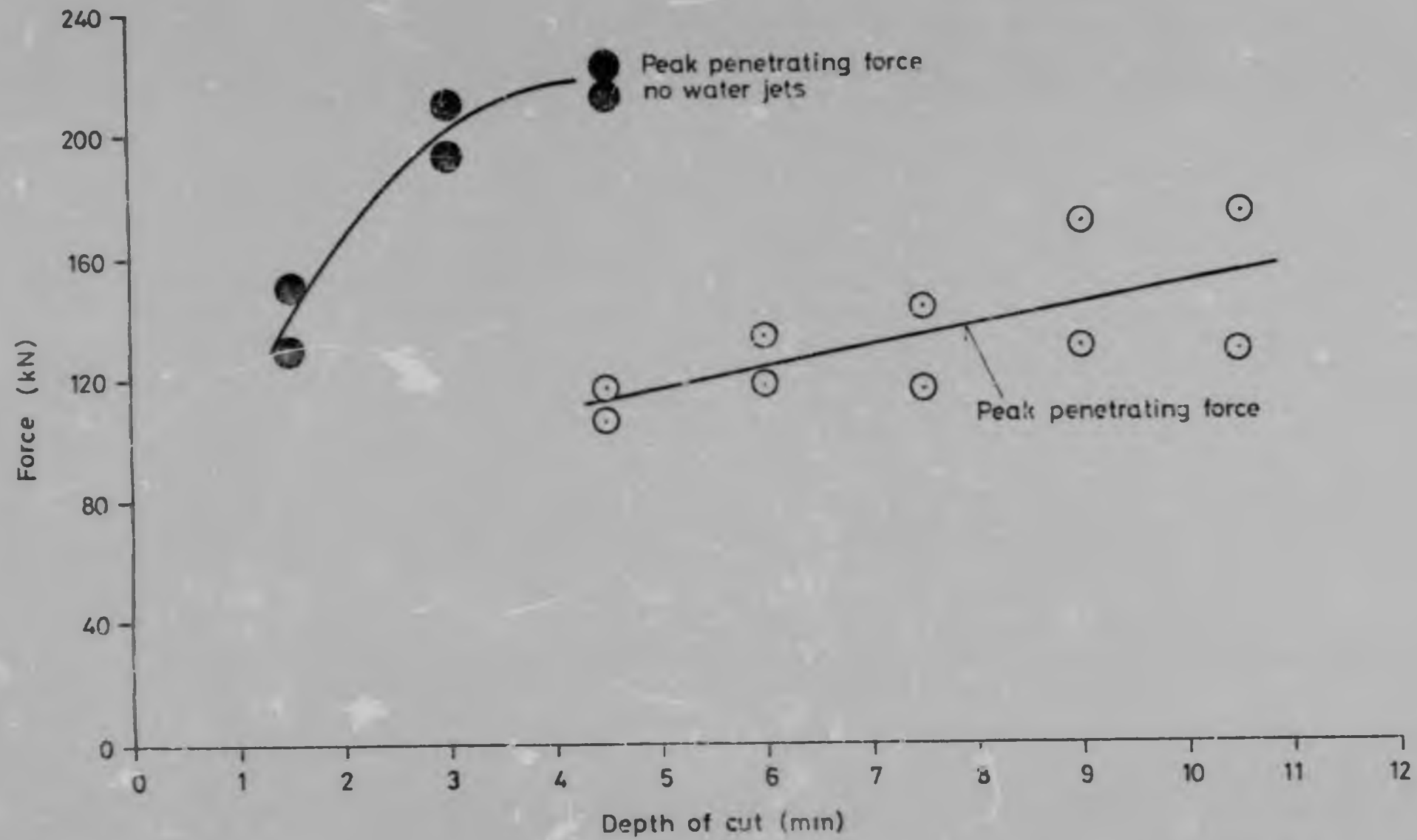


FIGURE 65 : Mean peak bit penetrating force plotted against depth of cut illustrating the reduction of the force required to cut the rock with 50 MPa water jets directed ahead of the bit.

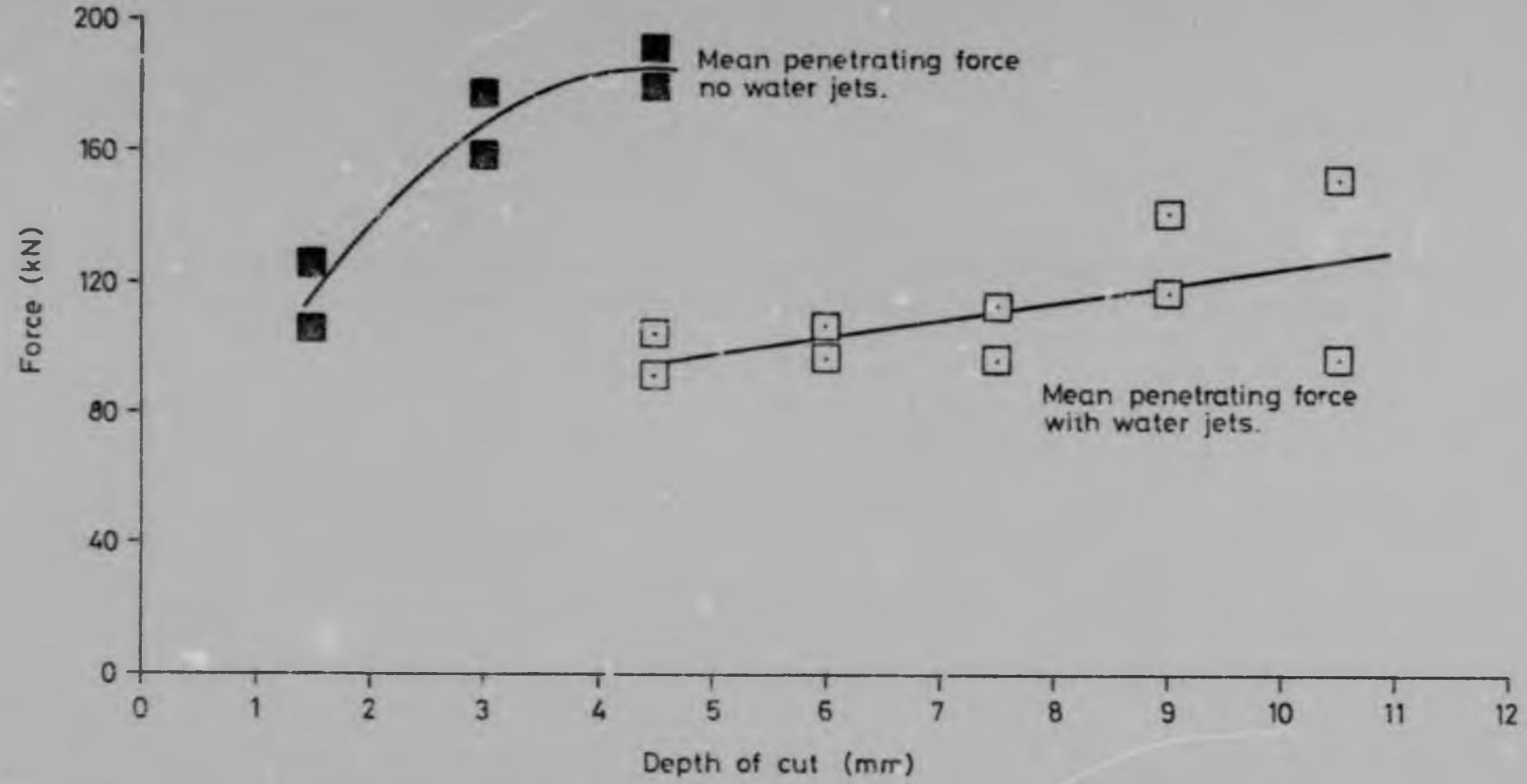


FIGURE 66 : Mean bit penetrating force plotted against depth of cut illustrating the reduction of the force required to cut the rock with 50 MPa water jets directed ahead of the bit.

10 MPa, are presented in Figures 67 to 70. The mean peak cutting force was halved when these jets were used, so that the maximum depth of cut doubled from 4,5 mm using no water jets, to 9 mm, (Figure 67). The mean cutting force was reduced significantly also (Figure 68), but not as effectively as when the 50 MPa jets were used, (Figure 64). Values of both the mean peak and the mean bit penetrating force were somewhat decreased by the use of the 10 MPa jets, (Figures 69 and 70). The reduction of this component of bit force was not nearly as marked as was observed when the 50 MPa water jets were used, (Figures 65 and 66).

Therefore the bit cutting force was decreased markedly when water jets were used to assist the cutting operation and the reduction of this force component was not influenced by the pressure of the water jets. On the other hand, the bit penetrating force was reduced dramatically only when the higher pressure jets were used.

6.4.2 Effect of direction of the water jets relative to the corners of the tungsten carbide bit inserts

In order to determine the importance of the direction of the water jets relative to the bit, an experiment was carried out with the nozzles aimed such that the jets struck the rock face approximately 2 mm ahead of the leading edge of the bit inserts. The included angle between the two jets was such that the jets struck the rock inside the corners of the tungsten carbide bit insert, (Figure 62b). Bit force measurements were recorded using water jets at a pressure of 10 MPa. These results were compared with bit force measurements using water jets at the same pressure directed outside

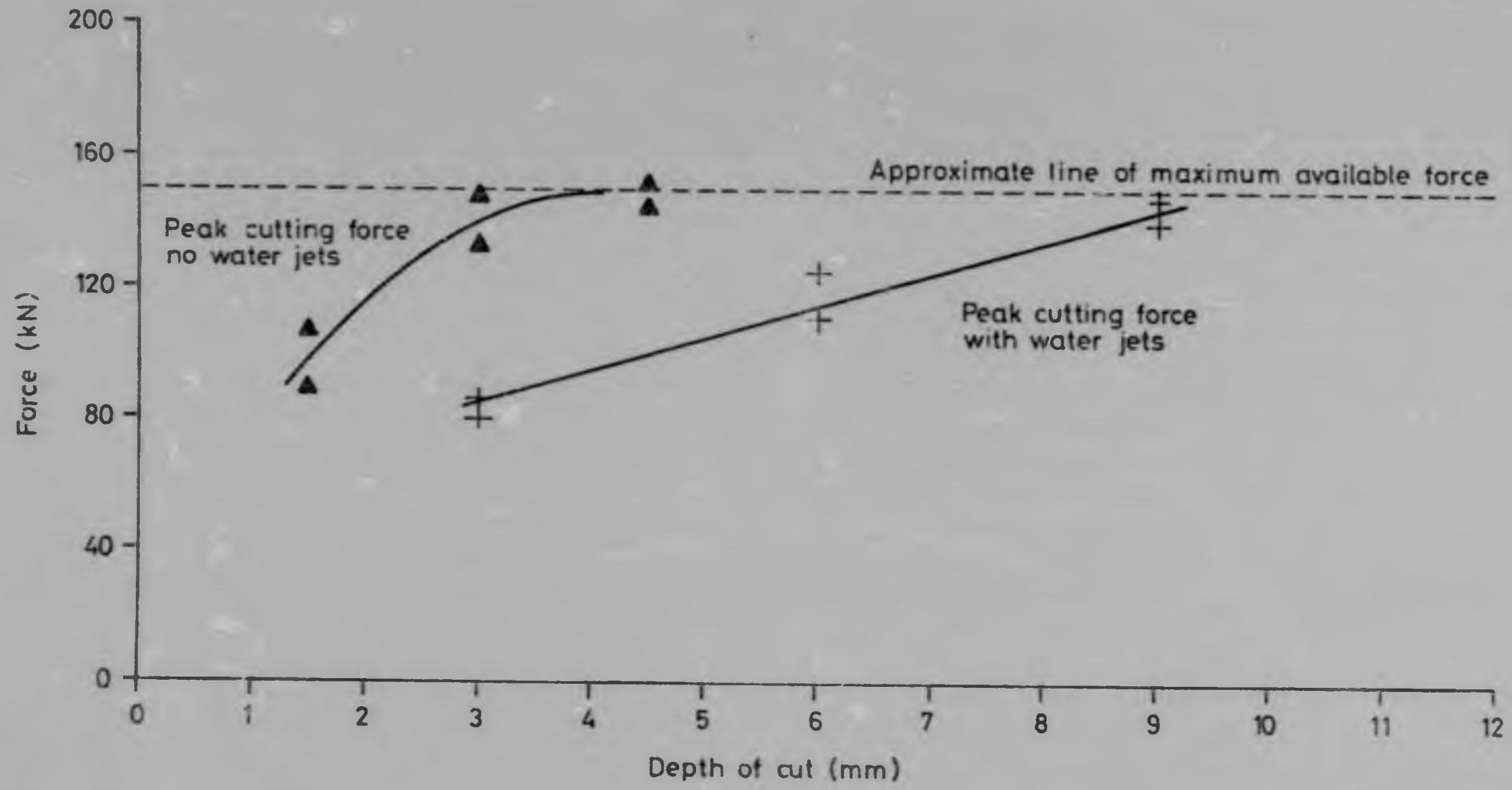


FIGURE 67 : Mean peak bit cutting force plotted against depth of cut, illustrating the reduction of the force required to cut the rock with 10 MPa water jets directed ahead of the bit.

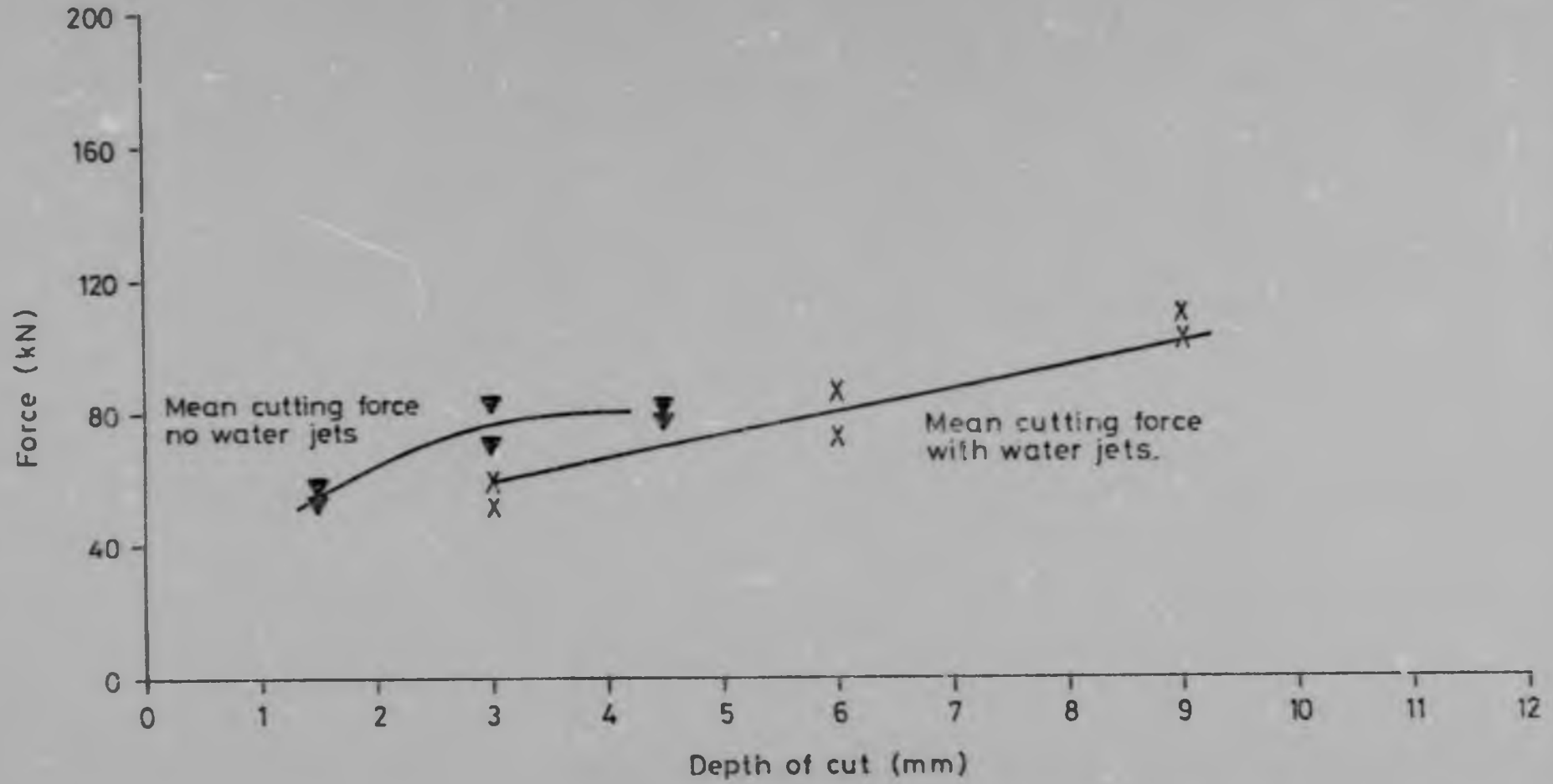


FIGURE 68 : Mean bit cutting force plotted against depth of cut, illustrating the reduction of the force required to cut the rock with 10 MPa water jets directed ahead of the bit.

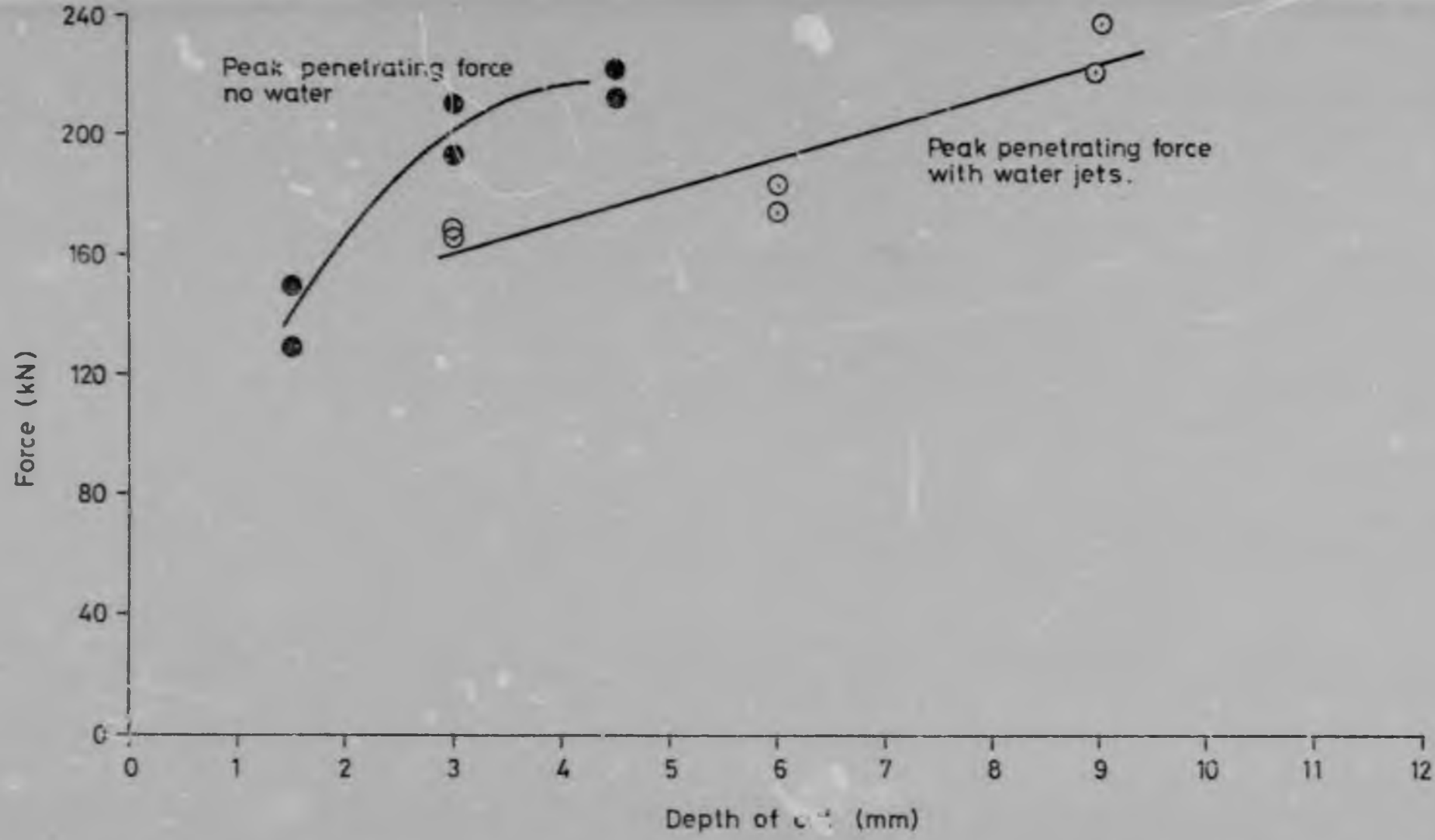


FIGURE 69 : Mean peak bit penetrating force plotted against depth of cut, illustrating the reduction of the force required to cut the rock with 10 MPa water jets directed ahead of the bit.

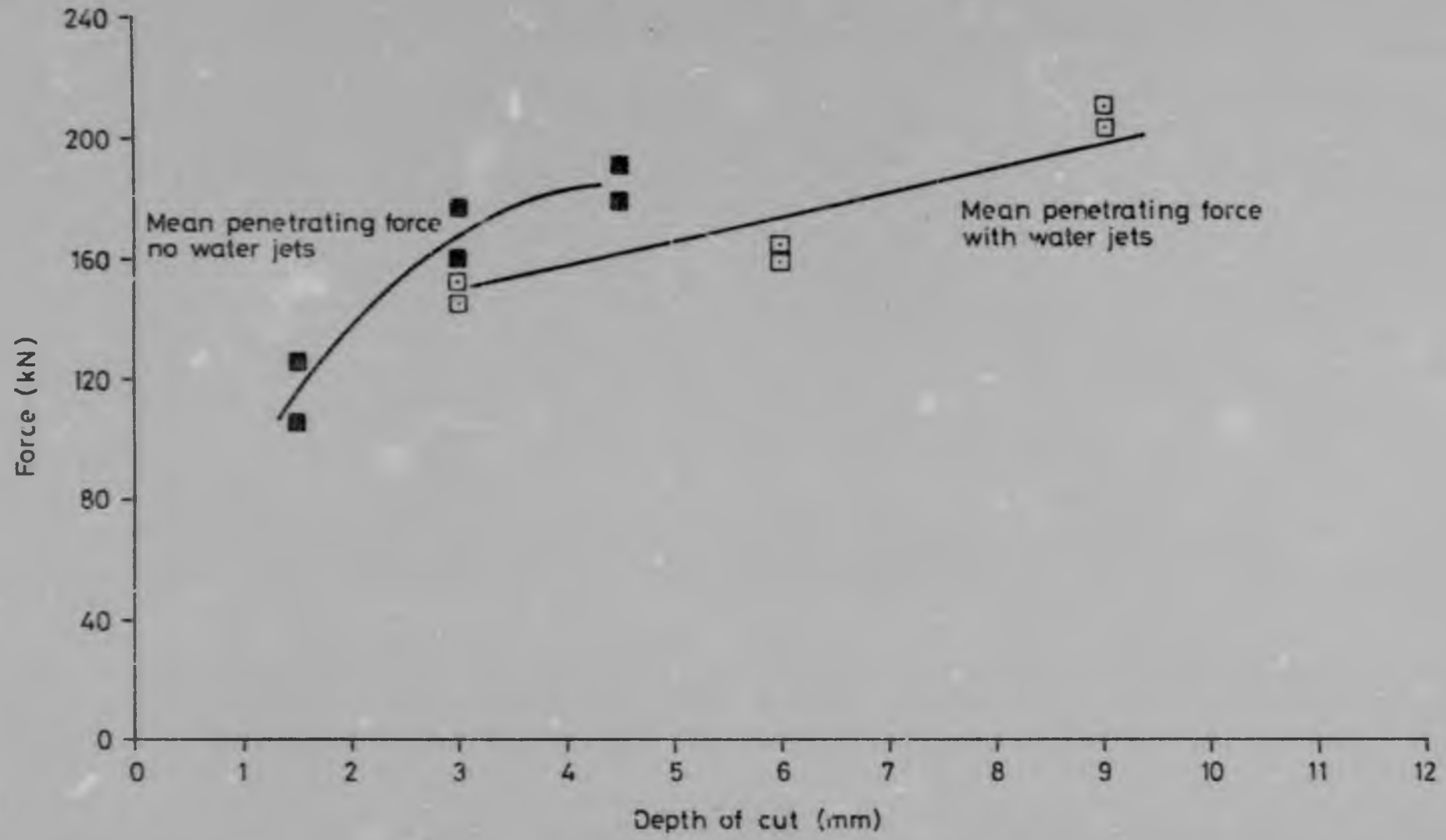


FIGURE 70 : Mean bit penetrating force plotted against depth of cut, illustrating the reduction of the force required to cut the rock with 10 MPa water jets directed ahead of the bit.

the corners of the tungsten carbide inserts, (Section 6.4.1).

Measurements of the components of the bit force which were made during these tests are plotted against depth of cut in Figures 71 to 74. These graphs show that only a small difference in the bit cutting force values was observed between two nozzle configurations, (Figures 62a and 62b). The bit penetrating force values were consistently lower with the jets directed inside the corners of the bit inserts in the path of the bit wearflat (Figures 73 and 74).

A further test was conducted to ascertain whether the position of the jet relative to the corners of the bit could affect the side force acting on the bit. The nozzles were mounted to direct the jets outside the corners of the tungsten carbide inserts, (Figure 62a). The upper nozzle was blocked so that only one jet, that which was directed towards the corner of the lower tungsten carbide bit insert, was used. The pressure of this jet was 50 MPa and the flow rate of the jet was about 0,33 ℓ/sec. Twenty cuts were made with the depth of cut a constant at 6 mm. The vertical force on the bit was measured during the cutting operation and following these tests the condition of the bit was examined. This experiment demonstrated effectively the pronounced effect of the water jets on the cutting ability of the drag bits. No marked difference to the vertical component of bit force was measured comparing the results of this test using one jet only and the experiment at the same pressure with two jets directed outside the corners of the bit inserts, Section 6.4.1. However, examination of the bit following this test with the single jet showed that the tungsten carbide insert, which did not have the water jet directed towards it, had been fractured and plastic flow of the

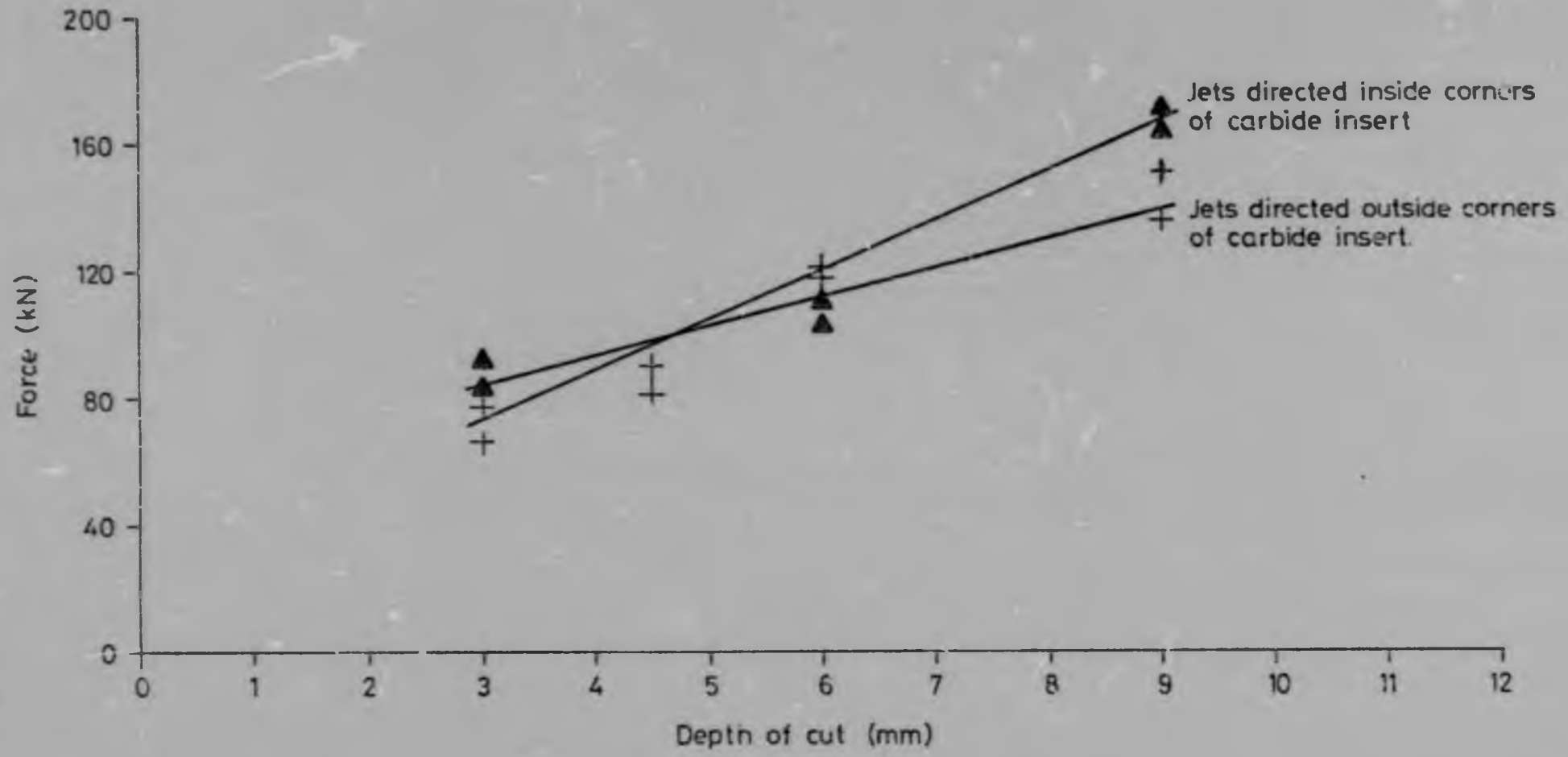


FIGURE 71 : Mean peak bit cutting force plotted against depth of cut with 10 MPa water jets directed adjacent to the corners of the tungsten carbide bit inserts.

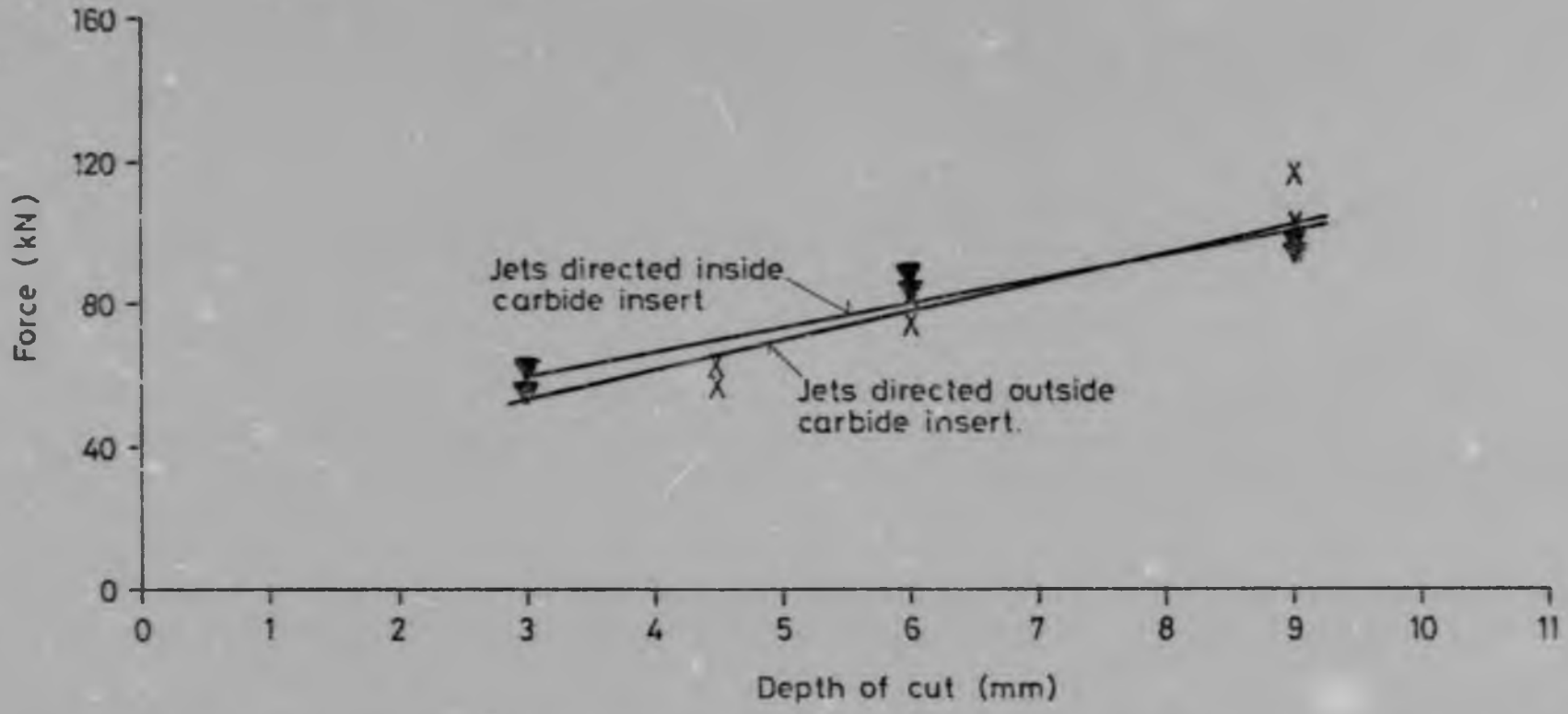


FIGURE 72 : Mean bit cutting force plotted against depth of cut with 10 MPa water jets directed adjacent to the corners of the tungsten carbide bit inserts.

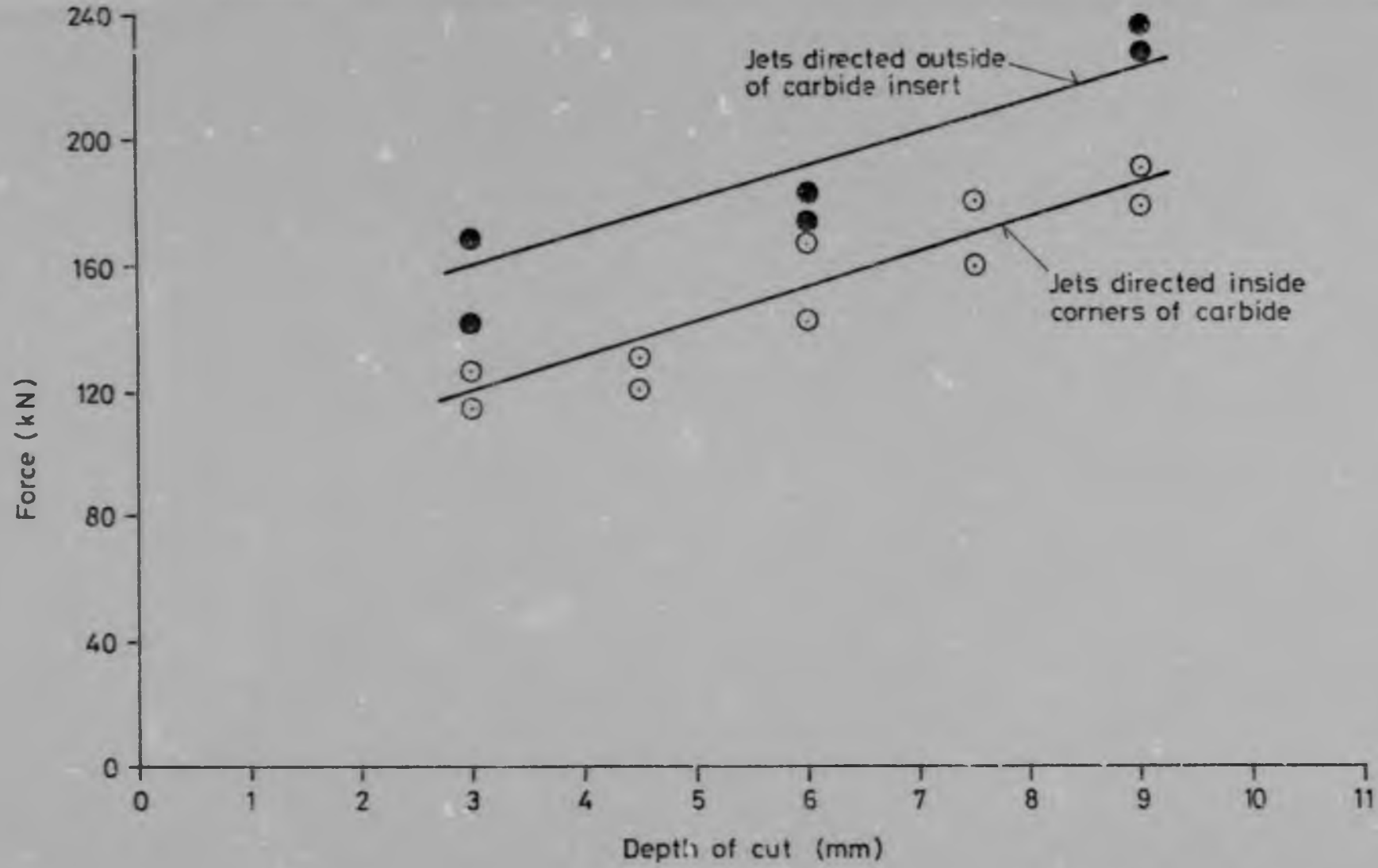


FIGURE 73 : Mean peak bit penetrating force plotted against depth of cut with 10 MPa water jets directed adjacent to the corners of the tungsten carbide bit inserts.

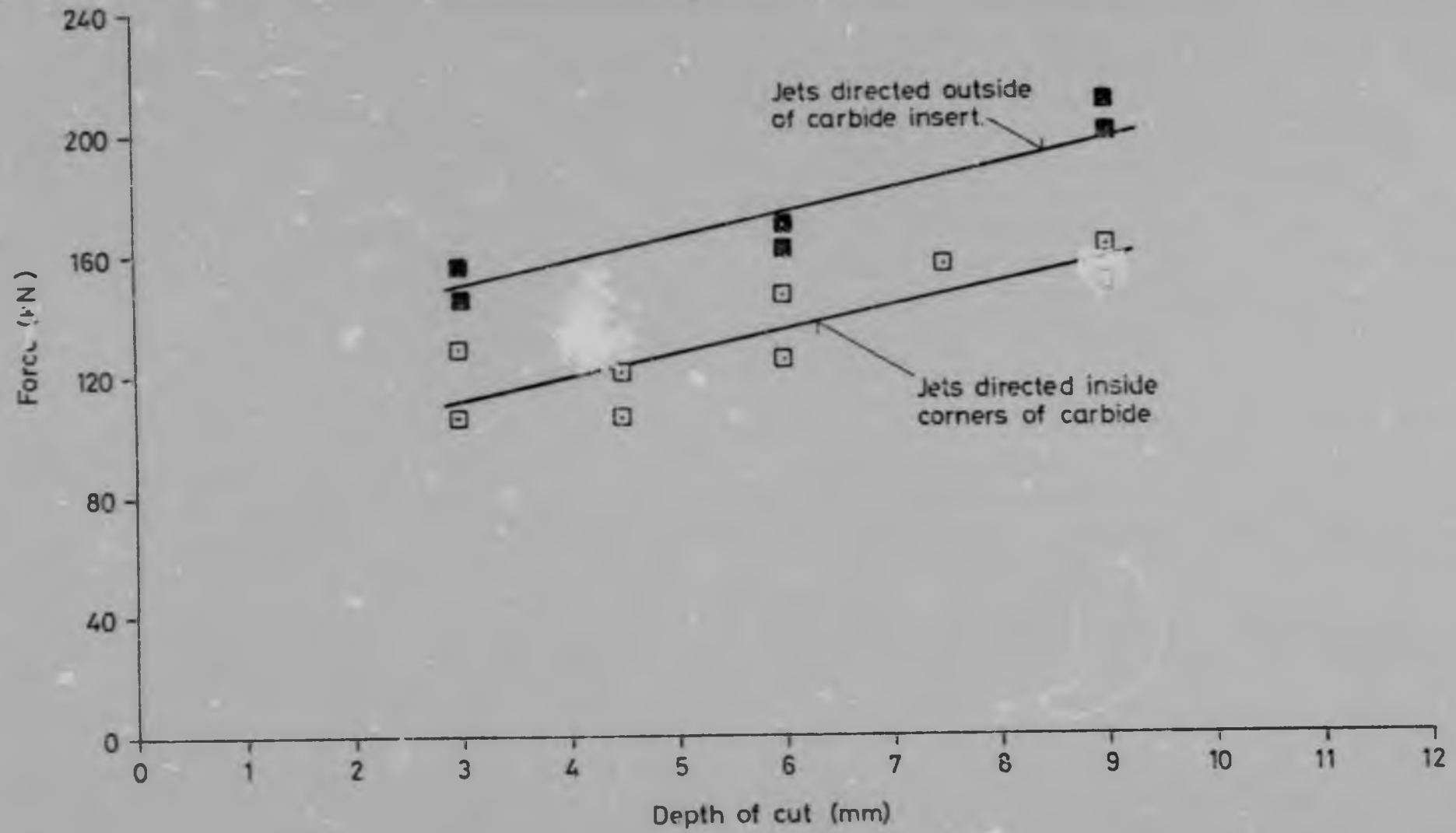


FIGURE 7a : Mean bit penetrating force plotted against depth of cut with 10 MPa water jets directed adjacent to the corners of the tungsten carbide bit inserts.

insert had occurred at the insert corner, (Figure 75). In contrast no visible damage of the bottom tungsten carbide insert had taken place.

This experiment provided dramatic evidence demonstrating the modification to the cutting action of the bit as a result of the use of high pressure water jets. The wear on the steel body of the bit when a single jet was directed outside the corner of the lower tungsten carbide insert took place on the upper face of the steel only. The lower steel face showed no wear, in fact the paint on this face was unscratched, (Figure 76).

An explanation of this phenomenon is shown in an exaggerated diagramatic form in Figure 77. A single water jet directed outside the corner of the lower tungsten carbide bit insert caused the upward vertical force acting on the bit to be reduced. Therefore, in effect, a downward component of vertical force was applied to the bit. This caused the blade to bend downwards and the upper surface of the bit to rub along the upper surface of the slot, (Figure 77). This would explain not only the marked wear pattern on the steel bit but also why no increase in the downward vertical bit force was observed. The method measuring the force acting on the bit was by measuring the reaction forces of the bit on the rock, (Section 4.1). With this experiment the effective downward vertical force applied to the tungsten carbide bit inserts, (V1 in Figure 77) was reacted by an upward vertical force from the steel bit body, (V2 in Figure 77), within the rock mass. Consequently no significant change in the vertical bit force was measured.



FIGURE 75. Photograph showing damage to a tungsten carbide bit insert when water jet was not directed towards the insert during the cutting operation.



FIGURE 76. Photograph showing wear of steel bit body when a water jet was not used.



FIGURE 76. Photograph showing wear of steel bit body when a water jet was not used.

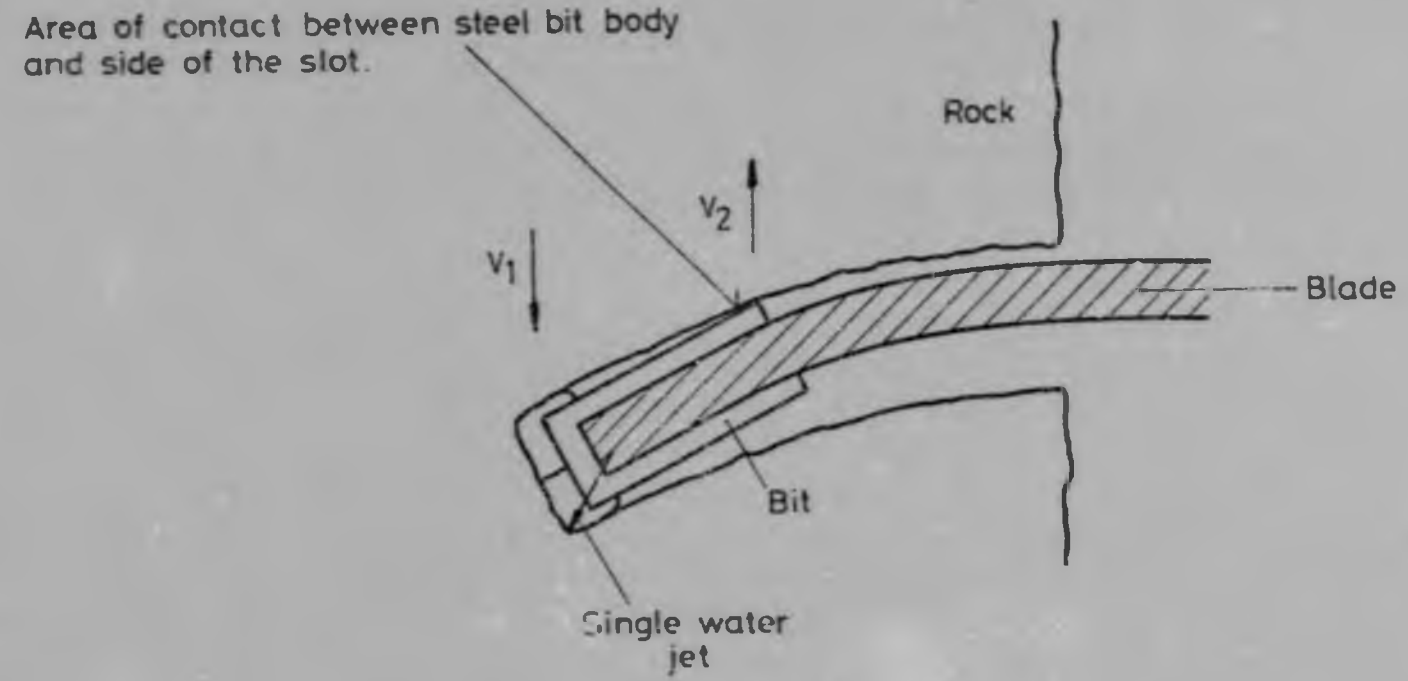


FIGURE 77 : Diagram illustrating the influence of water jets on the side force acting on the bit.

Examination of the rock which was cut during this experiment using only a single water jet to assist the drag bit, demonstrated that the predicted downward curve of the slot during the cut (Figure 77), did occur.

The fracturing of the upper tungsten carbide insert during this test was attributed to overloading while cutting. It was shown previously (Section 6.4.1), that the maximum depth of cut possible in norite for a given available machine force of about 150 kN, was 4,5 mm. With a single water jet the bit force was reduced so that the depth of cut was increased to 6 mm. However, since this jet was preferentially orientated towards the lower tungsten carbide bit insert, a higher force was applied to the upper bit insert which caused it to fracture. Thus this experiment demonstrated that bits of this design were operating close to the limits of their strength at 150 kN cutting force. The plastic flow of the tungsten carbide at the corners of the bit upper insert showed that a water jet with a flow rate of 0,33 ℓ/sec which was not applied directly onto the insert was insufficient to cool the tungsten carbide adequately during the cutting operation.

This experiment was repeated cutting a second slot in the same block of rock with the bottom nozzle blocked and only the top jet operating. Results of a similar nature were obtained. Identical damage to the bit was observed, only this time to the lower tungsten carbide insert. Wear took place only on the lower face of the steel bit body. The slot in the rock was observed to curve upwards.

It was concluded therefore that the position of the jets relative to the bit corners influenced significantly the side forces acting on the bit. This was of importance at the underground test site where one of the objectives was to cut up against the stope hanging-wall, (Section 3.1).

6.4.3 Point of impingement of the jets

It was observed during the test programme that the water jets, at the pressures used for these experiments, did no visible damage to the rock when traversed across the rock face without a bit. Although the mechanism of cutting rock with high pressure water jets is not well understood, empirical methods have shown that in order to cause appreciable damage to the rock with continuous, non-cavitating water jets, the pressure of the jets should exceed the uniaxial compressive strength of the rock, (Labus 1976). It is to be expected therefore that the water jets at pressures of 50 MPa and less, would not cause damage to the norite rock used during the laboratory experiments, since the norite has a uniaxial compressive strength of about 300 MPa. If the dramatic reduction of the bit forces when these relatively low pressure water jets were directed ahead of the bit was not attributable to preweakening of the rock by the jets, this must have been caused by an interaction between the jets and the fractured zone of rock adjacent to the bit. In order to discover the extent of the area ahead of the bit where the jets were effective in reducing the bit forces, an experiment was conducted with two jets directed 10 mm ahead of the leading edge of the bit, (Figure 62c). The jets were directed onto the rock in the path of the wearflat of the bit insert. The pressure of the water jets for this test was 15 MPa.

Measurements of the components of the bit force were recorded during this test with water jets directed onto the rock face. These are plotted together with force measurements made in the same block of rock without using water jets, (Figures 78 to 81). A different, block of norite with a somewhat higher uniaxial compressive strength, was used for these tests. For this reason the maximum depth of cut when no water jets were used was found to be reduced from 4,1 mm, which had been the typical maximum depth of cut in other norite blocks, to 3 mm, (Figure 78). These results show that maximum depth of cut was increased to 4,5 mm as a result of a relatively small reduction in the values of the bit cutting force when the water jets were used to assist the cutting operation, (Figures 78 and 79). The bit penetrating force was reduced also (Figures 80 and 81), although not to the same extent as when the jets were positioned closer to the leading edge of the bit, (Figures 69 and 70).

An experiment was conducted to ascertain whether the optimum position of the water jets was adjacent to the bit corners. A single water jet with a flow the same as the combined flow from the two jets used for the previous tests, 0,67 ℓ/sec, was directed at a pressure of 50 MPa towards the rock face along the centre of the bit inserts. The jet was directed 2 mm ahead of the leading edge of the inserts, (Figure 62d). The force measurements obtained during this experiment were compared with the measurements of bit forces when two water jets were directed, also at 50 MPa pressure, towards the corners of the carbide inserts.

The results of this experiment are presented graphically in Figures 82 to 85. The bit cutting force was shown to be reduced

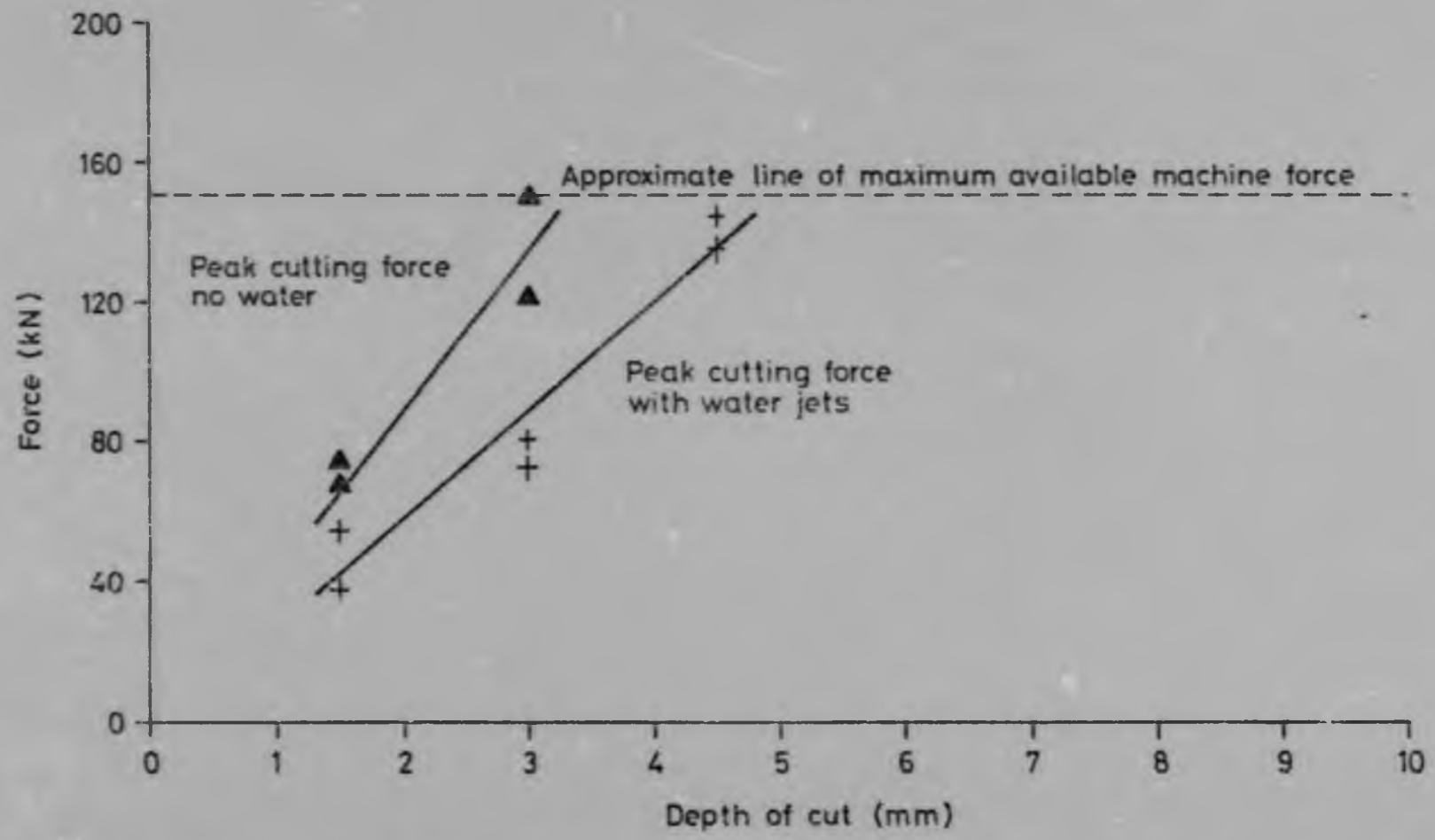


FIGURE 78 : Mean peak bit cutting force plotted against depth of cut, with water jets directed 10 mm ahead of the bit.

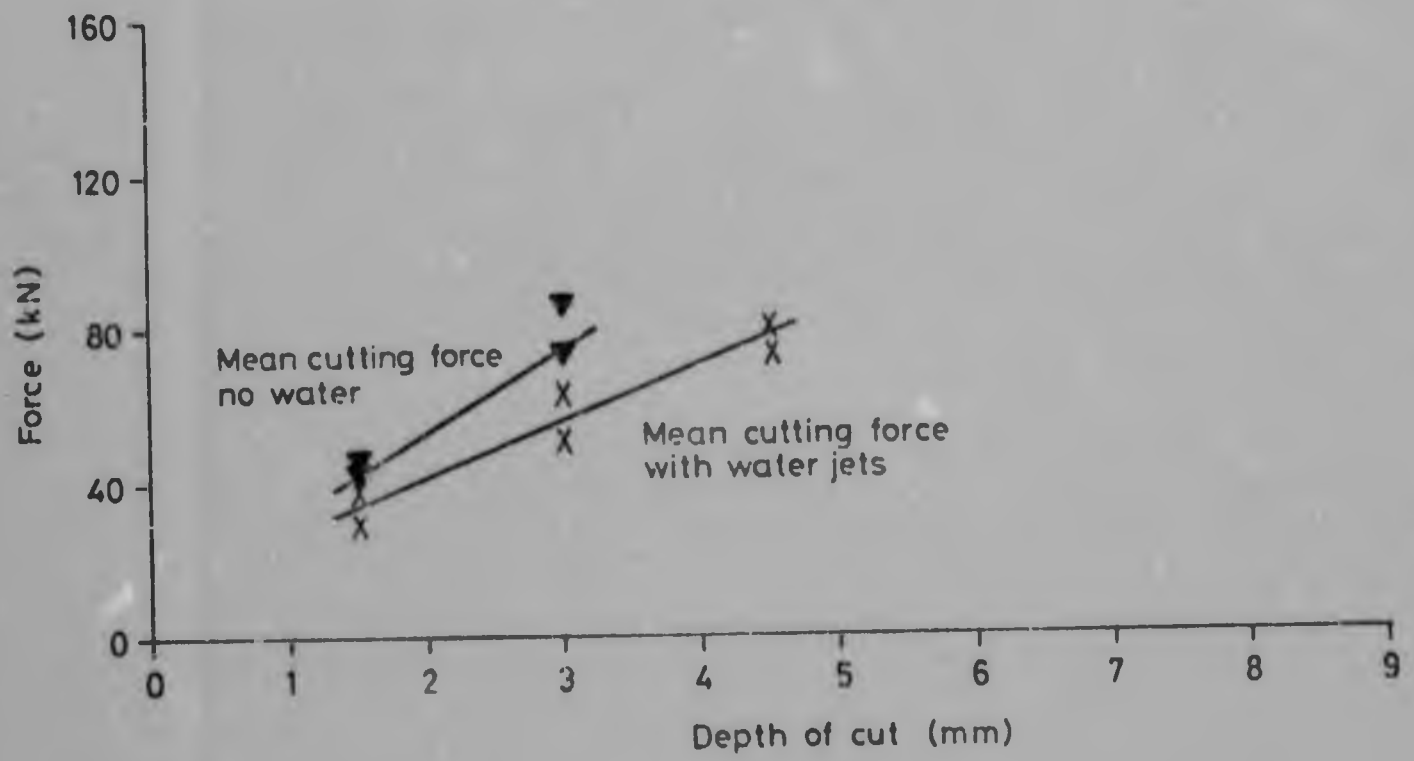


FIGURE 79 : Mean bit cutting force plotted against depth of cut, with water jets directed 10 mm ahead of the bit.

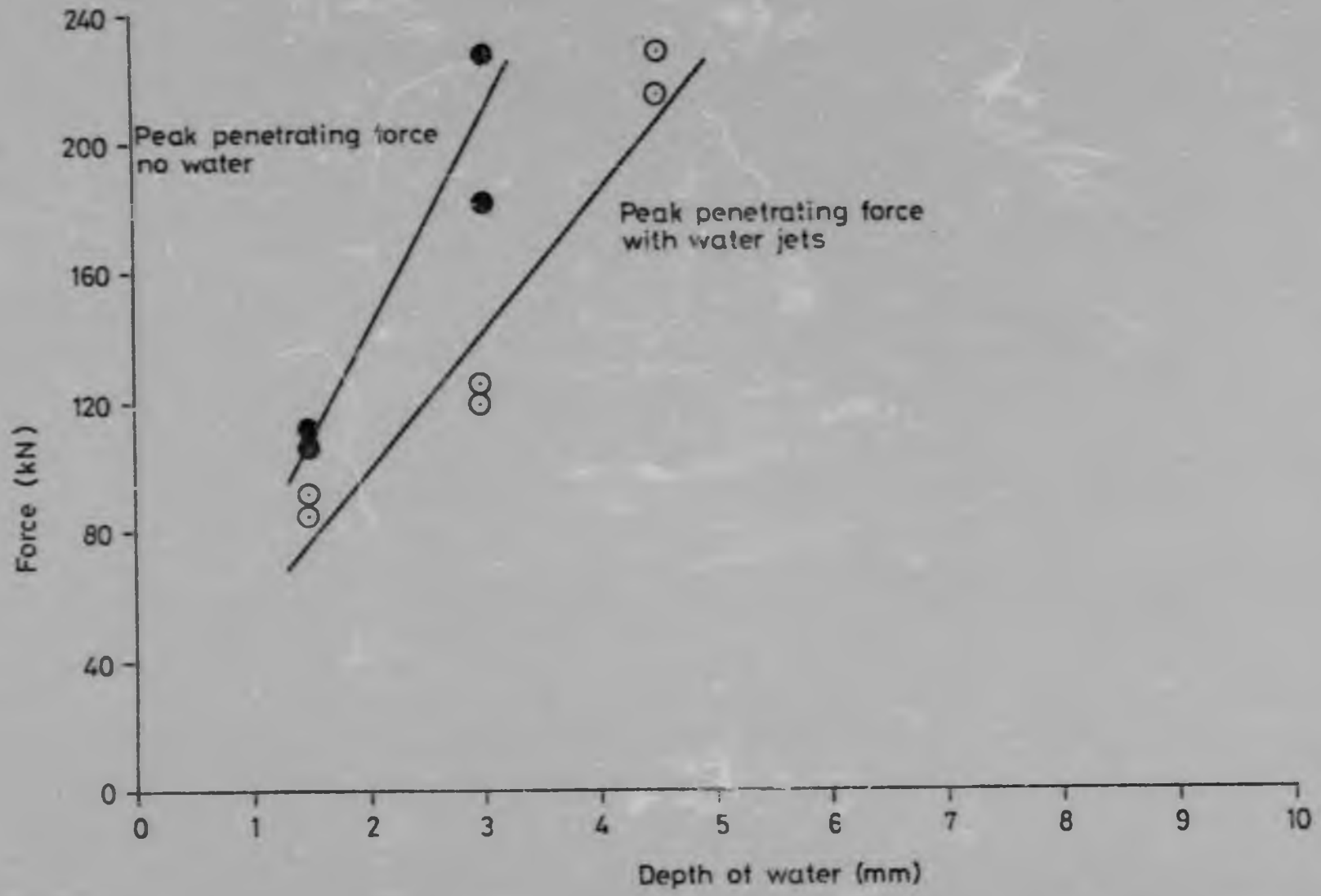


FIGURE 80 : Mean peak bit penetrating force plotted against depth of cut, with water jets directed 10 mm ahead of the bit.

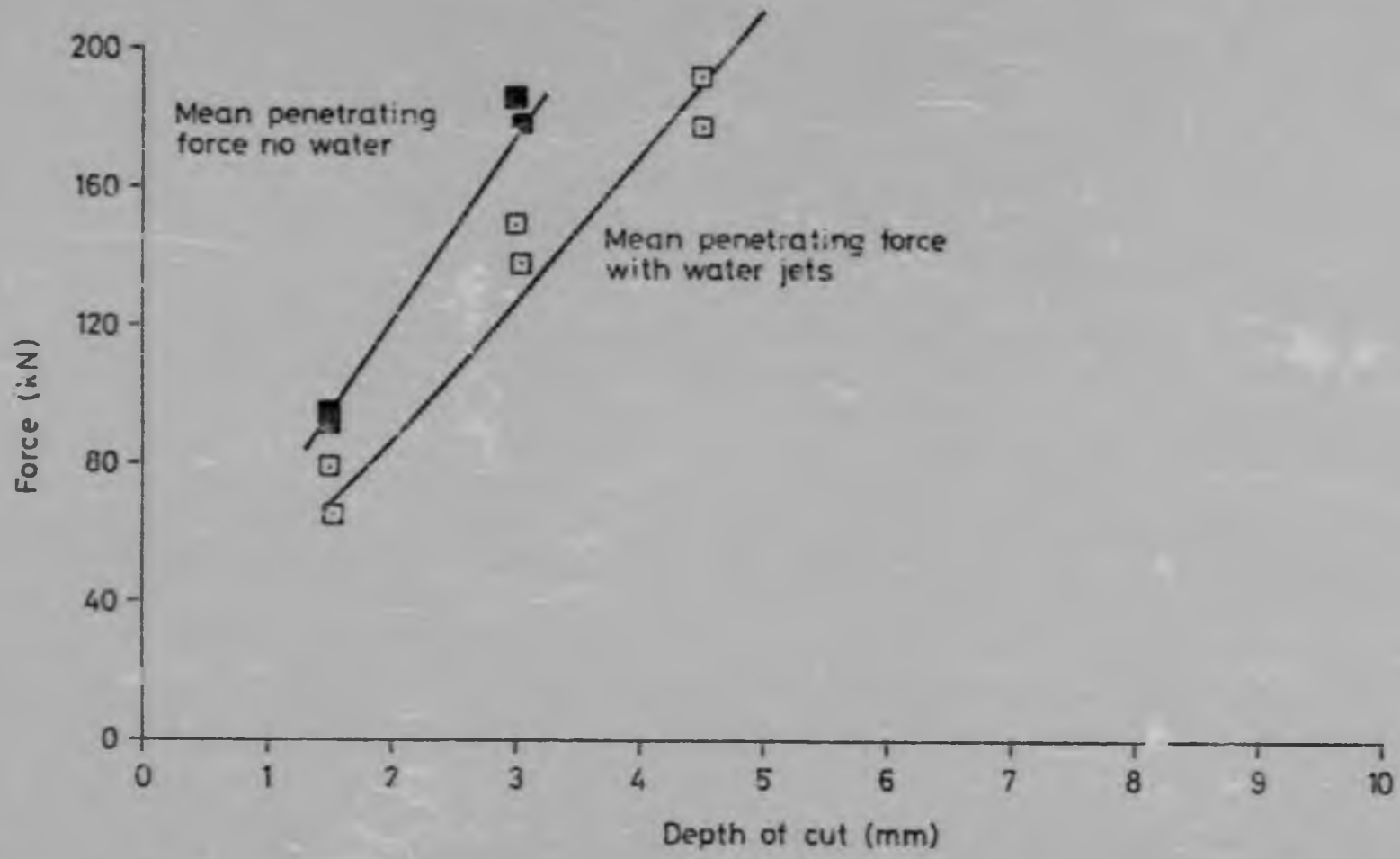


FIGURE 61 : Mean bit penetrating force plotted against depth of cut, with water jets directed 10 mm ahead of the bit.

equally well with both jets configurations, (Figures 82 and 83). However, the bit penetrating force which was decreased significantly with the jets directed towards the bit corners, was not much affected with a single jet directed along the centre of the tungsten carbide bit inserts, (Figures 84 and 85).

Therefore the forces acting on the bit were found to be particularly sensitive to the point of impingement of the water jets. The most important result showed that, in order to be effective in reducing the bit force, the jets should be directed as close as possible to the leading edge of the bit. The most significant reduction of the bit force occurred when two jets were directed towards the corners of the tungsten carbide bit inserts at the interface between the bit and the rock. The exact positioning of these jets relative to the bit corners was shown to affect the different components of the bit forces significantly. With the jets directed outside the bit corners the vertical component of the bit force was reduced, whereas with the jets directed inside these corners the bit penetrating force was decreased.

6.5 Testing water jets at the underground site

Five of the rockcutting machines at the Doornfontein trial site were fitted with the necessary equipment to direct high pressure water jets ahead of the bit during the cutting operation. The nozzle configuration chosen for these tests used two jets directed immediately ahead of the bit, towards the bit corners. The water pressure was adjusted to 40 MPa and the water flow rate through the nozzles was 0,67 ℓ/sec.

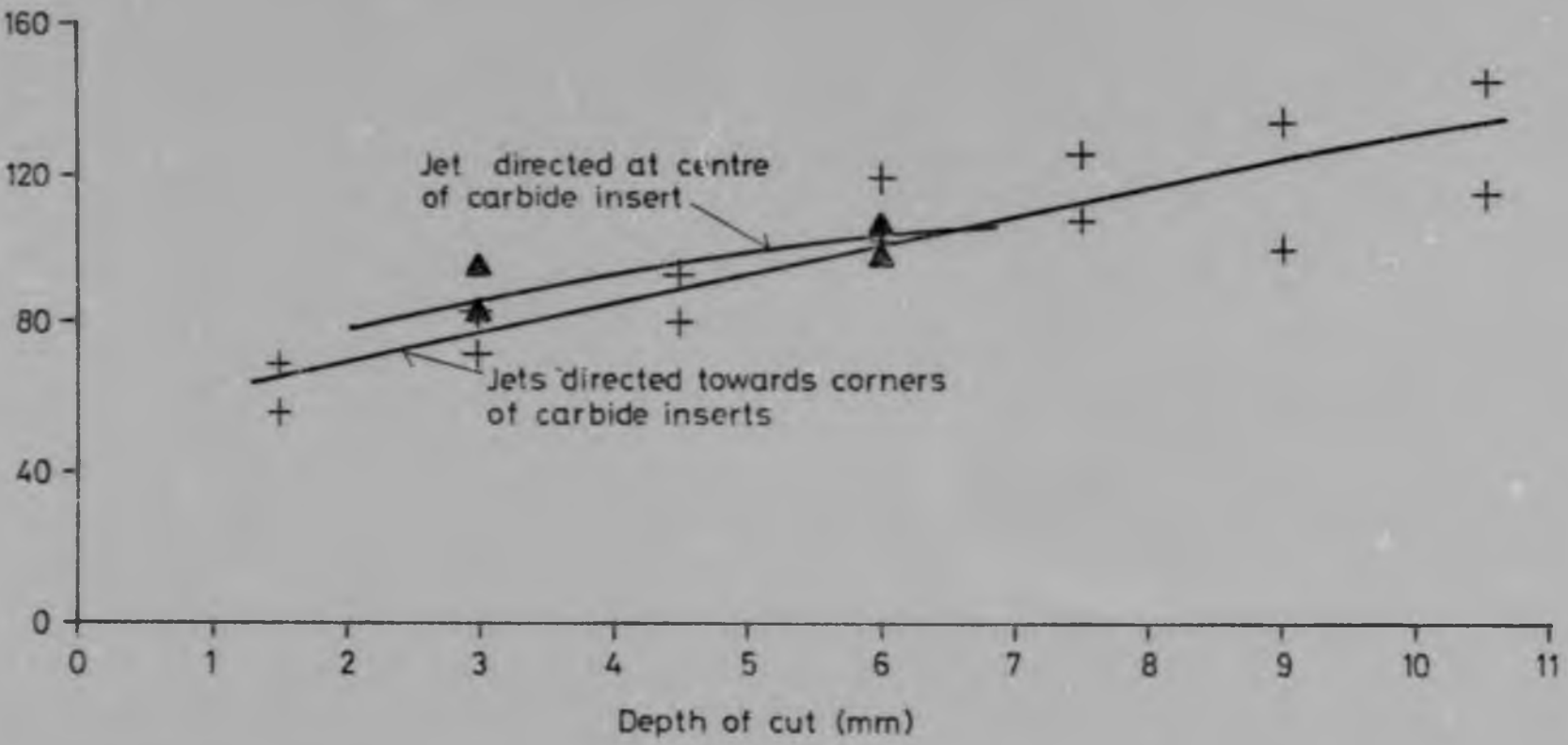


FIGURE 82 : Mean peak cutting force plotted against depth of cut, comparing force measurements using two water jets directed towards the bit corners with a single jet directed along the centre of the leading face of the bit.

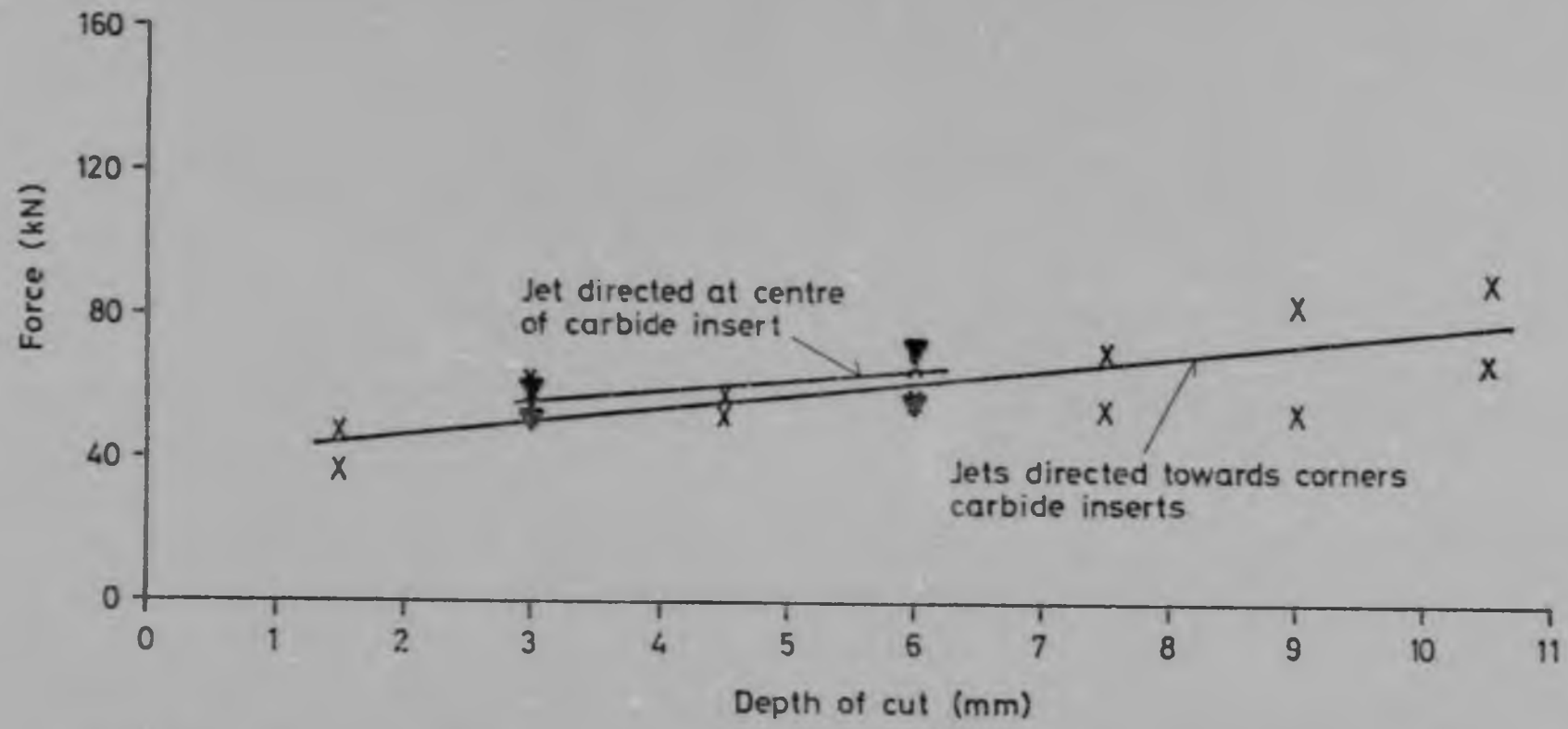


FIGURE 83 : Mean bit cutting force plotted against depth of cut, comparing force measurements using two water jets directed towards the bit corners with a single jet directed along the centre of the leading face of the bit.

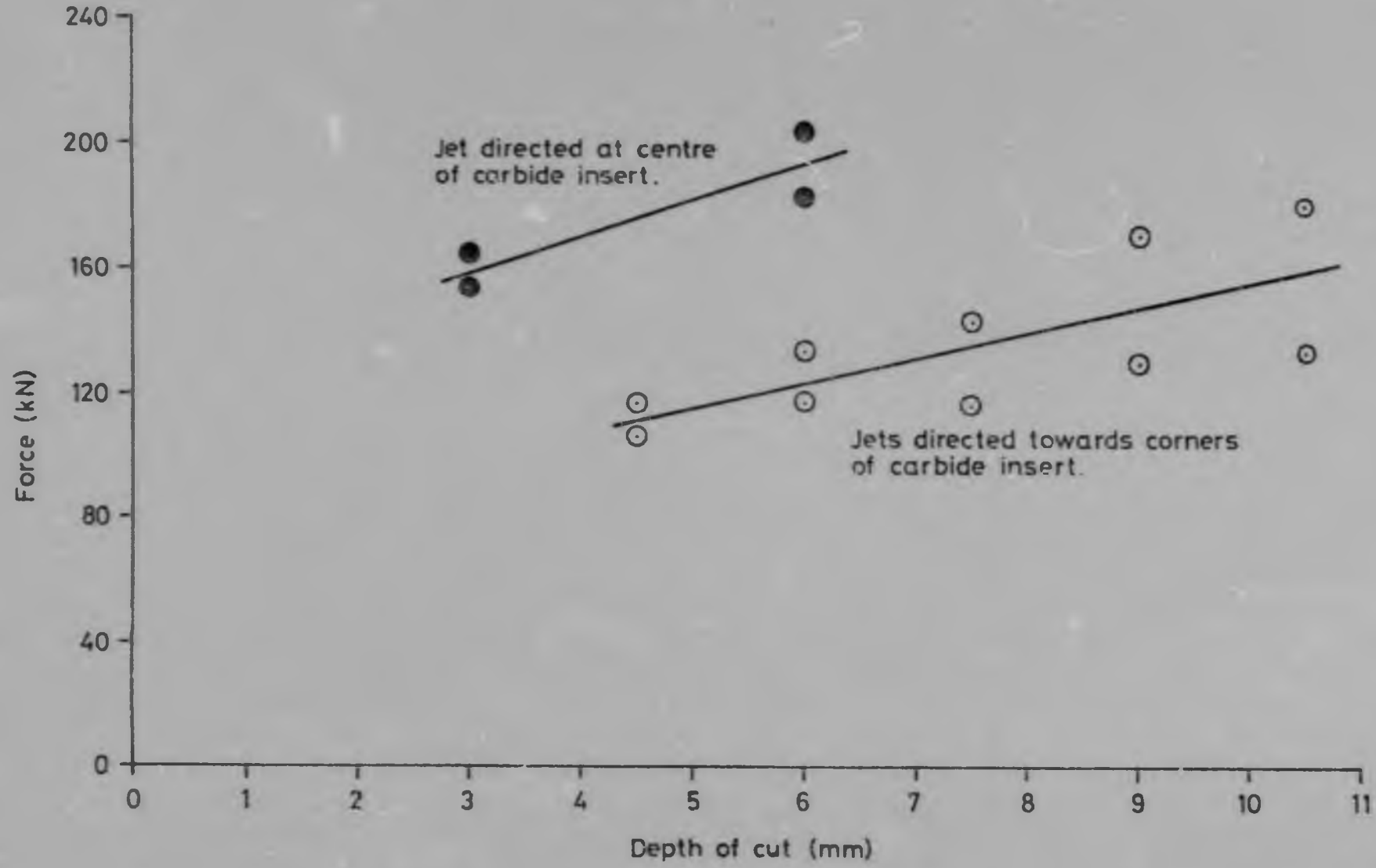


FIGURE 84 : Mean peak bit penetrating force plotted against depth of cut, comparing force measurements using two water jets directed towards the bit corners with a single jet directed along the centre of the leading face of the bit.

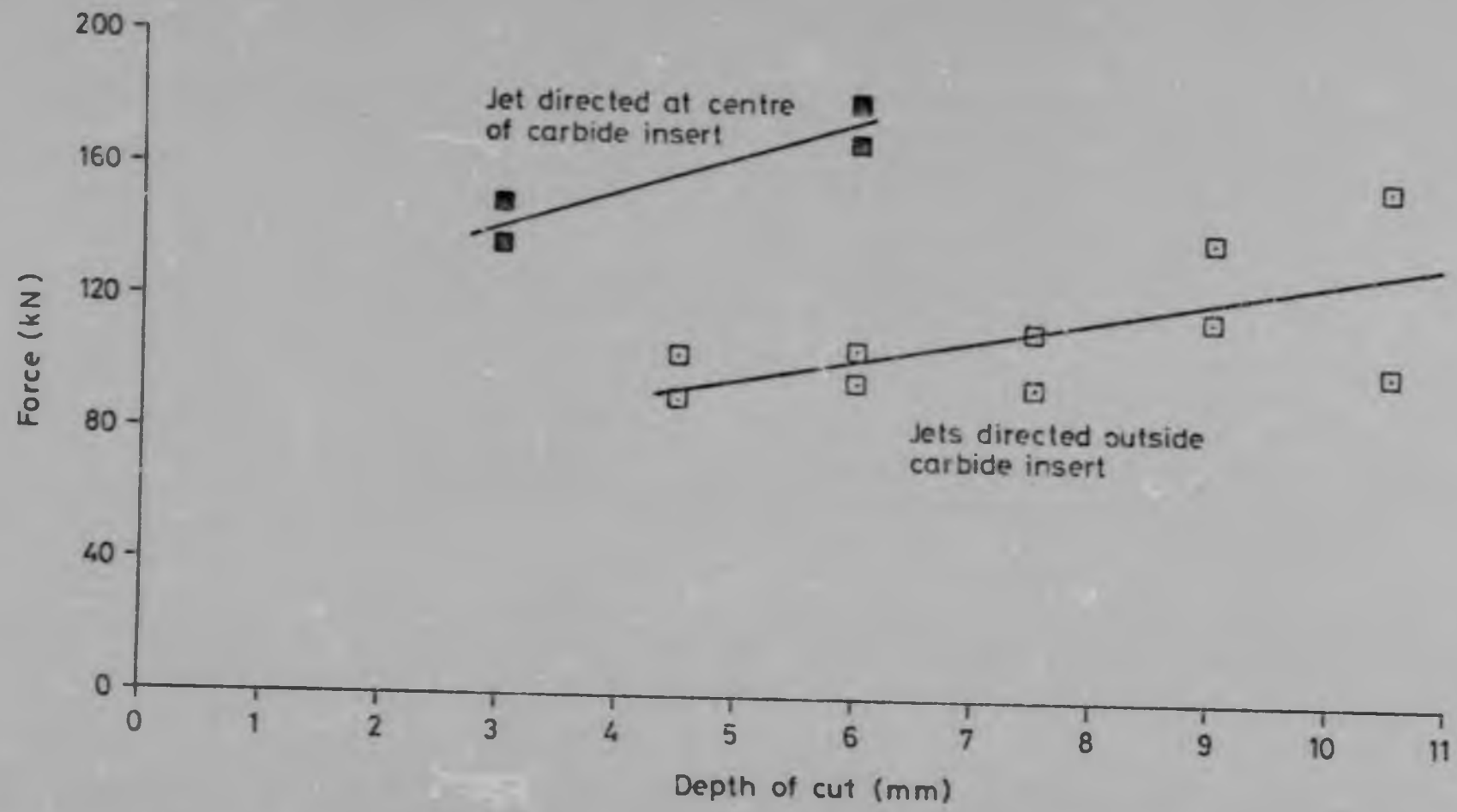


FIGURE 85 : Mean bit penetrating force plotted against depth of cut, comparing force measurements using two water jets directed towards the bit corners with a single jet directed along the centre of the leading face of the bit.

Detailed observations were made in order to assess how the use of these water jets influenced the cutting operation in the different rock conditions.

The maximum depth of cut without water jets was typically 2 mm to 3 mm cutting relatively unfractured quartzite at the Doornfontein test site. When water jets were directed towards the bit this was increased to between 10 mm and 15 mm. In highly-stressed, fractured ground the maximum depth of cut without water jets was between 8 mm and 10 mm which was increased to more than 40 mm when the water jets were used. Thus an average fivefold gain in depth of cut and therefore in the instantaneous cutting rate, was achieved with the assistance of high pressure water jets during the underground tests.

Excessive deflection of the blade caused by the high vertical force acting on the bit, which normally prevented slots from being cut up against the stope hangingwall, was shown to be greatly reduced when high pressure water jets directed towards the bit corners were used to assist the cutting operation. The application of these jets made it possible to establish a mining system whereby the machines were always set up to cut in the stope face against the hangingwall, thus achieving a significant mining advantage, (Section 3.1).

The tendency for the uppermost tungsten carbide insert of the bit to shatter when a slot was cut up against the hangingwall was found to be greatly affected by the position of the water jet relative to the corner of the bit insert. Laboratory tests had shown that the bit side force was influenced by the position of the jet relative to the bit corner (Section 6.4.2), and the underground experiments confirmed

this result. A test was carried out using sixty bits to cut up against the stope hangingwall. Thirty of these bits had jets directed outside the corners of the tungsten carbide bit inserts (illustrated in Figure 62a), and the remaining thirty bits had the jets directed inside the corners of the bit inserts, (Figure 62b). Twenty three of the bits with the jets directed inside the insert corners were removed from the machine with the top tungsten carbide insert shattered, after cutting an average of only 3,8 centares. In contrast, only five of the bits with the jets directed outside the insert corners were removed from the machine with damaged tungsten carbide insert, the remaining twenty five were discarded because of wear of the inserts. The average life of these bits was 6,4 centares per bit.

The more difficult rock conditions when cutting up against the hangingwall, caused the average life of the bits to be reduced from 11,6 centares (Table 7), to 6,4 centares. Nevertheless the mining system was changed so that the machines were set up always to cut against the hangingwall. Using this system it was shown that the effort required for secondary breaking was halved and, as a result, two men per machine panel were no longer needed in the stope. In addition to this substantial improvement in labour productivity, the smooth cut hangingwall created safer working conditions in the stope. These substantial advantages justified the higher cost of the bits.

The wear and failure pattern of the bits used for the tests underground also changed markedly when water jets were used. With no water jets the majority of the bits were removed from service because of failure of the braze joint or fracture of the tungsten carbide

inserts, (Section 6.2). The mechanism causing these failures was initiated both by a high rate of heat transfer to the bit causing thermal deterioration of the braze joint and the tungsten carbide (Section 6.1), and by excess loading which caused shattering of the tungsten carbide during the cut. The appreciable cooling effect of the water jets, combined with the reduced bit forces decreased the bit braze and bit insert failures to the extent that the bits were ultimately discarded because of excessive wear of the tungsten carbide inserts.

CHAPTER 7

7. INVESTIGATION OF THE MECHANISM OF FAILURE OF HARD ROCK, USING DRAG BITS ASSISTED BY WATER JETS

The reductions in the bit forces brought about when high pressure water jets were directed ahead of a drag bit were greater than had been expected in the light of existing knowledge that water jets by themselves in the pressure range at which these experiments were conducted, would not cause damage to the rock (Labus, 1976). Also, the effect was much greater than could be anticipated from improvements derived only as a result of better cooling of the bit, or better lubrication between the bit and the rock.

In order to investigate this phenomenon, work was directed towards establishing details of the interaction between the water jets and the rock adjacent to the bit. An interesting aspect of this reduction in the bit forces was that the bit penetrating force was more sensitive to a change in the parameters relating to the water jets, such as pressure or the position of the jets relative to the bit. than was the bit cutting force, (Chapter 6). An explanation of this behaviour was sought during these investigations.

7.1 The mechanism of fracture of strong rock using a drag bit with no water jets

In order to understand how water jets assist a drag bit when cutting in hard rock, it is necessary to examine the mechanism of rock fracture caused by a drag bit without water jets.

Riemann (1974), proposed that a drag bit cutting in strong rock acts in a similar fashion to a flat indentor moving through the rock. He suggested that the rock spalled ahead of the leading face of the bit and that this leading face therefore did not affect the rock breaking process, (Chapter 2). This theory is supported by experiments conducted by Cook (1973), in which the direction of the resultant force acting on the bit during the cut was measured. If, during cutting, the leading face of the bit was in continuous contact with the rock, or if this leading face was never in contact with the rock, then the direction of the resultant force would be expected to remain constant. However, if rock chips were formed ahead of the bit by indenting the rock surface with the bit wearflat and the forward motion of the bit frequently caused the leading face of the bit to impact against the rock, then large variations in the direction of the resultant force would be expected. Cook found that the direction of this force remained constant. He concluded therefore, that the rock was not broken as a result of the leading face of the bit impacting against the rock.

Evidence has been collected, during work carried out for this thesis, which supports the argument that the leading face of the bit is not in contact with the rock during the cutting process. A series of high-speed films was made of a bit cutting in a block of Witwatersrand quartzite in order to study, in a slow motion, the method of fracture of the rock adjacent to the bit. These films, which were taken at 3 000 frames a second using a revolving-prism type camera (Figure 86), showed that initial fracture was caused by indentation of the rock by the bit wearflat which produced a minor explosion

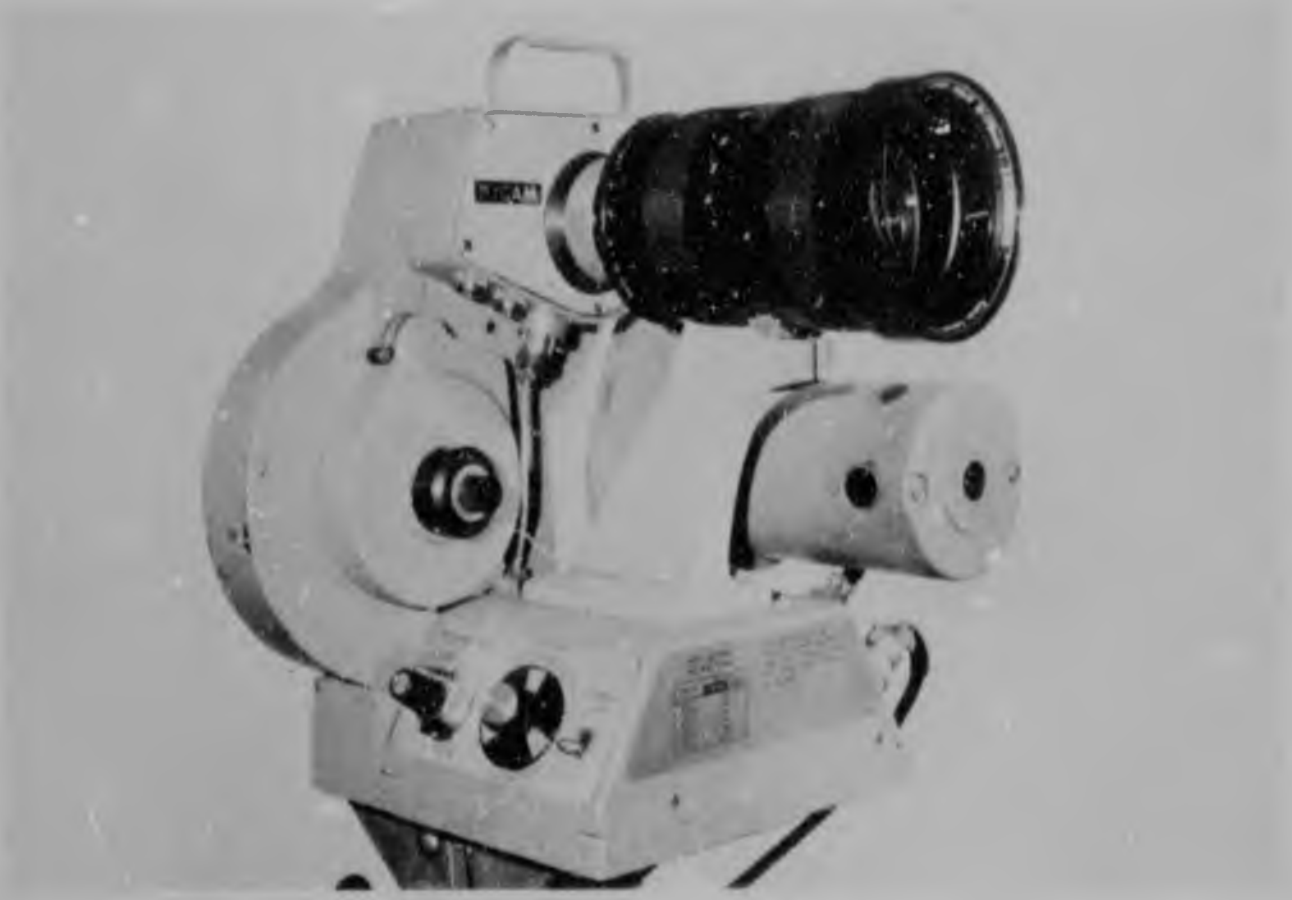
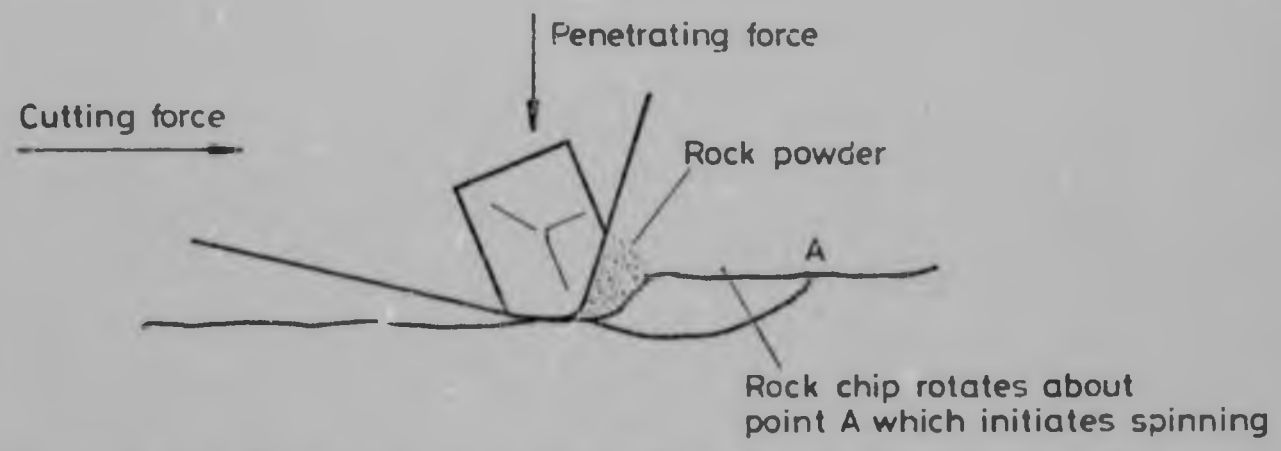


FIGURE 86 : High-speed camera.

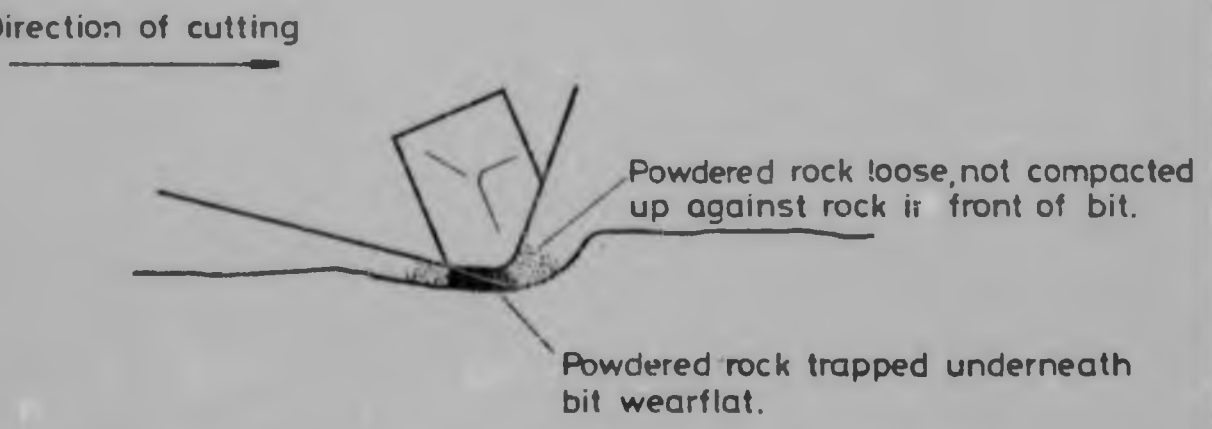
of the rock. A rock chip was formed ahead of the bit and this was observed to rotate whilst being ejected at a high velocity in the cutting direction. After the formation of the rock chip a large volume of crushed, powdered rock was visible ahead of the leading face of the bit. This powdered rock covered the bottom of the slot that was being cut, and became trapped under the bit wearflat as the bit advanced through the rock. This process of discontinuous chip formation, which is illustrated diagrammatically in Figure 87, continued along the length of the cut.

The plastic deformation of the tungsten carbide bit inserts during the cutting operation, described in Section 3.2.1, provided a further indication that the leading face of the bit did not affect the rock breaking process. The plastic flow of these inserts occurred in the direction ahead of the leading face of the bit. If this leading face had been used as a cutting surface, it would not have been possible for plastic deformation of the tungsten carbide to occur by flowing ahead of the bit. It was concluded therefore that the leading face of the bit was not in contact with the rock during the cutting operation.

As a consequence of the apparent validation by these experiments of the theory that the mechanism of rock breakage using a drag bit to cut strong rock is similar to that of an indentor, it is possible to apply two valuable techniques which can be used to study the fracture of rock adjacent to an indentor. Firstly, it should be possible to simulate the rock breaking process by a series of quasi-static indentation tests, using a press to indent the bit against the rock surface. Secondly, the stresses generated within an elastic medium when a punch



a) A rock chip forms in front of the leading face of the bit with a minor explosion. Rock powder is observed ahead of the bit, and the rock chip is ejected in the direction of the applied cutting force, rotating about point A.



b) As the bit advances through the rock, powdered rock is trapped underneath the wearflat.

c) Cycle is then repeated and another chip forms ahead of the leading face of the bit.

FIGURE 87 : Diagramatic representation of discontinuous chip formation during the cutting process.

is used to indent the surface of the medium, can be calculated. This problem was analysed originally by Bousinesque in a series of papers (Comptes Rendus 1878-1883), and more recently by Harding and Sneddon (1945). The results of such analysis can be compared with the known stresses and fracture patterns in rock failure.

7.2 Indentation tests - using a drag bit to indent a rock surface

The objectives of these experiments were firstly to find out whether the rock chip that was formed when a quasi-static indentation force was applied to a rock specimen, using a drag bit as the indentor, resembled the rock chips that were formed during the cutting operation. It was considered that if rock chips of a similar geometry could be produced by these two different methods then this would be a strong indication that rock fracture during the cutting process could be simulated, in a controlled fashion, by conducting a suite of indentation tests.

If this first objective was achieved, a technique was to be developed to enable the fractured rock zone in the vicinity of the bit to be studied with different applied indentation forces. In addition a shear force, equivalent to the bit cutting force, was to be superimposed on the normal force in a quasi-static test. The influence of these combined forces on the rock breaking process to be observed.

A stiff, 2 MN compression testing machine (Figure 88), was used as the press for applying known loads to the rock specimens throughout this test series. This rigid testing machine was used in order to



FIGURE 88 : Stiff compression testing machine.

measure accurately the force required to cause the specimen to fail and also to enable the post-failure characteristics of the rock to be studied. A detailed description of this machine is given in a paper / Hojem, et al (1975).

Cylindrical rock specimens, approximately 100 mm in diameter and 100 mm in length, were prepared. These were encased in a steel ring that was shrunk onto the specimens in order to confine the rock to prevent it from splitting when the load was applied. Samples of both quartzite and norite were prepared in this way.

The procedure followed was to place the rock on a fixed platen in the rigid-testing machine, with the bit inserted between the machine loading piston and the rock surface, (Figure 89). The bit was mounted in the machine with the entire bit wearflat in contact with the rock. Force was applied to the rock specimen using a fixed rate of displacement of the machine loading piston of $1{,}25 \times 10^{-3}$ mm/sec. Curves of the applied force against penetration of the bit were plotted continuously during the loading operation using the instrumentation built into the testing machine, (Hojem, et al, 1975).

7.2.1 Rock chips formed by an indentation force applied normal to the rock surface

Eight rock samples, four of norite and four of a strong, siliceous quartzite, were prepared. An indentation force was applied to the bit using the rigid testing machine, until a rock chip was formed adjacent to the bit, (Figure 90).

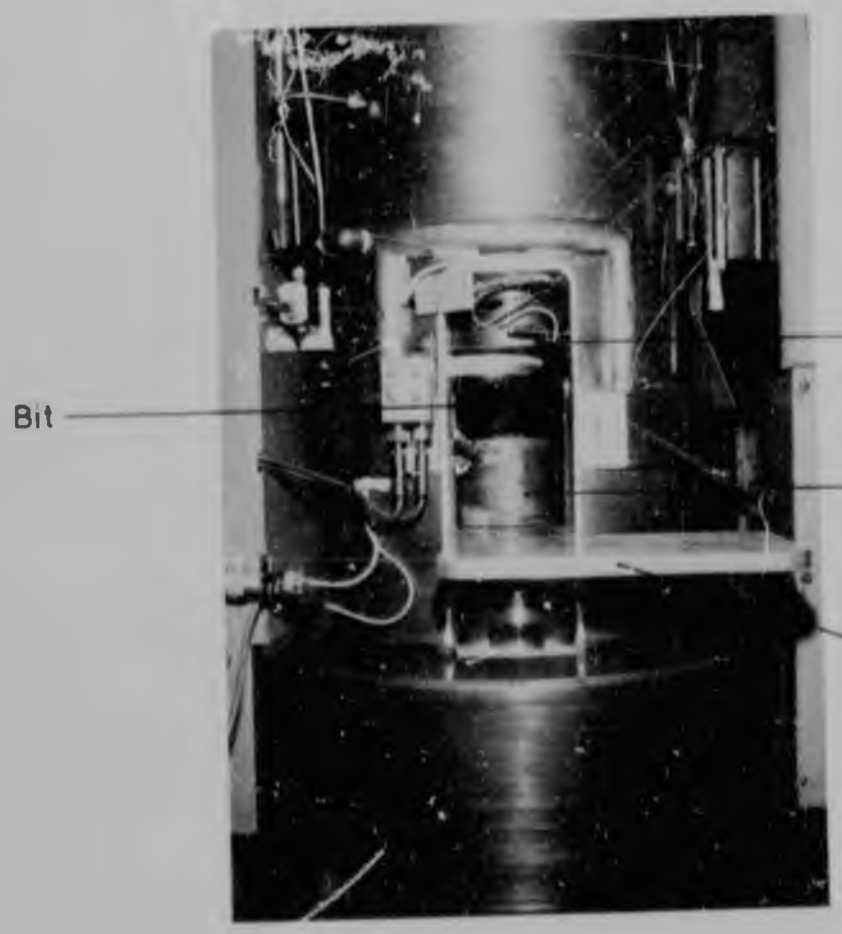


FIGURE 89 : Method of mounting the bit and the rock in the testing machine for indentation experiments.

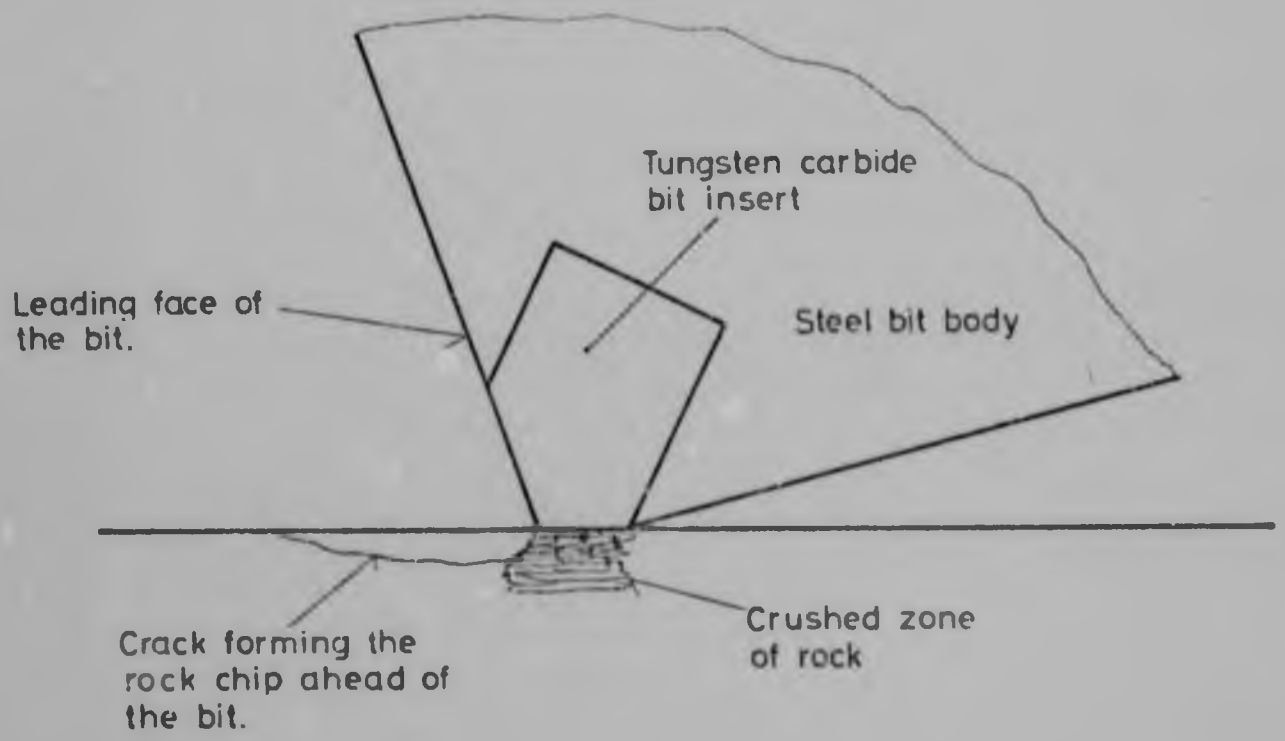


FIGURE 90 : Diagram illustrating formation of a rock chip during indentation tests.

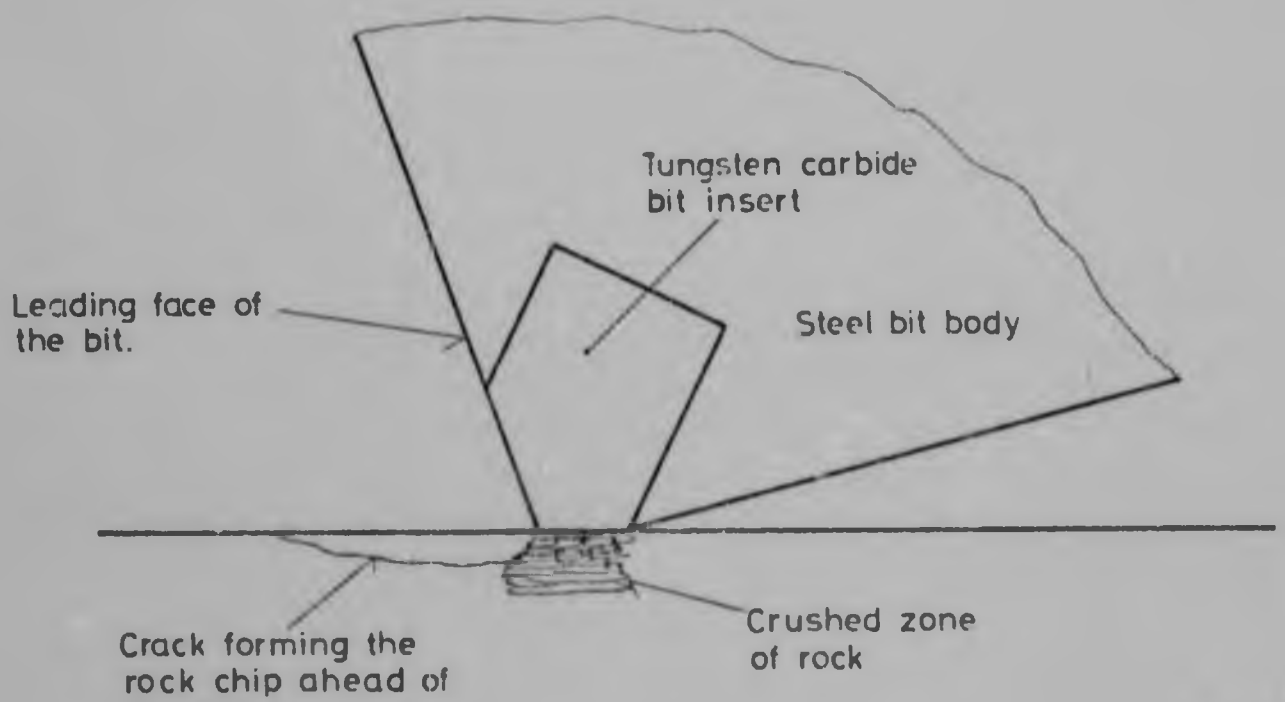


FIGURE 90 : Diagram illustrating formation of a rock chip during indentation tests.

It can be shown theoretically that when a rigid punch is applied to an elastic medium, stress concentrations are induced in the elastic medium beneath the corners of the punch, (Section 7.4). This was supported by observations made during these compression tests with both the norite and the quartzite specimens. Small rock chips about 2 mm in diameter and 0,5 mm thick, were observed to form next to the corners of the bit when the force applied was between 100 kN and 150 kN. This load was increased up to a point where a major rock chip was formed immediately ahead of the leading face of the bit. No other damage to the specimen in the form of cracking, other than this minor chipping in the vicinity of the bit corners, was visible until this major chip was formed. This large chip in front of the bit extended across the full 35 mm thickness of the bit, and for some 10 mm to 15 mm ahead of the bit. The force required to form this rock chip, in both the norite and the quartzite specimens, was between 250 kN and 350 kN. Examples of curves showing the applied load plotted against bit penetration for the norite and quartzite samples are given in Figures 91 and 92 respectively.

Rock chips would be expected to form symmetrically on either side of a flat-bottomed rectangular punch which was pressed against a flat rock surface. However, with all of the specimens tested during this experimental programme, the large rock chips were formed always on one side of the bit, ahead of the leading face. The reason for this preferential cracking ahead of the bit is given by the asymmetrical bit geometry. The steel bit body behind the rear face of the tungsten carbide insert was pressed against the rock during the indentation process. To support this argument, it was observed that paint was transferred from the steel bit body to the rock surface in

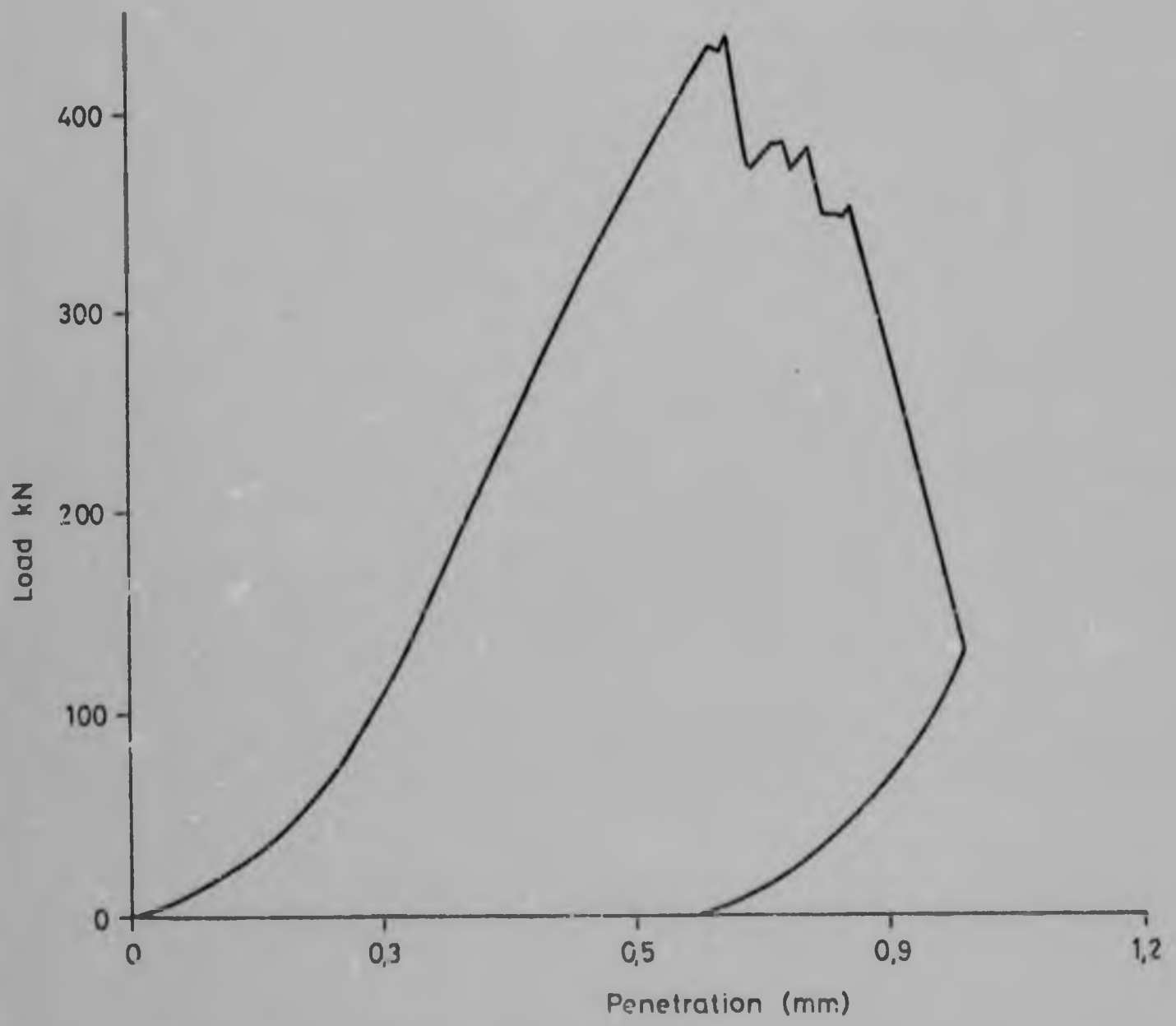


FIGURE 91 : Indentation force required to form a rock chip in norite, plotted against penetration of the bit.

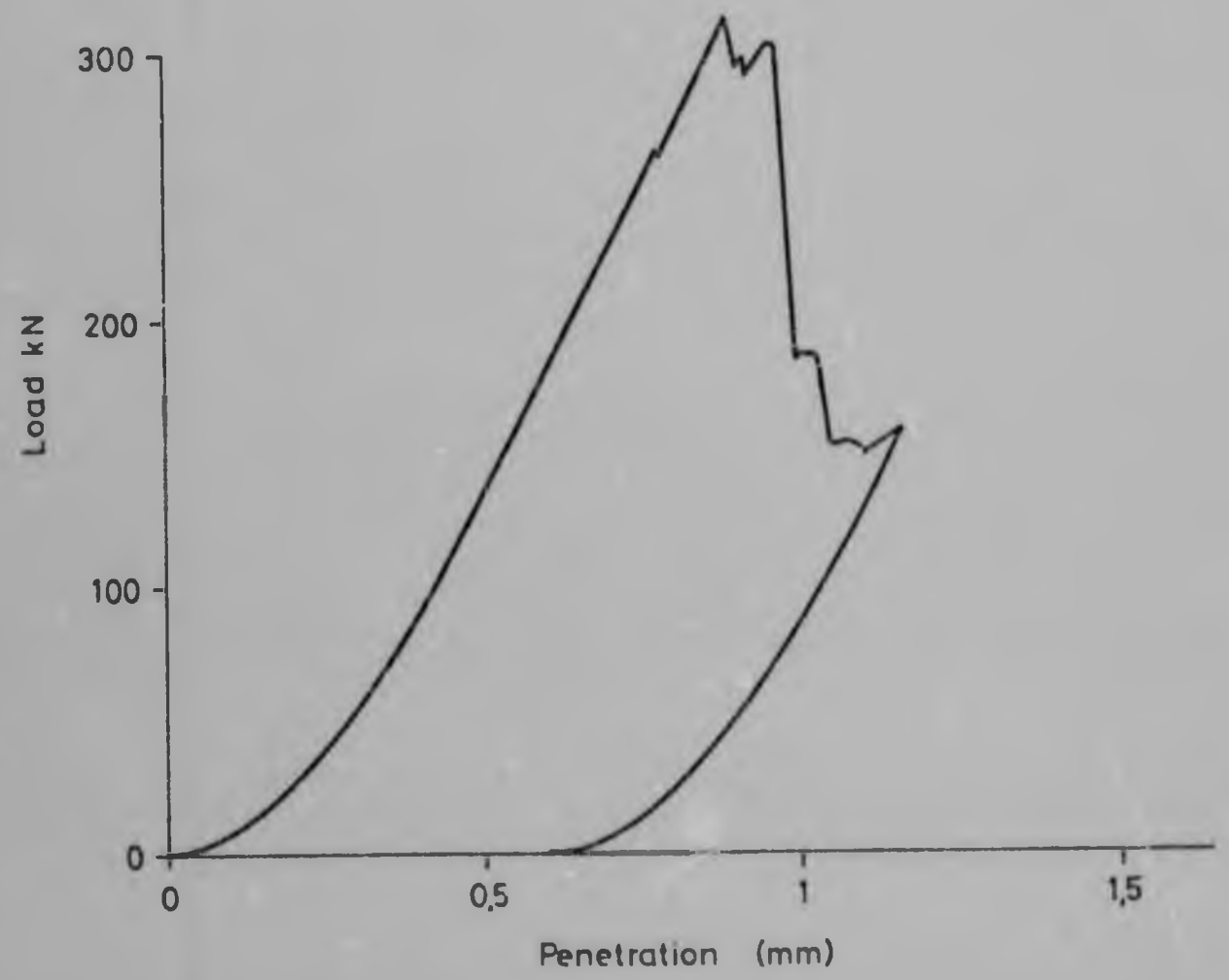


FIGURE 92 : Indentation force required to form rock chip in quartzite, plotted against penetration of the bit.

this region during these tests. Therefore, the steel applied a confining force to this area of the rock surface and inhibited the propagation of cracks.

In order to estimate the extent of this preferential cracking caused by the geometry of the bit, a test was carried out, using a quartzite specimen, where the application of the load was continued after the formation of the lar rock chip ahead of the bit. When the applied force reached 450 kN, approximately one and a half times the force required to form a rock chip ahead of the bit, a major rock fracture occurred behind the bit. The plot of load against penetration for this test is given in Figure 93. A discussion on the rock fracture in the vicinity of the bit is given in Section 7.3.

Examination of the rock chips formed ahead of the bit during these quasi-static indentation tests, showed that geometrically they resembled very closely the rock chips that were formed during the cutting process, (Figure 94). From this result it was concluded that quasi-static indentation tests could be used to study the process of rock fracture during the cutting operation.

7.2.2 Indentation tests with a shear force superimposed between the bit and the rock

The most apparent difference in results between the indentation tests (Section 7.2.1), and the cutting experiments (Chapter 5), in terms of the rock breaking process, was that during the indentation tests much higher values of the normal, or penetrating, force were required to break the rock. Typical penetrating force values when cutting in

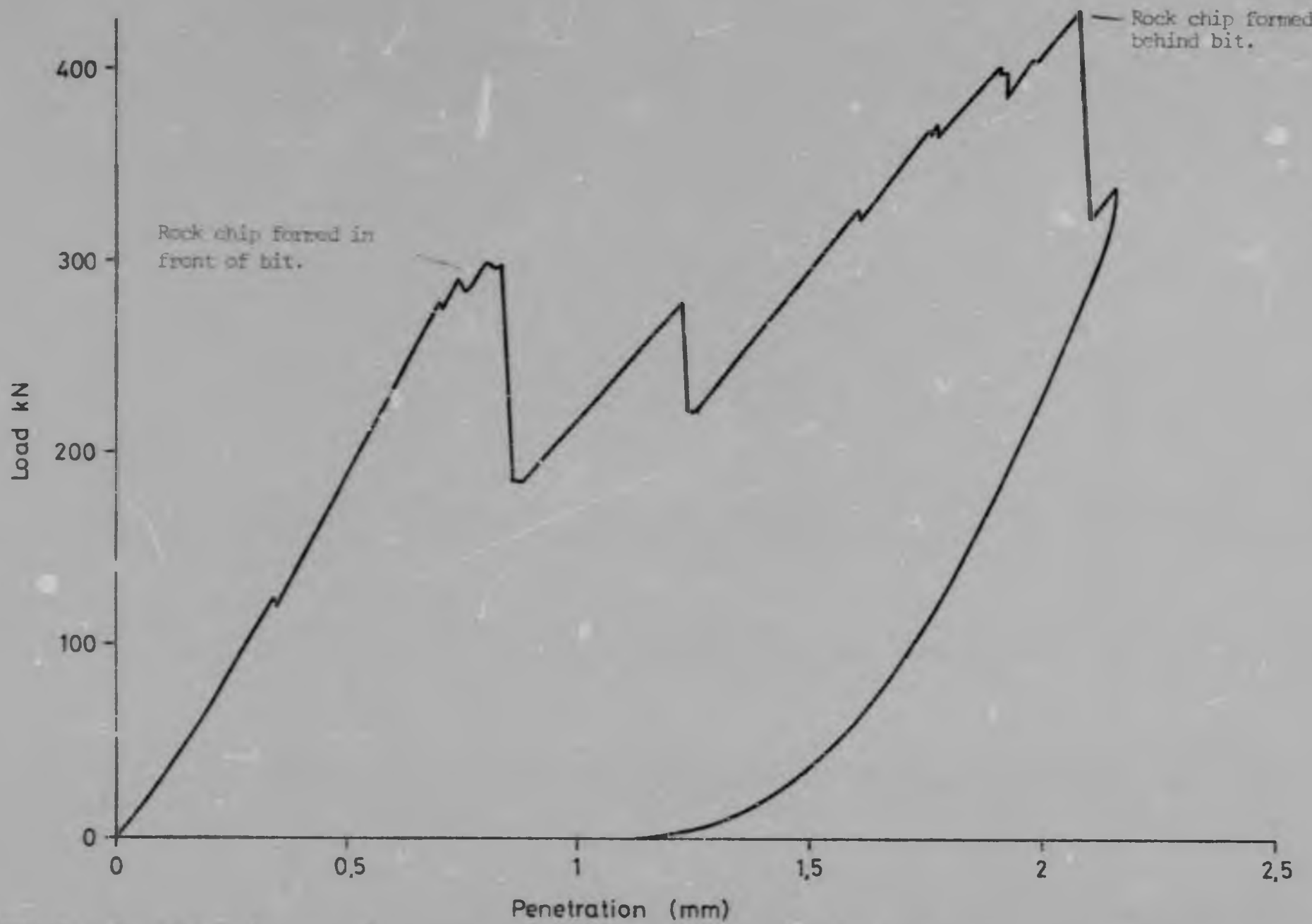


FIGURE 93 : Indentation force required to form a rock chip behind the bit plotted against bit penetration.



FIGURE 94 : Geometric similarity between rock chips formed during the cutting operation and those formed during indentation tests.

norite with a 35 mm thick drag bit were 100 kN to 250 kN. Results from the indentation tests, using a bit of the same design as an indentor, showed that in order to form a large rock chip in quartzite ahead of the leading face of the bit a force of between 250 kN and 350 kN was required and in norite a higher force of 400 kN to 500 kN was needed.

In order to account for this difference in force values it is necessary to examine differences between the cutting operation and the quasi-static indertation experiments. Two major factors which affect the force required to break the rock and which were not simulated by these indentation tests are, the absence of the shear force component, which is equivalent to the bit cutting force, and also the lack of impacting by the bit against the rock. This impacting normally is introduced during the cutting process by compliance of the hydraulic drive to the rockcutting machine, (Section 6.3.3).

In an attempt to simulate one of these factors, apparatus was constructed which enabled a shear force to be applied between the bit and the rock during an indentation test. This apparatus comprised a bit, mounted inside a right-angled frame which was positioned inside the testing machine, (Figure 95). The bit was applied normal to the rock surface in the usual manner, with the bit wearflat in contact with the rock. A steel ring was fitted over the rock specimen and, attached to this ring was a threaded bar which passed through the frame containing the bit, (Figure 95). A 300 kN centre-hole, hydraulic jack was mounted onto the threaded bar and held with a retaining nut. This jack was arranged to bear against the right-angled frame so that when pressure was applied to the jack, the

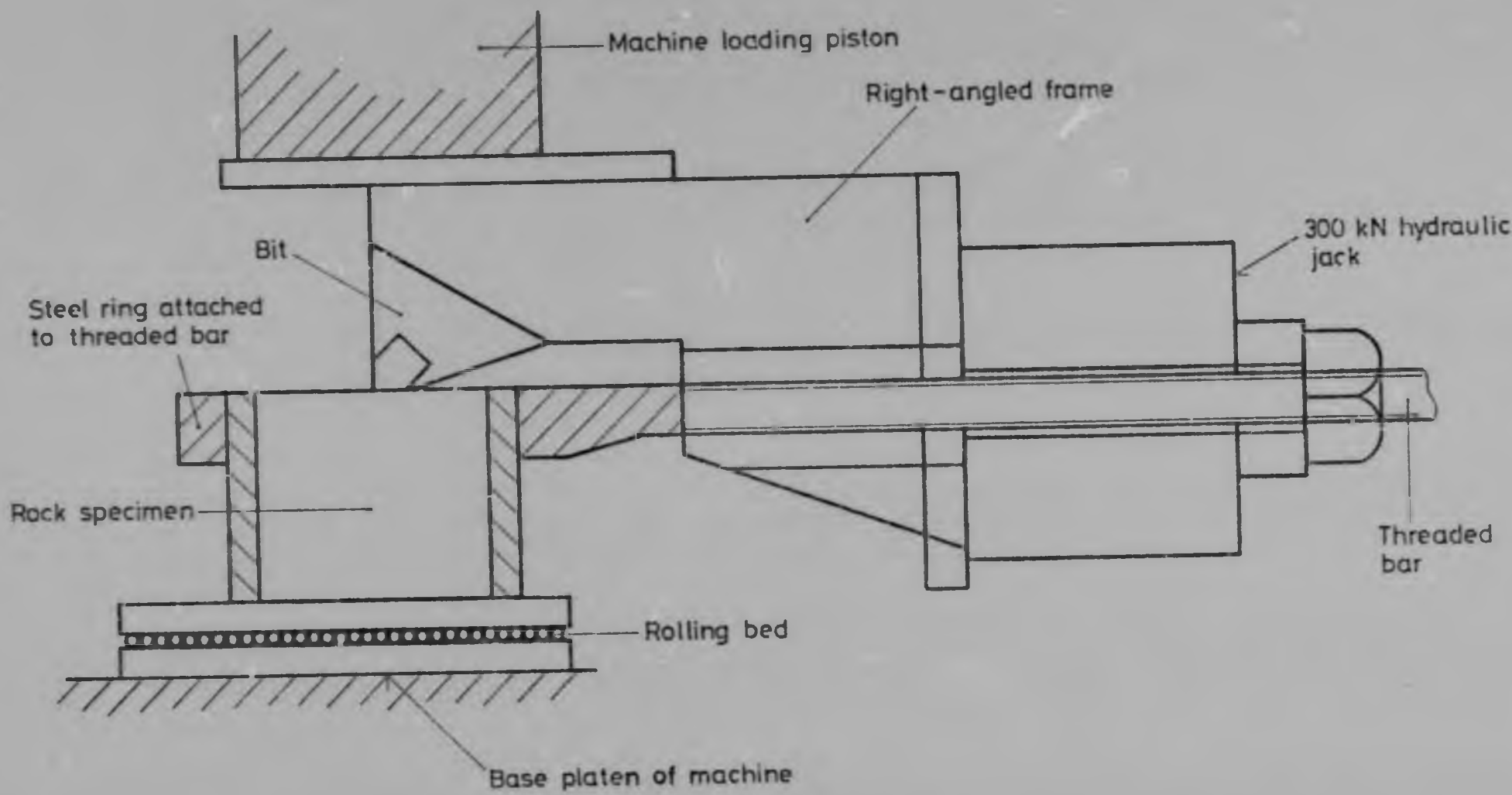


FIGURE 95 : Method by which a shear force was applied to the rock during indentation tests.

tensile force which was induced in the threaded bar was reacted by this frame. Therefore, when a normal force was acting on the bit and the jack was pressurized, a shear force would be applied to the rock by the bit, (Figure 95).

In order to ensure that a couple was not generated between the bit and the rock, the apparatus was arranged so that the steel ring, by means of which the 'pulling force' was applied to the rock, was mounted at the top of the rock specimen in the line with the bit. Also, the rock specimen was mounted on a 'rolling bed', which consisted of two flat plates with small diameter rollers trapped between them. This prevented a friction force from causing the rock specimen to tip up when pressure was applied to the jack.

The experimental procedure followed was to apply the force normal to the rock surface,using the loading piston of the testing machine, in the usual manner, (Section 7.2.1). As this force was increased, the hydraulic jack was pressurized in a controlled fashion using a hand pump, thereby applying a shear force to the rock. This shear force was measured by monitoring the pressure in the jack and then using the calibration which had been made previously with this jack, (Section 4.2.1). A dial indicator was placed against the rock specimen in order to monitor accurately relative movement between the bit and the rock specimen. The shear force was applied using the jack until small movements of the rock, less than $2{,}5 \times 10^{-2}$ mm, were observed to take place. When this occurred, pressurization of the jack was stopped until the normal force, which was applied continuously, had increased. The shear force was applied in this discontinuous manner to ensure that, at any given time, the shear force on the rock was a maximum for a

given normal force. The normal and the shear forces were recorded until a large rock chip formed ahead of the bit.

Four specimens of norite were tested in this manner and the rock chips that were formed were geometrically similar to those produced during the cutting operation. Measurements recorded during these experiments showed that the force normal to the rock surface which was required to form a rock chip ahead of the bit varied between 250 kN and 350 kN. This compared with values of 380 kN to 450 kN of this component of force, which had been measured when no shear force was superimposed on the rock (Section 7.2.1). Typical maximum values of the bit penetrating force which were measured during the cutting operation when water jets were not directed ahead of the bit, were in the range 200 kN to 250 kN. These experiments showed that the indentation force applied normal to the rock surface which was required to form a large rock chip, was only slightly higher than was measured during the cutting operation. This discrepancy in force values between these indentation tests and the cutting tests, probably is due to impacting of the bit during the cutting operation. It was shown previously that compliance of the hydraulic system introduced vibration of the bit which affected the forces applied to the bit, (Section 6.3.3).

Therefore, it was concluded that the mechanism of rock fracture when a blunt design of drag bit is used to cut strong rock, could be studied by performing a suite of quasi-static indentation tests, using the bit to indent the rock surface and then subsequently examining the rock.

7.3 The propagation of fracture in rock caused by a bit indenting the rock surface with the force applied normal to the surface

The objective of this experiment was to study in detail the mode of rock fracture caused by indentation, using a drag bit applied normal to the rock surface. It was anticipated that the results of these tests would indicate how high pressure water jets directed immediately ahead of the bit during the cutting operation, could assist the rock fracturing process.

A suite of indentation tests was carried out using specimens of both norite and quartzite. These specimens were made using the same core sections from which the rock samples for the previous tests had been prepared, (Section 7.2.1). In order to examine cracks as they developed in the rock when the load was applied, the compression was stopped at predetermined points along the curve of load against penetration, with special attention paid to points immediately prior to the peak of this curve. The rock speciments were then sectioned with a diamond saw and the fractured zone adjacent to the bit was studied. A scanning electron microscope was used to obtain a large depth of field in a magnified section of this fractured region.

A section through one of the quartzite specimens from the indentation tests (Figure 96), shows that the rock immediately underneath the bit wearflat was intensely crushed to a depth of several millimetres. The crack which indicates the formation of a major rock chip ahead of the leading edge of the bit, is marked "A" in Figure 96. Other major cracks, marked "B" and "C" in Figure 96, extended from the

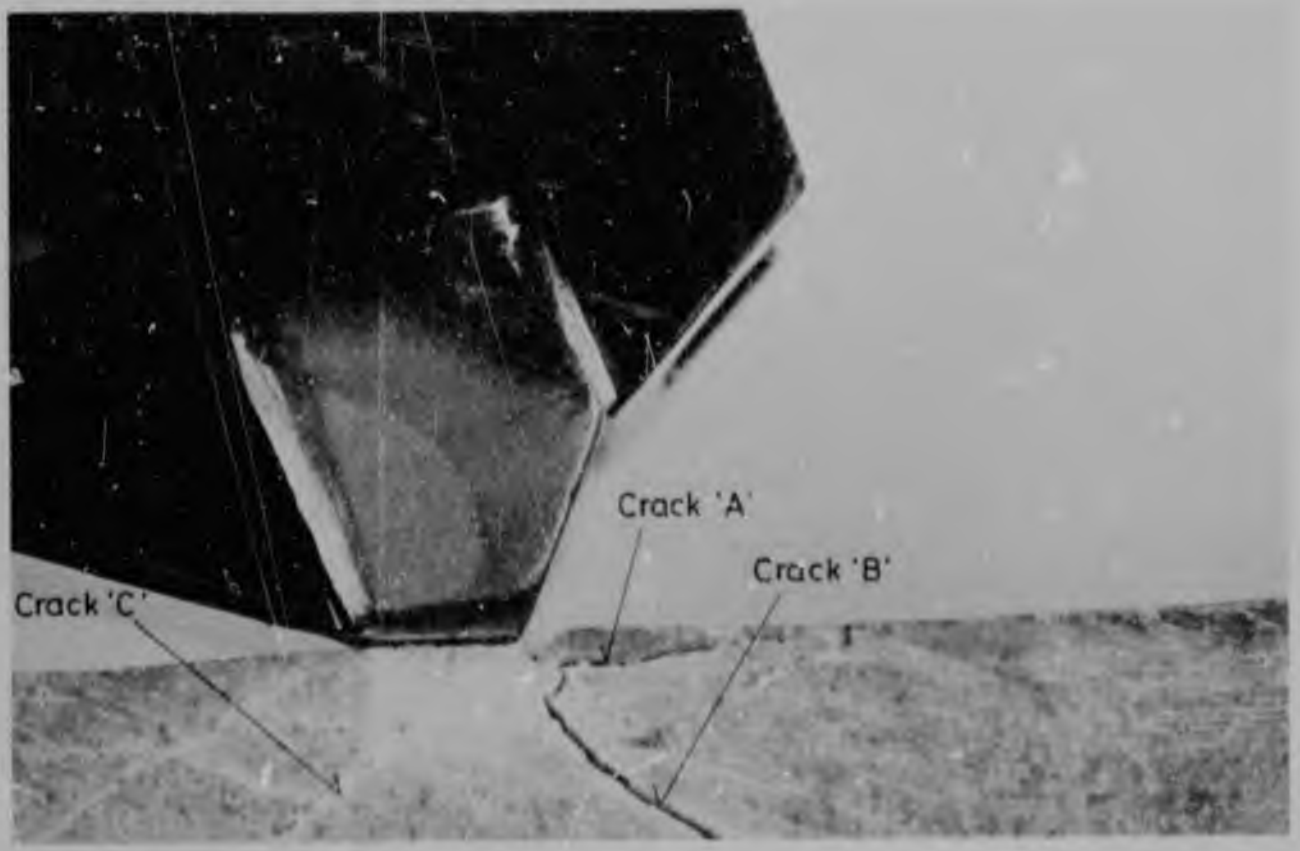


FIGURE 96 : Section through rock specimen, illustrating the position of a rock chip relative to the bit.

crushed rock zone to the sides of the specimen, (Figure 97). A crack once initiated develops towards a free surface to form a rock chip. Therefore the prominence of the cracks marked "B" and "C" was attributed to the limited size of the specimen. In a massive block of rock the only available free surface would be the face in contact with the bit wearflat and consequently, the crack marked "A" would be expected to develop in preference to the cracks "B" and "C".

A more detailed study of the propagation of the cracks adjacent to the bit was carried out using four rock specimens, two of norite and two of quartzite. A bit was used to indent the rock surface and the applied load was removed at selected points along the curve of load plotted against penetration. The graphs from these tests are given in .igures 98 to 101. The rock specimens were sectioned in a similar manner to that illustrated in Figure 96 and the region of interest, immediately underneath the bit wearflat and in front of the leading edge of the bit, was mounted on a scanning electron microscope specimen holder. Photographs were taken of the cracks made visible when the rock was examined using this microscope.

Figure 102 shows the fractures which developed in one of the norite samples as a result of indentation by the bit. The curve of load plotted against penetration made during this test is given in Figure 98. The most clearly defined fracture in Figure 102 is that closest to the rock surface. If the force applied to the indentor had not been removed, this crack would have extended to form a large rock chip. The shape of this rock chip is defined by the crack, and the geometric similarity between this chip and those from other indentation and cutting experiments (Figure 94), is apparent.

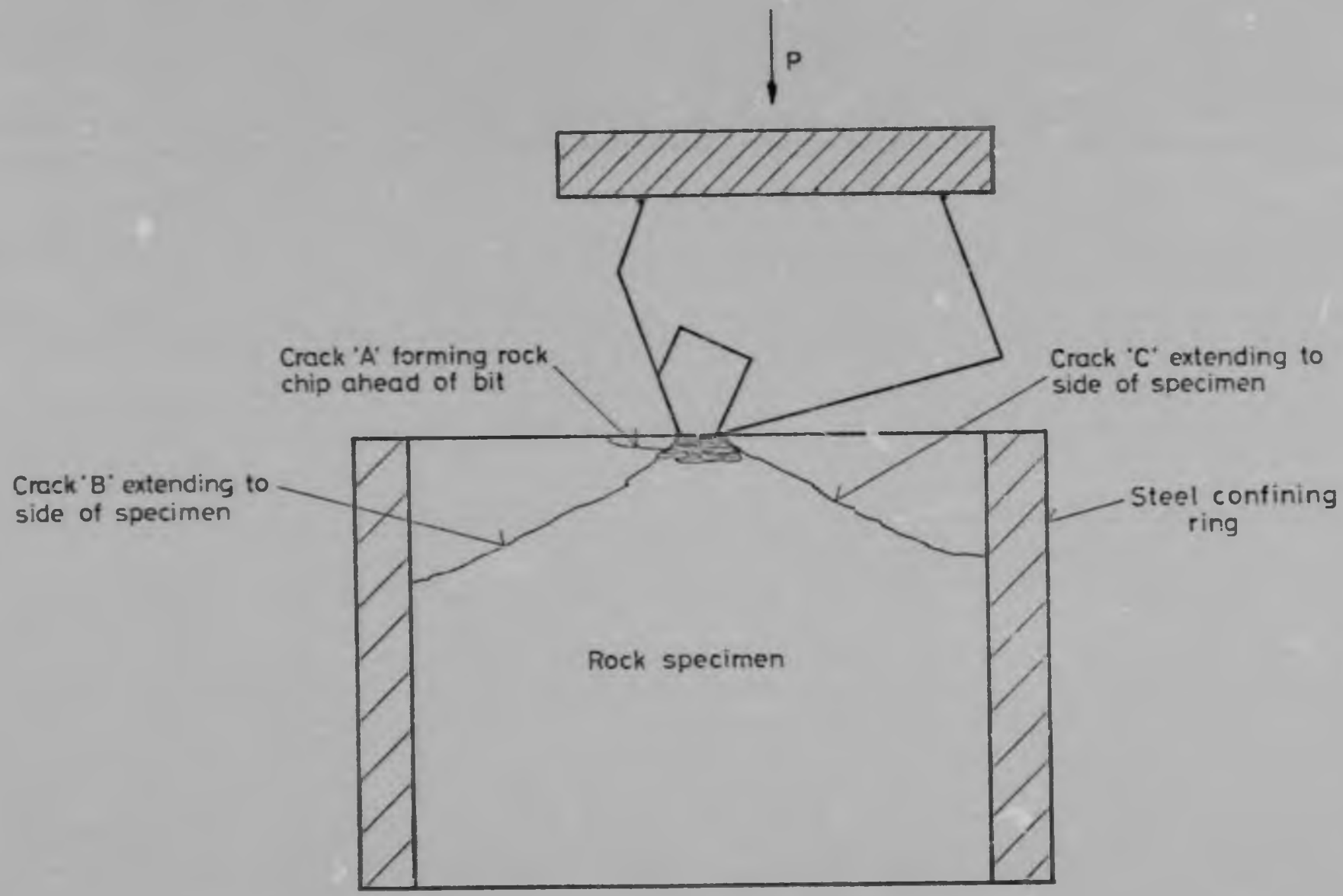


FIGURE 97 : Diagram illustrating cracks which developed as a result of the limited size of the specimen.

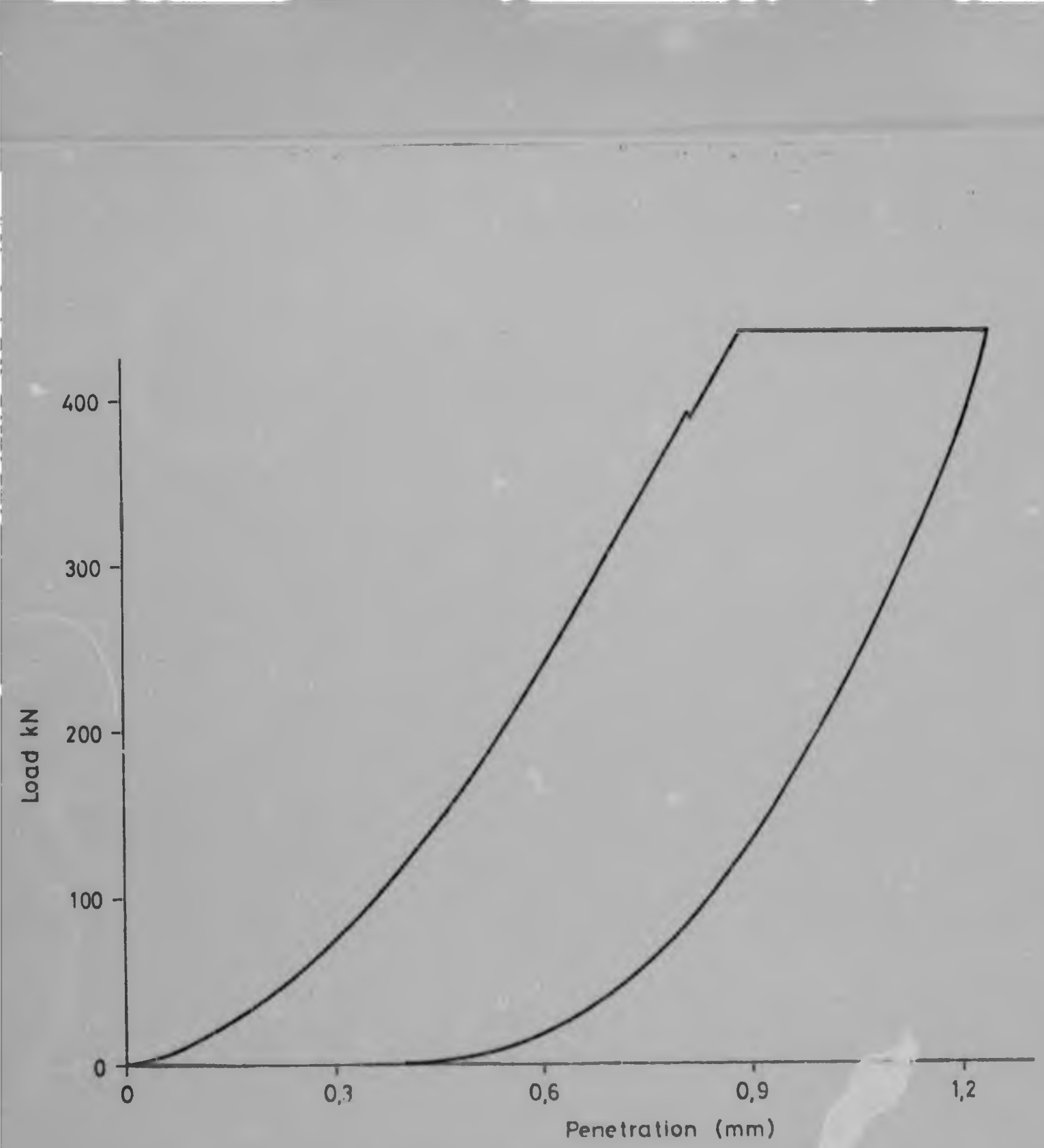


FIGURE 38: Indentation load plotted against bit penetration for first norite specimen.

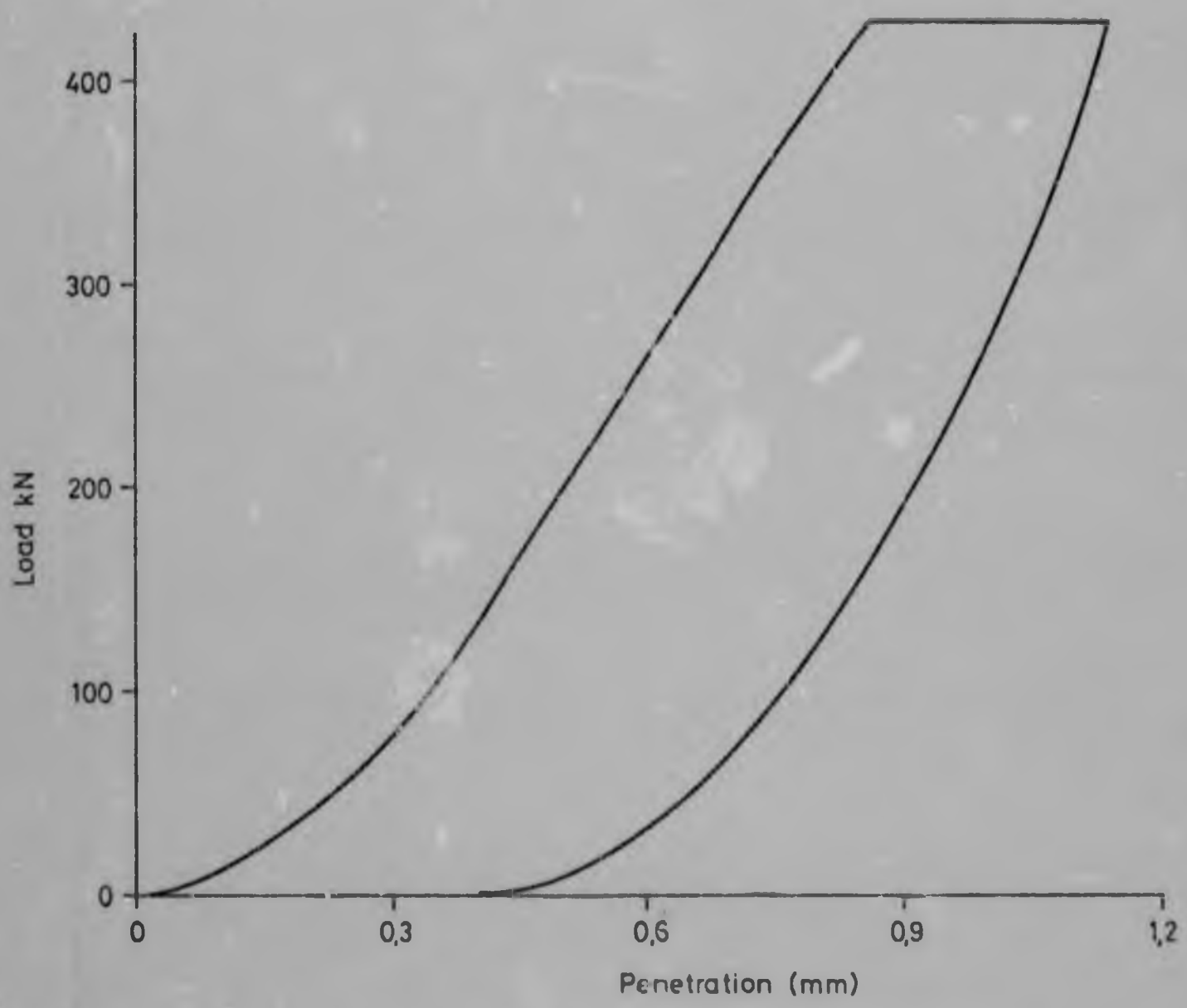


FIGURE 99 : Indentation load plotted against bit penetration for second norite specimen.

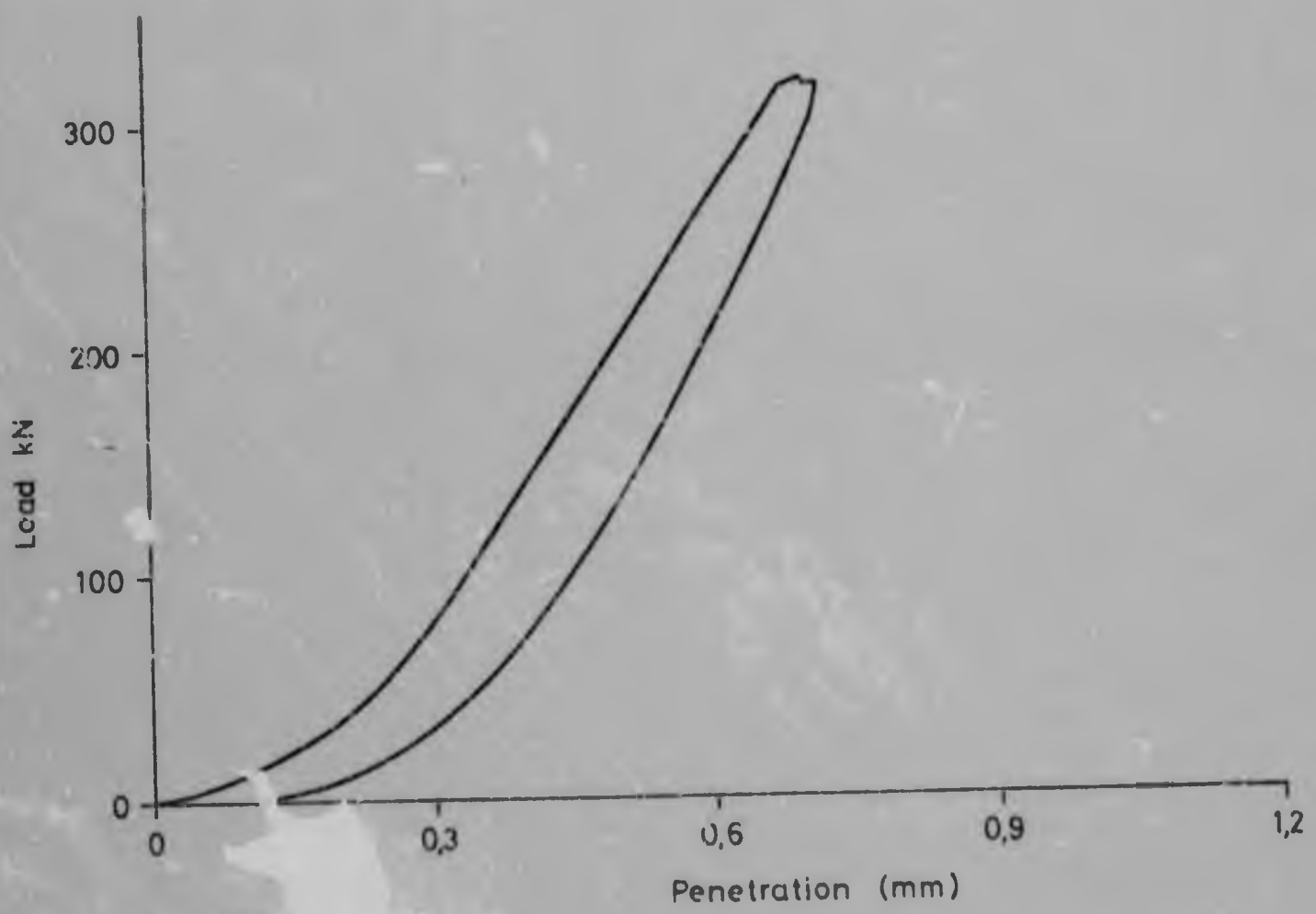


FIGURE 100 : Indenta... [illegible] plotted against bit penetration for first quartzite specimen.

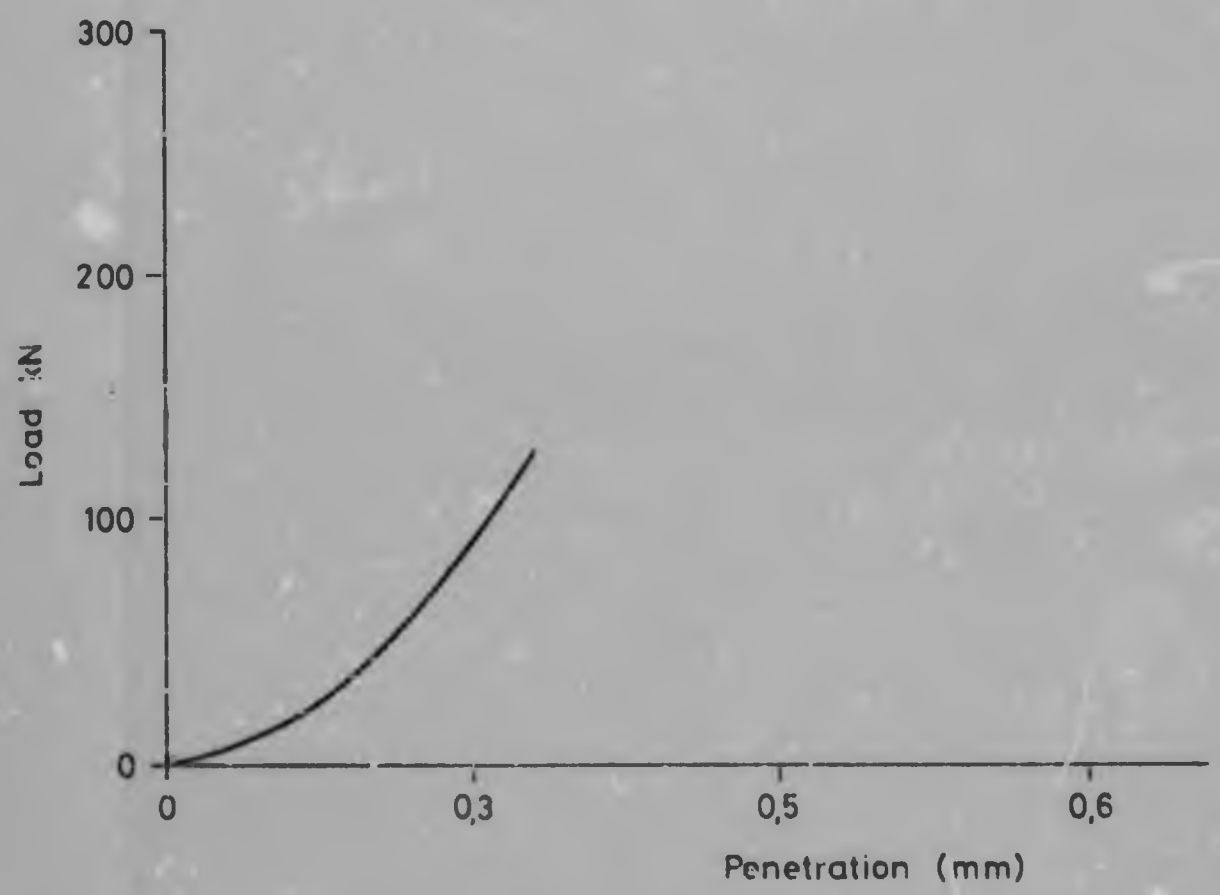


FIGURE 101 : Indentation load plotted against bit penetration for second quartzite specimen.

The rock immediately underneath the bit wearflat was intensely crushed. This is shown by the different appearance of the rock adjacent to the bit compared to that of surrounding rock, (Figure 102). This region of crushed, powdered rock extends ahead of the leading face of the bit by some 4 mm.

The graph of applied load plotted against penetration for the second norite specimen shows that the force applied was somewhat lower than was used for the first test, (Figure 99). Consequently the extent of rock fracturing is less marked, (Figure 103). Nevertheless, the crack near to the free surface, which indicates the formation of a rock chip, is clearly visible and is marked "A" in Figure 103.

A magnified section of the crack in the first quartzite specimen which was loaded close to failure of the rock (Figure 100), is given in Figure 104. This shows two cracks in the rock specimen immediately in front of the bit. These cracks have an orientation similar to those found in the norite specimens (Figures 102 and 103), although the major fracture close to the free surface is considerably longer and further below the surface than those observed in norite.

The load applied to the second quartzite specimen was removed at approximately half of the force necessary to form a rock chip ahead of the bit, (Figure 101). This was done in order to discover whether cracks in the rock could be detected at this force level. Figure 105 shows a section through the specimen; no marked crushing or cracking of the rock is evident in this Figure.



FIGURE 102 : Photo-micrograph of section through first norite specimen.

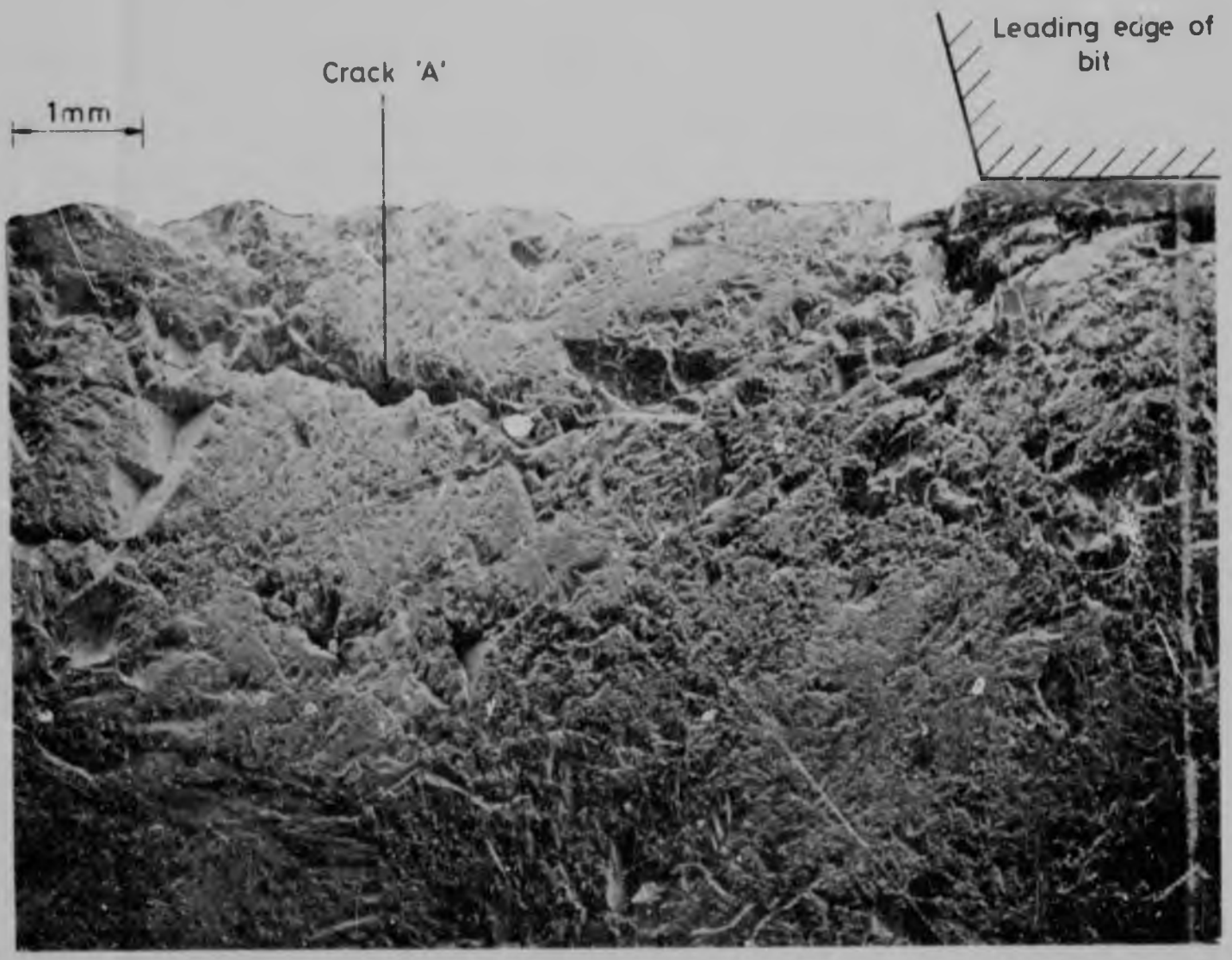


FIGURE 102 : Photo-micrograph of section through second norite specimen.

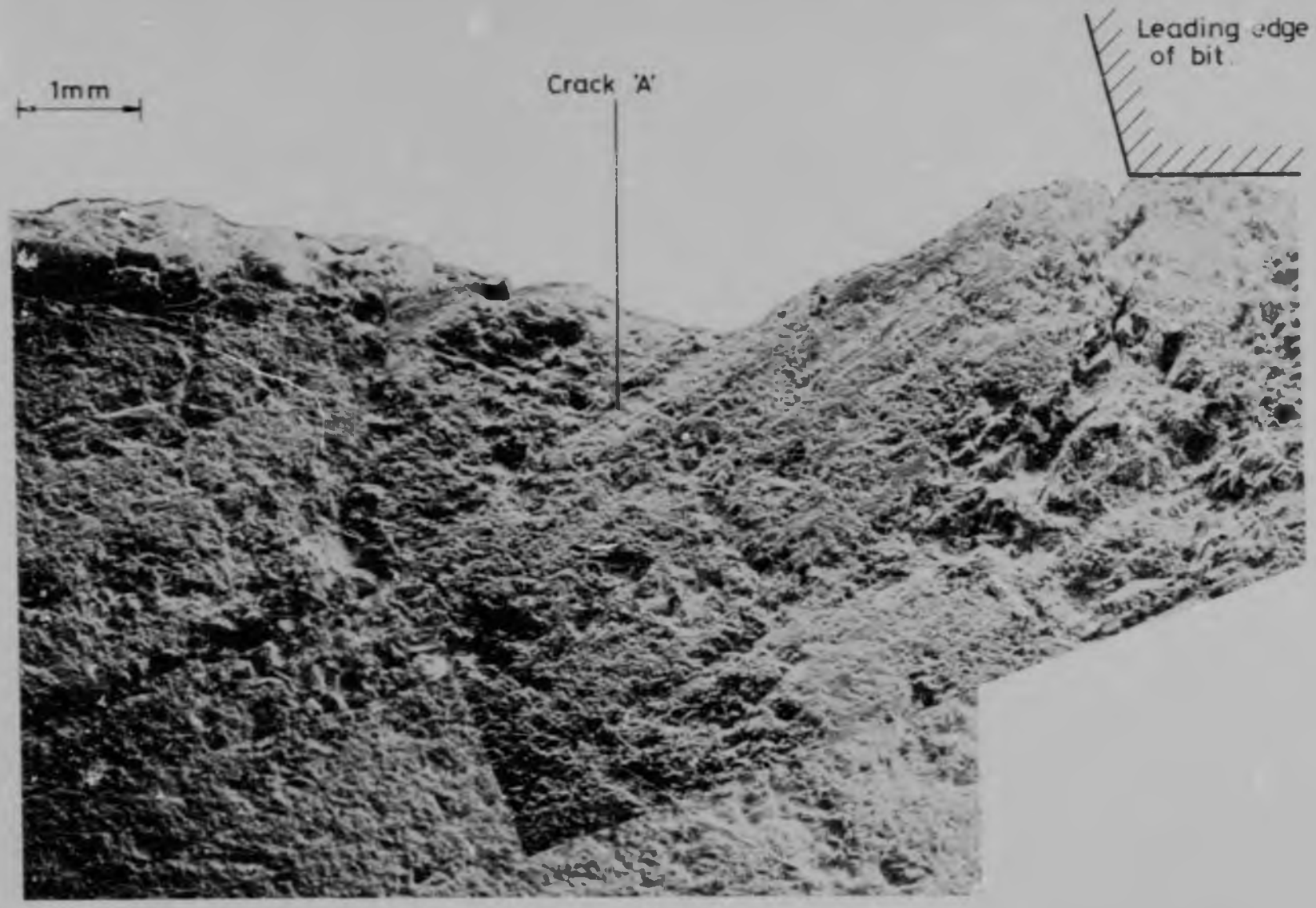


FIGURE 104 : Photo-micrograph of section through first quartzite specimen.

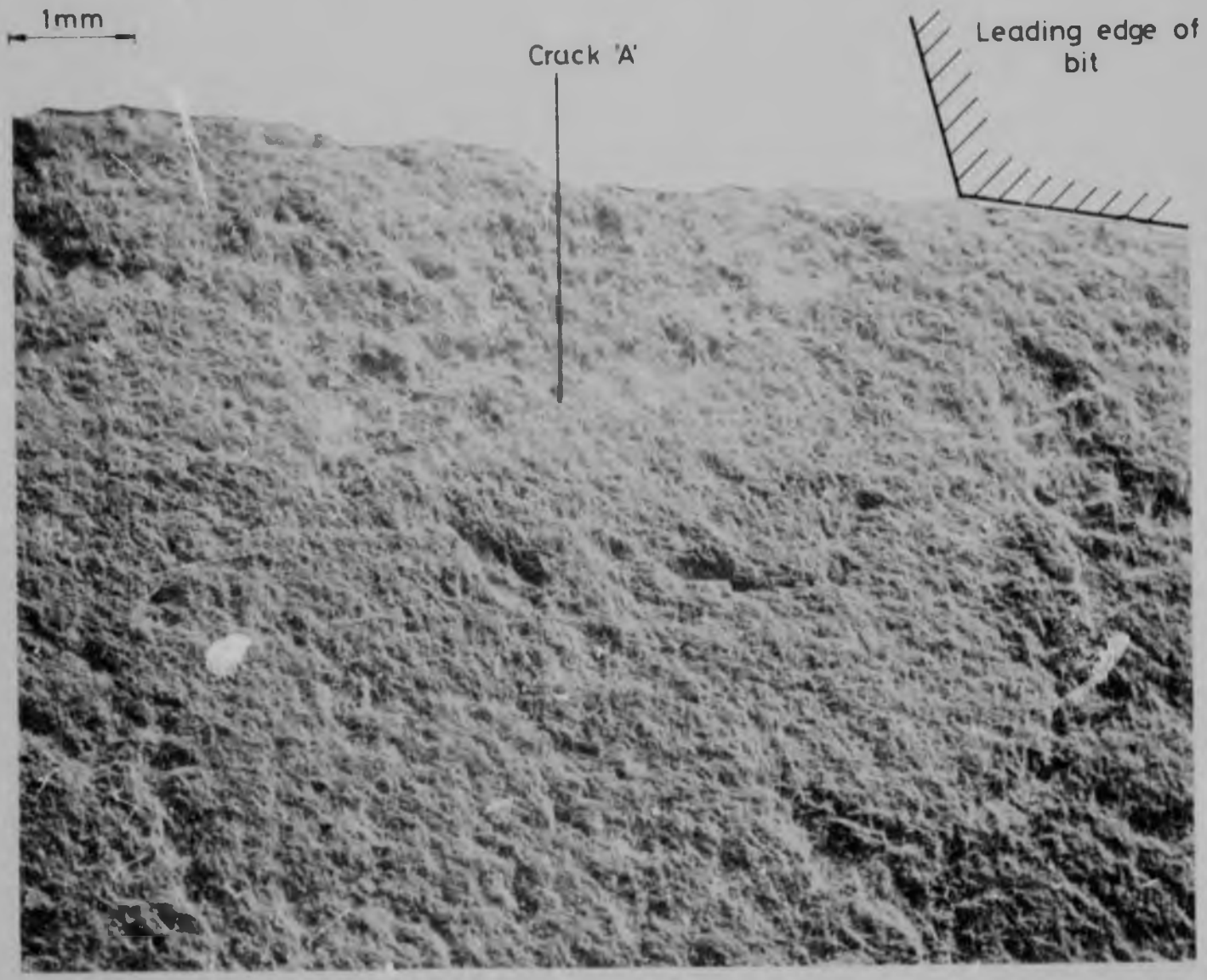


FIGURE 105 : Photo-micrograph of section through second quartzite specimen.

7.4 Calculation of the stress distribution in the rock adjacent to the bit

Experiments had shown that the indentation force necessary to form a rock chip ahead of a drag bit was reduced markedly when a shear force, applied parallel to the rock surface, was superimposed on the bit, (Section 7.2.3). In an endeavour to find an explanation for this and other related phenomena, use was made of mathematical analysis. The stress distribution in the rock adjacent to the bit was calculated by making the following assumptions :

(i) The rock behaves as a linear, isotropic, elastic material.

(ii) The bit applies a uniformly distributed load to the surface of the rock, which is taken to be a semi-infinite mass.

It has been shown that most hard rocks exhibit ideal elastic behaviour up to a critical stress level (Wagner and Schümann, 1971), and therefore the first of these assumptions is valid.

It can be shown that the stresses applied in an elastic material underneath a punch are dependent on the assumptions made about the nature of the punch. If the punch is assumed to be rigid then, in the regions underneath the corners of the punch, the stresses tend to infinity. On the other hand, finite stress values in the material are calculated if the stress along the contact area between the punch and the elastic body is taken to be uniformly applied. The application of the load when a blunt drag bit is used to cut hard rock, probably is a compromise between these two extreme methods of loading. Away from the contact area the stress fields induced by these two

loading conditions become virtually idential (Wagner and Schümann, 1971), for this reason one condition only, the latter condition was considered in this analysis.

A two dimensional analysis was used and the plane in which the rock stresses were calculated is illustrated diagramatically in Figure 7. Two separate loading conditions were considered :

(i) with a normal force only applied to the punch

(ii) with both a normal force and a shear force applied to the punch.

Contours of stresses parallel to the x axis and the y axis were calculated, together with the shear stresses. From these the principal stresses were calculated. The Mohr failure criterion was used to define a zone of excess stress underneath the punch. From a series of triaxial tests with norite specimens, the Mohr envelope for this rock type was plotted, (Figure 106). The radius of the Mohr circle is given by half the difference of the principal stresses and the distance from the y axis to the centre of the circle is given by half the sum of the principal stresses, that is :

$$R = \tfrac{1}{2}(\sigma_1 - \sigma_3)$$

and

$$A = \tfrac{1}{2}(\sigma_1 + \sigma_3)$$

where R and A are defined in Figure 107.

If the intercept of the Mohr envelope is given by S_o and the angle that the linear portion of this curve makes with the x axis is given by ϕ (Figure 107), then linear extrapolation of this curve gives that the intercept on the x axis is

$$x_1 = -\frac{S_o}{\tan \phi}$$

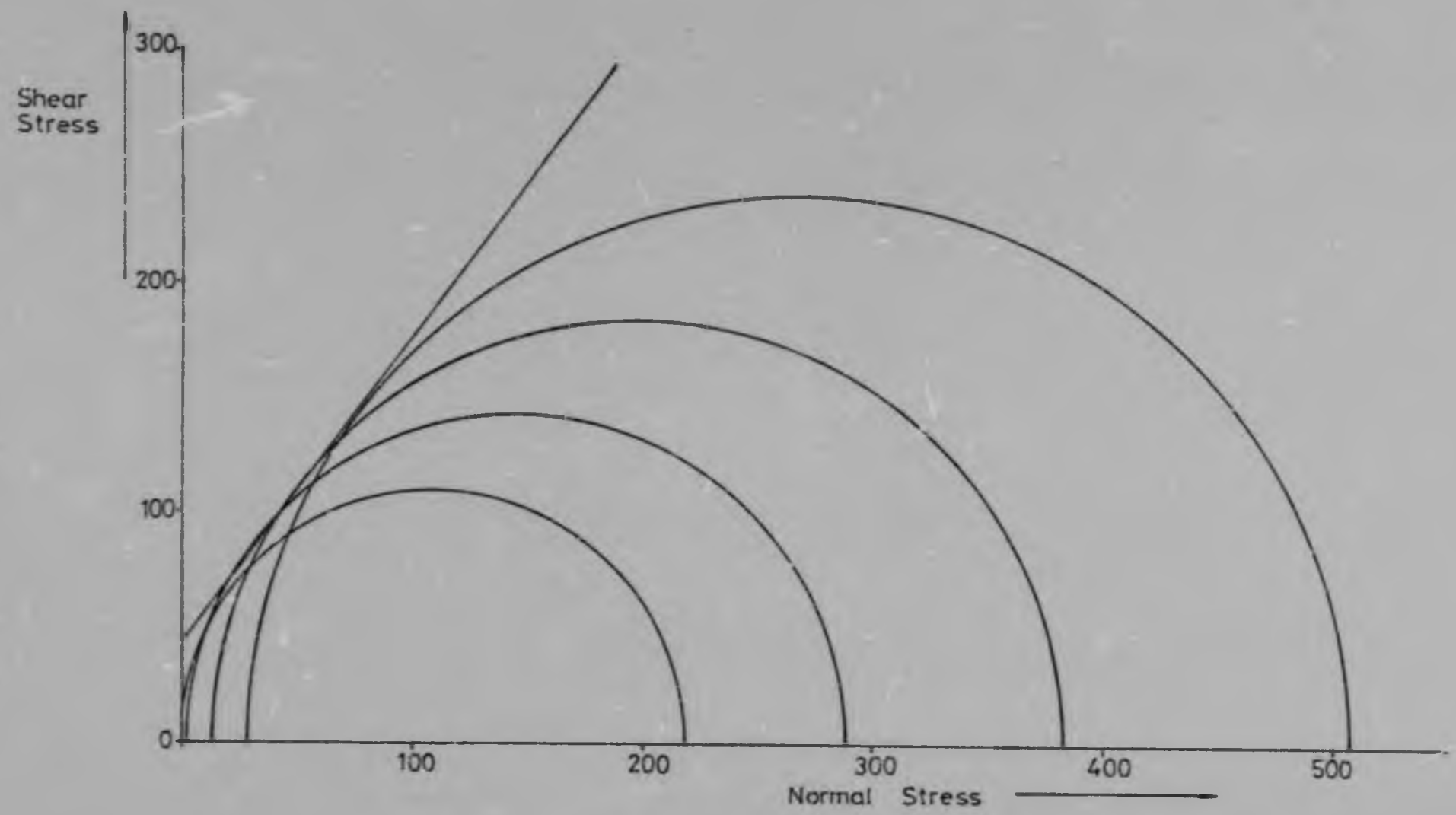


FIGURE 106 : Mohr envelope plotted for granite rock specimens.

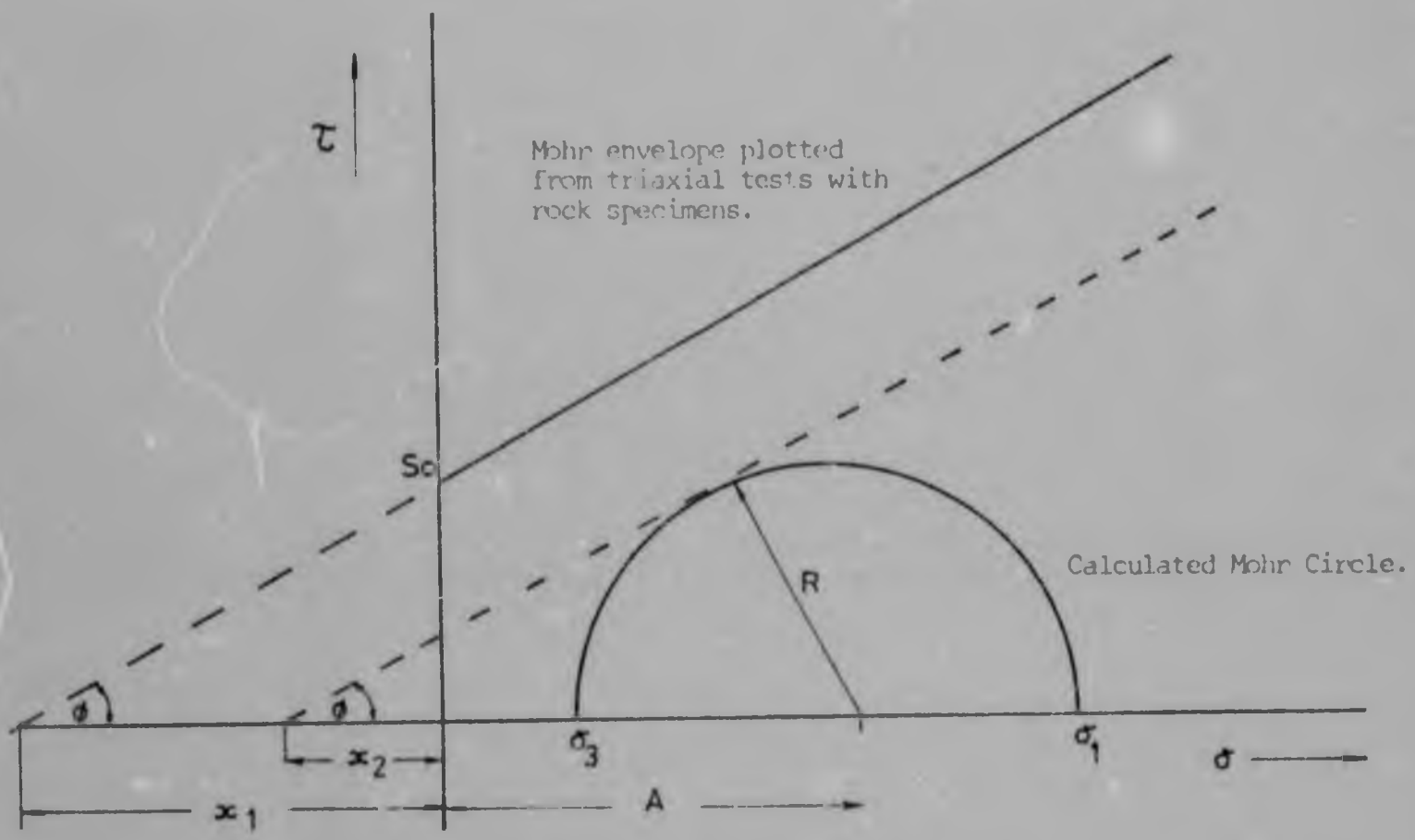


FIGURE 107 : Diagram illustrating the criterion used to determine the state of stress at points in the rock underneath an indentor.

Now, if the principal stresses are calculated at a point in the rock underneath a punch and the Mohr circle is plotted then the rock is defined as failed if the circle touches or crosses the Mohr envelope. From Figure 107 the intercept on the x axis from the Mohr circle is given by

$$x_2 = \frac{\frac{1}{2}(\sigma_1 - \sigma_3)}{\sin\phi} - \frac{1}{2}(\sigma_1 + \sigma_3)$$

$\therefore$ if $x_2 < x_1$ then rock has not failed.

But if $x_2 \geq x_1$ the rock has failed.

This criterion was used to define the regions of failed rock underneath the punch.

The mechanism by which fractures propagate in brittle rock is a subject which is not well understood. Investigations have been carried out by the staff of the Chamber of Mines to study rock fracture in the vicinity of underground excavations on the deep level gold mines of the Witwatersrand, (Van Proctor, 1977). These studies have shown that fractures propagate along the line of the maximum principal stress. It has been found, for example, that rock fracture occurs parallel to the stope face for a considerable distance ahead of the face on a section of a longwall which is mined by machines, and therefore where the fracture pattern is not confused by blasting, (Figure 10) Another example of brittle rock fracturing in the direction of the maximum principal stress, is the 'slabbing' on the side walls of a tunnel, (Figure 108). This phenomenon, which was discussed by Fairhurst and Cook (1966), but which otherwise is not documented in the

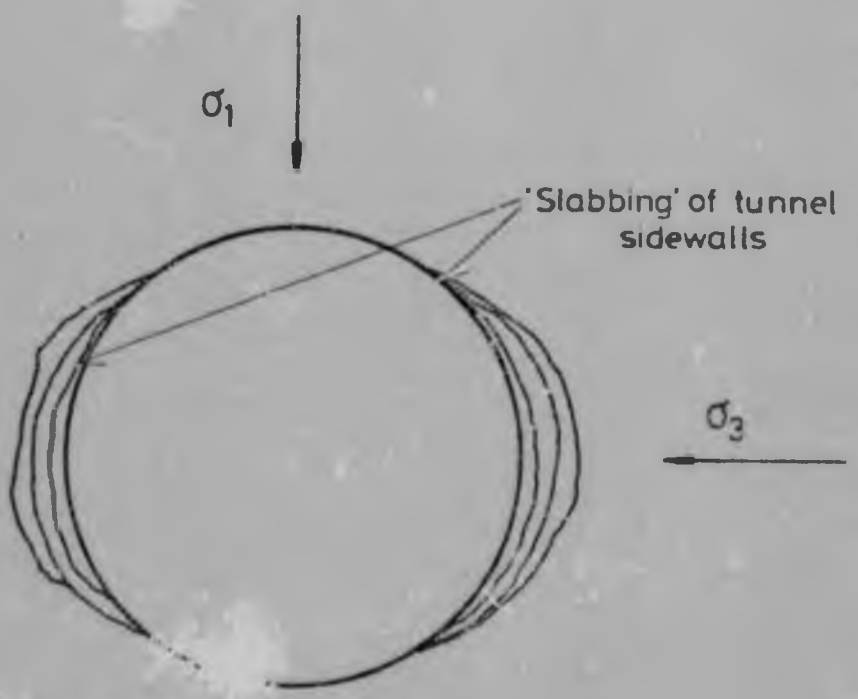


FIGURE 108 : Evidence of rock fracture parallel to the direction of the maximum principal stress illustrated by slabbing on the sidewalls of a tunnel.

literature, is so pervasive that research is being conducted by personnel at the Chamber of Mines to investigate it further. In order to investigate whether the cracks which developed in the rock adjacent to a drag bit followed in the direction of the maximum principal stress, the stress trajectories were calculated and plotted for both loading conditions.

7.4.1 Calculation of stress contours

A cross-section view of a punch applied to the surface of an elastic body is given in Figure 109. This shows a normal force P and a shear force T applied to the surface of a body by a punch with a contact length 2 L. A number of authors have developed the solution for the components of stress within the body when the normal force, P in Figure 109, is applied to the surface, (Love, 1929), (Harding and Sneddon, 1945). The stresses produced in the body when a shear force, T in Figure 109, is applied to the surface was calculated by Sneddon (1951), using Fourier transforms.

A cross-section view of a drag bit cutting in strong rock (Figure 7), shows that the penetrating force is equivalent to the normal force P in Figure 109, and that the cutting force is equivalent to the shear force T in this Figure. Because a drag bit cuts hard rock by an indentation process (Section 7.1), the bit cutting force is developed only as a result of the bit penetrating force. Therefore the stresses produced in an elastic body have been calculated for two separate cases. Firstly when only the normal force P is applied to the punch, and secondly when both the normal force P and the shear force T are applied simultaneously.

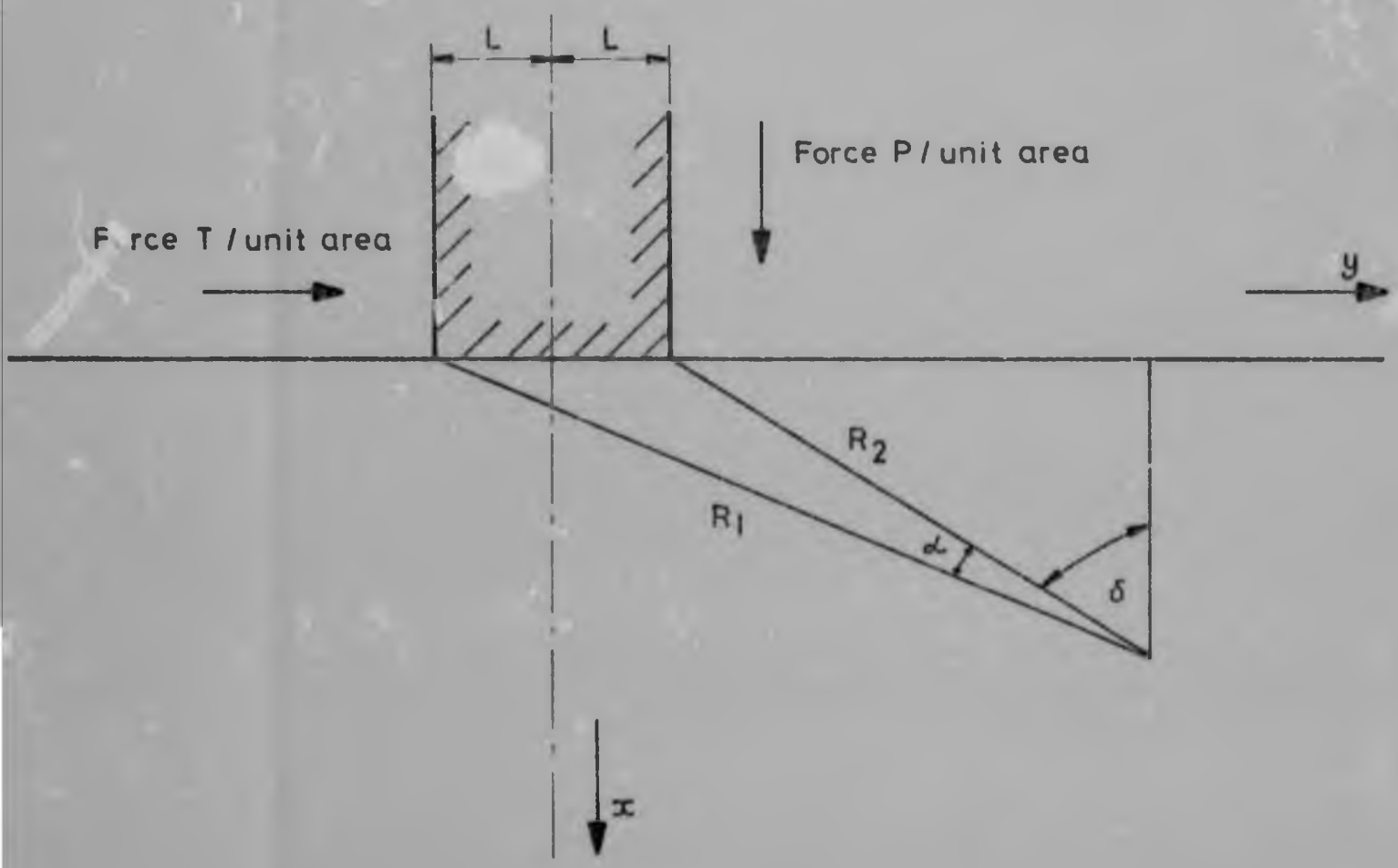


FIGURE 109 : Nomenclature for calculations of the stress induced in an elastic body when a punch is applied to the surface of the body.

The limiting values of the stress components, at a given point A, which do not vanish when the normal force P only is applied by the punch and when the appropriate boundary conditions are applied are :-

$$\sigma_{xx} = \frac{p}{\pi} \{ \alpha + \sin \alpha \cos (\alpha + 2\delta) \} \quad (1)$$

$$\sigma_{yy} = \frac{p}{\pi} \{ \alpha - \sin \alpha \cos (\alpha + 2\delta) \} \quad (2)$$

$$\tau_{xy'} = \frac{p}{\pi} \sin \alpha \sin (\alpha + 2\delta) \quad (3)$$

where p = force per unit area (after Jurgenson, 1934)

It can be shown that the principal stresses are given by :

$$\sigma_1 = \tfrac{1}{2}(\sigma_{xx} + \sigma_{yy}) + \{ \tau^2_{xy} + \tfrac{1}{4} (\sigma_{xx} - \sigma_{yy})^2 \}^{\frac{1}{2}} \quad (4)$$

$$\sigma_3 = \tfrac{1}{2}(\sigma_{xx} + \sigma_{yy}) - \{ \tau^2_{xy} + \tfrac{1}{4} (\sigma_{xx} - \sigma_{yy})^2 \}^{\frac{1}{2}} \quad (5)$$

(Jaeger and Cook, 1969)

Substituting equations (1), (2) and (3) into equations (4) and (5) gives

$$\sigma_1 = \frac{p}{\pi} \{ \alpha + \sin \alpha \} \quad (6)$$

$$\sigma_3 = \frac{p}{\pi} \{ \alpha - \sin \alpha \} \quad (7)$$

From Mohr's circle the maximum shear stress

$$\tau_{max} = \tfrac{1}{2} (\sigma_1 - \sigma_3)$$

$$= \frac{p}{\pi} \sin \alpha \quad (8)$$

Scott, (1963) developed a solution for the stresses underneath a punch when a shear force is applied to the punch. Combining the stress components to give the stress values when both a normal force and a shear

force is applied to the punch gives :-

$$\sigma_{xx} = \frac{P}{\pi}\{\alpha + \sin\alpha \cos(\alpha + 2\delta)\} + \frac{q}{\pi}\sin\alpha \sin(\alpha + 2\delta)\} \quad (9)$$

$$\sigma_{yy} = \frac{P}{\pi}\{\alpha - \sin\alpha \cos(\alpha + 2\delta)\} + \frac{q}{\pi}\{\log_e \frac{R_1^2}{R_2^2} - \sin\alpha \sin(\alpha+2\delta)\} \quad (10)$$

$$\tau_{xy} = \frac{P}{\pi}\sin\alpha \sin(\alpha + 2\delta) + \frac{q}{\pi}\{\alpha - \sin\alpha \cos(\alpha + 2\delta)\} \quad (11)$$

where q is the shear force per unit area.

The principal stresses, where these two forces were applied to the punch, were calculated by substituting the values from equations (9), (10) and (11) into equations (4) and (5).

A computer program was developed to calculate these different stress components for the two load conditions at a large number of points underneath the punch. A Data General Nova 3 mini computer with a Tektronix 4014 - 1 Graphic Display was used for this purpose. The stress contours were plotted by selecting :

(i) the load condition and values of the applied load(s).

(ii) the length of the contact area between the punch and the surface.

(iii) the size of the window to be studied.

(iv) the stress component of interest.

(v) a minimum and a maximum value of this stress component with an increment defined between these values.

The stresses within the window were calculated by the computer at

chosen points in the x - y plane. When a point was reached where a value was calculated which exceeded the required stress, the program calculated the coordinates of the point which corresponded to this stress by interpolating linearly between points. These coordinates were marked by plotting a symbol on the graphic display. The program continued in this manner, plotting a number of symbols which indicated points of known, constant stress. The selected stress values, up to the required maximum stress, were plotted in a similar fashion, using different symbols to mark different stress values. This program, together with an example of the output, is given in Appendix (iv).

Values of the loads applied to the punch were taken from the actual forces measured during the laboratory experiments cutting rock and from the indentation tests where a drag bit was pressed against the rock surface. Since all of the loads applied by the punch are expressed in terms of force per unit area, the force values must be divided by the area of the bit wearflat, which for a new bit is 35 mm x 6 mm = 210 mm^2.

From Chapter 6, the maximum cutting force applied to the bit = 150 kN.

$\therefore$ Maximum shear force per unit area = 714 MPa.

Also from Chapter 6, the maximum bit penetrating force when water jets were not used to assist the cutting operation was about 220 kN.

$\therefore$ Maximum normal force per unit area = 1048 MPa

When 50 MPa water jets were used the bit penetrating force was reduced to about 160 kN.

$\therefore$ Maximum normal force per unit area = 762 MPa.

The force applied normal to the rock surface required to form a rock chip during the indentation tests was about 420 kN in norite and 300 kN in quartzite, (Section 7...1). These correspond to pressures of 2 000 MPa and 1 429 MPa respectively. When a shear force was applied together with the normal force during the indentation tests (Section 7.2.2), the force normal to the surface of the norite specimen was reduced to about 300 kN with a shear force of about 50 kN. These correspond to pressures of 238 MPa from the shear force and 1 429 MPa from the normal force.

A complete suite of graphs, giving values of : σ_{xx}, σ_{yy}, τ_{xy}, σ_1,σ_3 and τ_{max} for the conditions both where the normal force only is applied, and where the normal and shear forces are applied to the punch, are presented in Figures 110 to 121. The applied normal stress has been taken as 1 050 MPa and the applied horizontal stress has been taken as 700 MPa. These graphs show that the stress distributions, which are symmetrical about the x axis when the normal force only is applied, are skewed over when the shear force is applied also. This has the effect of inducing higher stresses closer to the free surface ahead of the punch.

The calculations show that a zone exists behind the punch where the stresses parallel to the y axis are negative, when both the normal and shear forces are applied, (Figure 117). This indicates that tensile stresses are indiced at the rock surface in this region and, since most rocks are much weaker in tension than in compression, it was considered that tensile cracks might be developed behind the bit during the cutting operation. This is discussed further in Section 7.5.1.

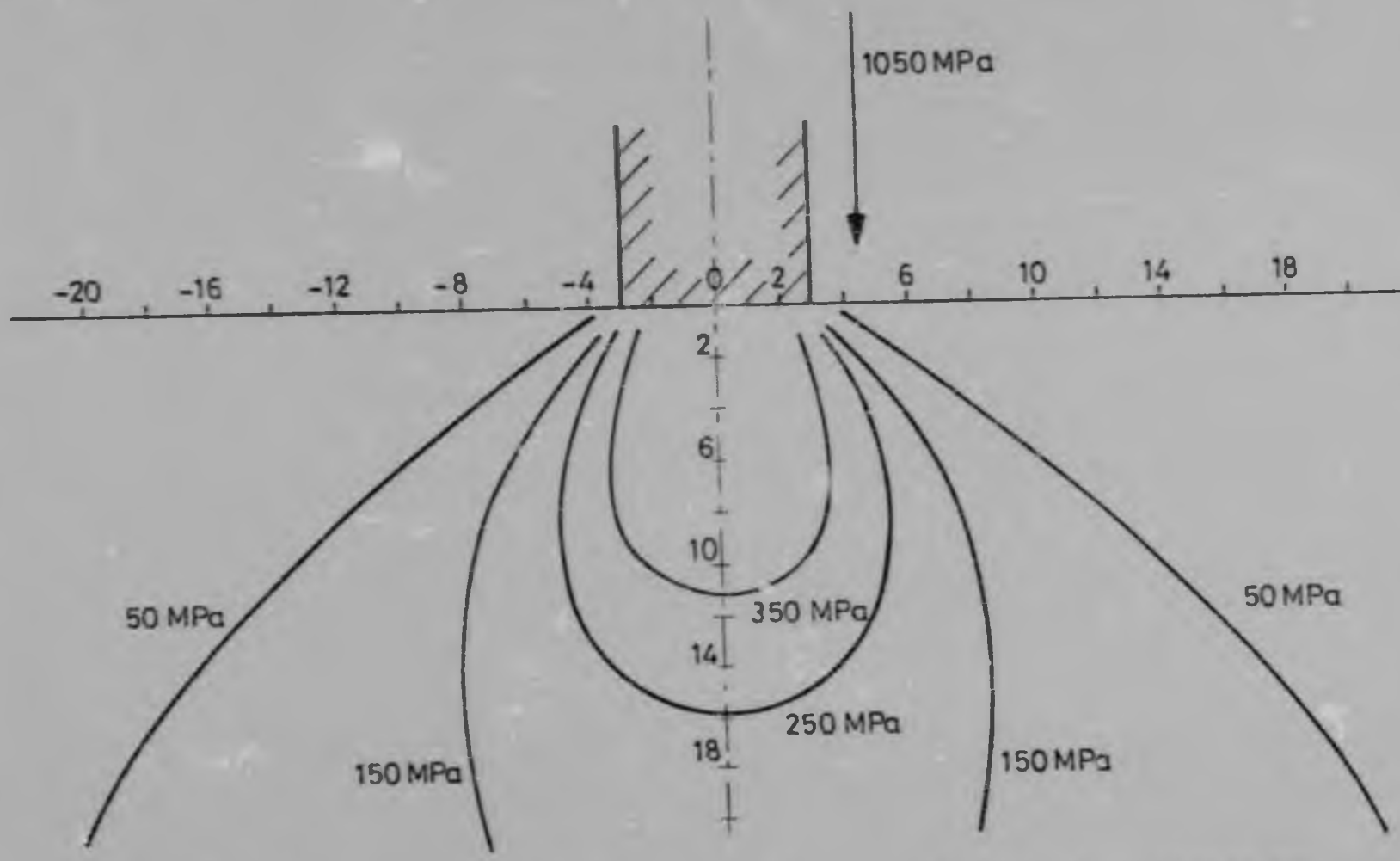


FIGURE 110 : Stress contours σ_{xx} when a normal pressure 1 050 MPa is applied to the surface of the body.

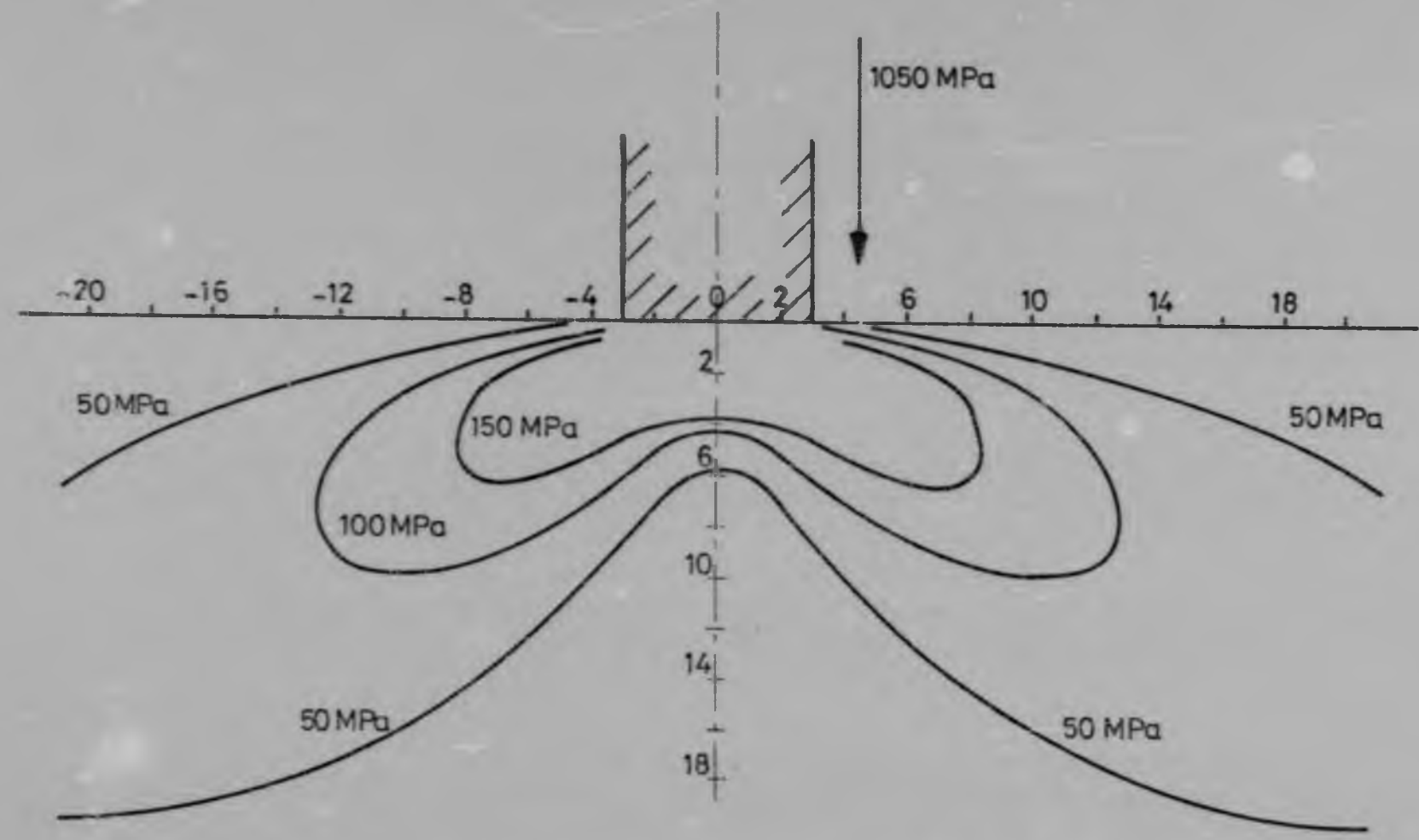


FIGURE 111 : Stress contours σ_{yy} when a normal pressure 1 050 MPa is applied to the surface of the body.

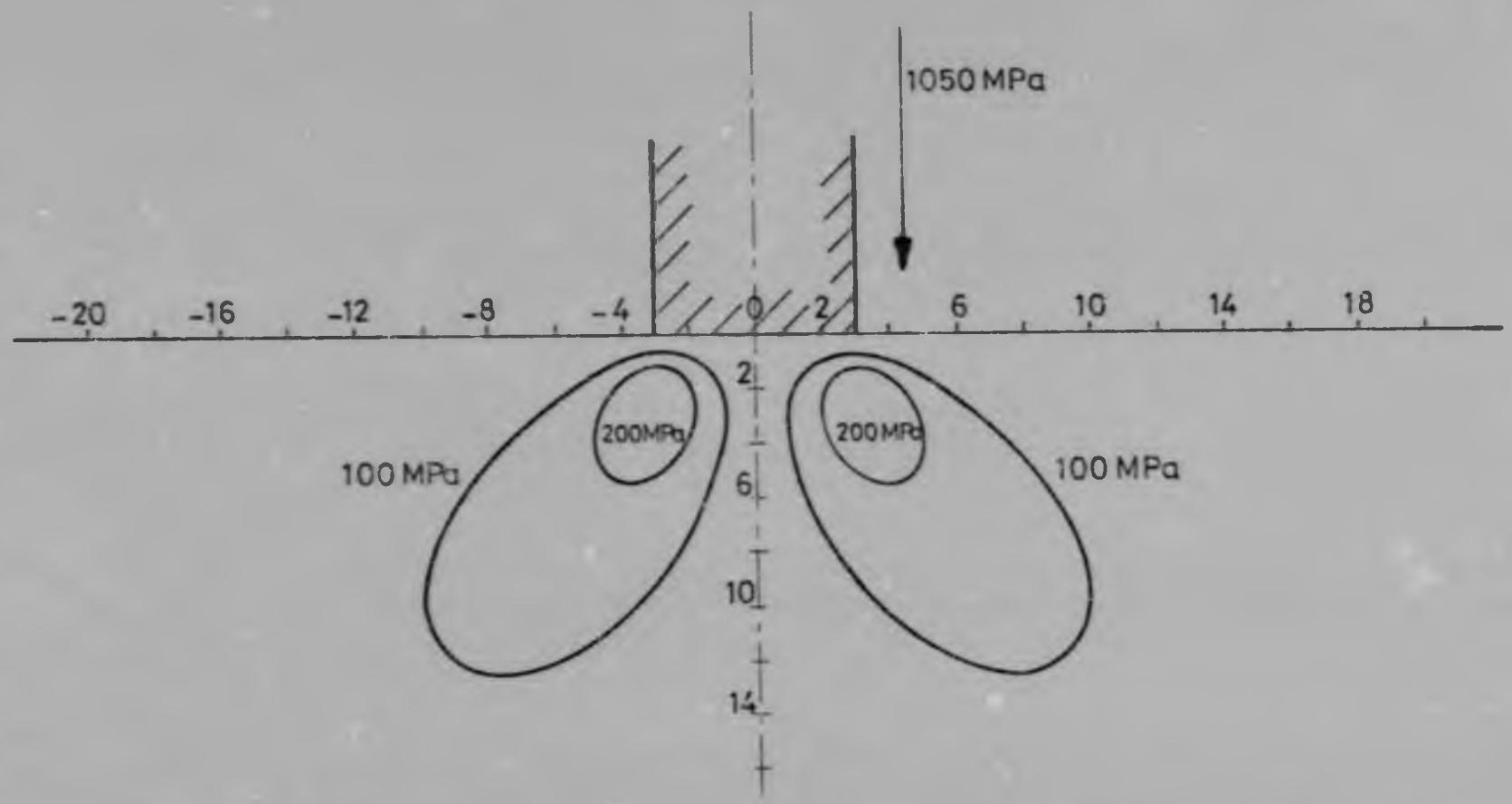


FIGURE 112 : Stress contours τ_{xy} when a normal pressure 1 050 MPa is applied to the surface of the body.

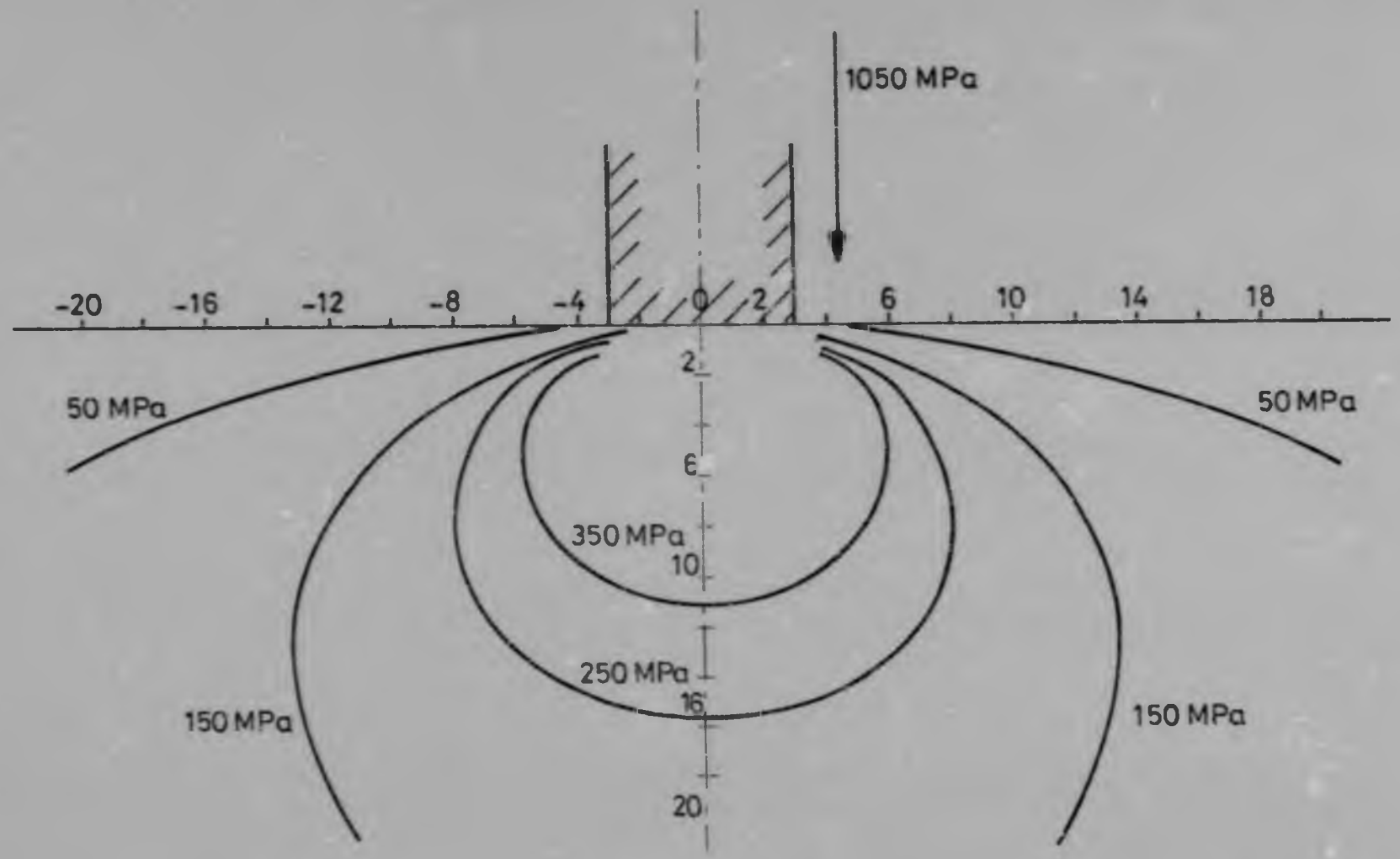


FIGURE 113 : Stress contours σ_1 (maximum principal stress) when a normal pressure 1 050 MPa is applied to the surface of the body.

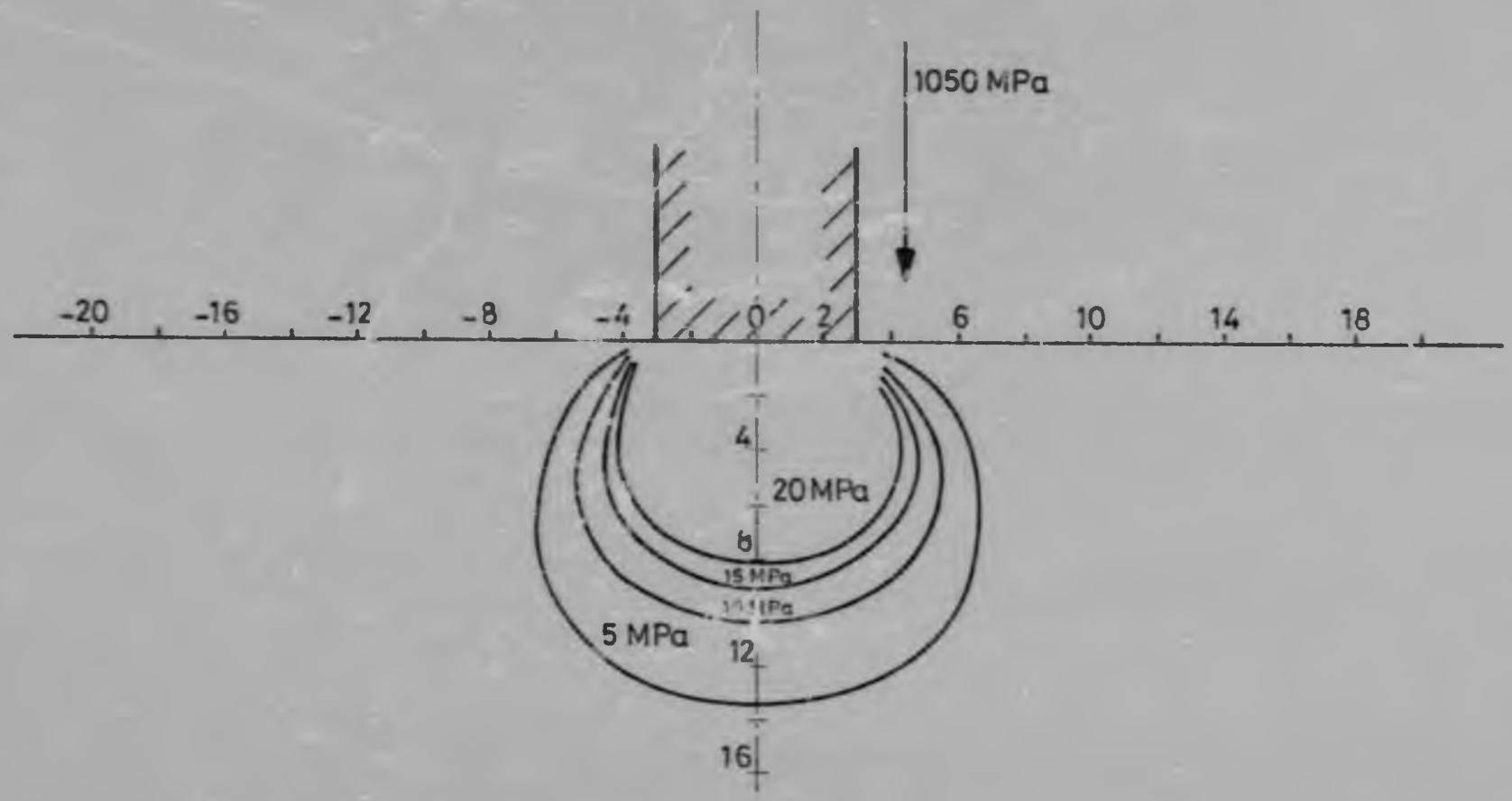


FIGURE 114 : Stress contours σ_3 (minimum principal stress) when a normal pressure 1 050 MPa is applied to the surface of the body.

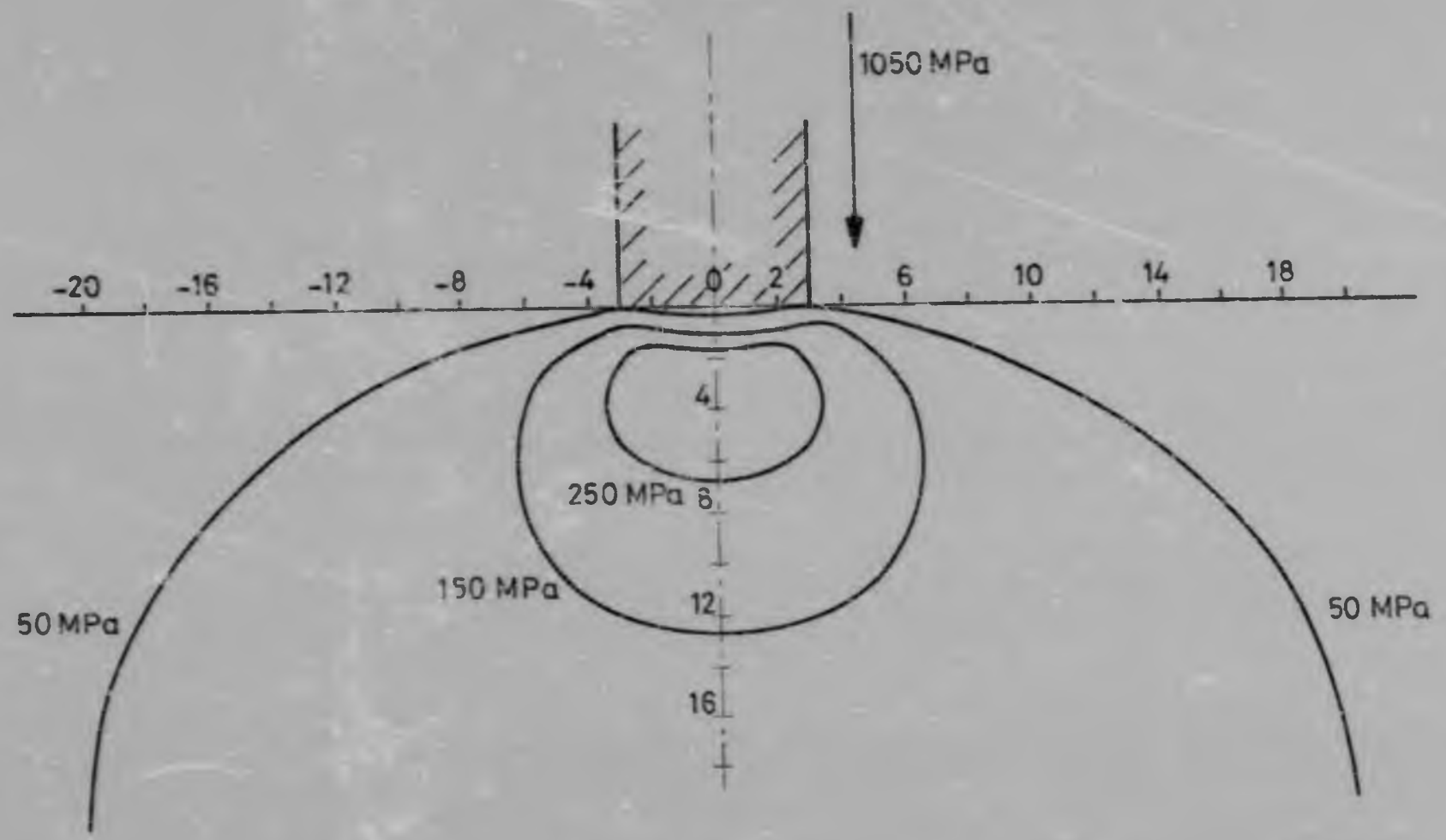


FIGURE 115 : Stress contours τ_{max} (maximum shear stress) when a normal pressure 1 050 MPa is applied to the surface of the body.

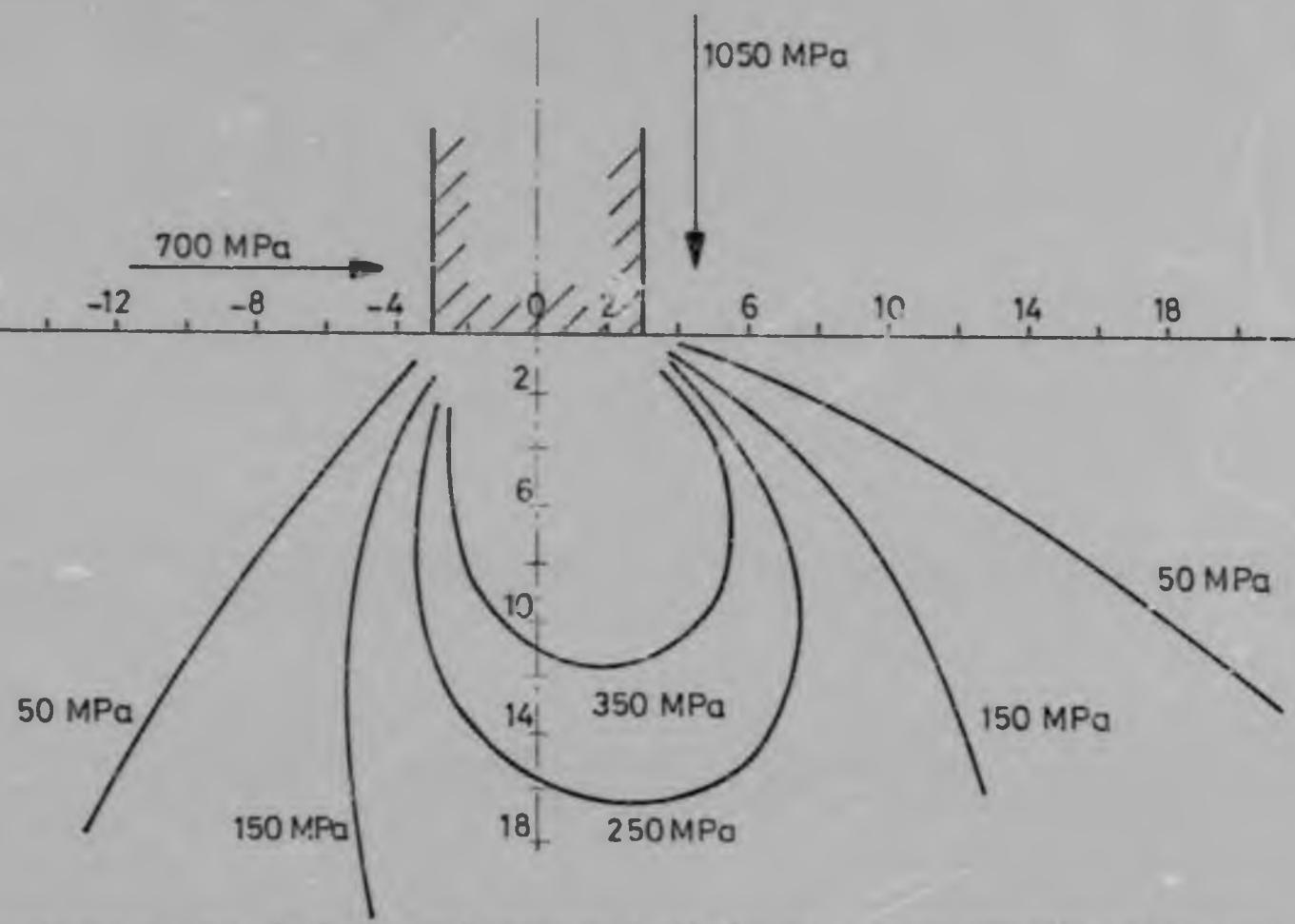


FIGURE 116 : Stress contours σ_{xx} when both a normal pressure 1 050 MPa and a shear pressure 700 MPa are applied to the surface of the body.

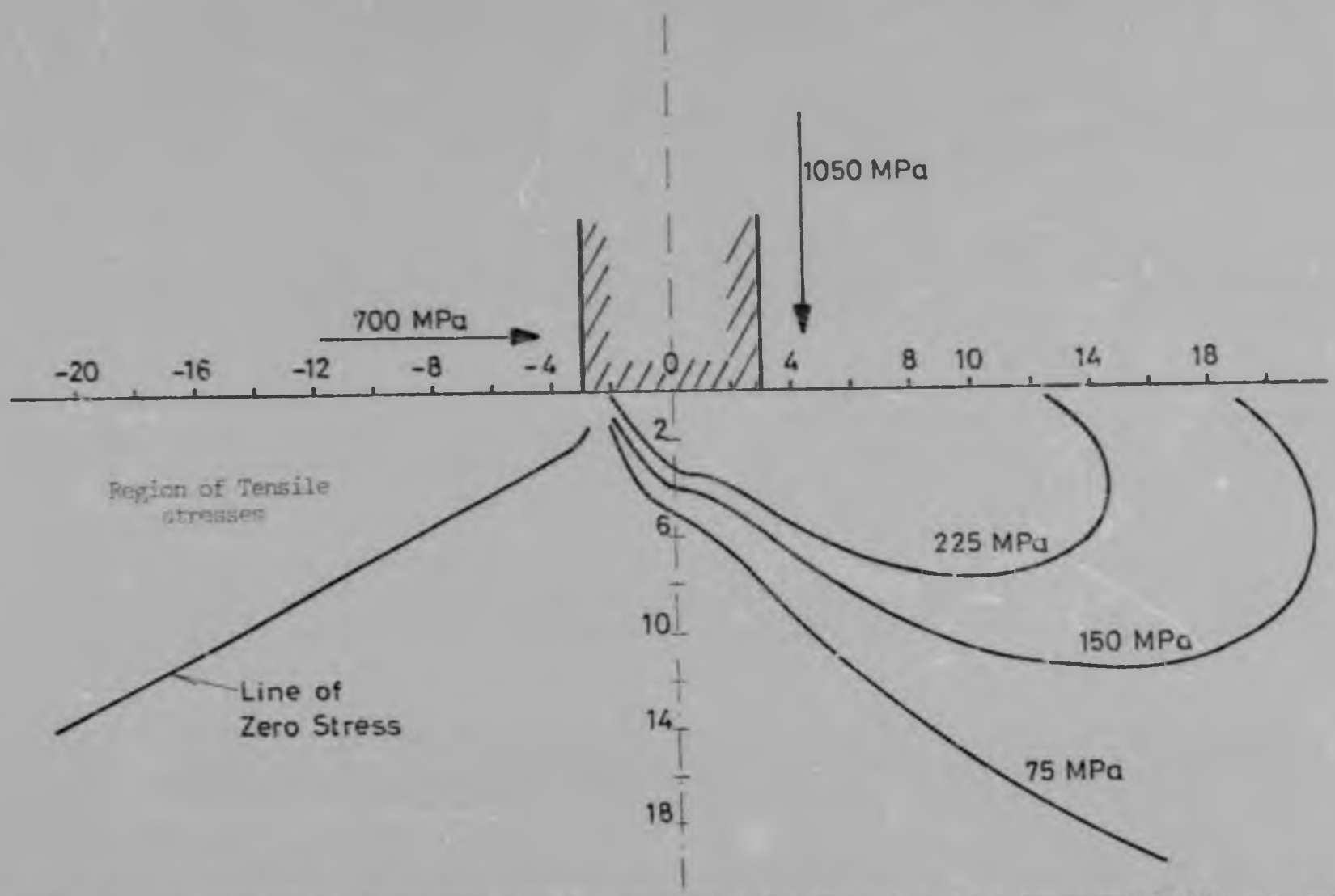


FIGURE 117 : Stress contours σ_{yy} when both a normal pressure 1 050 MPa and a shear pressure 700 MPa are applied to the surface of the body.

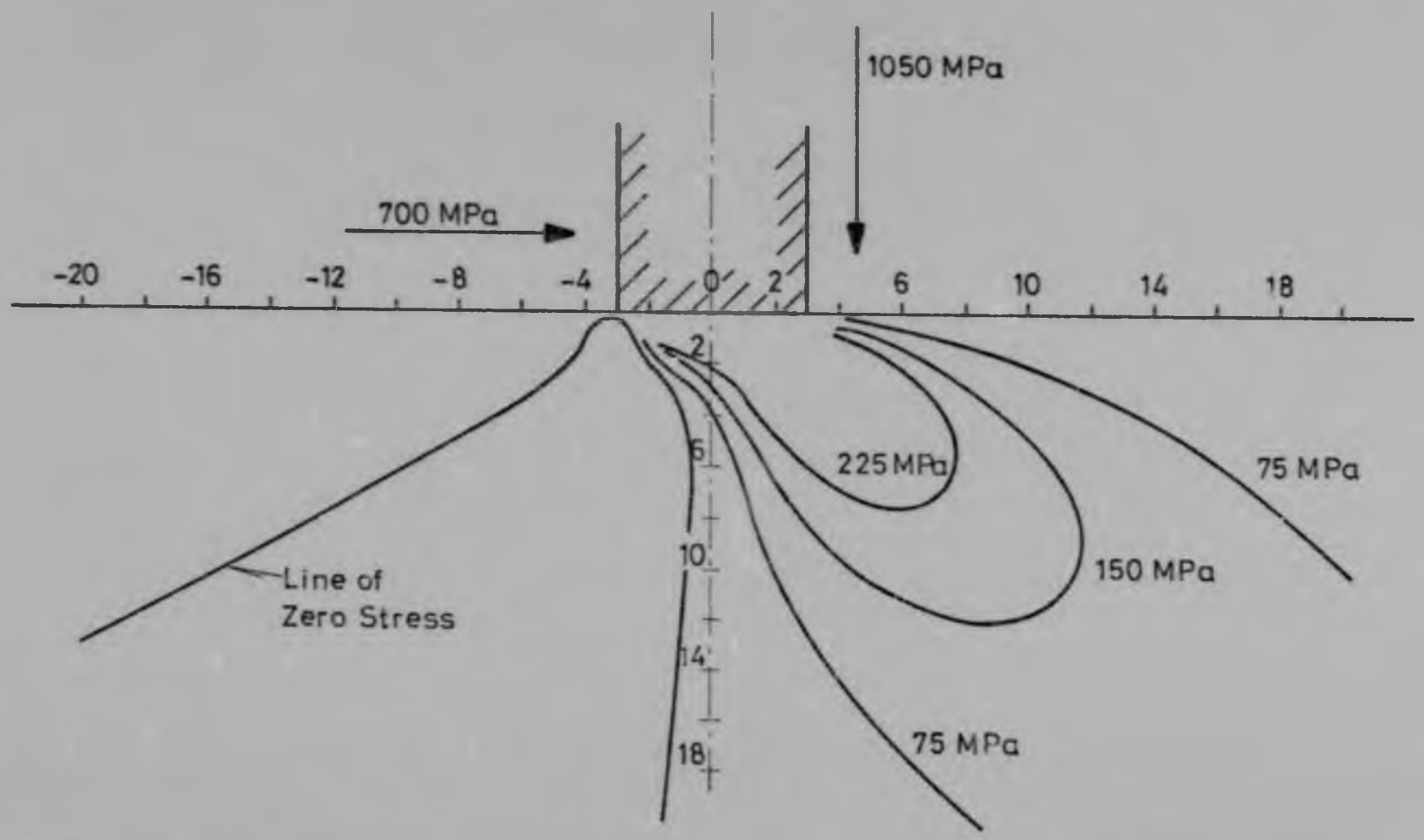


FIGURE 118 : Stress contours τ_{xy} when both a normal pressure 1 050 MPa and a shear pressure 700 MPa are applied to the surface of the body.

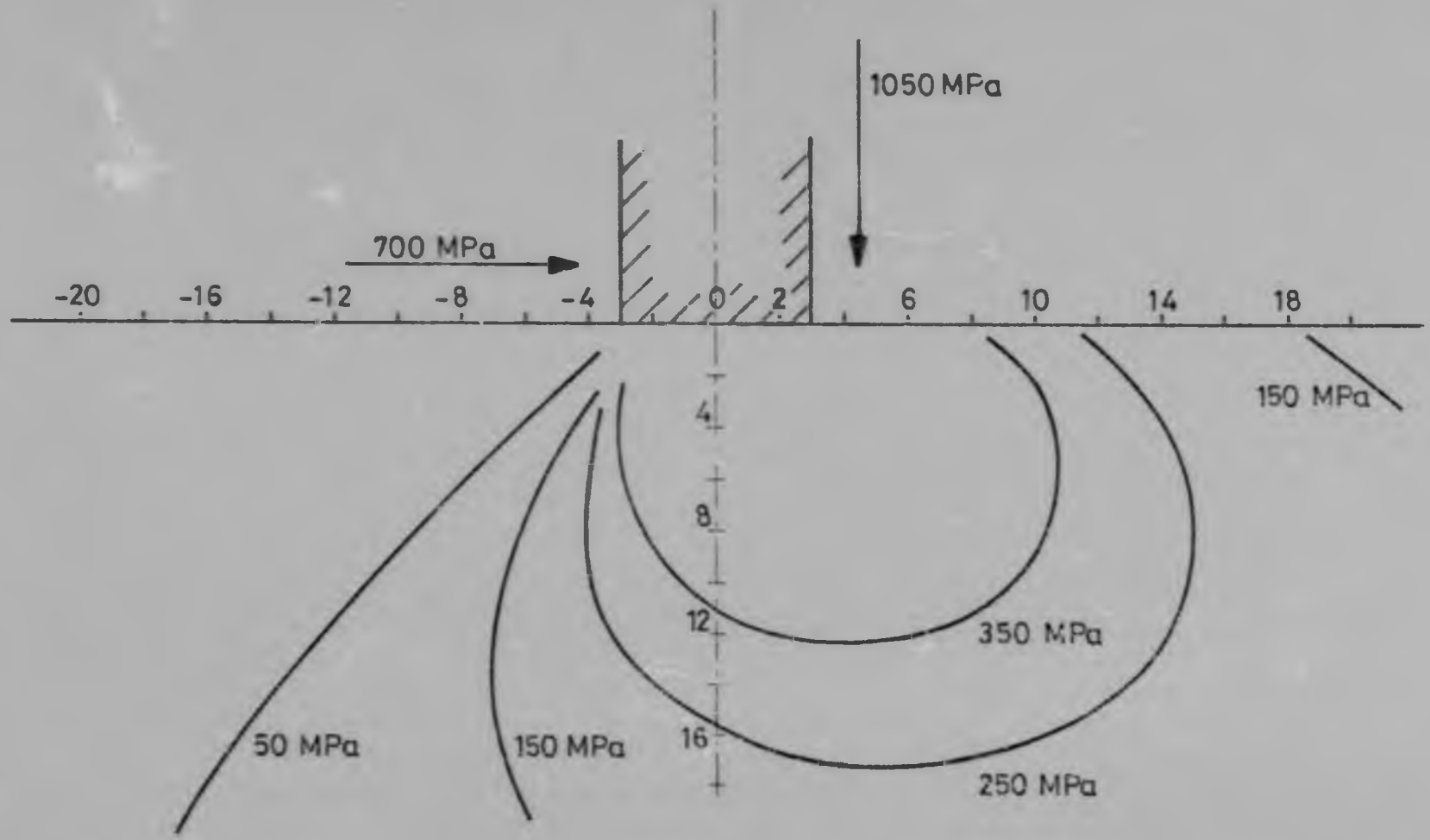


FIGURE 119 : Stress contours σ_1 when both a normal pressure 1 050 MPa and a shear pressure 700 MPa are applied to the surface of the body.

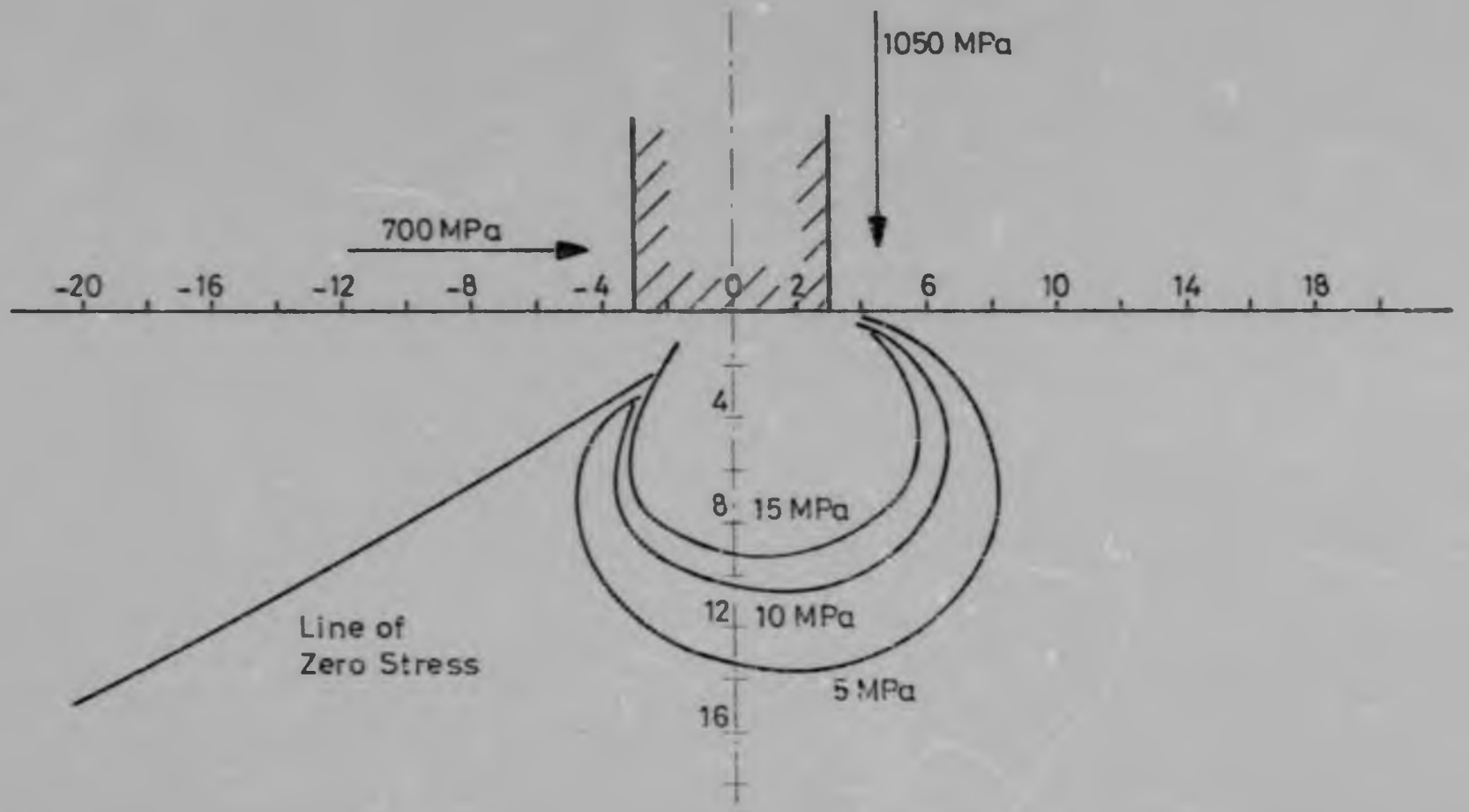


FIGURE 120 : Stress contours σ_3 when both a normal pressure 1 050 MPa and a shear pressure 700 MPa are applied to the surface of the body.

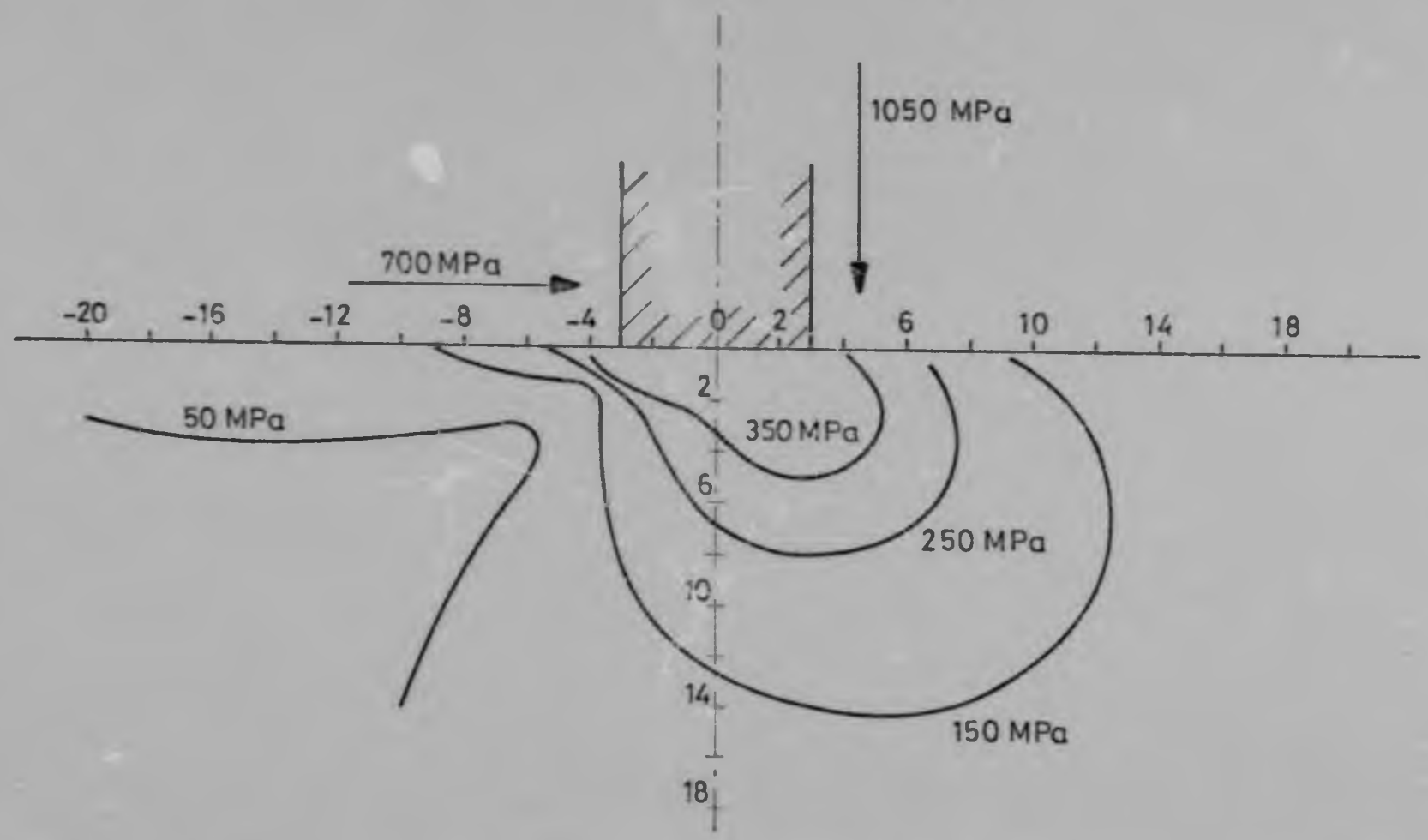


FIGURE 121 : Stress contours τ_{max} when both a normal pressure 1 050 MPa and a shear pressure 700 MPa are applied to the surface of the body.

When different forces are applied to the punch, the effect on the rock is illustrated by plots of the maximum principal stress and the maximum shear stress, (Figures 122 to 127). These show that :-

(i) When a constant shear stress of 700 MPa is applied to the rock by the punch, the stresses induced close to the surface of the rock ahead of the leading face of the punch are similar, whether the applied normal stress is high (1 050 MPa), or low (760 MPa), (Figures 119, 121 and 122, 123). From these Figures is can be seen that higher stresses are induced in the rock at shallower depths below the punch as the applied normal stress is increased.

(ii) When no shear force was applied to the punch then, in order to cause the rock to fracture, experiments had demonstrated that the applied stress normal to the rock surface had to be increased substantially, (Sections 7.2.1 and 7.2.2). These calculations show that this high applied stress causes high stresses to be induced in the rock both near to the rock surface and at depth below the punch (Figures 124 and 125).

(iii) When a relatively small shear stress (240 MPa), was applied to the rock surface by the punch, the applied normal stress required to cause the rock to fail was 1 430 MPa, (Section 7.2.2). The calculations show that when these stresses are applied to the rock surface, the maximum principal stress and the maximum shear stress induced in the rock close to the surface, ahead of the leading face of the punch, are at all times, the same as or greater than the stresses induced in the rock when the contact pressure underneath the punch applied normal to the surface, is 2 000 MPa, (Figures 126 and 127).

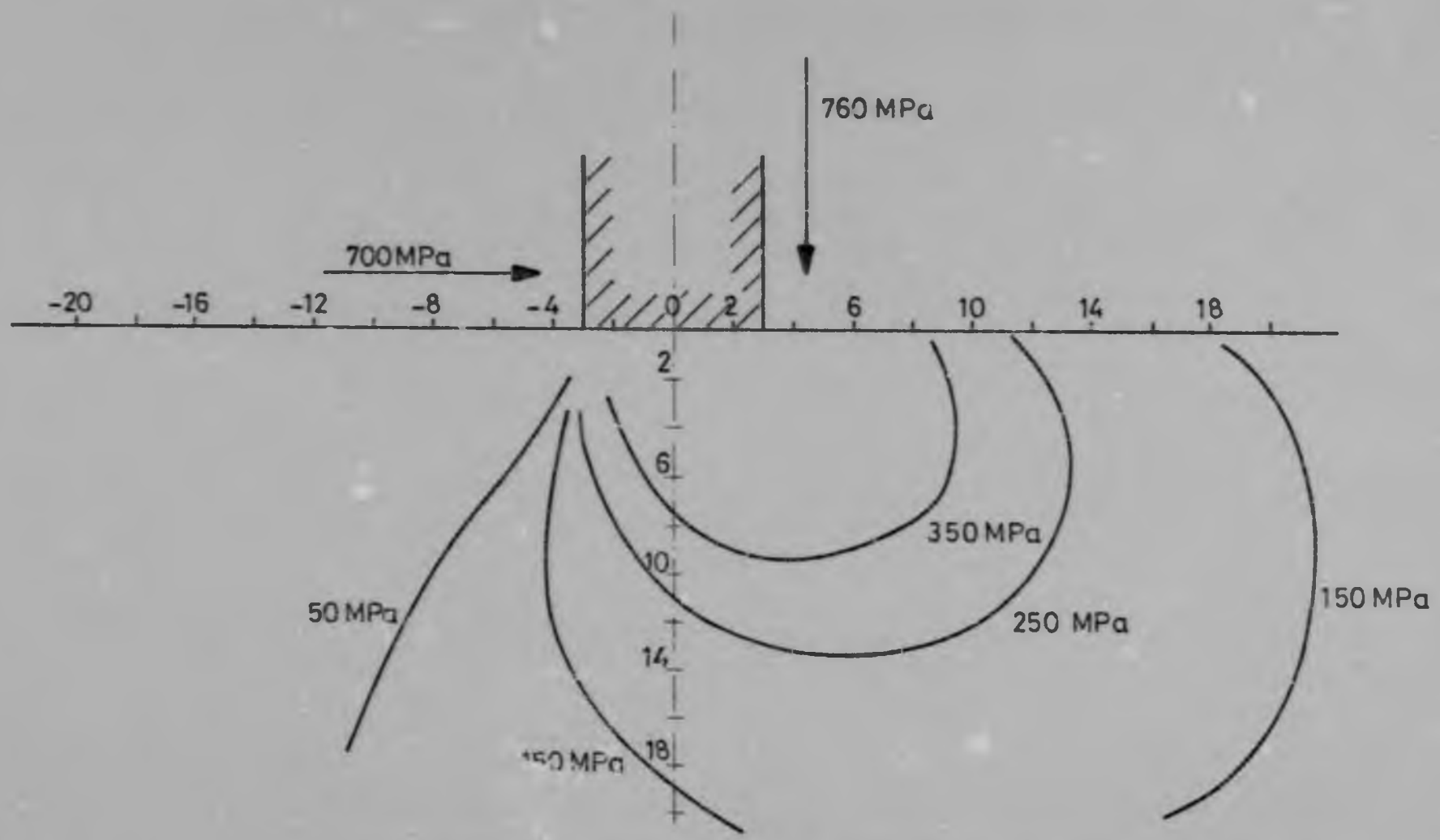


FIGURE 12? : Stress contours σ_1 when both a normal pressure 760 MPa and a shear pressure 700 MPa are applied to the surface of the body.

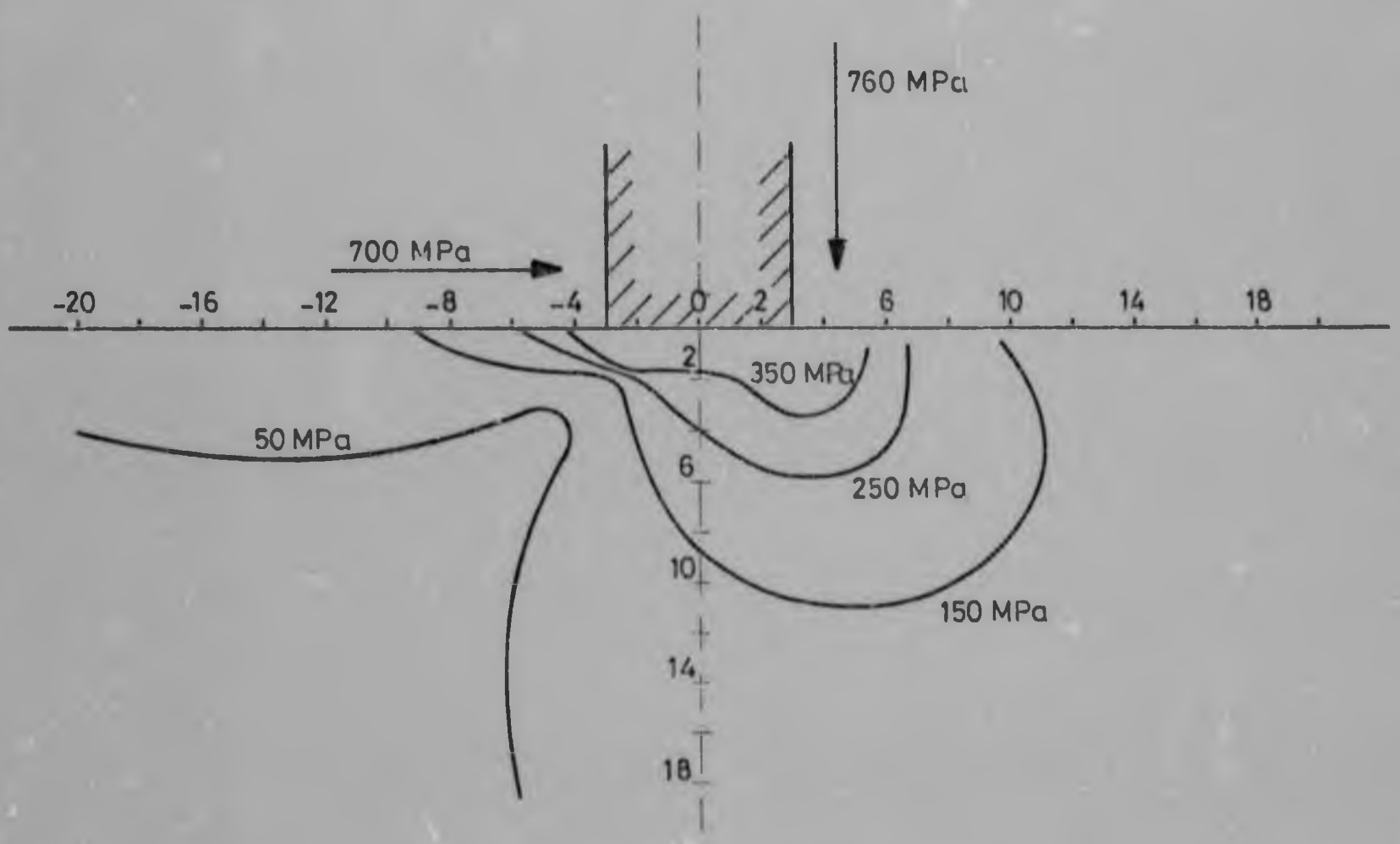


FIGURE 123 : Stress contours τ_{max} when both a normal pressure 760 MPa and a shear pressure 700 MPa are applied to the surface of the body.

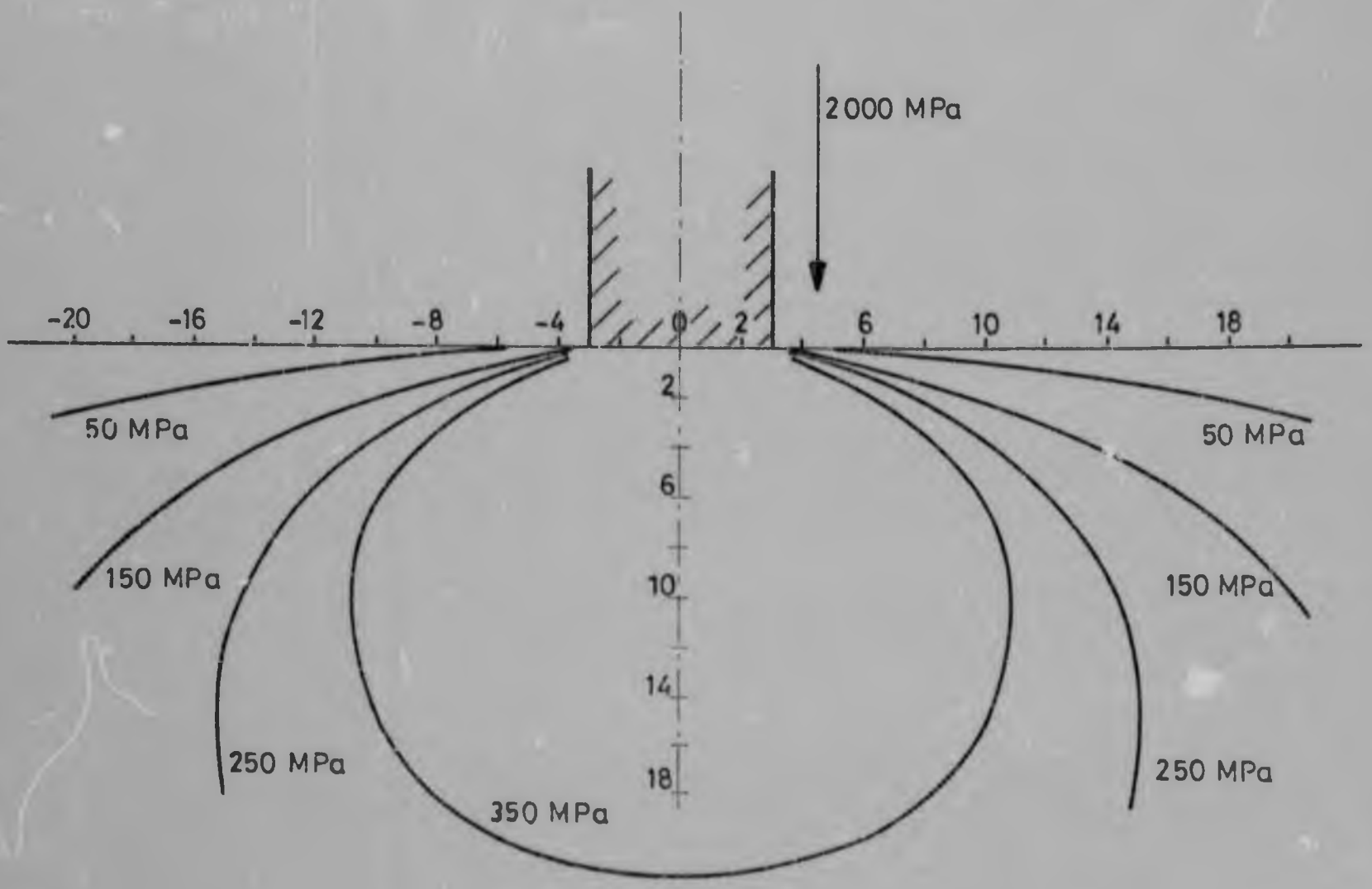


FIGURE 124 : Stress contours σ_1 when a normal pressure 2 000 MPa is applied to the surface of the body.

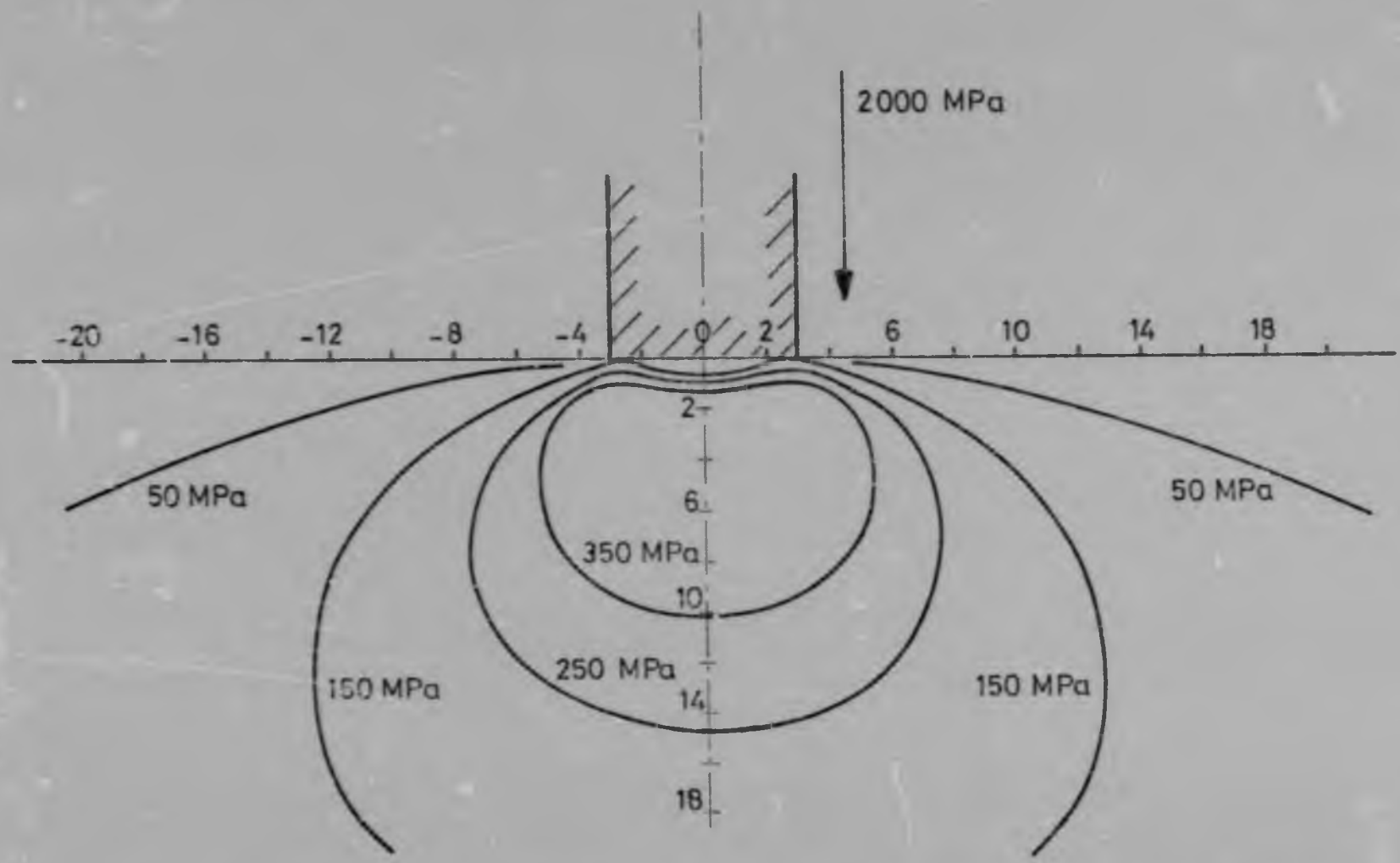


FIGURE 125 : Stress contours τ_{max} when a normal pressure 2 000 MPa is applied to the surface of the body.

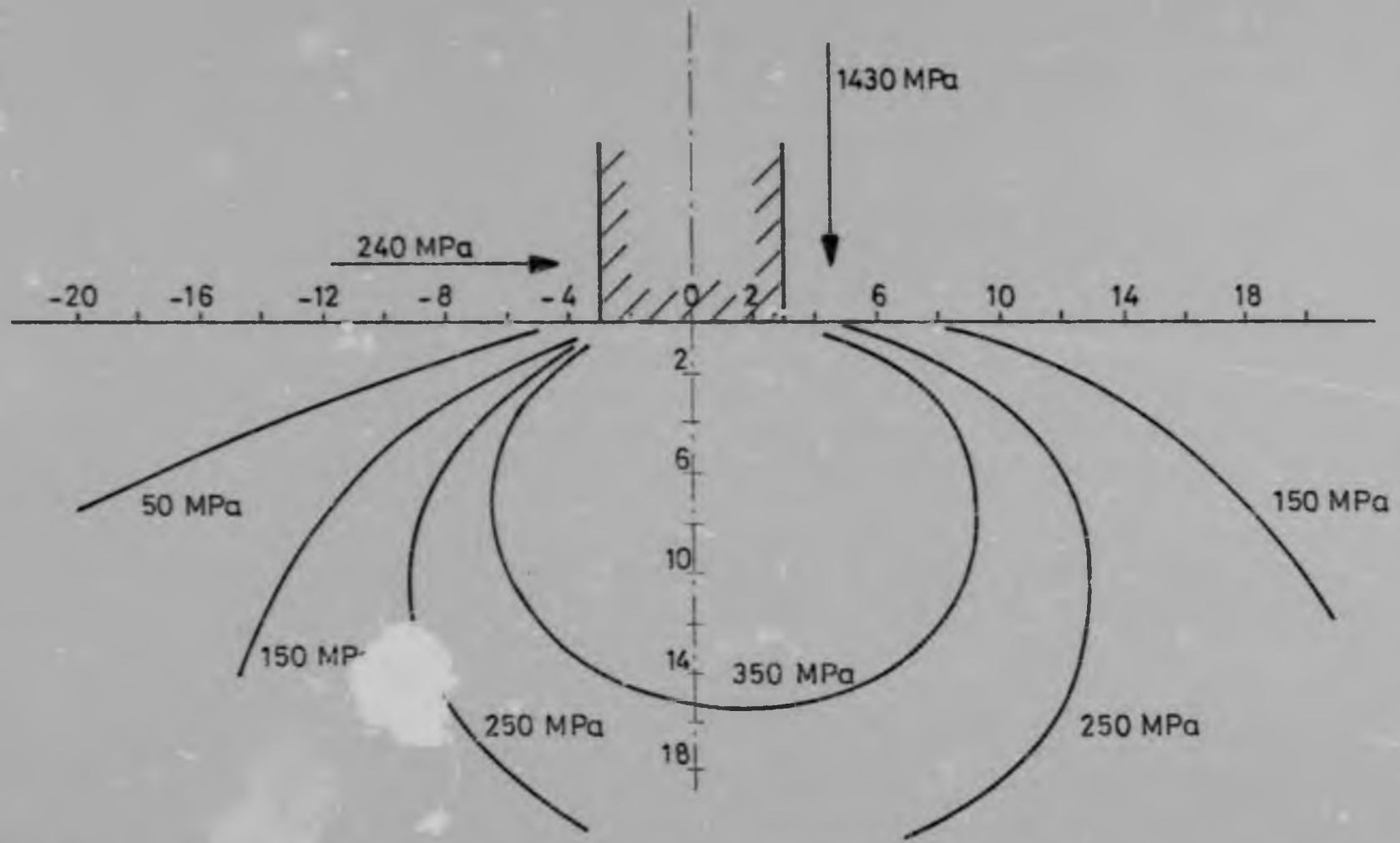


FIGURE 126 : Stress contours σ_1 when both a normal pressure 1 430 MPa and a shear pressure 240 MPa are applied to the surface of the body.

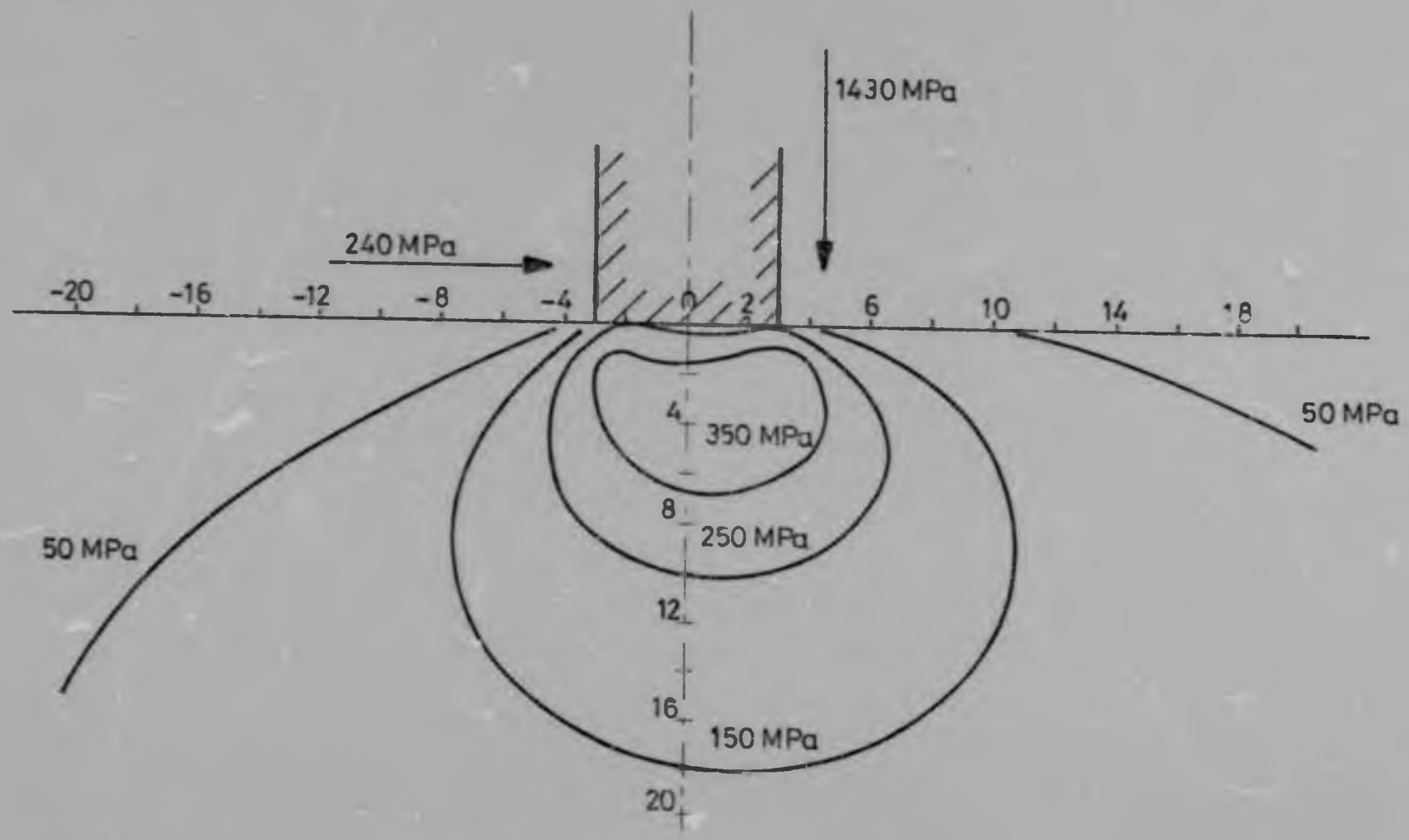


FIGURE 127 : Stress contours τ_{max} when both a normal pressure 1 430 MPa and a shear pressure 240 MPa are applied to the surface of the body.

7.4.2 Regions of excess stress

The variations in the sizes of these zones, when different loads are applied to the rock surface, are given in Figures 128 to 131. It is evident from these Figures that these regions of excess stress extend a fixed distance, between 8 mm and 10 mm, ahead of the leading face of the punch, no matter which load condition is applied. On the other hand, underneath the punch, these zones extend from 11 mm to 28 mm below the contact area, depending on the load(s) applied. This implies that the mechanism of rock fracture leading to the formation of rock chip may be related to a given area of 'failed rock' anead of the bit.

The regions of crushed rock underneath the bit wearflat and ahead of the leading face of the bit, that were observed when the rock samples used for the indentation tests (Section 7.3), were examined under the microscope, were smaller than these calculated zones of excess stress. For example, the specimen illustrated in Figure 102, shows that the crushed rock extended for some 4 mm ahead of the leading face of the bit and for about 8 mm beneath the contact area. This indicates that the rock is damaged to a greater extent than is evident by inspection of the visible, crushed region.

7.4.3 Stress trajectories

It can be readily shown that if the principal axes make an angle Θ with the existing Oxy axes then :-

$$\tan 2\Theta = \frac{2\tau xy}{\sigma xx - \sigma yy} \qquad (12)$$

(Section 2.3, Jaeger and Cook, 1969).

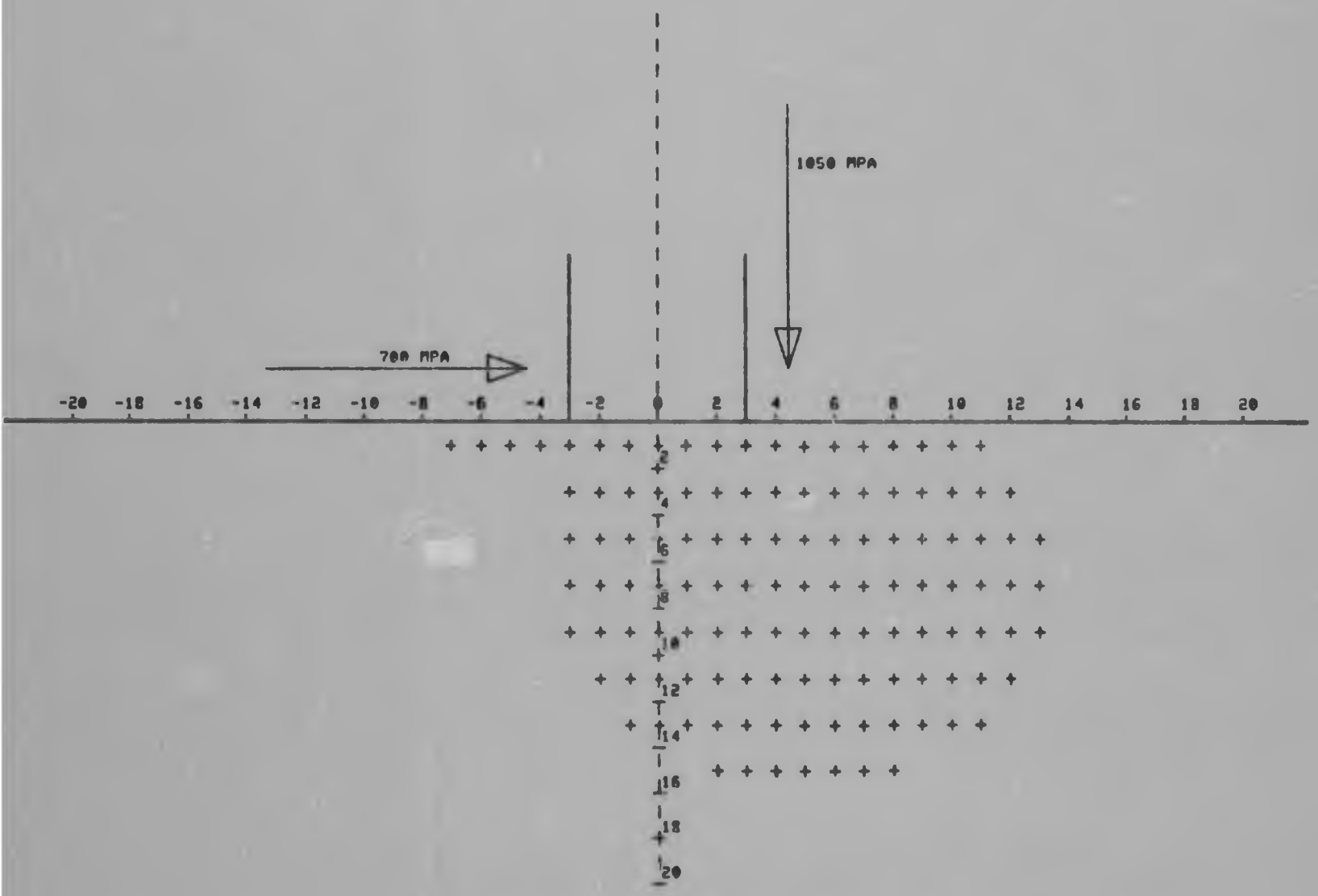


FIGURE 128 : Zone of excess mass when both a normal pressure 1 050 MPa and a shear pressure 700 MPa are applied to the surface of the body.

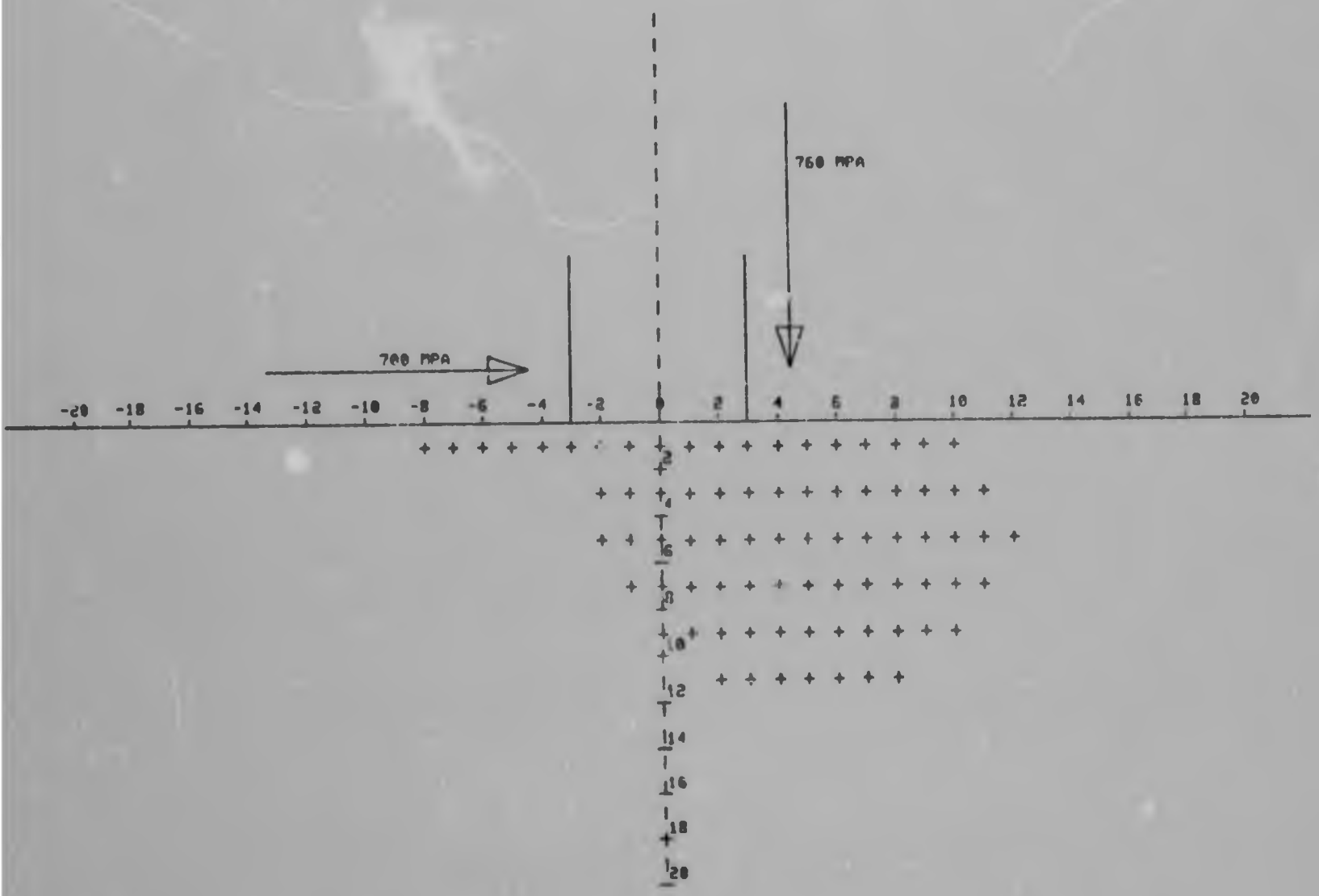


FIGURE 129 : Zone of excess stress when both a normal pressure 760 MPa and a shear pressure 700 MPa are applied to the surface of the body.

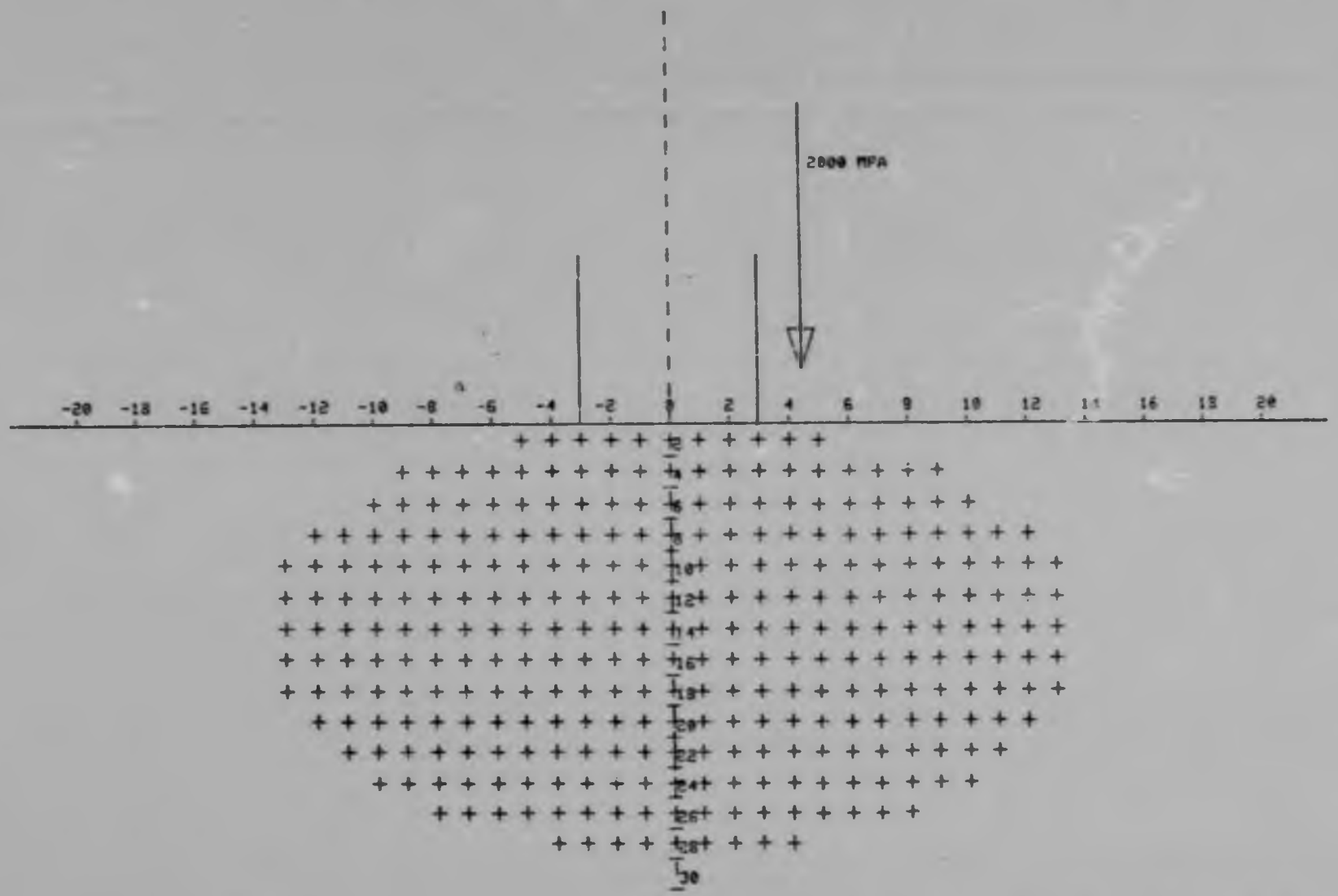


FIGURE 130 : Zone of excess stress when a normal pressure 2 000 MPa is applied to the surface of the body.

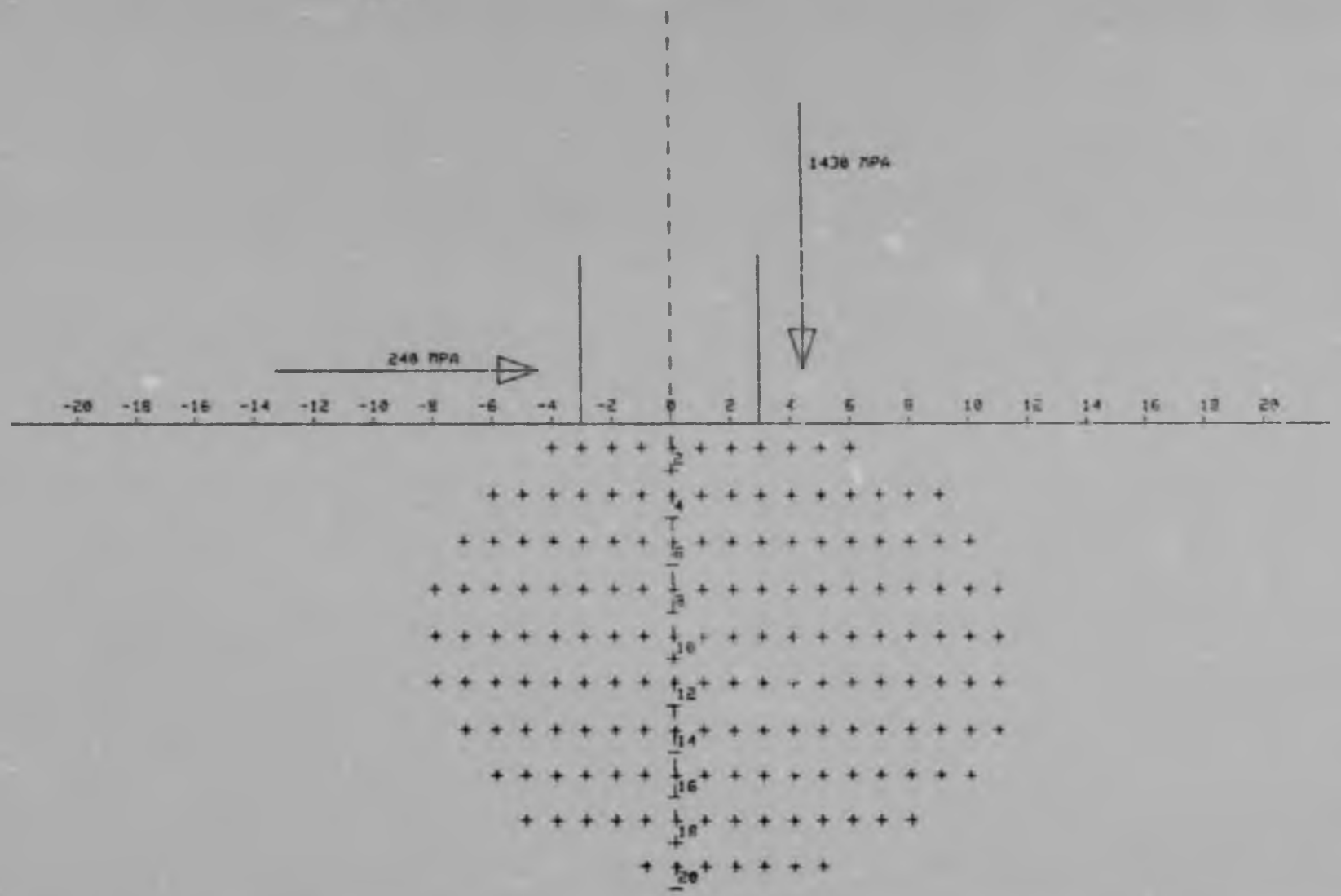


FIGURE 131 : Zone of excess stress when both a normal pressure 1 430 MPa and a shear pressure 240 MPa are applied to the surface of the body.

Values of σxx, σyy and τxy were taken from the calculations given in 7.4.1 and substituted into equation 12. Therefore these stress trajectories apply when a uniform stress is applied to the surface of an elastic body by a punch.

When the normal force P only is applied the values of σxx, σyy and τxy are given by equations 1, 2 and 3 respectively. Substituting from these equations into equation 12, gives :-

$$\tan 2\Theta = \tan(\alpha + 2\delta)$$

$$\therefore \Theta = \tfrac{1}{2}(\alpha + 2\delta) \qquad (13)$$

From this equation it can be shown that the stress trajectories are confocal ellipses and hyperbolae, with foci at the corners of the punch, (Figure 132).

The stress trajectories when the normal force P only was applied and when the combined forces P + T were applied were calculated from equation 12. The directions of the principal stresses at a large number of points close to the surface of the body, adjacent to the punch, were computed using programs developed for a Hewlett-Packard 9830a calculator. These programs, together with extracts from the tabled results, are given in Appendix (iv).

A comparison of the stress trajectory plots for the two loading situations (Figures 132 and 133), shows that an area behind the punch, along the 'y' axis in the negative direction, is distorted when the shear force T is superimposed. Ahead of the punch, along the 'y' axis in the positive direction, the stress trajectories are not altered

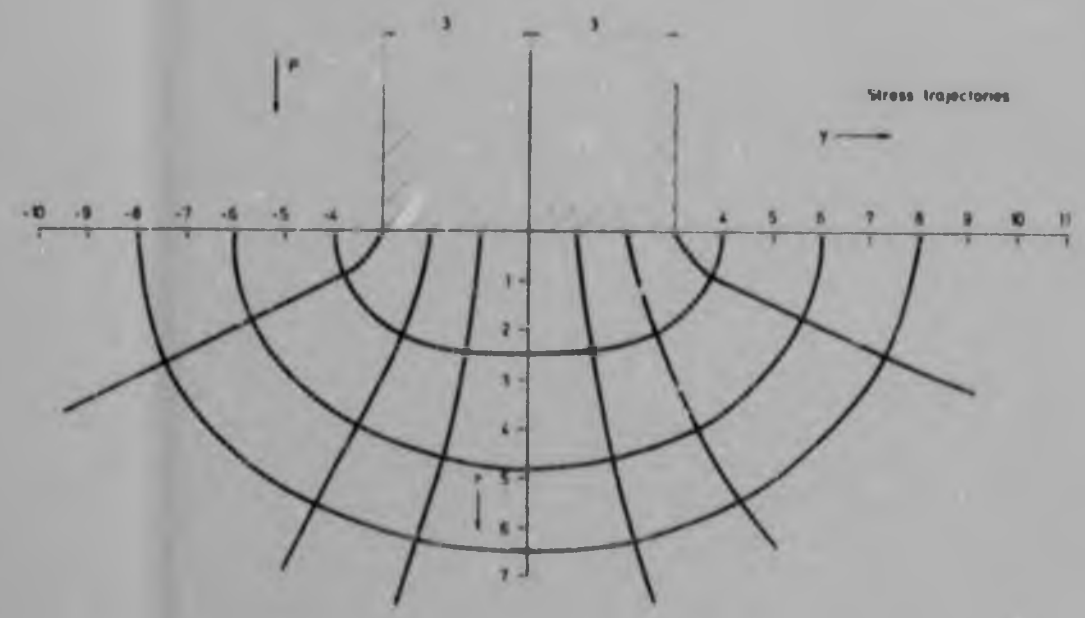


FIGURE 132 : Stress trajectories when a normal pressure only is applied to the surface of the body.

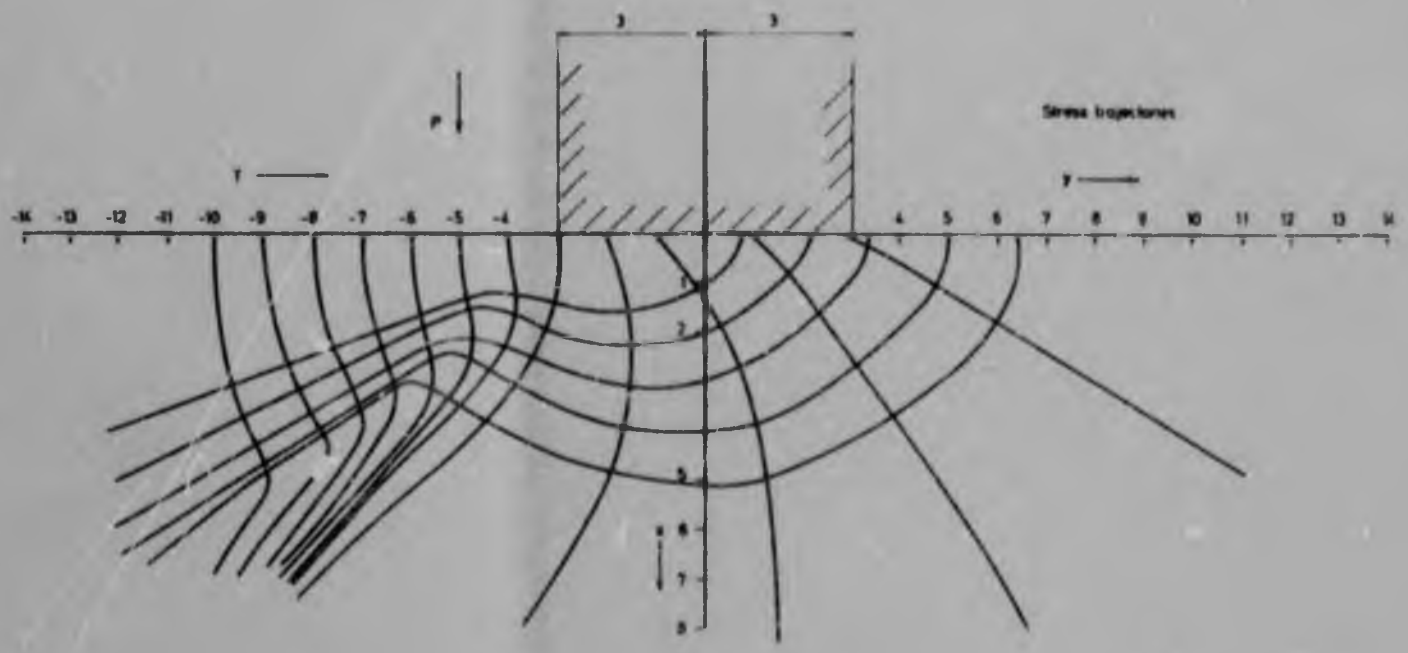


FIGURE 133 : Stress trajectories when both a normal pressure and a shear pressure are applied to the surface of the body.

significantly by the superimposition of the shear force T. Therefore, the predicted crack orientation and mode of failure of the rock would be the same, whether a normal force only was applied to the rock surface, or whether both a normal and a shear force was applied. However, since the stresses near to the free surface ahead of the punch are calculated to be higher when the shear force is added (Section 7.4.1), cracks would be expected to develop at lower values of the normal force in this situation.

Thus the theory conforms to the experimental results, since indentation tests with a shear force superimposed on the normal force caused the major rock chip ahead of the bit to be formed at reduced values of the indentation force, (Section 7.2.3). In addition, the geometry of the cracks was shown to be similar during indentation tests with a normal force only applied to the rock and when a shear force combined with a normal force was applied to the rock, (Section 7.2.3).

7.5 Experiments to study the effect of high pressure water jets on the rock breaking process

7.5.1 Examination of hypotheses

The mathematic analysis (Section 7.4), indicated that during the cutting operation tensile stresses were induced in the rock close to the surface behind the bit. If these stresses were large enough to cause cracks to develop in the rock surface then on the next cutting stroke, if the bit wearflat caused water to be trapped in these cracks, very high water pressures would be generated as a result of the high contact pressure between the bit and the rock. This could cause

'hydraulic fracturing' of the rock which would result in rock chips being formed with relatively low forces applied to the bit. Hydraulic fracturing is a technique often used by rock mechanics specialists for determining stresses in-situ in a rock mass and involves pressurizing a hole until a tensile fracture is induced in the rock, (Zolack et al, 1977).

An alternative hypothesis to explain the effect of water jets on the cutting operation was that the very high temperatures generated at the bit wearflat (Section 6.1.1), caused water injected into this region to be converted to steam. Rock fracture ahead of the bit might then take place by a process of steam shattering and this could result in a reduction of the bit forces during the cutting operation.

Experiments were conducted to test these two hypotheses. First an examination of rock samples was made for cracks which might have developed behind the bit. Rock specimens used for the indentation tests where both a normal force and a shear force were applied for the bit (Section 7.2.2), were used for these investigations. The rocks were sectioned and the region of interest, immediately behind the bit, was examined using a scanning electron microscope. No evidence of cracks was found.

Before stating categorically that cracks behind the bit did not exist and that the mechanism described in the first hypothesis therefore was not applicable, an additional experiment was conducted. Tests were made cutting in a norite block in the test rig. Several cuts were taken without water jets to establish a slot in the rock. The blade feed was then increased to take a depth of cut of 6 mm. It has been

shown previousl that the power of this machine limited the depth of cut to 4,5 mm when water jets were not used. However, a blade feed of 6 mm did not cause the machine to stall immediately, and the saddle travelled approximately 0,5 m in a jerky fashion before the stall condition. Once the machine had stalled an equilibrium position was reached and the saddle made no further motion. At this point, with full force still applied to drive the machine, two coherent water jets at 40 MPa pressure were directed towards the corners of the tungsten carbide bit inserts. This had the effect of immediately breaking the stalled condition of the machine, and the bit, assisted by the water jets, continued to cut smoothly until the end of the slot. This experiment was repeated a large number of times cutting in different norite blocks and this result was achieved consistently.

These experiments demonstrated that it was not necessary to have water pre-injected into existing cracks in order to benefit the cutting operation. In addition the tests showed that the machine could be left in the stalled condition for a long period of time, allowing the bit to cool, and that when the water jets were applied the cut was continued immediately. Therefore, the second hypothesis, which proposed shattering of the rock by steam, was discounted also.

7.5.2. Indentation tests using high pressure water jets

A series of indentation tests was conducted to investigate whether, when high pressure water jets were directed immediately ahead of the bit, the force necessary to form a rock chip ahead of the bit was decreased.

The stiff-testing machine (Figure 88), did not provide sufficient space to enable a bit connected to a high pressure water supply, to be mounted in this machine. Therefore, an alternative press comprising a steel frame with a 6 MN hydraulic jack, was used for these tests, (Figure 134). The bits used for these experiments were of a modified design, in that the nozzles were incorporated in the steel body of the bit, (Figure 135). The nozzles were positioned so that the jets were directed towards the corners of the tungsten carbide inserts in the bit, approximately 2 mm ahead of the leading face of the bit. The bit was mounted on a foreshortened blade which was connected to the high pressure water pump. Cylindrical rock specimens of both norite and quartzite were prepared in the usual way, (Section 7.2).

The 6 MN jack was pressurized using a hand pump, (Figure 134). The relationship between the pressure of the hydraulic fluid in the jack and the force applied by the jack was found using a pre-calibrated strain-gauge instrumented load cell to measure the force. The hydraulic pressure was measured using a calibrated pressure gauge. The calibration curve obtained is given in Appendix (iii).

The rock specimen was placed on the base platen of the press and the bit with the attached blade section was inserted between the jack and the rock in the usual way. (Figure 136). The procedure followed was to apply the load slowly to a value approximately half that required to form a rock chip ahead of the bit, that is between 150 kN and 200 kN. The stress in the rock at the corners of the bit with this applied force was sufficient to form small chips in this region, (Section 7.2.1). At this juncture the water jets were applied at 40 MPa pressure with a flow rate of 0,5 ℓ/sec. When these jets struck

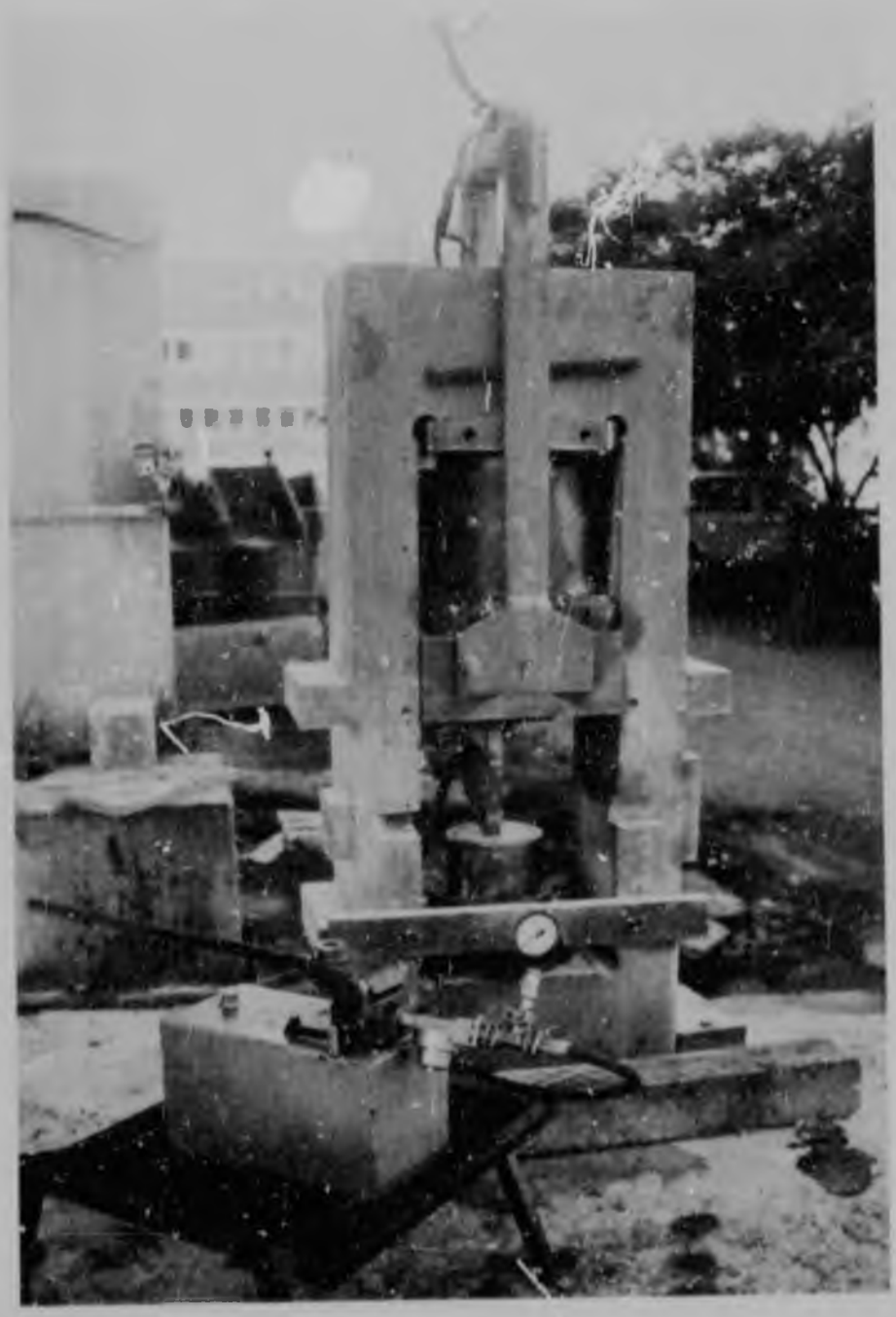


FIGURE 134 : Press used for indentation tests with high pressure water jets.



FIGURE 135 : Drag bits with nozzles for high pressure water jets built in to the steel bit body.



FIGURE 136 : Method of mounting bit and rock specimen in the press prior to conducting indentation tests assisted by water jets.

the rock surface the rock chip formed ahead of the bit almost immediately. The rock chip formation was noted by recording a fall in pressure of the hydraulic fluid in the jack since the water spray prevented direct observations. It was observed also that powdered rock ahead of the leading face of the bit, underneath the rock chip (Section 7.2.1), was flushed away when water jets were used. The crushed rock beneath the bit wearflat however was not removed by the jets.

This experiment was repeated ten times using different specimens of both norite and quartzite. The results were consistent in demonstrating that when water jets were used only about half of the normal indentation force was required to form a rock chip ahead of the bit. It was not possible, using this apparatus, to correlate different combinations of the pressure of the water jets with the applied load necessary to form the rock chip. The limitations of the apparatus which prevented this correlation were the compliance of the frame and the hydraulic system and the inexact method used to measure the applied force. Nevertheless, it was demonstrated that, when water jets were used to assist the rock breaking operation, the force normal to the rock surface required to form a rock chip ahead of the bit, was reduced substantially.

Previous experiments had shown that cracks were initiated close to the leading face of the bit and that as the applied load was increased, these cracks propagated and a rock chip was formed, (Section 7.3). These experiments using water jets during the indentation process had shown that these jets reduced the force required to form a rock chip. The mechanism proposed to explain this force reduction was that cracks

were initiated ahead of the bit with a relatively low applied force; when the jets were applied water was forced into these cracks causing them to propagate and form a rock chip.

7.6 A model to explain how high pressure water jets affect the cutting operation

Experiments conducted to investigate the mechanism of fracture of strong rock using blunt drag bits showed that the bit penetrating force caused the bit to indent the rock and form rock chips ahead of the leading face of the bit, (Section 7.1). In addition, it was shown that the leading face of the bit is not in contact with the rock during the cutting operation (Section 7.1), which indicates that the bit cutting force is required largely to overcome friction between the bit and the rock. Further tests together with calculations, demonstrated that the bit cutting force assists the rock breaking operation by increasing the stress in the rock ahead of the bit, (Sections 7.2. and 7.4).

The ability of water jets to reduce the forces acting on the bit during the cutting operation was found not to depend on cracks pre-existing in the rock or on the heat of the bit reacting with the water and generating steam which shattered the rock, (Section 7.5.1). Instead, a series of indentation tests showed that when 40 MPa water jets were directed immediately ahead of the bit, the force required to form a rock chip was reduced by a factor of at least two, (Section 7.5.2). The experiments cutting rock (Chapter 6), had shown that the most effective point of impingement of the jets was immediately ahead of the leading force of the bit, (Section 6.4.3). It was in this region that cracks were initiated in the rock, (Section 7.3). Taken together

were initiated ahead of the bit with a relatively low applied force; when the jets were applied water was forced into these cracks causing them to propagate and form a rock chip.

7.6 A model to explain how high pressure water jets affect the cutting operation

Experiments conducted to investigate the mechanism of fracture of strong rock using blunt drag bits showed that the bit penetrating force caused the bit to indent the rock and form rock chips ahead of the leading face of the bit, (Section 7.1). In addition, it was shown that the leading face of the bit is not in contact with the rock during the cutting operation (Section 7.1), which indicates that the bit cutting force is required largely to overcome friction between the bit and the rock. Further tests together with calculations, demonstrated that the bit cutting force assists the rock breaking operation by increasing the stress in the rock ahead of the bit, (Sections 7.2. and 7.4).

The ability of water jets to reduce the forces acting on the bit during the cutting operation was found not to depend on cracks pre-existing in the rock or on the heat of the bit reacting with the water and generating steam which shattered the rock, (Section 7.5.1). Instead, a series of indentation tests showed that when 40 MPa water jets were directed immediately ahead of the bit, the force required to form a rock chip was reduced by a factor of at least two, (Section 7.5.2). The experiments cutting rock (Chapter 6), had shown that the most effective point of impingement of the jets was immediately ahead of the leading force of the bit, (Section 6.4.3). It was in this region that cracks were initiated in the rock, (Section 7.3). Taken together

these experiments indicated that the mechanism by which the water jets assisted the rock breaking process was by penetrating and then propagating the cracks which developed ahead of the bit.

This proposition has an interesting consequence. It was found during laboratory experiments cutting rock (Chapter 6), that the bit penetrating force was reduced progressively as the pressure of the water jets was increased. This implies that the crack ahead of the bit propagated gradually in a stable manner to cause a rock chip to form. In the field of hydraulic fracturing it is normally assumed that because large stress concentrations are induced at the tip of a fracture, the crack propagates rapidly in an unstable manner even when only moderate fluid pressure is applied to the fracture, (Zoback et al, 1977).

In order to explain this apparent contradiction between the experimental results and the existing theory it is suggested that in the situation where two discrete jets are directed towards the edges of a crack having a width of the order of the bit thickness (35 mm), the water pressure within the fracture is relatively low. This is because water is free to escape continuously from the crack. Consequently the stress intensity at the tip of the fracture decreases as the crack length increases. This represents the case of stable crack growth, requiring an increase in the jet pressure to produce an increase in the crack length.

Stable crack propagation has been observed during other experiments using hydraulic fracturing techniques to break rock. Observations reported by Zoback et al, (1977) showed that when a viscous fluid was

pressurized in a borehole, the cracks emanating from the borehole were extended in a stable fashion. The hypothesis proposed by the authors to explain this phenomenon noted that with a viscous fluid the pressure drop along the crack would be large, and consequently the stress concentration at the tip of the crack was likely to be insufficient to cause unstable crack growth. Therefore, it has been shown that crack growth in brittle materials is a stable phenomenon under certain conditions. This subject has not been pursued further since the topic of fracture propagation is complex and the development of cracks in the situations described above requires special study. It is recommended that this subject should be investigated in detail in future work.

The propagation of cracks by water jets ahead of the bit was taken to be the major influence affecting the reduction of the bit penetrating force during the cutting operation. Another factor, which was considered to exert a secondary influence, was the flushing of the powdered rock from ahead of the leading face of the bit, (Section 7.5.2). It was shown during the indentation tests that the crushed rock underneath the bit wearflat was not removed by water jets (Section 7.5.2), and therefore that the substantial reduction of the bit indentation force during these quasi-static tests was a result of jet-assisted crack propagation. Consequently in the dynamic, cutting situation, it was assumed that this could be the major influence also.

The bit cutting force was reduced substantially when water jets were used to assist the cutting operation, almost irrespective of the pressure or point of impingement of the jets, (Section 6.4). It was concluded that the water acted as a lubricant between the bit and the rock which caused the coefficient of friction between these two bodies

to be reduced. Thus, provided the water jets were directed close to the bit, the bit cutting force was reduced. It was shown that when the jets were directed 10 mm ahead of the leading face of the bit, the bit cutting force was not reduced markedly, (Section 6.4.3). It was concluded that with this jet configuration, the volume of water at the point of contact between the bit and the rock was insufficient to decrease the friction force effectively.

CHAPTER 8

8. SUMMARY OF CONCLUSIONS

Experiments designed to investigate the causes of bit failure and to improve the strength of drag bits used for cutting in hard rock had shown that very nigh temperatures were generated at the interface between the tool and the rock. It was established that the major reason for discarding bits from service at the underground test site was thermal deterioration of the bit braze joint. Efforts to strengthen this joint by using a braze metal with a higher remelt temperature and by increasing the area of contact between the braze joint and the tungsten carbide inserts, did improve the overall bit life. In addition it was shown during the course of laboratory tests that the temperatures at the bit braze joint could be controlled to an acceptable level if a large volume of water was used to flood the bit during the cutting operation.

Three different experimental techniques were attempted in an attempt to reduce the mean force acting on the bit during the cutting operation. Bits with a reduced wearflat area were shown to decrease the components of force acting on the bit, but the tungsten carbide bit inserts were weakened substantially by reducing this area. Therefore, this line of experimentation was not continued. A second experiment whereby the vibration of the bit was increased during the cutting stroke of the machine, demonstrated that this caused the mean peak values of the penetrating force to be reduced. Significantly lower values of the bit penetrating force were measured also in the course of a third experiment using a 'flat- fan' water jet directed ahead of the bit

during the machine cutting stroke.

As a result of these preliminary tests a comprehensive investigation was carried out to study the potential for reducing the components of the bit force using coherent high pressure water jets directed ahead of the bit during the cutting operation. The use of water jets to assist the rock breaking operation was selected as the most promising approach since the previous experiment had shown that, with this technique, it was possible not only to reduce the mean bit force but also to provide adequate cooling to the bit.

It was demonstrated that when suitable high pressure water jets were used in combination with drag bits to cut hard rock, the force on the bits was reduced significantly allowing deeper cuts to be taken. Also, in general, bluntness caused by wear became the overriding criterion for bit discard compared with the situation where water jets were not used, when failure of either the tungsten carbide inserts or the bit braze joint were the usual reason for bit discard.

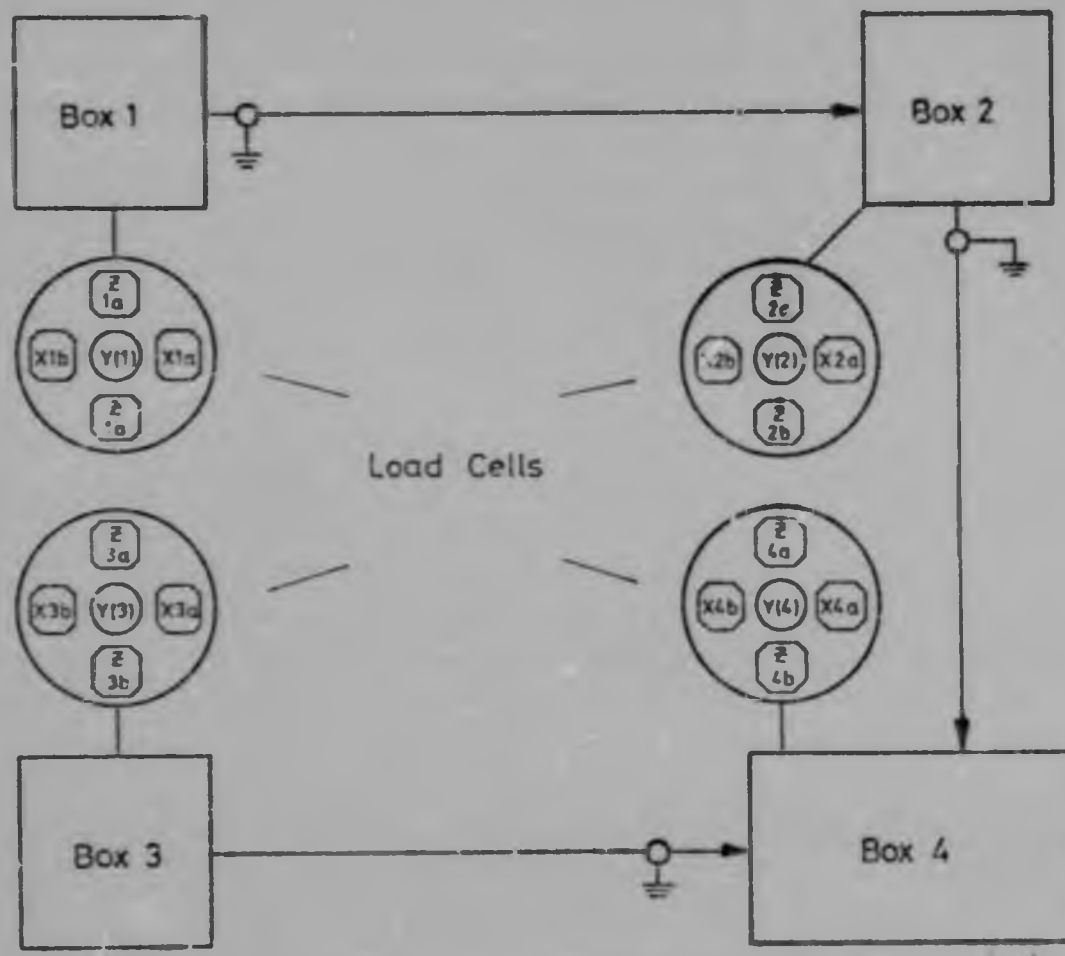
It is possible that the use of drag bits in combination with water jets, will spread to hard rock applications in the field of rock cutting since these bits are more efficient cutting tools than the various types of roller cutter in current general use. However, in order to promote a widespread use of drag bits, high values of bit life are necessary. It has been shown that in a situation where drag bits were used to cut into a corner in very strong highly abrasive quartzite the majority of the bits were discarded because of wear of the bit inserts. It is encouraging that the bits did not break in this application but a high rate of wear of the tungsten carbide bit inserts

was observed. Further work is necessary to study the wear mechanism and to help to minimise it.

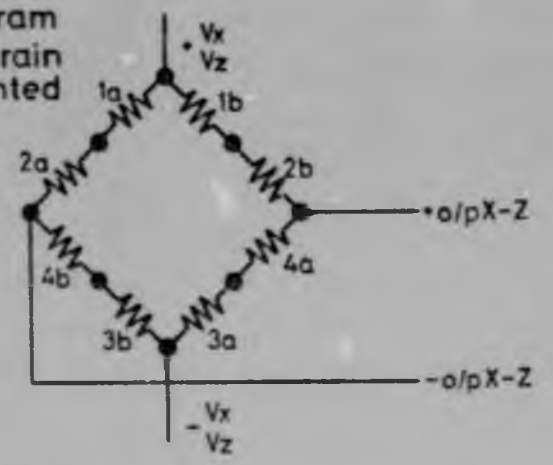
The results of the investigation into the mechanism by which a drag bit cuts hard rock and into the effects of high pressure water jets on this rock breaking process, have important implications. It was shown that the bit fractures the rock in a similar manner to an indentor. The water is injected into cracks which form adjacent to the bit and the water pressure helps to propagate the cracks. Thus it is probable that water jets at similar pressures could be used to assist other methods of rock cutting where the mechanism of rock breaking is also an indentation process. For example, evaluation of any benefits to be derived by using high pressure water jets in conjunction with disc roller cutters in tunnel boring and raise boring applications is a potential direction for future investigations.

APPENDIX (i)

Circuit and connection diagrams for test rig instrumentation.



Connection diagram for horizontal strain gauge instrumented billets.



Connection diagram for vertical strain gauge instrumented billets.

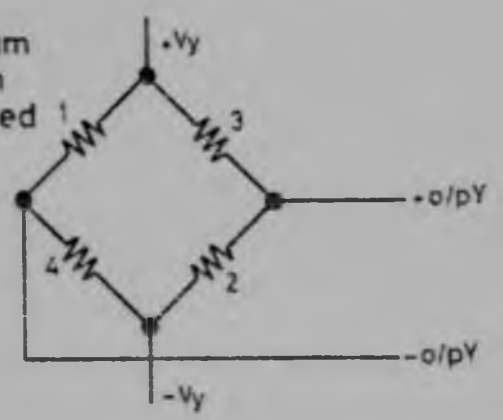


FIGURE 1.16 Instrumentation of the test frame used for experiments cutting rock.

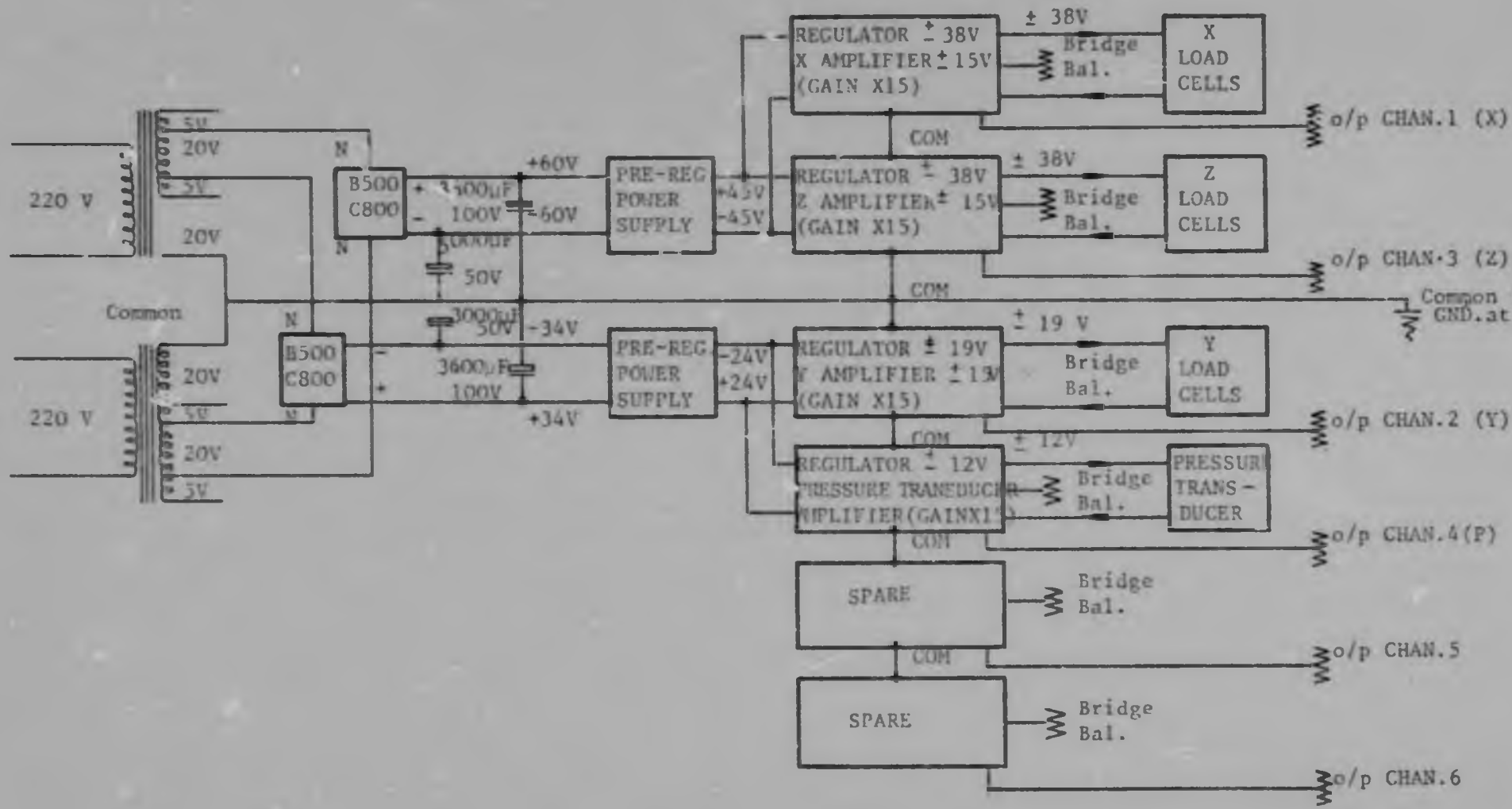


FIGURE 1.1(b) INSTRUMENTATION FOR TEST STOPE OF PRODUCTION ROCK CUTTERS.

BLOCK DIAGRAM OF INSTRUMENTATION.

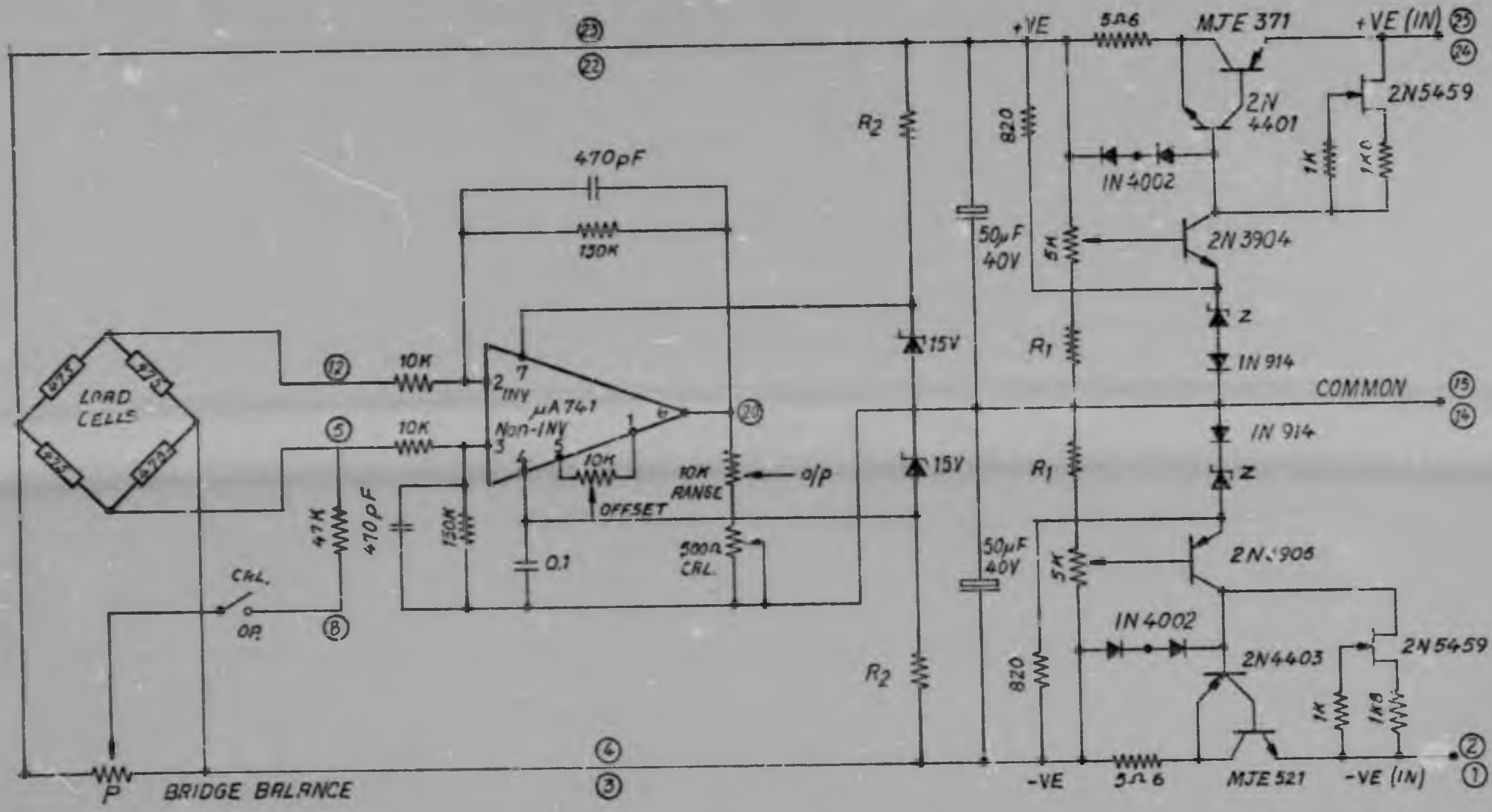


FIGURE 1.2 Pre-amplifier and bridge supply for test frame instrumentation.

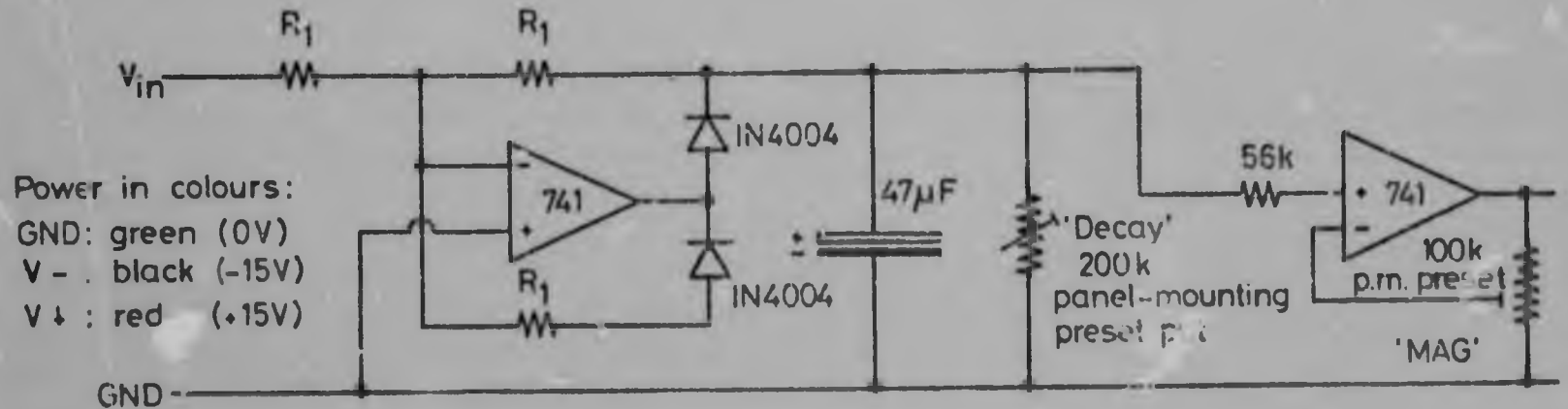


FIGURE 1.1 Peak level detector circuit diagram.

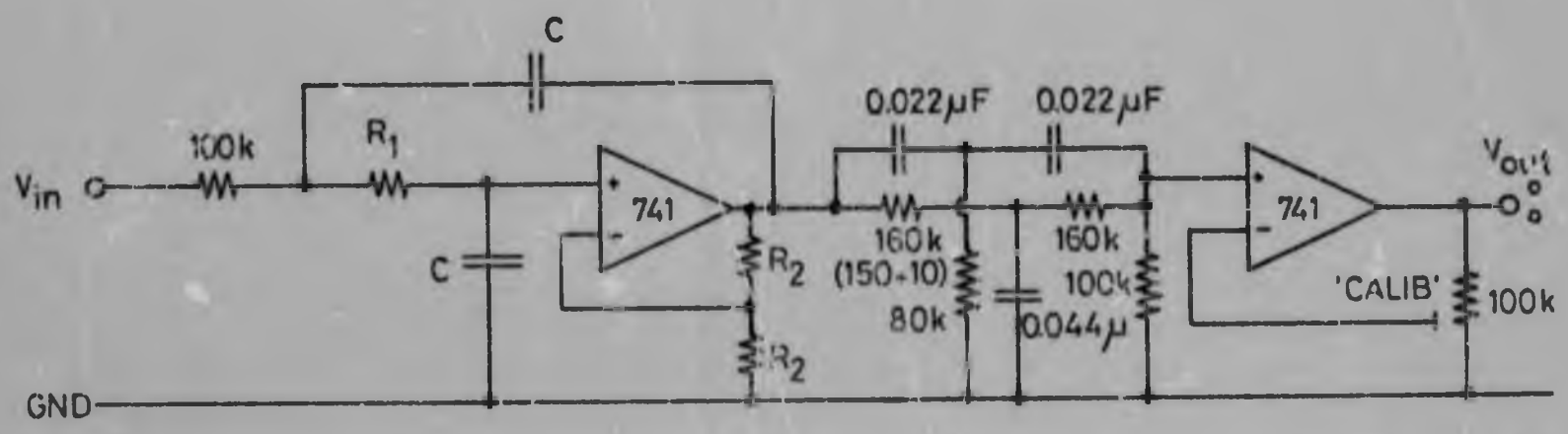
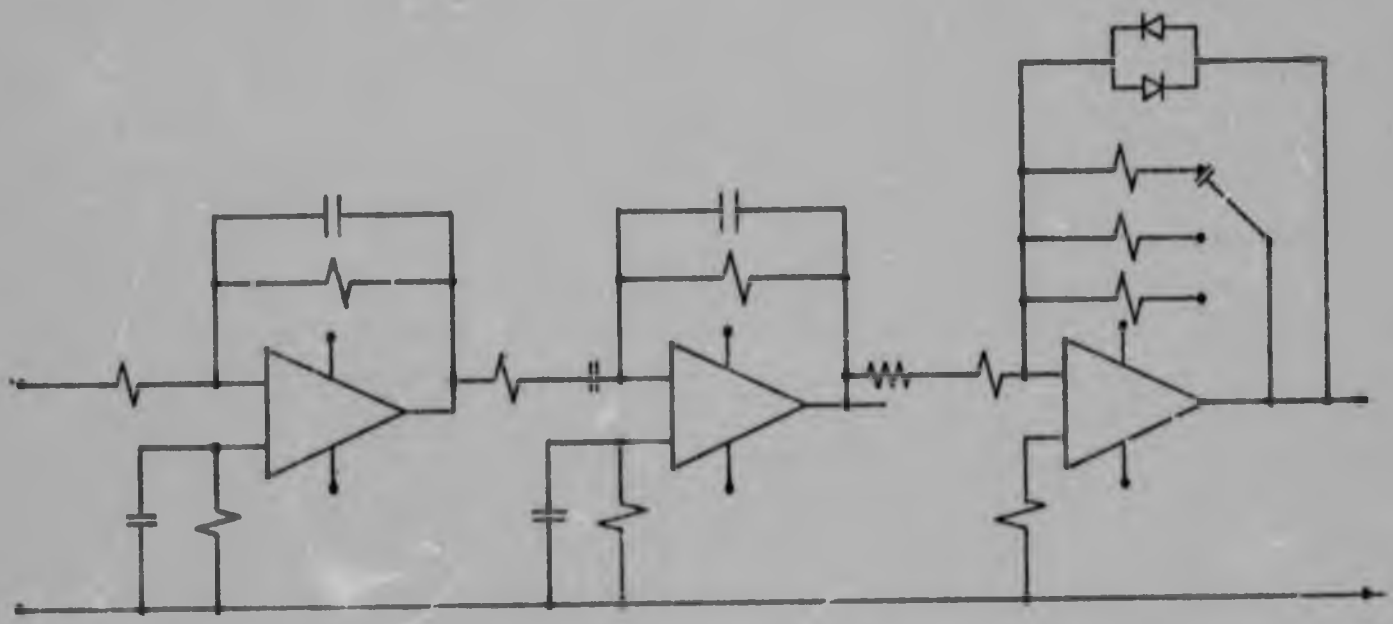


FIGURE 1.4 Low-pass filter diagram.



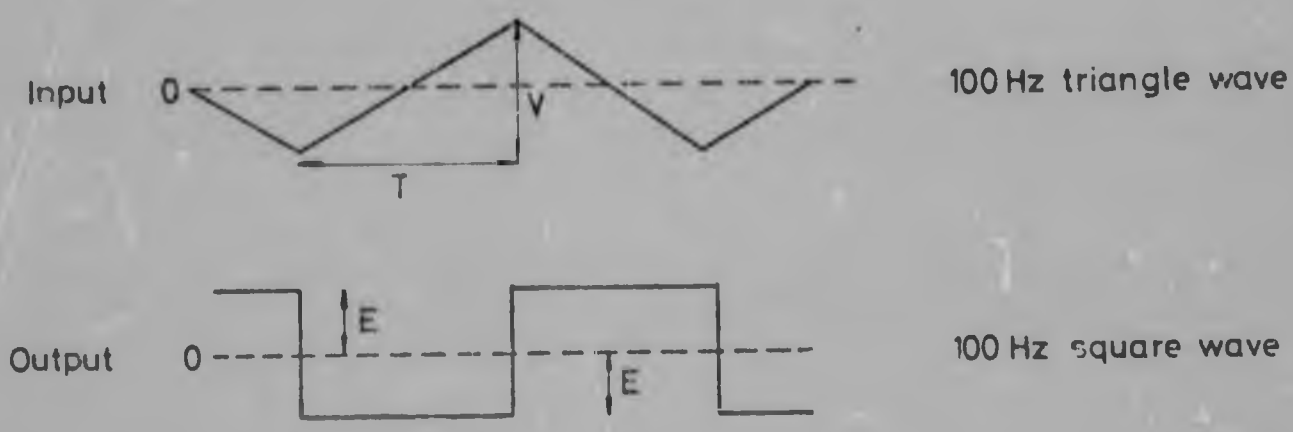


FIGURE 1.5 Differentiator Circuit Diagram.

APPENDIX (ii)

Calibration curves.

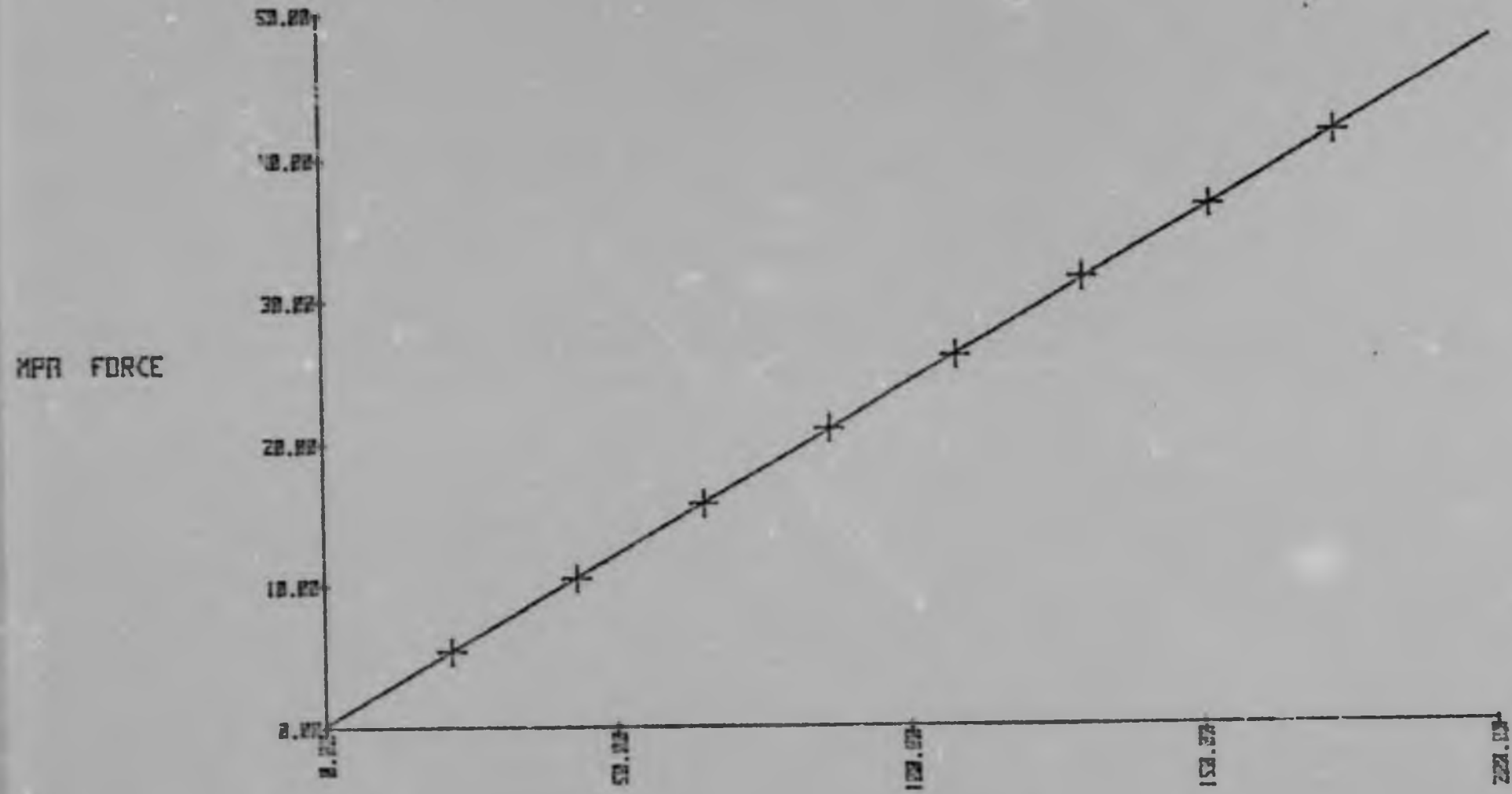


FIGURE 2.1 Calibration of 300 kN hydraulic jack.

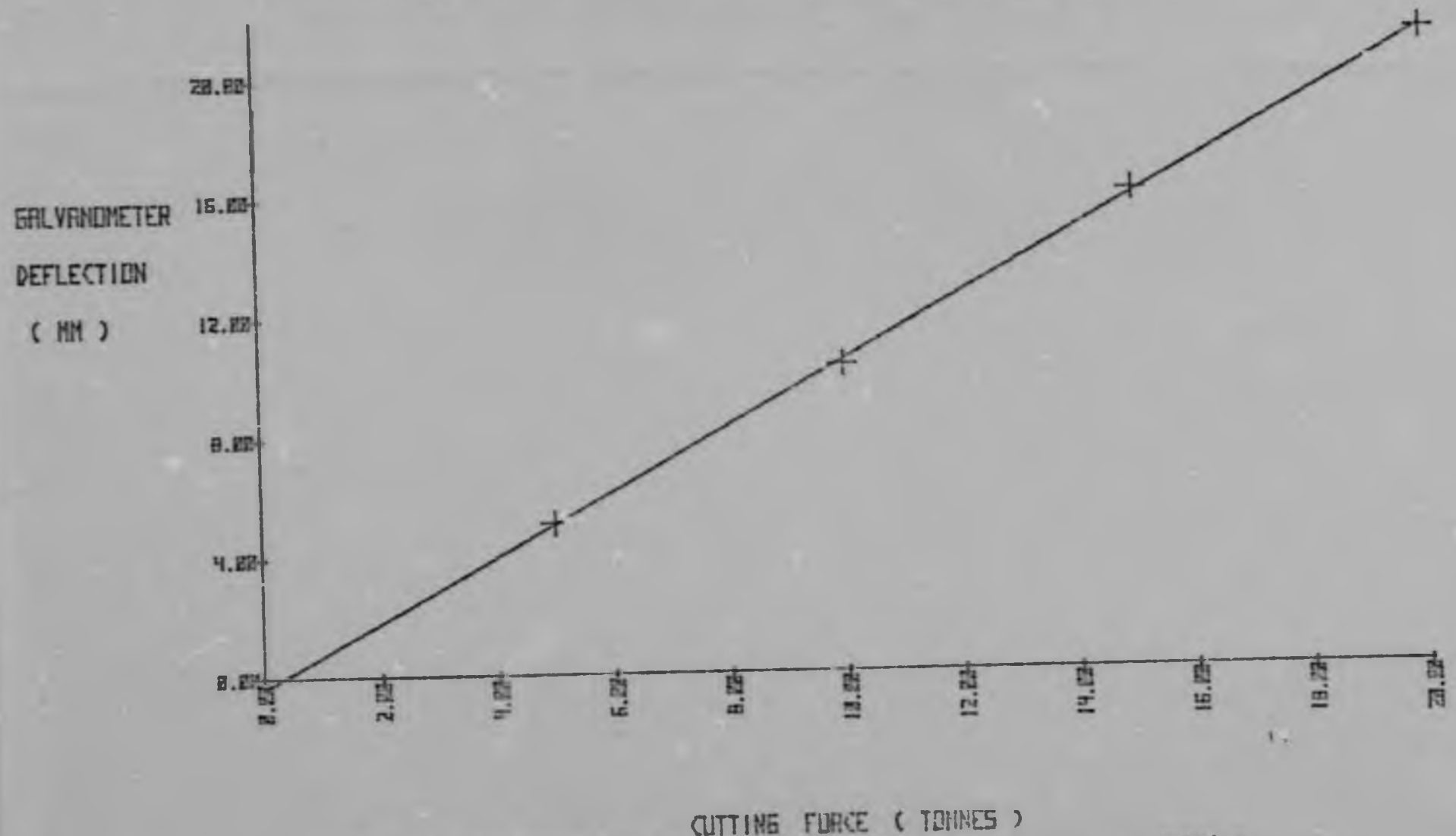


FIGURE 2.2. Calibration of test frame load cells in the direction of cutting.

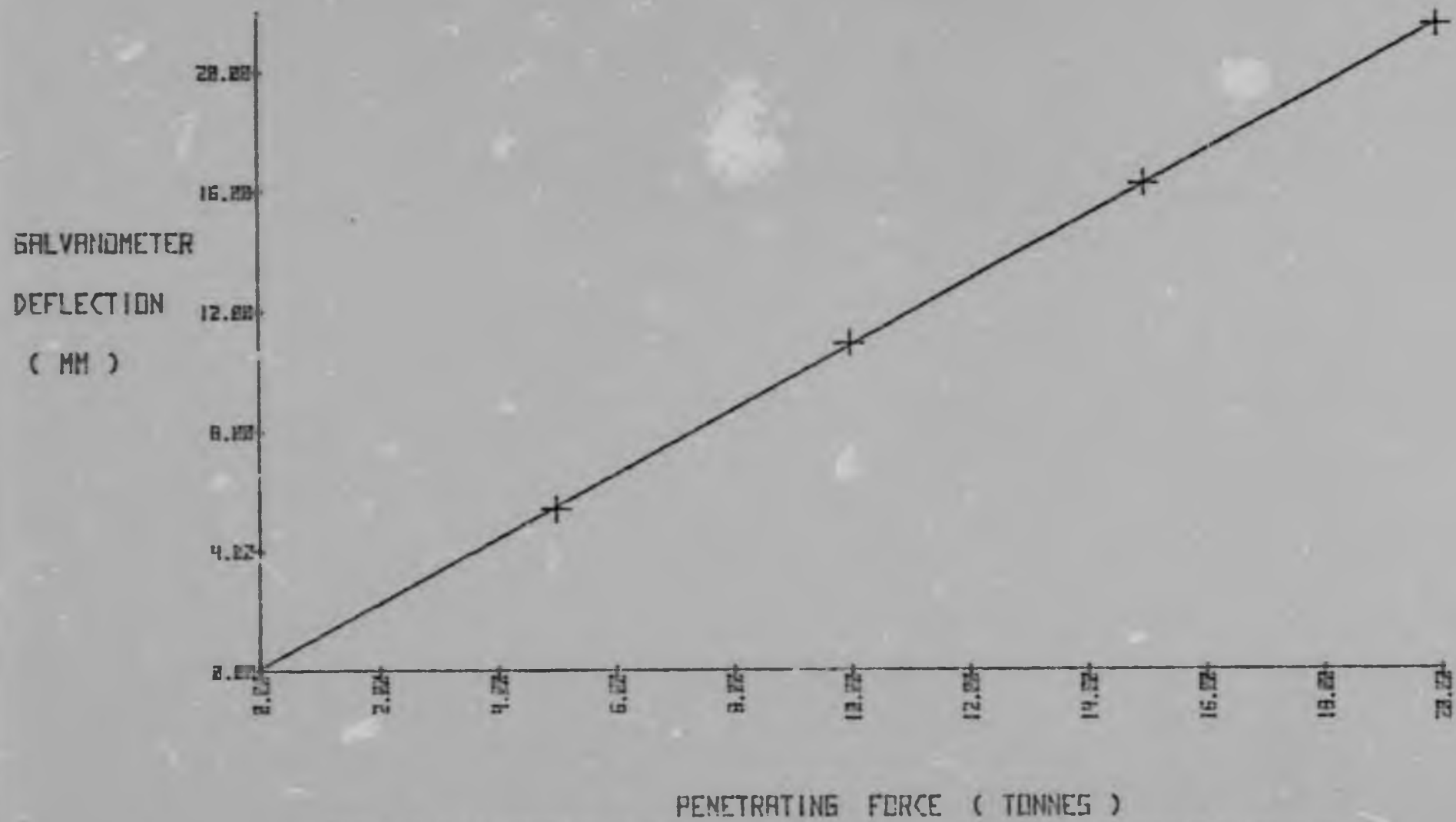


FIGURE 2.3 Calibration of the test frame load cell normal to the cutting direction.

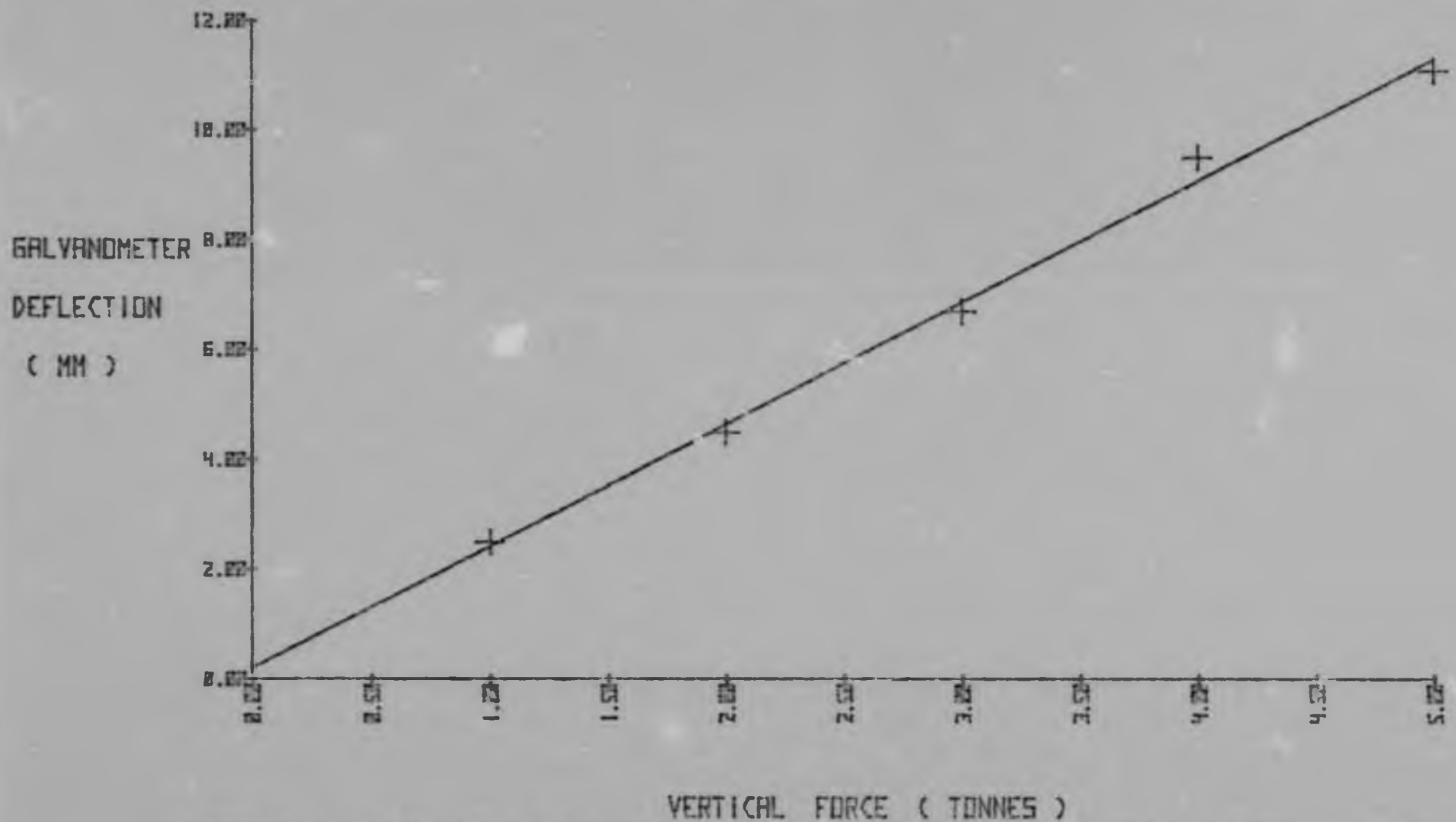


FIGURE 2.4 Calibration of the test frame load cells orthogonal to the cutting and normal directions.

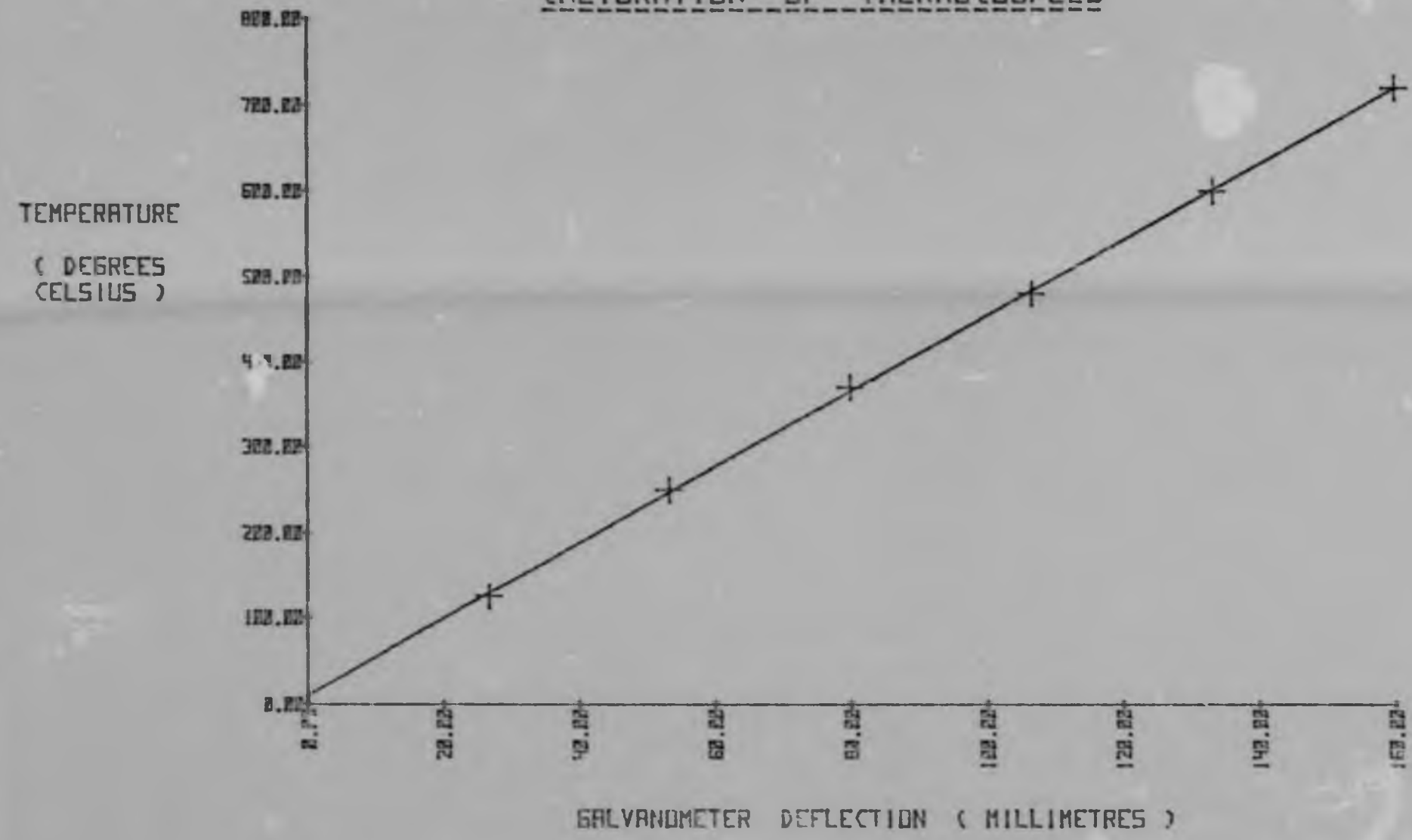


FIGURE 2.5 Thermocouple calibrations.

APPENDIX (iii)

A comparison of the power required to cut a unit area of slot in rock using : -

a) A jet channeling torch

b) A rockcutting machine

A calculation of the rate at which heat is generated using a jet channeling torch gives :

Fuel used is kerosene.

Assuming a fuel density = 800 kg/m^3

and specific heat of fuel = 42 000 kJ/kg.

From the manufacturers specifications, the fuel consumption of the torch using a standard nozzle = 40 ℓ/hr.

40 litres of fuel/hr = 32 kg of fuel/hr.

. . Rate at which heat is generated = 373 kW.

It has been shown, using similar torches in quarries, that the rate of cutting slots varies between one square metre an hour and three square metres an hour, depending on the type of rock being cut, (Union Carbide equipment specification, form ~~AE~~ 910-C). The same rate of cutting is achieved using rockcutting machines, however, the power required to drive these machines is 30 kW.

A calculation to show the change in the 'stiffness' of the hydraulic machine drive using different operating pressures and flow rates.

The hydraulic fluid operating the rockcutting machine main ram is supplied through flexible hoses. The elasticity of these hoses and the compressibility of the hydraulic fluid causes the hydraulic drive to act as a spring pulling a mass, the saddle, across a surface. Reducing the stiffness of the spring in this system, has the effect of reducing the vibrational frequency and increasing the amplitude of vibration of the mass.

The theoretical variation in the stiffness in the hydraulic machine is calculated for two different system pressures and flow rates.

Stiffness is defined as the force F required to deform a spring by a distance Δx.

$$\therefore \quad R = \frac{F}{\Delta x} \qquad (1)$$

Experiments were conducted at two system pressures. The power to the machine was the same for both of these test conditions, therefore the main cylinder diameter was reduced using the higher operating pressure, so that the available bit force remained constant. The cutting speed was kept constant also.

The hydraulic fluid used was an emulsion of 95 per cent water and 5 per cent soluable oil. Therefore the bulk modulus of the fluid was

taken to be that of water. The main cylinder was assumed to be rigid and thus the amount of fluid compressed in the cylinder was calculated from the bulk modulus of water only. The bulk modulus of the fluid in the hoses was calculated from an experiment whereby a hose was pressurized to a given value and the increased volume of the fluid in the hose was measured and compared with the volume occupied by the fluid at atmospheric pressure.

$$\text{By definition, Bulk modulus } \beta = \frac{V\ \Delta P}{\Delta V} \qquad (2)$$

The stiffness of the hydraulic drive can be calculated using the bulk modulus to obtain the increased volume of fluid in the hoses (ΔV_h), and in cylinder (ΔVc), for a given change in pressure. Then, the total increase in volume of the hydraulic fluid at a given pressure

$$\Delta V_T = \Delta V_h + \Delta V_c \qquad (3)$$

If the system pressure is now reduced to atmospheric pressure, this increased volume of hydraulic fluid will cause the piston to be displaced by a distance Δx.

$$\therefore \quad \Delta x = \frac{\Delta Vc}{Ac} \qquad (4)$$

where Ac = the cross-section area of the main cylinder.

$$\text{The force applied to the cylinder } \Delta F = \frac{\Delta P}{Ac} \qquad (5)$$

Thus the stiffness κ can be calculated using equation 1. The total volume of the main cylinder Vc was calculated with the piston in the middle of the cylinder, that is, two metres from the cylinder end.

$\therefore$ $Vc = 2 \times Ac$ (m) (6)

The experiment (Section 4.3.3.) was carried out using system pressures of 14 MPa and 25,5 MPa. The calculations of the respective drive stiffness at these pressures show :-

		Experiment 1	Experiment 2
Pressure	ΔP	14 MPa	27,5 MPa
Cross-Section area of hose	Ah	$3,14 \times 10^{-4} m^2$	$3,14 \times 10^{-4} m^2$
Length of hose	lh	20m	20m
Volume of hose	Vh	$6,28 \times 10^{-3} m^3$	$6,28 \times 10^{-3} m^3$
Cross-section area of cylinder	Ac	$1,21 \times 10^{-} m^2$	$6,19 \times 10^{-3} m^2$
Volume of cylinder	Vc	$2,42 \times 10^{-2} m^2$	$1,24 \times 10^{-2} m^2$
Bulk Modulus of hose and fluid	βh	$6,08 \times 10^{2} MN/m^2$	$6,08 \times 10^{2} MN/m^2$
Bulk Modulus of cylinder and fluid	βc	$2,25 \times 10^{3}$ MN/m^2	$2,25 \times 10^{3}$ MN/m^2
Since $\Delta V = \frac{V}{\beta} \Delta P$			
ΔVh		$1,45 \times 10^{-4} m^3$	$2,84 \times 10^{-4} m^3$
ΔVc		$1,51 \times 10^{-4} m^3$	$1,52 \times 10^{-4} m^3$
$\therefore$ ΔVt		$2,96 \times 10^{-4} m^3$	$4,36 \times 10^{-4} m^3$
Δx		$2,45 \times 10^{-2} m$	$7,04 \times 10^{-2} m$
ΔF		169 kN	170 kN
$\therefore$ Stiffness κ		6,9 MN/m	2,4 MN/m

APPENDIX (iv)

Computer programs used for plotting stress contours and for calculation of zones of excess stress

```
0010 PRINT
0020 PRINT
0030 PRINT "CALCULATION OF PRINCIPAL STRESSES"
0050 PRINT "WHICH STRESS DO YOU WANT ?"
0060 PRINT "X1=1,Y1=2,Z1=3,K1=4,K2=5,T1=6."
0070 PRINT "NORMAL+SHEAR FORCES;"
0080 PRINT "X4=7,Y4=8,Z4=9,K4=10,K5=11,T2=12."
0090 INPUT O
0110 INPUT "PENETRATING FORCE= ",P
0120 INPUT "HORIZONTAL FORCE=",Q
0140 INPUT "HALF FLAT LENGTH/2= ",L
0150 INPUT "LENGTH ALONG Y AXIS= ",C
0160 INPUT "LENGTH ALONG X AXIS= ",D
0170 INPUT "STEP INCREMENT ALONG X AXIS= ",S
0180 INPUT "STEP INCREMENT ALONG Y AXIS= ",T
0190 INPUT "1ST STRESS LINE=?",S3
0200 INPUT "LAST STRESS LINE=?",S2
0210 INPUT "IN STEPS OF?",M
0220 INPUT "NO OF FURTHER DIVS OF Y=",G
0225 INPUT "NO OF FURTHER DIVS OF X=",H
0230 GOTO 1300
0240 FOR N=S3 TO S2 STEP M
0250   LET S1=N
0270   FOR J=-C TO C STEP T/(G+1)
0280     LET Y=J
0310     LET K3=0
0320     FOR I=0 TO D STEP S/(H+1)
0330       LET X=I
0335       IF I=0 THEN LET X=.1
0340       LET R1=((Y+L)^2+X^2)^.5
0350       LET R2=((Y-L)^2+X^2)^.5
0360       IF Y>L THEN GOTO 0450
0380       IF Y<-L THEN GOTO 0480
0420       LET D3=ATN((L-Y)/X)
0430       LET A1=ATN((L+Y)/X)+D3
0440       GOTO 0520
0450       LET D3=ATN((Y-L)/X)
0460       LET A1=ATN((Y+L)/X)-D3
0470       GOTO 0520
0480       LET D3=ATN((L-Y)/X)
0490       LET A1=D3-ATN((-Y-L)/X)
0500       GOTO 0520
0510       IF (Y-2)=.5*L THEN LET A1=ATN(2*L/X)
0520       LET P1=3.14159
0525       IF Y<L THEN LET D3=-D3
0530       LET X1=(P/P1)*(A1+SIN(A1)*COS(A1+(2*D3)))
0540       LET X4=X1+(Q/P1)*SIN(A1)*SIN(A1+2*D3)
0550       LET Y1=(P/P1)*(A1-SIN(A1)*COS(A1+(2*D3)))
0560       LET Y4=Y1+(Q/P1)*(LOG((P1-2)/(R2-2))-SIN(A1)*SIN(A1+(2*D3)))
0570       LET Z1=(P/P1)*SIN(A1)*SIN(A1+(2*D3))
0580       LET Z4=(Q/P1))*(A1-SIN(A1)*COS(A1+2*D3))+Z1
0590       LET  K1=(P/P1)*(A1+SIN(A1))
0600       LET K4=.5*(X4+Y4)+((Z4)^2+.25*((X4-Y4)^2))^.5
0610       LET K2=(P/P1)*(A1-SIN(A1))
0620       LET K5=.5*(X4+Y4)-((Z4)^2+.25*((X4-Y4)^2))^.5
0625       LET T1=(P/P1)*SIN(A1)
0627       LET T2=(K4-K5)/2
0630       IF O=1 THEN LET K1=X1
0640       IF O=2 THEN LET K1=Y1
0650       IF O=3 THEN LET K1=Z1
0660       IF O=5 THEN LET K1=K2
0670       IF O=6 THEN LET K1=T1
0680       IF O=7 THEN LET K1=X4
```

FIGURE 5.1.(a) : Program used for stress contour plots.

```
0690        IF O=8 THEN LET K1=Y4
0700        IF O=9 THEN LET K1=Z4
0710        IF O=10 THEN LET K1=K4
0720        IF O=11 THEN LET K1=K5
0730        IF O=12 THEN LET K1=T2
0740        GOSUB 1110
0750      NEXT I
0770    NEXT J
0780 NEXT N
0781 MOVE,0,-350
0800 END
0810 GOTO 1110
0820 FOR J=-C TO C STEP T
0830   MOVE,J*450/C,0
0840   ILINE,0,5
0850   IMOVE,-10,5
0860   PRINT J
0870 NEXT J
0880 FOR K=S TO D STEP S
0890   MOVE,0,-K*350/D
0900   ILINE,5,0
0910   ILINE,-10,0
0920   IMOVE,-9,3
0930   PRINT K
0940 NEXT K
0950 MOVE,100,240
0960 ILINE,0,-200
0970 ILINE,10,30
0980 ILINE,-20,0
0990 ILINE,10,-30
1000 IMOVE,0,150
1010 PRINT P' MPA'
1020 IF Q=0 THEN GOTO 0240
1030 MOVE,-100,40
1040 ILINE,-30,10
1050 ILINE,0,-20
1060 ILINE,30,10
1070 ILINE,-200,0
1080 IMOVE,100,10
1090 PRINT Q'MPA'
1100 GOTO 0240
1110 IF K1=S1 THEN GOTO 1620
1120 IF K1<S1 THEN GOTO 1150
1130 IF K1>S1 THEN GOTO 1170
1140 GOTO 1290
1150 IF K3>S1 THEN GOTO 1240
1160 GOTO 1280
1170 IF K3=0 THEN GOTO 1280
1180 IF K3<S1 THEN GOTO 1200
1190 GOTO 1280
1200 LET E=K1-K3
1210 LET F=K1-S1
1220 LET X=X-(F/E)*S
1230 GOTO 1620
1240 LET E=K3-K1
1250 LET F=S1-K1
1260 LET X=X-(F/E)*S
1270 GOTO 1620
1280 LET K3=K1
1290 RETURN
1300 ERASE
1301 PRINT
1302 PRINT
1310 IF O=1 THEN PRINT 'SIGMA X,STRESS IN X PLANE'
1320 IF O=2 THEN PRINT 'SIGMA Y,STRESS IN Y PLANE'
1330 IF O=3 THEN PRINT 'TAU XY, SHEAR STRESS IN XY PLANE'
1340 IF O=4 THEN PRINT 'SIGMA 1'
1350 IF O=5 THEN PRINT 'SIGMA 2'
1360 IF O=6 THEN PRINT 'TAU MAX'
1370 IF O=7 THEN PRINT 'SIGMA X'
1380 IF O=8 THEN PRINT 'SIGMA Y'
1390 IF O=9 THEN PRINT 'TAU XY'
1400 IF O=10 THEN PRINT 'SIGMA 1'
1410 IF O=11 THEN PRINT 'SIGMA 2'
1415 IF O=12 THEN PRINT 'TAU MAX'
1420 PRINT 'FROM'S3'MPA TO'S2'MPA IN STEPS OF'T'MPA.'
1430 LET X=0
1440 LET Y=0
1450 WHERE,X,Y
1460 IMOVE,-X,-Y
1470 ORIGIN
1480 MOVE,500,400
1490 ORIGIN
1500 LINE,500,0
1510 LINE,-500,0
1520 FOR Y=250 TO -350 STEP -20
1530   MOVE,0,Y
1540   ILINE,0,10
1550 NEXT Y
1560 MOVE,L*450/C,0
1570 ILINE 0,125
1580 MOVE,-L*450/C,0
1590 ILINE,0,125
1600 MOVE,0,0
1610 GOTO 0820
1620 MOVE,(X*450/C),-X*350/D
1630 IF N=S3 THEN GOTO 1710
1640 IF N=S3+M THEN GOTO 1770
1650 IF N=S3+2*M THEN GOTO 1820
1655 IF N=S3+5*M THEN GOTO 1710
1660 ILINE,-3,-5
1670 ILINE,6,0
1680 ILINE,-3,5
1685 IF N=S3+4*M THEN GOTO 1710
1690 GOTO 1280
1700 RETURN
1710 ILINE,3,0
1720 ILINE,-6,0
1730 ILINE,3,0
1740 ILINE,0,3
1750 ILINE,0,-6
1755 IF N=S3+7*M THEN GOTO 1820
1760 GOTO 1280
1770 ILINE,4,0
1780 ILINE,0,-4
1790 ILINE,-4,0
1800 ILINE,0,4
1810 GOTO 1280
1820 IMOVE,3,3
1830 ILINE,-6,-6
1840 IMOVE,0,6
1850 ILINE,6,-6
1860 GOTO 1280
```

FIGURE 4.1. (b) : Program used for stress contour plots.

SIGMA :
FROM 100MPA TO 400MPA IN STEPS OF 100MPA.

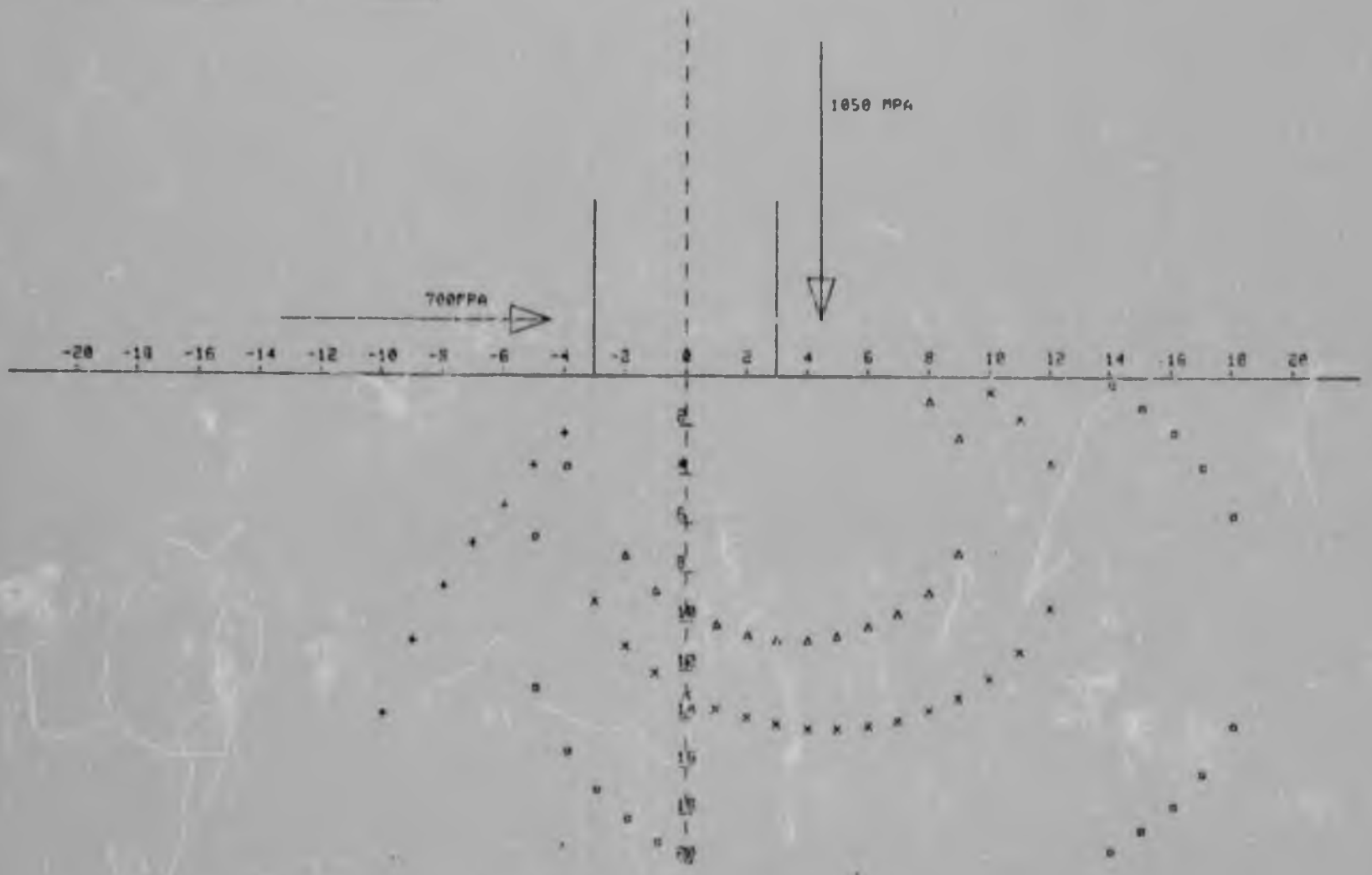


FIGURE 12 : An example of the computer plot of stress contours.

```
0010 ERASE
0020 PRINT
0030 PRINT "CALCULATION OF PRINCIPAL STRESSES"
0040 PRINT "NORMAL AND SHEAR FORCES"
0050 PRINT
0060 INPUT "PENETRATING FORCE ",P
0070 INPUT "HORIZONTAL FORCE ",Q
0080 PRINT
0090 INPUT "WEARFLAT LENGTH/2 ",L
0100 INPUT "LENGTH ALONG Y AXIS ",C
0110 INPUT "LENGTH ALONG X AXIS ",D
0120 INPUT "STEP INCREMENT ALONG X AXIS ",S
0130 INPUT "STEP INCREMENT ALONG Y AXIS ",T
0140 PRINT "WHICH CONDITION, DO YOU WANT?"
0150 PRINT "NF ONLY=1, INF+SF ONLY=2, INF+SF AND INF=3"
0160 INPUT O
0170 ERASE
0180 GOTO 1000
0190 FOR J=-C TO C STEP T
0200   LET Y=J
0210   FOR I=1 TO D STEP S
0220     LET X=I
0270     IF Y<L THEN GOTO 0320
0290     IF Y<-L THEN GOTO 0350
0290     LET DJ=ATN((L-Y)/X)
0300     LET A1=ATN((L+Y)/X)+DJ
0310     GOTO 0370
0320     LET DJ=ATN((Y-L)/X)
0330     LET A1=ATN((L+Y)/X)-DJ
0340     GOTO 0370
0350     LET DJ=ATN((L-Y)/X)
0360     LET A1=DJ-ATN((-L-Y)/X)
0370     LET PI=3.14155
0380     IF Y<L THEN LET DJ=-DJ
0390     LET R1=((Y+L)↑2+X↑2)↑.5
0400     LET R2=((Y-L)↑2+X↑2)↑.5
0410     LET X1=(P/PI)*(A1+SIN(A1)*COS(A1+(2*DJ)))
0420     LET X4=(Q/PI)*(SIN(A1)↑2*SIN(A1+2*DJ))+X1
0430     LET Y1=(P/PI)*(A1-SIN(A1)*COS(A1+(2*DJ)))
0440     LET Y4=Y1+(Q/PI)*((LOG(R1↑2/R2↑2))-SIN(A1)↑2*SIN((A1+2*DJ)
0450     LET Z1=(P/PI)*SIN(A1)↑2*SIN(A1+(2*DJ))
0460     LET Z4=(Q/PI)*(A1-SIN(A1)*COS(A1+2*DJ)))+Z1
0470     LET K1=(P/PI)*(A1+SIN(A1))
0480     LET K4=(X4+Y4)/2+((Z1)-2+.25*((X4-Y4)↑2))↑.5
0490     LET K2=(P/PI)*(A1-SIN(A1))
0500     LET K5=(X4+Y4)/2-((Z4)↑2+.25*((X4-Y4)↑2))↑.5
0570     LET U=47
0580     LET A=PI/180*52
0590     LET Y2=((K1-K2)/2)/SIN(A)-((K1-K2)/2)
0600     LET Y3=((K4-K5)/2)/SIN(A)-((K4-K5)/2)
0610     LET X2=U/TAN(A)
0670     GOSUB 1190
0680   NEXT I
0690 NEXT J
0700 END
0710 FOR J=-C TO C STEP (T*2
0720   MOVE,J*450/C,0
0730   ILINE,0,5
0740   IMOVE,-10,5
0750   PRINT J
0760 NEXT J
0770 FOR K=(S*2) TO D STEP (S*2)
0780   MOVE,0,-K*350/D
0790   ILINE,5,0
0800   ILINE,-10,0
0810   IMOVE,0,5
0820   PRINT Y
0830 NEXT K
0840 MOVE,100,240
0950 ILINE,0,-200
0860 ILINE,10,30
0870 ILINE,-20,0
0880 ILINE,10,-30
0900 IMOVE,0,150
0900 PRINT P" MPA"
0910 IF Q=0 THEN GOTO 0190
0920 MOVE,-100,40
0930 ILINE,-30,10
0940 ILINE,0,-20
0950 ILINE,30,10
0960 ILINE,-200,0
0970 IMOVE,80,5
0980 PRINT Q" MPA"
0990 GOTO 0190
1000 LET X=0
1010 LET Y=0
1020 WHERE,X,Y
1030 IMOVE,-X,-Y
1040 ORIGIN
1050 MOVE,500,400
1060 ORIGIN
1070 LINE,500,0
1080 LINE,-500,0
1090 FOR Y=300 TO -350 STEP -20
1100   MOVE,0,Y
1110   ILINE,0,10
1120 NEXT Y
1130 MOVE,L*(450/C),0
1140 ILINE,0,125
1150 MOVE,-L*(450/C),0
1160 ILINE,0,125
1170 MOVE,0,0
1180 GOTO 0210
1190 IF Y2<X2 THEN GOTO 1280
1200 IF O=2 THEN GOTO 1280
1210 MOVE,(Y*450/C),(-X*350/D)
1220 ILINE,5,0
1230 ILINE,-10,0
1240 ILINE,5,0
1250 ILINE,0,5
1260 ILINE,0,-10
1270 IF O=1 THEN RETURN
1280 IF Y3<X2 THEN RETURN
1290 IF O=1 THEN RETURN
1300 MOVE,(Y*450/C),-X*350/D
1310 IMOVE,0,3
1320 ILINE,-3,-6
1330 ILINE,6,0
1340 ILINE,-3,6
1350 RETURN
```

FIGURE 4.3 . Computer program used for calculation of zones of excess stress.

ACKNOWLEDGEMENTS

This work was carried out at the Chamber of Mines, Mining Technology Laboratory and I should like to thank this Organisation for allowing me to submit these studies for this degree.

In addition I should like to thank the Management and staff of Doornfontein Gold Mining Company, Limited and the staff at the field trials site from the Mining Technology Laboratory, for their cooperation and assistance.

I am indebted to my supervisors Dr. N.C. Joughin and Mr. R.A. Sesink-Clee for their help and guidance; to Mr. C. de Roo and Miss J. Collins for their assistance, and to Mrs. S. Furman for typing the script.

REFERENCES

Bárdendsen, P. (1970). Tunnelling with machines working on the undercutting principle. The technology and potential of tunnelling; S.A. Tunnelling Conf. Vol. 1.

Borchers, R. (1961). Exploration of the Witwatersrand system its extensions. Trans. 7th Commonwealth Min. Metall. Congr., Vol. II Johannesburg.

Bousinesque (1878 - 1883). 'Comptes Rendus' 'Applications des potentiels a l'etude de l'equilitre ..... des solids elastiques .....', Paris, 1885.

Cook, N.G.W., Joughin, N.C., Wiebols, G.A. (1968). Rockcutting and its potentialities as a new method of mining. J.S.Afr. Inst. Min. Metall., 68, (10), 435.

Cook, N.G.W., Immelman, D.A., Mrost, M. (1969). Planning research and development policy for large South African gold mines - an economic analysis. 9th Commonwealth Mining and Metallurgy Congress. London. May.

Cook, N.G.W., and Joughin, N.C. (1970). Rock fragmentation by mechanical, chemical and thermal methods. Paper 1c. 6. 6th Int. Min. Congress. Madrid.

Cook, N.G.W. (1973). Private Communication.

Ernst-Merchant (1945). Merchant, M.E. Basic Mechanics of the metal cutting process. J. App. Mech. 11(4) A 168 - A 175.

Evans, I. (1962). A theory of the basic mechanics of coal ploughing. Proc. Int. Symp. of Min. Res., Vol. 2, London, Pergamon Press. p. 761.

Evans, I. (1965). The force required to cut coal with blunt wedges. Int. J. Rock. Mech. Min. Sci. Vol. 2 p 1-12.

Fairhurst, C. and Lacabanne, W.D. (1957). Hard rock drilling techniques. Mine and Quarry Engineer. April, 1957.

Fairhurst, C. and Cook, N.G.W. (1966). The phenomenon of rock splitting parelled to the direction of maximum compression in the neighbourhood of a surface. Proc. 1st. Cong., Int. Soc. Rock. Mechs.

Fowell, R.J. (1974). The application of percussively activated tools to reef slotting in some South African Quartzites.

Frocht, H.H. (1948). Photoelasticity. Vol. II. pub. John Wiley and Sons Inc. 1948.

Harding, J.W. and Sneddon, I.N. (1945). The elastic stresses produced by the indentation of the plane surface of a semi-infinite elastic solid by a rigid punch. Cambridge Philos. Soc. Proceedings. Vol. 41, p. 16.

Hewitt, K.S. (1975). Aspects of the design an application of cutting systems for rock excavation. PhD. Thesis. University of Newcastle-upon-Tyne., Dec.

Hojem, J.P.M., Joughin, N.C., Demitriou , C. (1971). The design and development of a rockcutting machine for gold mining, J.S. Afr. Inst. Min. Metall. Vol. 71 No. 7 Feb. p.135 - 147.

Hojem, J.P.M., Cook, N.G.W. and Heins, C.(1975). A stiff two meganewton testing machine for measuring the work softening behaviour of brittle materials. J.S.Afr. Inst. Min. Metall. Vol. 25 No. 9 p. 250 - 270.

Hood, M. (1973). A comparison between percussive and non percussive cutting in the field of hard rock machining. Dissertation for BSc. (Hons) degree. University of Newcastle-upon-Tyne.

Jaeger, J.C., and Cook, N.G.W. (1969). Fundamentals of rock mechanics. Lond. Metheun.

Jager , A.F. (1976). Private communication.

Joughin, N.C. (1966). The measurement and analysis of earth motion resulting from underground rock failure, PhD. Thesis. Univ. of Witwatersrand.

Joughin, N.C. (1974). Private communication.

Joughin, N.C. (1976). Potential for the mechanisation of stoping in gold mines. J.S.Afr. Inst. Min. Metall., Vol. 76, No. 6; p.285 - 300.

Jurgenson, L. (1934). The application of theories of elasticity and plasticity to foundation problems contributions to soil mechanics. Boston Soc. of Civ. Engrs. 1925 - 1940.

Kanellopoulos, A. and Ball, A. (1975). The fracture and thermal weakening of quartzite in relation to comminution. J.S.Afr. Inst. Min. Metall. Vol. 76 p.45 - 52.

Labus, T.J. (1976). Energy requirements for rock penetration by water jets. 3rd. Int. Symp. Jet Cutting Technology, Paper No. E.3, Chicago.

Laurellio, P.J. and Fritch, C.A. (1974). Design and economic constraints of thermal rock weakening techniques. Int. J. Rock Mech. Min. Sci. and Geomech. Abst. Vol. II pp. 31 - 39. Pergamon Press 1974.

Leach, D.J. and Walker, G.L. (1966). Some aspects of rock cutting by high speed water jets. Roy. Soc. Lond. A, Vol. 260, p.295 - 308.

Love, A.E.H. (1929). The stress produced in a semi-infinite solid by pressure on part of the boundary, Roy. Soc. Phil. Trans. 228, A, p. 337 - 420.

Maurer, W.C. (1966). The state of rock mechanics knowledge in drilling. 8th Symp. on Rock Mechs., Univ. of Minn. Sept. Ch.15.

Nikonov, G.P. and Shavlovski, S.S. (1961). Gornyt Mashing, i Avtomatika, Nauchno - Tekh. Sb. 1. (18). 5.

Pomeroy, C.D. and Brown, D.H. (1968). Laboratory investigations of cutting processes applied to coal winning machines. J. of Strain Anaylsis.

Pomeroy, C.D. (1968). Mining application of the deep cut principle. Min. Eng. June p. 506.

Potts, E.L.J. and Shuttleworth, P. (1959). A study of the plough-ability of coal with special references to the effects of blade shape, direction of planing to the cleat , planing speed and the influence of water infusion. Trans. Inst. Min. Engrs., 117, 8 May 519 - 553.

Riemann, K.P. (1974). Die zerspanung von hartgesteinen beim schlitzhobeln. Dissertation. T.U. Hanover.

Rittinger, P. van. (1867). Lehrburch der Aufbereitungskunde, Berlin.

Rollaston, E.C. (1968). Metallurgy for engineers. 3rd Edition, pub. Edward Arnold Ltd. London.

Roxborough, F.F. (1973). Cutting rock with picks. Min. Engr. 132. 153 June. p. 445 - 455.

Roxborough, F.F. and Rispin, A. (1973). A laboratory investigation into the application of picks for mechanised tunnel boring in the Lower Chalk. Min. Engr. V. 133. No. 156. Oct.

Scott, R.F. (1963). Principles of soil mechanics. Pub. Addison-Wesley Publishing Company, Inc.

Sneddor, I.N. (1951). Fourier Transforms. McGraw-Hill Co. Inc. 1951.

Stokes, R.S.G. (1961) Contributed Editorial. Quart. New Bull. Geol. Soc. S. Afr., Vol. 4, No. 1

Van Proctor, R.J. (1977) Private Communication.

Wagner, H. and Schümann, E.H.R., (1971). The stamp-load bearing strength of rock. An experimental and theoretical investigation. Rock Mechs. Vol. 3/4, p. 185 - 207.

Whiller, A. (1974). Private communication.

Whittaker , B.N. (1967) An investigation into the design factors influencing the performance of the variable geometry coal plough. PhD. Thesis. University of Newcastle-upon-Tyne. May.

Zolack, M.D. Rummel, F., Jung, R., Raleigh, C.B. (1977) Laboratory hydraulic fracturing experiments in intact and pre-fractured rock. Int. J. Rock. Mech. Min. Sci. & Geomech. Abstr, Vol. 14 p. 49-58. Pergamon Press 1977.

Author Hood M
Name of thesis A Study of Methods to improve the Performance of Drag Bits used to cut hard Rock 1977

PUBLISHER:
University of the Witwatersrand, Johannesburg
©2013

LEGAL NOTICES:

Copyright Notice: All materials on the University of the Witwatersrand, Johannesburg Library website are protected by South African copyright law and may not be distributed, transmitted, displayed, or otherwise published in any format, without the prior written permission of the copyright owner.

Disclaimer and Terms of Use: Provided that you maintain all copyright and other notices contained therein, you may download material (one machine readable copy and one print copy per page) for your personal and/or educational non-commercial use only.

The University of the Witwatersrand, Johannesburg, is not responsible for any errors or omissions and excludes any and all liability for any errors in or omissions from the information on the Library website.